UTS UNIVERSITY OF TECHNOLOGY SYDNEY

The role of the endometrial microbiome and the implications for the outcome of *In Vitro* Fertilisation (IVF)

by Ciara Joy Bryant

Thesis submitted in fulfilment of the requirements for the degree of

Doctor of Philosophy

under the supervision of Professor Wilhelmina Huston, Dr Bentotage Fernando, and Dr Laurence Luu

University of Technology Sydney
Faculty of Science

January, 2026

CERTIFICATE OF ORIGINAL AUTHORSHIP

I, Ciara Joy Bryant, declare that this thesis is submitted in fulfilment of the requirements for the award of Doctor of Philosophy, in the Faculty of Science at the University of Technology Sydney.

This thesis is wholly my own work unless otherwise referenced or acknowledged. In addition, I certify that all information sources and literature used are indicated in the thesis.

This document has not been submitted for qualifications at any other academic institution.

This research was supported by an Australian Government Research Training Program (RTP) Scholarship doi.org/10.82133/C42F-K220.

Signature:

Production Note:
Signature removed prior to publication.

Date: 9/01/2026

Acknowledgements

First and foremost, I would like to express how grateful I am to have had the opportunity to complete a PhD. It has been something I have wanted to do since I was in undergrad! I can't believe I made it to the end! I am also grateful to have found such an interesting and fulfilling project to work on for the last four years.

I would like to thank my supervisor, Professor Willa Huston, for her ongoing support and reassurance throughout my project. I would also like to thank my co-supervisors, Dr Bentotage Fernando and Dr Laurence Luu, for all their help with protocols, data analysis, and feedback throughout my project. I would also like to thank the UTS technical officers and the UTS Microbial Imaging Facility staff for training me and for their help with various broken machines over the years!

Over the last few years, I have had ongoing support from my family and friends, in particular, my partner Tess, who has always been there to cheer me up and encourage me to keep going. I have also made some wonderful friends along the way, including Hannah Nugent and Brittany Jury, who were always keen for a coffee break and a walk. I would also like to thank Niamh, Kate, and Jess for letting me vent and complain whenever I needed it. What would I have done without you!

This thesis is formatted as a conventional thesis.

Table of Contents

Acknowledgements ..... *iii*

List of Figures ..... *xi*

List of Tables ..... *xv*

Abstract ..... *xviii*

1 Literature Review *20*

1.1 Menstruation, conception and implantation **21**

1.1.1 The structure of the female reproductive tract and menstruation 21

1.1.2 Endometrial receptivity 24

1.1.3 Early embryo development and implantation 25

1.2 *In Vitro* fertilisation (IVF) **30**

1.2.1 What is infertility? 30

1.2.2 What is IVF? 30

1.2.3 How IVF success and failure are defined 34

1.2.4 IVF in Australia and the current challenges 35

1.3 The reproductive bacterial microbiome **37**

1.3.1 Studying the reproductive microbiome 37

1.3.2 The eubiotic vaginal microbiome 39

1.3.3 The dysbiotic vaginal microbiome 41

1.3.4 The importance of microbiota-associated metabolites in the vagina 43

1.3.5 The endometrial microbiome 47

1.3.6 The microbiome throughout pregnancy 50

1.4 The factors involved in the outcome of IVF **51**

1.4.1 The endometrial microbiome and IVF failure 51

1.4.2 The endometrial microbiome, receptivity, and the immune response 54

1.4.3 Modelling the endometrial environment and the microbiome 57

1.5 Knowledge gap **66**

1.6 Endometrial model design **67**

1.7 Hypothesis and aims **71**

1.7.1 Hypothesis 71

1.7.2 Aims 72

2 Materials and Methods 73

2.1 Cell Culture 74

2.1.1 Culture and maintenance of endometrial epithelial cell lines 74

2.1.2 Culture and maintenance of the JAR cell line 75

2.1.3 Culture and maintenance of innate immune cell lines 76

2.1.4 Differentiation of THP-1 cells into macrophages 78

2.1.5 Authentication of cell lines 78

2.1.6 Mycoplasma testing 79

2.2 Preparation of Metabolites 80

2.2.1 Stock Metabolite Solutions 80

2.3 Viability of cells treated with microbiota-associated metabolites 81

2.3.1 MTS reagents 81

2.3.2 MTS assays for cell viability 81

2.4 Culture of cells with microbiota-associated metabolites 84

2.4.1 Treatment and collection of supernatant and cell samples 84

2.5 Culture of epithelial cells with conditioned media 87

2.5.1 Preparation of conditioned media 87

2.6 RNA extraction and Reverse-Transcription -quantitative (RT-q)PCR 88

2.6.1 RNA extraction and cDNA synthesis 88

2.6.2 Reverse Transcription-quantitative (RT-q) PCR 91

2.7 Glucose-uptake assay 95

2.7.1 Seeding and treatment of cells 95

2.7.2 Glucose-uptake assay 95

2.7.3 Analysis and figure generation for glucose-uptake assays 97

3 Microbiota-associated metabolites impact the functionality of the endometrial environment 98

3.1 Introduction 99

3.2 Hypothesis and aims 102

3.2.1 Hypothesis 102

3.2.2 Aims 103

3.3 Methods 103
3.3.1 Cell culture 103
3.3.2 MTS assays and the concentration of metabolites used in culture 103
3.3.3 Glucose-uptake assay: 104
3.3.4 Transepithelial Electrical Resistance (TEER): 104
3.3.5 Wound Healing Assay 107
3.3.6 Immunohistochemical staining for Zonula Occludens (ZO-1) 108
3.3.7 RNA extraction and Real-Time- Quantitative PCR (RT-qPCR) 111
3.4 Results: 114
3.4.1 Endometrial epithelial cells and innate immune cells are viable when cultured with microbiota-associated metabolites 114
3.4.2 Succinic acid decreases glucose uptake in NK-92 cells 116
3.4.3 L-lactic acid decreases epithelial migration in Ishikawa and RL95-2 cells 118
3.4.4 D-lactic acid and acetic acid decrease the expression of ZO-1 in Ishikawa cells 120
3.4.5 Ishikawa and RL95-2 cells do not polarise 122
3.4.6 Microbiota-associated metabolites downregulate the expression of involved in receptivity in both endometrial epithelial and innate immune cell lines. 124
3.5 Discussion: 127
3.6 Conclusion and future directions 137
4 The immunomodulatory effect of microbiota-associated metabolites in the endometrial environment 139
4.1 Introduction 140
4.2 Hypothesis and Aim 144
4.2.1 Hypothesis 144
4.2.2 Aim 144
4.3 Methods 144
4.3.1 Cell culture 144
4.1.1 Treatment of cells and sample collection 145
4.1.2 Generation of conditioned media 145

4.1.3 Quantification of cytokines and chemokines using a cytometric bead array 145
4.1.4 RT-qPCR 147
4.4 Results 149
4.4.1 L-lactic acid and acetic acid induce decreased secretion of pro-inflammatory cytokines by endometrial epithelial cells 149
4.4.2 Microbiota-associated metabolites modulate NK-92 secretion of IL-6, IL-8, and IL-10 151
4.4.3 L-lactic acid induces increased THP-1 secretion of IL-8 but decreases secretion of RANTES 154
4.4.4 L- and D-lactic acid treatments modulate inflammatory gene expression in endometrial epithelial cells. 155
4.4.5 L-lactic acid and acetic acid treatment was associated with downregulation of pro-inflammatory genes in natural killer cells but not in macrophages 158
4.4.6 Succinic acid induces an increase in IDO1 mRNA expression in NK-92 cells 159
4.4.7 Conditioned media generated by THP-1 cells treated with L-lactic acid, decreases RL95-2 *IL8* expression 161
4.5 Discussion 163
4.6 Conclusion and future directions 175
5 Microbiota-associated metabolites and embryo implantation 178
5.1 Introduction 179
5.2 Hypothesis and Aim 182
5.2.1 Hypothesis 182
5.2.2 Aim 182
5.3 Methods 183
5.3.1 Cell culture 183
5.3.2 MTS Assays 183
5.3.3 Treatment of cells and sample collection 183
5.3.4 Glucose-uptake assay 184
5.3.5 Western blots 184
5.3.6 RT-qPCR 188

5.3.7 Spheroid Attachment Model 190

5.4 Results 194

5.4.1 JAR cell viability at physiologically relevant concentrations of microbiota-associated metabolites 194

5.4.2 Microbiota-associated metabolites do not impact JAR cell glucose uptake 195

5.4.3 MMP and TIMP expression is not impacted by microbiota-associated metabolites 197

5.4.4 Microbiota-associated metabolites do not impact endometrial epithelium's ability to facilitate attachment 200

5.4.5 Microbiota-associated metabolites do not impact JAR spheroids' ability to attach to endometrial epithelium 201

5.4.6 The NK-92 secretome, after exposure to microbiota-associated metabolites, inhibits spheroid attachment to endometrial epithelium 203

5.5 Discussion 206

5.6 Conclusion and future directions 215

6 General Discussion and Future Directions 217

6.1 Determining the role of endometrial microbiota-associated metabolites in IVF 218

6.2 Do microbiota-associated metabolites in the endometrium have a similar role to metabolites in the vaginal environment? 222

6.3 The relationship between receptivity, the immune response and implantation 224

6.4 The limitations of modelling the endometrium and future directions ... 226

6.5 The microbiome and IVF in the future 231

6.6 Conclusion 234

Appendix 1 235

Cell line authentication 235

Appendix 2 236

Wound healing assay using Ishikawa cells 236

Wound healing assay using RL95-2 cells **237**

ZO-1 western blot images **238**

Reference gene C_t values **239**

ΔC_t values for genes associated with receptivity from cells treated with microbiota-associated metabolites **242**

Fold change analysis of receptivity genes **246**

Appendix 3 ..... ***250***

Cytometric Bead Array (CBA) analysis of cytokines and chemokines **250**

Cytokine and chemokine secretion by Ishikawa cells 251

Cytokine and chemokine expression by RL95-2 cells 255

Cytokine and chemokine expression by NK-92 cells 259

Cytokine and chemokine secretion by THP-1 cells 263

C_t values of reference genes in conditioned media models **267**

ΔC_t values for genes associated with the immune response from cells treated with microbiota-associated metabolites **269**

ΔC_t values for genes associated with the immune response from cells treated with conditioned media **274**

Fold change analysis of immune response genes **277**

Appendix 4 ..... ***282***

C_t Values for reference genes in JAR cells **282**

ΔC_t Values for TIMP and MMP genes in JAR cells **283**

Spheroid Attachment Assay **284**

Expression of MMP9 by JAR Cells **288**

Bibliography ***289***

List of Figures

Figure 1. The female reproductive tract.. 22
Figure 2. The menstrual cycle. 23
Figure 3. Embryo implantation. Implantation occurs in three stages; apposition, adhesion, and invasion into the endometrium. 27
Figure 4. Standard IVF treatment cycle.. 31
Figure 5. The viability (%) of endometrial epithelial cells and innate immune cells treated with microbiota-associated metabolites 115
Figure 6. The glucose uptake of endometrial epithelial cells and innate immune cells after treatment with microbiota-associated metabolites. 117
Figure 7. The wound closure of endometrial epithelial cells treated with microbiota-associated metabolites..... 119
Figure 8. The decreased expression of ZO-1 in Ishikawa cells after treatment with microbiota-associated metabolites. 121
Figure 9. Transepithelial electrical resistance of endometrial epithelial cells.. 123
Figure 10. Relative gene expression of genes involved in receptivity compared to untreated cells. 126
Figure 11. Ishikawa and RL95-2 cells cytokine response to microbiota-associated metabolites.. 150
Figure 12. NK-92 cells cytokine response to microbiota-associated metabolites.. 153
Figure 13. THP-1 cells cytokine response to microbiota-associated metabolites. 155
Figure 14. Relative gene expression of genes involved in the immune response in endometrial epithelial cells compared to untreated cells..... 157
Figure 15. Relative gene expression of genes involved in the immune response in NK-92 cells compared to untreated cells. 159
Figure 16. Relative gene expression of IDO1 in NK-92 cells compared to untreated cells. 160
Figure 17. Relative expression of genes involved in the immune response in epithelial cells treated with conditioned media compared to untreated controls..... 162
Figure 18. JAR Spheroid attachment assay workflow. 191

Figure 19. The viability (%) of JAR cells treated with microbiota-associated metabolites.. 195
Figure 20. The glucose uptake JAR cells after treatment with microbiota-associated metabolites. 196
Figure 21. Relative gene expression of MMP2, MMP9, TIMP1, and TIMP2 by JAR cells treated with microbiota-associated metabolites compared to untreated cells. .. 198
Figure 22. Protein expression of MMP2 relative to GAPDH in JAR cells treated with microbiota-associated metabolites. 199
Figure 23. Spheroid attachment to endometrial epithelial cells treated with microbiota-associated metabolites..... 201
Figure 24. Attachment of JAR cells treated with microbiota-associated metabolites to untreated endometrial epithelial cells.. 202
Figure 25. Spheroid attachment to endometrial epithelial cells treated with media conditioned by NK-92 cells cultured with microbiota-associated metabolites.. 204
Figure 26. Spheroid attachment to endometrial epithelial cells treated with media conditioned by differentiated THP-1 cells cultured with microbiota-associated metabolites.. 205
Figure 27. Proposed model of the impact of microbiota-associated metabolites on endometrial epithelium and innate immune cells..... 220
Figure 28. The impact of microbiota-associated metabolites on Ishikawa cells' wound closure.. 236
Figure 29. The impact of microbiota-associated metabolites on RL95-2 cells' wound closure. 237
Figure 30. Representative images of protein expression of ZO-1 in Ishikawa cells treated with microbiota-associated metabolites.. 238
Figure 31. The relative expression of genes associated with receptivity in Ishikawa cells treated with microbiota-associated metabolites. 246
Figure 32. The relative expression of genes associated with receptivity in RL95-2 cells treated with microbiota-associated metabolites.. 247
Figure 33. The relative expression of genes associated with receptivity in NK-92 cells treated with microbiota-associated metabolites. 248
Figure 34. The relative expression of genes associated with receptivity in PMA differentiated THP-1 cells treated with microbiota-associated metabolites.. 249

Figure 35. Cytokine expression by Ishikawa cells treated with L-lactic acid (LLA)... 251
Figure 36. Cytokine expression by Ishikawa cells treated with D-lactic acid (DLA).. 252
Figure 37. Cytokine expression by Ishikawa cells treated with acetic acid (AA). 3.... 253
Figure 38. Cytokine expression by Ishikawa cells treated with succinic acid (SA)..... 254
Figure 39. Cytokine expression by RL95-2 cells treated with L-lactic acid (LLA)..... 255
Figure 40. Cytokine expression by RL95-2 cells treated with D-lactic acid (DLA)..... 256
Figure 41. Cytokine expression by RL95-2 cells treated with acetic acid (AA)..... 257
Figure 42. Cytokine expression by RL95-2 cells treated with succinic acid (SA)..... 258
Figure 43. Cytokine expression by NK-92 cells treated with L-lactic acid (LLA).. 259
Figure 44. Cytokine expression by NK-92 cells treated with D-lactic acid (DLA).. ... 260
Figure 45. Cytokine expression by NK-92 cells treated with acetic acid (AA).. 261
Figure 46. Cytokine expression by NK-92 cells treated with succinic acid (SA).. 262
Figure 47. Cytokine expression by THP-1 cells treated with L-lactic acid (LLA).. 263
Figure 48. Cytokine expression by THP-1 cells treated with D-lactic acid (DLA)..... 264
Figure 49. Cytokine expression by THP-1 cells treated with acetic acid (AA)..... 265
Figure 50. Cytokine expression by THP-1 cells treated with succinic acid (SA). 266
Figure 51. The relative expression of genes associated with the immune response in Ishikawa cells treated with microbiota-associated metabolites..... 277
Figure 52. The relative expression of genes associated with the immune response in RL95-2 cells treated with microbiota-associated metabolites..... 278
Figure 53. The relative expression of genes associated with the immune response in NK-92 cells treated with microbiota-associated metabolites. 279
Figure 54. The relative expression of genes associated with the immune response in THP-1 cells treated with microbiota-associated metabolites.. 280
Figure 55. The relative expression of IDO1 in NK-92 cells treated with microbiota-associated metabolites..... 281
Figure 56. Spheroid attachment to endometrial epithelial cells treated with microbiota-associated metabolites..... 284
Figure 57. Attachment of JAR cells treated with microbiota-associated metabolites to untreated endometrial epithelial cells.. 285
Figure 58. Spheroid attachment to endometrial epithelial cells treated with media conditioned by NK-92 cells cultured with microbiota-associated metabolites. 286

Figure 59. Spheroid attachment to endometrial epithelial cells treated with media conditioned by differentiated THP-1 cells cultured with microbiota-associated metabolites.. 287
Figure 60. Protein expression of MMP9 and GAPDH in JAR cells treated with microbiota-associated metabolites 288

List of Tables

Table 1. Dominant bacteria in the vaginal CSTs. 40
Table 2. Bacteria present in the vagina in dysbiotic conditions 43
Table 3. Metabolites produced by vaginal bacteria in eubiosis and dysbiosis. 45
Table 4. The advantages and disadvantages of different modelling formats. 60
Table 5. Preparation of microbiota-associated metabolites from purchased stock. 80
Table 6. Concentration range of individual microbiota-associated metabolites used in MTS Viability Assays. 83
Table 7. The concentration range of microbiota-associated metabolites used to treat cells. 86
Table 8. cDNA synthesis reaction components. 90
Table 9. Reverse Transcriptase reaction components. 90
Table 10. Thermal cycling conditions used to synthesise cDNA. 91
Table 11. RT-qPCR master mix components 93
Table 12. Thermal cycling conditions used to conduct RT-qPCR reactions. 93
Table 13. Reference gene primer sequences. 94
Table 14. 2DG6P Detection Reagent. 96
Table 16. The concentration range of microbiota-associated metabolites used to treat cells in RT-qPCR experiments. 112
Table 17. Primer sequences for markers of receptivity and cellular function 113
Table 19. Products purchased from BD to conduct CBA experiments. 146
Table 20. Inflammatory marker primer sequences. 148
Table 22. The primary and secondary antibodies used in western blot experiments. 187
Table 23. Primer sequences for genes involved in MMP regulation by JAR cells 189
Table 24. The results of cell line genotyping using CLASTR 235
Table 25. Average C_t values of HPRT1 in Ishikawa cells treated with microbiota-associated metabolites and controls. 239
Table 26. Average C_t values of HPRT1 in RL95-2 Cells treated with microbiota-associated metabolites and controls. 240

Table 27. Average C_t values of GADPH in NK-92 cells treated with microbiota-associated metabolites and controls. 240
Table 28. Average C_t values of ACTB in THP-1 cells treated with microbiota-associated metabolites. 241
Table 29. ΔC_t values from Ishikawa cells treated with microbiota-associated metabolites.. 242
Table 30. ΔC_t values from RL95-2 cells treated with microbiota-associated metabolites. 243
Table 31. ΔC_t values from NK-92 cells treated with microbiota-associated metabolites.. 244
Table 32. ΔC_t values from THP-1 cells treated with microbiota-associated metabolites.. 245
Table 33. Average C_t values of HPRT1 in Ishikawa cells cultured with THP-1 conditioned media.. 267
Table 34. Average C_t values of HPRT1 in Ishikawa cells cultured with NK-92 conditioned media. 267
Table 35. Average C_t values of HPRT1 in RL95-2 cells cultured with THP-1 conditioned media.. 268
Table 36. Average C_t values of HPRT1 in RL95-2 cells cultured with NK-92 conditioned media.. 268
Table 37. ΔC_t values from Ishikawa cells treated with microbiota-associated metabolites. 270
Table 38. ΔC_t values from RL95-2 cells treated with microbiota-associated metabolites. 271
Table 39. ΔC_t values from NK-92 cells treated with microbiota-associated metabolites.. 272
Table 40. ΔC_t values from THP-1 cells treated with microbiota-associated metabolites.. 273
Table 41. ΔC_t values from Ishikawa cells cultured with NK-92 cell-conditioned media. 274
Table 42. ΔC_t values from Ishikawa cells cultured with THP-1 cell-conditioned media.. 275

Table 43. ΔC_t values from RL95-2 cells cultured with NK-92 cell-conditioned media.. 275
Table 44. ΔC_t values from RL95-2 cells cultured with THP-1 cell-conditioned media. 276
Table 45. Average C_t values of GAPDH in JAR cells treated with microbiota-associated metabolites and controls.. 282
Table 46. ΔC_t values from JAR cells treated with microbiota-associated metabolites. 283

Abstract

Infertility is a common diagnosis for people globally. One treatment for infertility is *in vitro* fertilisation (IVF), where oocytes are collected, fertilised *in vitro*, and then transferred back into the uterine cavity to implant into the endometrium. Currently, in Australia and New Zealand, 33.1% of fresh embryo transfers achieve a clinical pregnancy, and 25.9% of fresh transfers achieve a live birth. This is an improvement on the initial IVF success rates, but these numbers have shown little change over the last 10 years. This is of concern as IVF is a costly and physically and mentally challenging procedure for patients.

With the introduction of next-generation sequencing, the endometrial microbiome has been profiled, and different compositions of bacteria have been associated with IVF outcomes. *Lactobacillus* dominance is associated with successful outcomes such as clinical pregnancy and live birth. Whereas, diverse polymicrobial profiles are associated with poor outcomes, including implantation failure. Thus, this project aimed to investigate the factors involved in the relationship between IVF outcome and microbiome composition. This was done by incorporating microbiota-associated metabolites in cell culture models to determine the impact of metabolites on the development of receptivity, the endometrial immune response, and embryo implantation. Lactic acid isomers were used to represent *Lactobacillus,* and acetic and succinic acids were used to represent diverse bacteria.

L-lactic acid, representing *Lactobacillus,* reduced endometrial epithelial cell migration. D-lactic acid and acetic acid reduced the expression of tight junction protein

ZO-1 in epithelial cells. Treatment with the metabolites also reduced the expression of genes involved in the development of receptivity include *TGFBR1*. This suggests that metabolites could affect processes like the epithelial-to-mesenchymal transition which are required for receptivity. Interestingly, L-lactic acid decreased the secretion of pro-inflammatory cytokines in endometrial epithelial cells. On the other hand, D-lactic acid increased the secretion of IL-6, IL-8, and IL-10 in NK cells, which may be beneficial for controlling embryo invasion and developing maternal tolerance. Furthermore, media conditioned by NK cells treated with metabolites reduced spheroid attachment to epithelial cells, suggesting the metabolites could adversely affect the interaction between innate immune cells and endometrial epithelium. This study has shown that microbiota-associated metabolites are capable of impacting important factors in the development of receptivity, the immune status of the endometrium, and embryo implantation.

1 Literature Review

1.1 Menstruation, conception and implantation

1.1.1 The structure of the female reproductive tract and menstruation

The female reproductive tract is divided into two sections: the lower and upper reproductive tract. The lower reproductive tract is comprised of the vagina and cervix (Figure 1). The vagina is lined by a mucosal layer of non-keratinised stratified squamous epithelium and has underlying layers of fibrous connective tissue and indistinct smooth muscle [1]. The cervix sits at the top of the vaginal canal, connecting the vagina to the uterus. It is lined by simple columnar epithelium and cervical glands [1]. The upper reproductive tract includes the uterus, uterine cavity, fallopian tubes and ovaries (Figure 1). The uterus is made of three layers of tissue. The outermost is the perimetrium, consisting of mesothelium, and loose connective and elastic tissue [1]. The intermediate layer, or myometrium, consists of three defined layers of smooth muscle [1]. The innermost layer is the endometrium, which consists of the stratum functionalis and the stratum basalis. The stratum functionalis consists of simple columnar epithelium, glands, stroma, and blood vessels. The stratum basalis is beneath the stratum functionalis and is a much thinner layer of regenerative tissue. The fallopian tubes extend from the uterus and are lined with ciliated and non-ciliated simple columnar epithelium [1, 2]. The ovaries contain follicles surrounded by germinal epithelium and connective tissue. The follicles develop and are released from the ovary during ovulation [2].

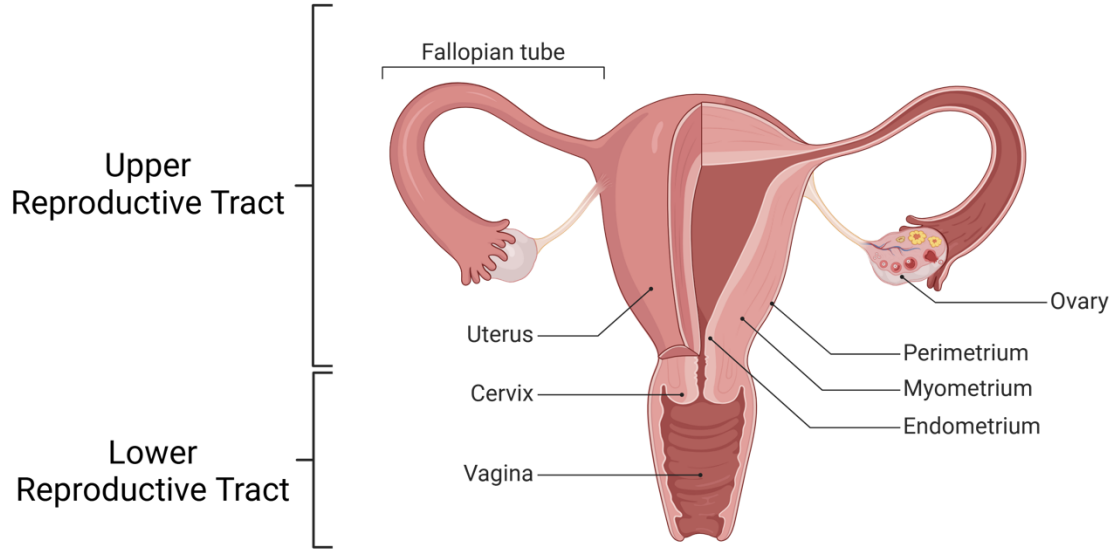


Figure 1. The female reproductive tract. Adapted from BiorRender. Female reproductive system anatomy. 2025 Available from: https://app.biorender.com/biorender-templates/figures/all/t-601c1bd881f68e3bd0dd9807-female-reproductive-system-anatomy

The endometrium undergoes structural changes throughout the menstrual cycle, which are driven by hormonal fluctuations in two stages [1]. The first stage is known as the follicular stage and is controlled by follicle-stimulating hormone (FSH) produced by the pituitary gland (Figure 2). This stage begins on the first day of menstruation, lasting for approximately 14 days, and during this time FSH drives the maturation of follicles [3]. Towards the end of the follicular stage, FSH levels decline, and estradiol (E_2) is produced by the dominant follicle, promoting the development of the endometrial tissue (Figure 2) [3]. At the same time, progesterone (P_4) levels begin to rise (Figure 2) [4]. Estradiol peaks and remains high for 36 hours, stimulating the hypothalamus to release gonadotrophin-releasing hormone (GnRH), triggering greater FSH production and the luteinising hormone (LH) surge [3]. The end of the follicular stage is marked by ovulation and the release of an oocyte (Figure 2). The second stage is known as the luteal stage,

which approximately begins on the fifteenth day of the cycle and lasts to the twenty-eighth day (Figure 2) [3]. At this point, the follicle develops into the corpus luteum and produces high progesterone levels [3]. This promotes the secretory phase, where the endometrial tissue proliferates and thickens, preparing for the implantation of an embryo. If embryo implantation does not occur, the endometrium will progress to the menstrual phase as the corpus luteum degrades into the corpus albicans [3]. The degradation of the tissue causes decreased production of progesterone and estradiol. The endometrial tissue begins to shed and is excreted from the body (Figure 2) [5].

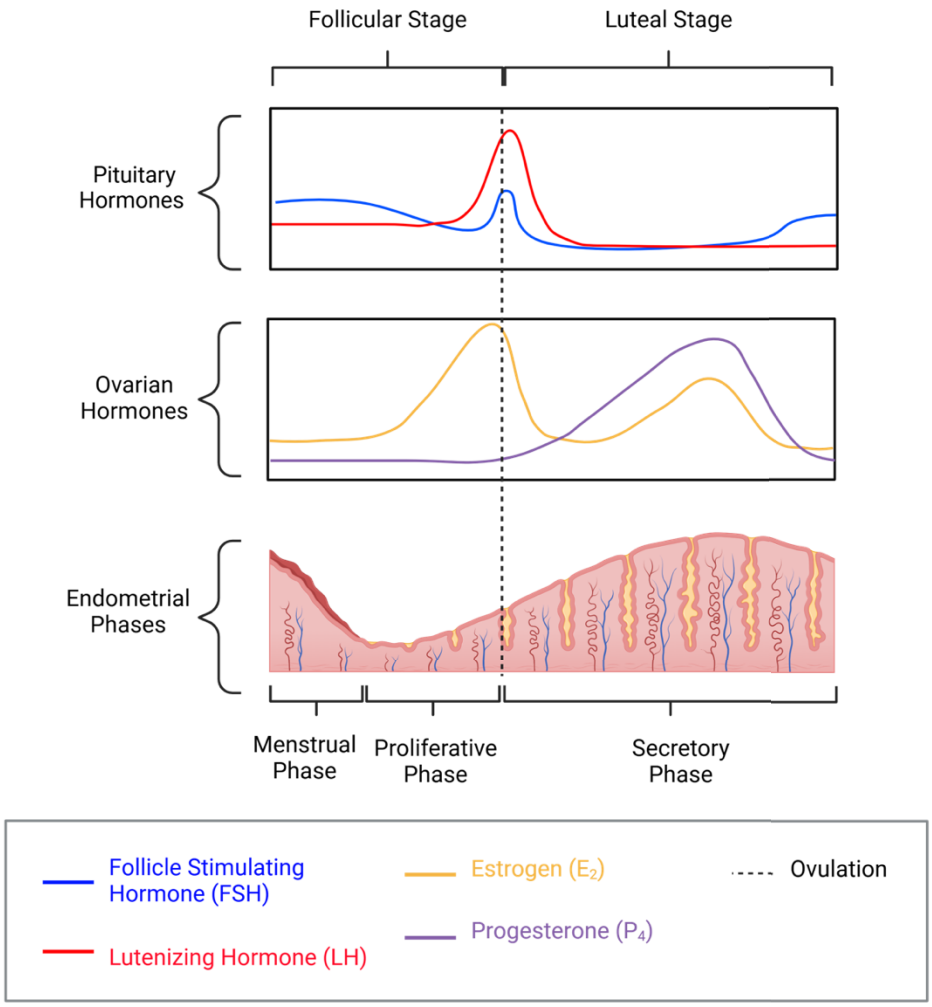


Figure 2. The menstrual cycle. Created in https://BioRender.com.

1.1.2 Endometrial receptivity

Endometrial receptivity is the stage in the menstrual cycle where the endometrium has developed enough to allow the successful attachment and implantation of a blastocyst [6]. The window of implantation (WOI) describes the short period of time when the endometrium is receptive and the blastocyst has also adequately developed to implant. The endometrium is receptive for approximately four to six days in the mid-luteal stage and is regulated by estradiol and progesterone. In the 1930s, the histological characteristics of a receptive endometrium were identified [7]. This was followed by the development of the Noyes criteria, which outlined several histological features that enabled the endometrium to be 'dated', meaning the endometrial phase and receptive status could be identified from a biopsy [8]. These features included gland mitoses, pseudostratification of nuclei, basal vacuolation, glandular secretions, stromal oedema, stromal mitoses and the infiltration of leucocytes. These criteria are still used today to date endometrial tissue. In addition, several markers are associated with receptivity, including the development of pinopodes, the loss of microvilli, and changes in cell polarity and tight junctions [9, 10]. In a clinical setting, morphological markers such as endometrial thickness, volume, pattern, blood flow, and contractions are used to determine receptivity. However, their use is cautioned as they have a limited ability to predict clinical pregnancy [11]. In more recent years, molecular techniques have been used to evaluate receptivity. Extensive analysis of gene expression in endometrial tissue was conducted during the proliferative phase and the window of implantation [12]. Comparison of upregulated and downregulated genes showed several significant changes, particularly in cholesterol transport, lipid signalling, immunomodulation, peptidases, and ion transport during the window of implantation [12].

One of the most significant developments in determining receptivity was the endometrial receptivity array (ERA). The ERA was first proposed in 2011 and was developed as a microarray for endometrial biopsies that could ultimately be used to determine receptivity [13]. In total, 238 genes were analysed, 134 of which were determined to be exclusively expressed during the receptivity stage and defined the transcriptomic signature of receptivity. Several biomarkers were identified, and these were related to immune response, the cytoskeleton, adhesion, signalling, and cellular proliferation [13]. However, the ERA has become somewhat contentious. Some studies showed that it is superior to histological dating conducted by a pathologist and can improve *in vitro* fertilisation (IVF) outcomes, but others showed it does not improve the outcome of IVF and may even hinder treatments [14-16]. More recently, a molecular staging model was developed using RNA-sequencing and identified over 3400 endometrial genes that fluctuate daily [17]. The model successfully dated the endometrium and showed highly dynamic gene expression patterns, especially during the luteal stage. Overall, it is understood that endometrial receptivity is a complex and highly regulated process that involves the endometrial tissue undergoing significant structural and molecular changes.

1.1.3 Early embryo development and implantation

During ovulation, an oocyte is released from the ovary and leaves behind the corpus luteum. It travels down the fallopian tubes and can be fertilised with sperm. After fertilisation, the oocyte becomes a zygote and travels to the uterine cavity as it undergoes cell division. After approximately five to six days, the zygote will have developed into a blastocyst through blastulation [18]. The blastocyst comprises an outer layer of cells

called the trophectoderm and the inner cell mass, which consists of two cell types: the epiblast and the hypoblast [18]. The trophoblastic cells come into contact with the maternal tissue and are involved in complex interactions at the maternal-fetal interface during implantation and placentation [19, 20].

Implantation is a complex process divided into three stages: apposition, adhesion, and invasion (Figure 3). Apposition can be described as the stage where the blastocyst is in close proximity to the endometrial epithelium and forms an initial loose adhesion (Figure 3) [21-23]. Adhesion follows apposition and occurs when a strong bond between the trophectoderm of the blastocyst and the epithelium forms (Figure 3) [22]. This is a strong and stable attachment that is thought to be initiated at the embryonic pole [21, 24, 25]. Adhesion is mediated by cell adhesion molecules expressed by the embryo and maternal tissue and includes cadherins, integrins, mucins and cell membrane glycoproteins. Cadherins are involved in maintaining the epithelial layer and enabling implantation [26, 27]. They respond to hormonal cycling and embryo adhesion, where they reorganise, and epithelial cells undergo an epithelial-to-mesenchymal transition (EMT) [26]. Integrins are thought to act as linkers between the embryo and the epithelium, binding to bridging molecules [24]. Mucins are thought to act as an anti-adhesive layer in the endometrium but may also promote the recognition and initial adhesive events [28]. Cell membrane glycoproteins like intercellular adhesion molecule-1 (ICAM-1) aid in cell-to-cell adhesions during embryo implantation [29].

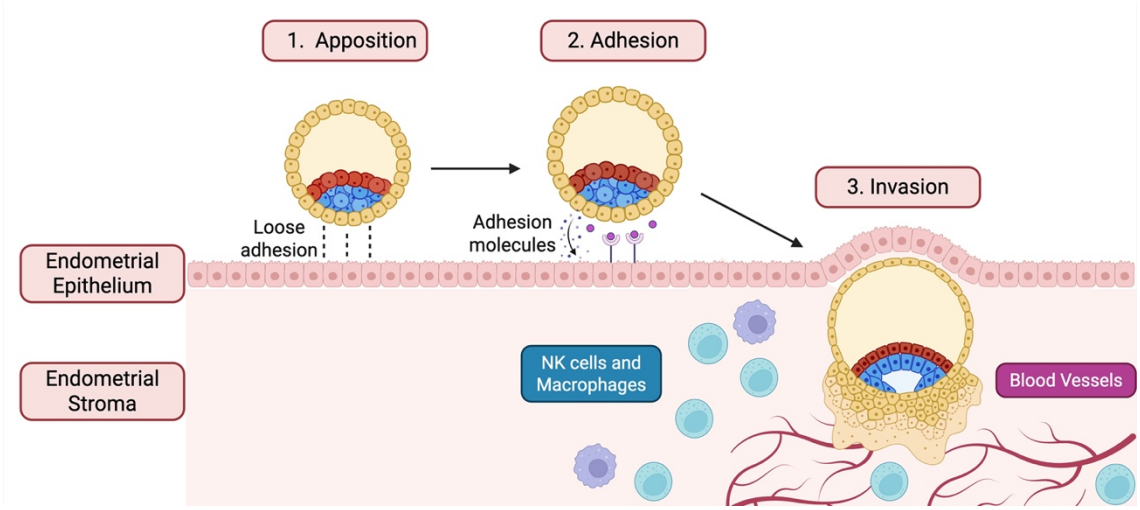


Figure 3. Embryo implantation. Implantation occurs in three stages; apposition, adhesion, and invasion into the endometrium. Adapted from Delrose, N. Human embryo implantation. 2025; Available from: https://app.biorender.com/biorender-templates/figures/all/t-6632e1957932da70946caa5e-human-embryo-implantation.

Invasion occurs once there is stable adhesion between the embryo and epithelium (Figure 3) [30]. Our current understanding of this process is based mainly on non-human primate models, few human histological specimens and *in vitro* culture-based models; thus is limited and somewhat speculative. Bentin-Ley et al. (2000) used primary endometrial cells and human embryos to model the early stages of embryo implantation [31]. They observed that the embryo undergoes intrusive penetration by separating the epithelial cells at the plasma membrane, rather than fusion penetration or displacement penetration. This model also demonstrated that the trophoblast likely induces lysis of interepithelial apical junctional complexes and desmosomes, then subsequently regenerates the junctions with the trophoblast cells [31]. It is thought that this occurs simultaneously as the trophoblastic cells proliferate and differentiate. The layers of daughter cells form a primitive cytotrophoblast and undergo cell fusion promoted by contact with endometrial epithelium, generating the syncytiotrophoblast, which becomes

invasive [32, 33]. This layer becomes the only layer in contact with maternal tissue, fully surrounding the embryo but in close contact with blood vessels and glands, ensuring access to nutrients [32]. The syncytiotrophoblastic cells also produce human chorionic gonadotropin (hCG), which promotes this production of progesterone by the corpus luteum, aiding in maintaining the pregnancy [34]. Both the trophoblast cells, and the maternal epithelium and stromal cells undergo an epithelial-to-mesenchymal-like transition, enabling migration and invasion [27, 35]. At this point, the embryo is entirely embedded within the stroma. During the secretory phase, spiral arteries develop from straight arteries present in the proliferative phase [36]. The spiral arteries form a vascular network that supplies the functionalis layer of the endometrium, and consist of disorganised smooth muscle layers and dilated vessels, creating low resistance in the blood flow [36-38]. This is essential as it allows the embedded embryo to access nutrients (Figure 3).

Embryo implantation and invasion is an inflammatory process. During the development of receptivity and early implantation, approximately 75% of innate immune cells within the endometrium are decidual natural killer (dNK) cells (Figure 3) [39]. dNK cells are a specific phenotype of NK cells in the endometrium, showing a distinct cytokine and gene expression profile with lower cytotoxicity than peripheral NK cells [40-42]. There is also an abundance of macrophages, which comprise approximately 20% of innate immune cells (Figure 3) [43]. These macrophages do not align with M1/M2 categories as they produce cytokines and chemokines that are both pro- and anti-inflammatory [44]. There are also abundant dendritic cells and T cells present. During implantation, various pro-inflammatory cytokines are secreted by innate immune cells, epithelium and stromal tissue. Epithelial cells produce cytokines and chemokines,

including interleukin (IL)-8, IL-6, regulated on activation, normal T cell expressed and secreted (RANTES), and tumour necrosis factor (TNF) [45-48]. These are thought to be involved in the recruitment of immune cells to the endometrium, angiogenesis, and cross-talk between the maternal tissue and the embryo. dNK cells produce a similar range of cytokines and chemokines, which are involved in the modulation of embryo invasion and remodelling of spiral arteries [49-53]. Similarly, macrophages also produce cytokines and chemokines, which play a role in controlling embryo invasion and angiogenesis [54-56]. However, dNK cells and macrophages also produce anti-inflammatory cytokines like IL-10 and IL-4 during embryo invasion. This is essential to promoting maternal tolerance to the semi-allogeneic embryo and preventing an inflammatory reaction that is detrimental to the maintenance of pregnancy [57-60]. The overarching inflammatory response becomes anti-inflammatory as pregnancy progresses into the second trimester. This is promoted by T regulatory cells (Tregs), which have an immunosuppressive profile that aids in maintaining tolerance to the embryo [61]. Cell-to-cell contact or the secretion of cytokines by Tregs suppresses the expansion and activation of effector T cells, subsequently protecting the foetus and creating an anti-inflammatory environment [62]. Reduced numbers of Treg cells is thought to result in poor outcomes such as spontaneous abortion [63, 64]. In the final trimester and during parturition, there is a switch back to a pro-inflammatory response, with the activation of the nuclear factor-kappa B (NF-κB) pathway and an influx of immune cells [65].

1.2 *In Vitro* fertilisation (IVF)

1.2.1 What is infertility?

Infertility is defined as the inability to attain a clinical pregnancy after a minimum of 12 months of regular unprotected intercourse [66]. The World Health Organisation (WHO) estimates globally that one in six people will experience infertility [67]. In the western pacific ocean region, which includes Australia, 23.2% of all people will experience infertility in their lifetime [67]. Numerous causes of infertility affect both women and men. The most common reasons include ovulatory disorders, physical disorders or abnormalities of the female reproductive tract, abnormalities in embryo development and implantation, male factor infertility (sperm production and quality), and other conditions that affect multiple aspects of the body, such as immunological disorders [68]. A diagnosis of infertility is made by clinicians after the investigation of the patient's medical history, clinical examination, semen analysis, ultrasound, and endocrine assessment [69]. However, after clinical investigation, patients may receive a diagnosis of unexplained or idiopathic infertility. Within Australia and New Zealand, 27.3% of patients presenting for IVF treatment in 2022 were diagnosed with unexplained infertility [70].

1.2.2 What is IVF?

In vitro fertilisation, or IVF, is a form of artificial reproductive technology involving external oocyte fertilisation [66]. IVF was introduced in the late 1970s to early

1980s and has since become a readily used treatment for infertility. Patients undergoing IVF can either undergo a natural cycle IVF protocol or begin with an ovarian stimulation protocol (Figure 4). There are two types of IVF ovarian stimulation protocols; the GnRH agonist protocol and the GnRH antagonist protocol (Figure 4). Overall, stimulation protocols aim to promote the development of multiple follicles, prevent premature luteinisation, and control oocyte maturation so oocytes can be collected [71]. The chosen protocol depends on the patient's response, risk factors, and the goal of the stimulation protocol [72].

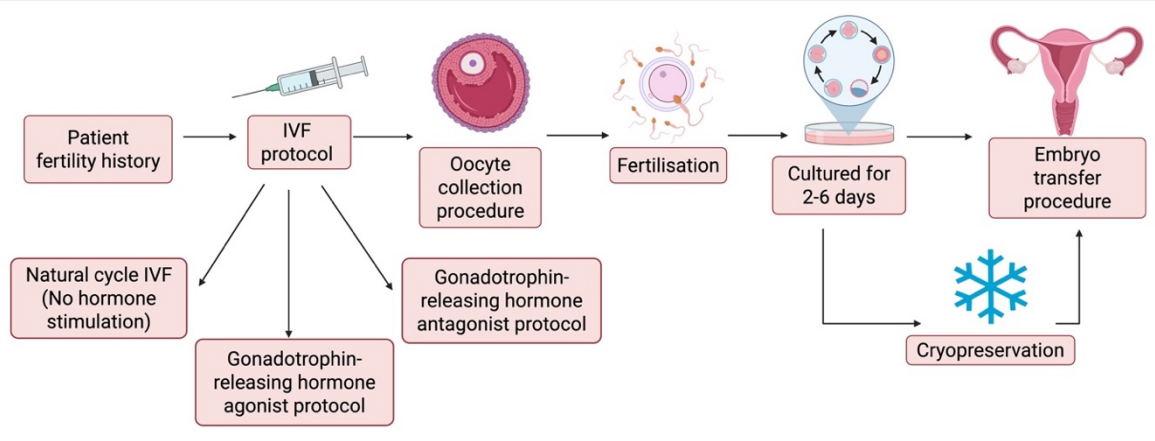


Figure 4. Standard IVF treatment cycle. Created in https://BioRender.com.

Natural cycle IVF was the first IVF protocol to achieve a live birth [73]. A natural cycle indicates that the individual's standard menstrual cycle is followed. The procedure is conducted without ovarian stimulation, and the developing follicles are monitored using transvaginal ultrasound (Figure 4) [74]. Once the follicles reach maturity, the oocytes can be retrieved. Patients may also undergo a modified natural cycle, where hCG is administered when follicles reach maturity to trigger ovulation, and drugs can be given to prevent premature luteinisation [66]. Natural cycle IVF has several advantages, including

its low cost, it does not require a resting cycle between IVF cycles, and is less physically and mentally stressful [74]. The rate of successful embryo implantation may also be higher in advanced-age patients undergoing a natural cycle [75]. However, it does not significantly reduce the risk of complications like ovarian hyperstimulation syndrome (OHSS) compared to other forms of IVF [74]. OHSS is an iatrogenic complication which is thought to be triggered by the administration of hCG [76]. It results in the cystic enlargement of the ovaries and fluid build-up in the abdomen. It is a serious and potentially life-threating complication [76, 77].There is a higher risk of cancellation due to a premature LH surge, and this protocol is not clinically recommended for high responders, who are patients that may produce more than 5-10 oocytes [72].

The GnRH agonist protocol can be performed in two ways: the short or long protocols. During the short protocol, a GnRH agonist is given from the first or second day of menses and ovarian stimulation is initiated with FSH two to three days after [71]. Both are administered until the follicles are an appropriate size, then hCG is given, and oocytes can be collected. This method initially promotes follicular development and then prevents luteinisation by downregulating the pituitary gonadotropin production [71]. Alternatively, the long protocol involves initially downregulating the pituitary gonadotropin production by administering a GnRH agonist for a minimum of two weeks [71]. When downregulation of gonadotropin production is confirmed, FSH is given concurrently until hCG can be administered and oocytes can be collected. This protocol can be used for poor responders to ovarian stimulation but is also considered equally as effective as the antagonist protocol [72].

The GnRH antagonist protocol alternatively begins by initiating ovarian stimulation with FSH and then administering an antagonist [71]. The antagonist competitively binds with GnRH receptors, preventing gonadotropin release, luteinisation, and ovulation. The GnRH antagonist can be given either in multiple doses from the sixth day of ovarian stimulation or in a single dose from day seven [71]. When the follicles have reached an appropriate size, hCG is given, and oocytes can be collected. This is the safer protocol for women who respond normally to ovarian stimulation or have a high response, producing a large number of follicles and are at risk of ovarian hyperstimulation syndrome [72].

Across all IVF protocols, after the oocytes have been collected, they are fertilised by either culture with sperm or intracytoplasmic sperm injection (ICSI) and incubated for 2-6 days to develop (Figure 4). Once the embryo has reached either the cleavage stage or the blastocyst stage, it is transferred to the uterine cavity via a catheter (Figure 4). Single or multiple embryos can be transferred. However, according to guidelines, multiple-embryo transfer is discouraged due to the risks and the better outcomes seen in single-embryo transfer [78, 79]. Additionally, embryos can be cryopreserved and transferred later (Figure 4). Cycles involving cryopreservation and delayed transfer are called freeze/thaw cycles. Freeze/thaw cycles are increasingly used in Australian and New Zealand clinics [80]. However, there is mixed evidence for whether this improves embryo transfer outcomes [81, 82].

1.2.3 How IVF success and failure are defined

Several outcomes can define either the success or failure of IVF treatment. The earliest measure is the diagnosis of a biochemical pregnancy, which is confirmed by the detection of hCG 10-14 days after embryo transfer [66]. However, a biochemical pregnancy may not develop any further. Thus, the pregnancy is officially confirmed by an ultrasound of the gestational sac and heartbeat six to eight weeks after transferring the embryo [66]. This is defined as a clinical pregnancy. However, if the gestational sac or heartbeat is not observed, this is considered implantation failure or embryo transfer failure [83]. If this occurs repeatedly, without other contributing factors, after transferring at least three high-quality euploid blastocysts, it is considered repeated or recurrent implantation failure (RIF) [84]. RIF was previously considered to occur somewhat frequently in IVF patients. However, more recent analysis has determined that true RIF occurs in less than 5% of patients with infertility [84]. After the initial scan at 6-8 weeks, a second-trimester scan is performed at 19-20 weeks to confirm an ongoing pregnancy and observe any structural anomalies. If there is a loss of the clinical pregnancy at this point, it is considered a miscarriage [66]. During the third trimester, other adverse outcomes can occur, including preterm birth, where the baby is born before 37 weeks of gestation; preterm rupture of membranes (PROM), where the foetal membranes rupture before term; and stillbirth. At the end of the third trimester, if the baby is born able to breathe, has a heartbeat, and is capable of movement, it is considered a successful live birth [66]. Live birth is the most important outcome of IVF for patients undergoing treatment. However, many studies generally use clinical pregnancy as a measure of success [85-87]. These studies tend to be focused on the factors involved with IVF embryo transfer success, with

later measures irrelevant to the aim of the study. However, it is important to recognise that later outcomes, like ongoing pregnancy and live births, are the most relevant outcomes for patients undergoing IVF treatment.

1.2.4 IVF in Australia and the current challenges

IVF use within Australia has steadily increased since its introduction. Initially, in the 1980s, there were mixed success rates of IVF embryo transfers. Several studies reported rates of pregnancy between 12% to 26% [88-92]. Currently, the rate of clinical pregnancy per embryo transferred in Australian and New Zealand clinics is 33.1%, and the rate of live births per embryo transfer is 25.9% [70]. The rate of live births per initiated cycle is currently 9.2% [70]. While these rates have improved compared to the initial success rates, this has only marginally increased over the last ten years, with a 2.4% increase in clinical pregnancies per embryo transferred and a 1.6% increase in live births per embryo transferred since 2015 [93]. Globally, IVF outcomes are measured by the pregnancy and delivery rates per aspiration, which are currently reported as 26.5% and 19.9%, respectively [94]. However, these rates differ greatly between regions, likely due to the number of embryos transferred and the accuracy of the data reported. Additionally, it is important to consider that this analysis does not include data from China and several Middle Eastern countries [94]. The reported delivery rate per oocyte aspiration was 23.9% in 2005, but since then, it has only marginally improved [95].

While it is positive that IVF success rates have improved since its introduction, it is of concern that the success rate has remained low with minimal increase over the last 10 years. Several factors contribute to this concern, including the high cost of treatment.

In Australia, it was calculated that one cycle, beginning with a fertility assessment to having a live birth with one embryo transfer, costs €4108.00 or approximately $8400.00 AUD [96]. This cost alone is expensive, and it is important to consider that, on average, Australian patients undergo approximately two cycles a year (with multiple embryo transfers), and only 38.9% of patients have a live birth within their first cycle [70]. Thus, this value may underestimate the true cost for patients who do not achieve a live birth after their first embryo transfer. Additionally, it was determined that clinics offer, on average, 3.1 add-ons to an IVF cycle [97]. Add-ons are extra procedures offered to patients to improve their chances of success, including preimplantation genetic testing (PGT), enriched culture media, and endometrial receptivity testing. However, add-ons can greatly increase the cost of treatment, ranging from $0 to $3700 per add-on, and often are not supported by strong evidence for their use in the literature [97]. Overall, as success rates continue to improve minimally, the cost of IVF treatment can quickly add up for patients, as most undergo multiple cycles with add-ons.

Furthermore, another concern around the lack of improvement in IVF success rates is the mental and physical burden of the treatment. IVF cycles and ovarian stimulation protocols are time-consuming and physically challenging for the patients, with many experiencing physical discomfort during treatment [98]. It has also been demonstrated that women's fertility-related quality of life significantly decreases as patients experience failed embryo transfers and undergo further attempts at IVF [99]. Many patients have limited knowledge of IVF, overestimating their chances of success and leading to negative psychological impacts [100]. Additionally, many experience a sense of loss and grief after failed cycles or if they remain childless after ending treatment

[98, 101]. Thus, as the success rate remains low, patients are more likely to experience a greater mental and physical burden when undergoing IVF.

1.3 The reproductive bacterial microbiome

1.3.1 Studying the reproductive microbiome

The human microbiome is the ecological community of commensal microorganisms colonising the body or a particular organ [102]. These microorganisms include bacteria, fungi, viruses, and archaea, and all have a role in maintaining homeostasis. This project focuses on the bacterial microbiome. However, it is important to acknowledge that the vagina and endometrium have commensal viruses, fungi, and archaea [103]. Like the bacterial microbiome, these organisms also play a role in the health of the reproductive tract. For example, decreased diversity of the viral microbiome in the cervicovaginal environment is associated with genital inflammation [104]. Additionally, in the endometrium, a shift in the fungal community structure to a dominance of *Penicillium* species is associated with the development of endometrial cancer [105]. While these interactions are also highly interesting, the scope of this study only extends to the bacterial microbiome, which will be explored in the following sections.

The vaginal and endometrial bacterial microbiome have been investigated using various next-generation sequencing techniques, but primarily 16s ribosomal RNA (rRNA) gene amplicon sequencing is used. 16s rRNA gene amplicon sequencing utilises the 16s rRNA gene, which is highly conserved in all bacterial genomes, to identify bacteria [106]. Nine hypervariable regions (V1-V9) in the 16s rRNA gene are commonly

targeted, with specific regions used dependent on the study's goal. The data generated can be analysed using various bioinformatics platforms, such as the commonly used QIIME platform. These bioinformatics platforms assign operation taxonomic units (OTUs) to identify bacteria by comparing them with a reference database [107, 108]. OUT can be used to calculate alpha (species richness and diversity) and beta (similarly of two or more communities) diversity and construct phylogenetic trees [107-109].

While 16s rRNA gene amplicon sequencing has been used for both vaginal and endometrial studies, it has limitations. Often, studies use the V4 region to avoid amplification of the host genome and thus enable the identification of more bacteria in vaginal samples, however it results in lower resolution [110, 111]. Furthermore, some studies do not classify bacteria beyond the genus level as there is insufficient resolution in the variable region, which can result in misleading conclusions on different species' role in disease or infertility and may not adequately profile high diversity, low biomass environments like the endometrium [110]. Metagenomic sequencing can also be used to profile the reproductive microbiome. Rather than targeting specific regions of the 16s gene, metagenomic sequencing sequences all DNA in a sample [112]. This enables higher resolution for species identification and functional analysis to determine the role of each bacteria present [113]. However, metagenomic sequencing is expensive as it requires deeper sequencing to overcome high amounts of host DNA that is present in samples [112, 114]. Furthermore, metatranscriptomics can be used to classify the microbiome. This sequences all the RNA in a sample, meaning the sequencing reads reflect active transcription [114]. While this provides valuable data on what genes are expressed and the active pathways, it does not account for bacteria that may not be active when samples are collected [114]. While techniques like 16s rRNA gene amplicon sequencing,

metagenomics, and metatranscriptomics are culture-independent techniques, culturomics is an upcoming approach to profiling the microbiome using high-throughput culture-based techniques. Culturomics uses a range of culture conditions and media to isolate a range of microbiota present in a sample, which are identified using matrix-assisted laser desorption ionisation time-of-flight (MALDI-TOF) mass spectrometry [115]. However, this technique relies on fresh samples and requires a higher workload to culture bacteria using multiple conditions [115]. Therefore, culture-independent methods are still primarily used for vaginal and endometrial samples [116].

1.3.2 The eubiotic vaginal microbiome

The reproductive tract harbours a particularly unique microbiome, dominated by a unique community of bacteria largely consisting of *Lactobacillus* and other lactic acid-producing bacteria. In 1892, *Lactobacillus* was first isolated and identified as the dominant genus of bacteria present in the vagina and was later theorised to have a protective function [117, 118]. The dominance of *Lactobacillus* is thought to be related to glycogen present in the vaginal epithelium and fluid, as well as the low pH created by lactic acid production [119, 120]. A higher concentration of glycogen in the human vagina has been proposed as a result of human dietary habits, which are distinct from those of other mammals and many higher-order primates [121]. Glycogen is also related to the production of estrogen, as it has been shown that increasing estrogen and a subsequent increase in glycogen during puberty drives a shift towards *Lactobacillus* dominance [122]. A similar result is seen in post-menopausal women who undergo estrogen therapy [123]. Further analysis of the microbiome showed that there are several species of *Lactobacillus* present in the human vagina, with the dominant species differing between

individuals [124]. However, these studies used culture-based methods such as agar plates and analytical profile index (API) strips to identify the bacteria present, thus limiting what genera and species could be isolated and identified.

With the development of advanced molecular-based techniques like next-generation sequencing, more recent studies have revealed the composition of a healthy vaginal microbiome. These studies reaffirmed that *Lactobacillus* commonly is the dominant bacteria present in the vagina, but also revealed that other bacteria, such as *Fannyhessea*, *Gardnerella*, *Prevotella*, and *Streptococcus,* can be present in healthy asymptomatic individuals [125]. In 2011, 16S rRNA gene amplicon sequencing of the vaginal microbiome revealed five distinct microbial communities in a cohort of 396 asymptomatic participants, termed the community state types (CST) [126]. This analysis revealed different species of *Lactobacillus* dominate four of the CSTs, which can be seen in Table 1 [126]. *Lactobacillus* does not dominate CST IV; rather, it is a more diverse community of lactic acid-producing strict and facultative anaerobes [126]. It was shown that the CSTs fluctuated and had varying stability throughout the menstrual cycle, with the most instability occurring during menses [127].

Table 1. Dominant bacteria in the vaginal CSTs [126].

CST	Dominant bacteria
I	*Lactobacillus crispatus*
II	*Lactobacillus gasseri*
III	*Lactobacillus iners*
IV	Diverse bacteria
V	*Lactobacillus jensenii*

One challenge of using the CST classification system is that it does not capture the diversity of the entire vaginal microbial community present in women. The VALENCIA study redefined the CST classifications using vaginal samples from 1975 women and 16s rRNA sequencing [128]. They defined 13 CSTs that more accurately classified profiles and more specifically defined CSTs that lack *Lactobacillus* and are dominated by other lactic acid-producing bacteria like *Bifidobacterium*. Similarly, a more recent investigation of the vaginal microbiome in 3323 participants, again reaffirmed that the CSTs do not capture the reality of the microbiome. They found many participants had co-occurring *Lactobacillus* species and did not clearly fall into a specific CST [129]. Furthermore, Vagitypes have also been proposed as a method of classification of the vaginal microbiome [130]. This study used samples from 6755 participants to create 13 Vagitypes using non-negative matrix factorisation. The Vagitypes more specifically defined diverse microbiomes and were successfully used to demonstrate the association between variables like lifestyle, social and environmental factors and composition [130]. Similarly, metagenomics has also been used to redefine the CSTs by metagenomic subspecies, which were associated with demographic factors, stability, ability to produce D-lactic acid and bacterial vaginosis [131]. While there are varying methods to classify the microbiome, they all highlight the importance of *Lactobacillus* and other lactic acid-producing bacteria in the maintenance of vaginal health.

1.3.3 The dysbiotic vaginal microbiome

An unhealthy microbiome or ‘dysbiotic’ microbiome occurs when the microbiota profile shifts from what is considered normal flora [132]. An important characteristic of

the eubiotic vaginal microbiome is the low diversity of bacteria. Dysbiosis occurs when there is an increase in diverse genera with a subsequent decrease in lactic acid-producing genera [133]. There are several forms of dysbiosis in the vaginal environment, but the most common is bacterial vaginosis (BV). BV is diagnosed using the Nugent score to grade the presence of diverse bacteria using a Gram stain and is considered the gold standard in diagnosing BV [134]. The Amsel criteria are most commonly used and bases diagnosis on the presence of abnormal vaginal discharge with clue cells, pH greater than 4.5, and a fishy odour when 10% potassium hydroxide is added [135]. In terms of the composition of the microbiome, BV is associated with the presence of diverse bacteria, shown in Table 2 [136-139]. BV is associated with several adverse health outcomes, including increased risk of acquiring sexually transmitted infections (STIs) like human immunodeficiency virus (HIV), and pelvic inflammatory disease [140-142]. Additionally, the presence of diverse bacteria in the vaginal environment is associated with embryo implantation failure [143, 144].

Aerobic vaginitis is another dysbiotic condition in the vagina. While a component of aerobic vaginitis is a decreased abundance of *Lactobacillus*, it differs from BV as there is also severe inflammation and the presence of bacteria shown in Table 2 [145-147]. Similarly to BV, there is an association between aerobic vaginitis and IVF outcomes, typically those that occur in the final trimester. There are many studies demonstrating an increased risk of preterm birth and other poor outcomes in women with aerobic vaginitis in late pregnancy [148-151].

Table 2. Bacteria present in the vagina in dysbiotic conditions

Type of vaginal dysbiosis	Bacteria present
Bacterial vaginosis	*Gardnerella vaginalis* *Fannyhessea vaginea* *Megashaera curtisii* *Prevotella bivia*
Aerobic vaginitis	*Streptococcus agalactiae* *Escherichia coli* *Staphylococcus aureus* *Enterococcus faecalis*

1.3.4 The importance of microbiota-associated metabolites in the vagina

An important function of the vaginal microbiome is the production of metabolites with the most important of these being lactic acid. There are two isoforms of lactic acid: L-lactic acid and D-lactic acid. L-lactic acid can be produced by host tissue and bacteria, but only D-lactic acid is produced by bacteria. Thus, the ratio of D/L-lactic acid was used to determine that lactic acid in the vagina is primarily produced by bacteria [152]. Different species of *Lactobacillus* produce different ratios of D/L-lactic acid, except for *Lactobacillus iners*, which produces only L-lactic acid (Table 3) [153]. D-lactic acid is considered the more protective isomer, protecting against infection, squamous intraepithelial lesions, and cervical cancer [153-155]. In the vaginal environment, the concentration of lactic acid creates a low pH of 3.5-3.8 on average [156, 157]. The acidic conditions and high concentration of lactic acid are thought to prevent pathogenic

colonisation and infection with STIs [153, 155, 158, 159]. Lactic acid is also known to modulate the vaginal inflammatory response via interleukin-1 receptor antagonist (IL-1RA) promoting an anti-inflammatory response with decreased expression of cytokines and chemokines like IL-8, IL-6, TNF, RANTES, and macrophage inflammatory protein-3 (MIP3α) when vaginal cells were stimulated with lipopolysaccharide (LPS), Pam3CSK4, or polyinosinic–polycytidylic acid (PIC) in conjunction with L- and D-lactic acids [160]. Furthermore, lactic acid promotes the expression of tight junction proteins like claudin-1 and claudin-4, and increases transepithelial resistance in vaginal and cervical cell models, demonstrating the role of lactic acids in maintaining the integrity of the epithelial barrier [161]. *Lactobacillus* in the vaginal environment also produces a range of other metabolites, as shown in Table 3, including amino acids, acetic and succinic acids [162]. However, these are produced in much lower concentrations compared to lactic acids [162]. The concentration of these metabolites has been shown to negatively correlate with *Lactobacillus* abundance [163].

Table 3. Metabolites produced by vaginal bacteria in eubiosis and dysbiosis.

	Bacteria	**Metabolites produced**	**Reference**
Eubiosis	*Lactobacillus crispatus* *Lactobacillus gasseri* *Lactobacillus jensenii* *Lactobacillus iners*	L-lactic acid D-lactic acid (except *Lactobacillus iners*) Amino acids Succinic acid Acetic acid	[153, 162-164]
Dysbiosis	*Gardnerella vaginalis* *Fannyhessea vaginae* *Prevotella bivia* *Megasphaera curtisii* *Sneathia*	Acetic acid Succinic acid Propionic acid Lactic acids Butyric acid Amines Formic acid Isopropanol Ethanol Amino acid catabolites	[162-164]

In a dysbiotic state, when the composition of the microbiome shifts, there is a change in the metabolites produced in the vaginal environment. It has been demonstrated that in dysbiotic conditions like BV, when there is a decrease in *Lactobacillus* abundance, there is a subsequent decrease in lactic acid in vaginal fluid [163-165]. Metabolomic analysis of vaginal fluid using chromatographic separation and mass spectroscopy

determined a correlation between metabolites and bacteria. This study found that 62% of the 279 metabolites detected in vaginal fluid significantly differed between healthy controls and women with BV [164]. The authors linked diverse bacteria with succinic acid, cadaverine, putrescine, tryramine, and deoxycarnitine [164]. It was proposed that these metabolites have a role in the increased pH of vaginal fluid and the presence of clue cells [164]. Additionally, BV status showed a negative correlation with phenylalanine, and a positive association with N-acetylputrescine, pipecolate, cadaverine, and deoxycarnitine [164]. Interestingly, many BV-associated bacteria can produce biogenic amines which create a fishy odour in vaginal discharge [165]. It has also been shown that increased acetic acid is an important marker of BV, alongside an increase in short-chain fatty acids, including propanoic and butyric acid, in vaginal discharge [166].

More recently, one study cultured bacteria associated with BV, including *Gardneralla, Fannyhessea,* and *Prevotella* in brain heart infusion media and showed that all produce high concentrations of acetic acid (Table 3) [162]. *Prevotella* produces high concentrations of succinic acid, and *Fannyhessea* produces high concentrations of ethanol and formic acid (Table 3) [162]. Interestingly, these bacteria can also produce lactic acid but in much lower concentrations compare to *Lactobacillus* (Table 3) [162]. The production of these metabolites in the vaginal environment has a significant impact on the epithelium. It has been shown that vaginal cell lines exposed to short-chain fatty acids like acetic acid and butyric acid, increased secretion of inflammatory cytokines and chemokines like IL-8, IL-6, and IL-1β [167]. Similar results and increased TNF secretion were seen when the cells were stimulated with LPS, Pam3CSK4, and imiquimod in conjunction with acetic acid and butyric acid [167]. Furthermore, one study used a dysbiotic solution containing lactic, acetic, succinic, propionic, and butyric acids in

culture to mimic the microbial composition of BV [168]. When stimulated cervical cells were exposed to this solution for 24 hours, a significant increase in IL-8 and TNF was observed, with a significant decrease in secreted RANTES and IP-10, demonstrating how metabolites derived from diverse bacteria can promote a pro-inflammatory response [168]. A more recent study cultured vaginal cells with a solution that consisted of lactic, acetic, succinic, and butyric acids, to represent dysbiosis [169]. This solution significantly decreased transepithelial resistance and increased dextran leakage, demonstrating its detrimental impact on epithelial barrier integrity. The same study also reaffirmed that a dysbiotic solution increased the mRNA expression of pro-inflammatory cytokines and chemokines, including IL-6, IL-8, TNF, and RANTES, after 24 hours [169]. Thus, it is clear microbiota-associated metabolites derived from diverse bacteria can have a detrimental impact on the vaginal immune response and epithelial barrier integrity.

1.3.5 The endometrial microbiome

The endometrium was previously thought to be sterile, as the cervix was considered to be a barrier between the vaginal environment and the upper reproductive tract [170, 171]. Early studies attempted to culture bacteria from endometrial samples with varied results. Some studies demonstrated a total lack of growth from samples, and others showed that bacteria could be cultured, yet it remained widely accepted that the uterine cavity was sterile [170, 172, 173]. With the introduction of 16S rRNA gene amplicon sequencing, researchers challenged this theory, demonstrating that bacteria associated with the vagina can be found in the endometrium and may have ascended from the lower reproductive tract into the uterine cavity [174, 175]. One study used species-specific qPCR on endometrial swabs collected during hysterectomies [174]. The most

common species found in the upper reproductive tract were *Lactobacillus iners, Prevotella, Lactobacillus crispatus, Gardnerella vaginalis, Fannyhessea vaginea,* and *Lactobacillus jensenii* [174]. Alternatively, another study of 19 participants identified that 90% of the women had an endometrial microbiome with approximately 30% of bacteria from the genus Bacteroides [175]. One of the most in-depth analysis of the reproductive microbiome conducted showed bacteria was present in the vagina, cervix, endometrium, fallopian tubes, and peritoneal fluid using 16s rRNA gene amplicon sequencing [176]. The researchers determined that each site had a unique microbial profile and bacteria are continuous throughout the reproductive tract, but there is a lower biomass in the upper reproductive tract [176]. Interestingly, this study showed that *Lactobacillus* was not the dominant bacteria in the upper reproductive tract, and that the microbiome was diverse [176]. The authors outlined that diverse bacteria identified in endometrial samples included *Pseudomonas*, *Acinetobacter*, *Vagococcus* and *Sphingobium* [176]. This was also observed in recent studies that found that *Lactobacillus* does not dominate the endometrial microbiome and that high diversity may be beneficial to reproductive outcomes [103, 177]. Sola-Levy et al. (2021) found that the most abundant bacteria across 14 endometrial samples included *Klebsiella pneumoniae, Clostridium botulinum, Pasteurella multocida*, and *Hydrogenophaga* species. Reschini et al. (2022) identified that *Lactobacillus* only contributes up to 30% of the endometrial microbiome, with diverse bacteria such as *Propionibacterium*, *Pelomonas, Pseudomonas, Streptococcus* and *Escherichia* comprising the rest of the microbiome. However, these findings were controversial, with several studies contradicting them, identifying *Lactobacillus* as the dominant bacteria in an eubiotic profile and often in association with successful reproductive outcomes [177-183].

It is important to consider that these studies often have several limitations which hinder the current understanding of the endometrial microbiome. Many studies have low sample sizes, limiting the interpretations that can be made. This is likely due to the invasive nature of the samples [184]. Similarly, the analysis of endometrial samples is limited due to the low biomass of the microbiome. It has been shown that the vaginal microbiome may have up to four orders of magnitude more bacteria than the endometrium [176]. Low biomass, coupled with potential contamination of samples with vaginal bacteria during intravaginal collection and a lack of adequate controls, may greatly limit how much the data from sequencing studies can be interpreted [184]. Likewise, it is also important to consider biofilms in the endometrial environment. It has been shown that biofilms of *Gardnerella* are able to form in the endometrium of women with BV [185]. However, little is known about the importance of biofilm formation in the endometrium and the interplay between biofilms and the endometrial microbiome. Additionally, the methodology used to profile the microbiome in these studies varies. While most use 16s rRNA gene amplicon sequencing, they use different variable regions, which can impact the diversity detected and the ability to determine both genus and species [186]. Furthermore, the composition of the endometrial microbiome is known to fluctuate through the menstrual cycle. A higher abundance of *Lactobacillus* is present in the luteal phase in endometrial fluid [187]. Then, *Lactobacillus* decreases in abundance after menstruation and begins increasing in abundance during the proliferative stage of the menstrual cycle [187]. Another study found that the follicular phase is dominated by Firmicutes, which increased throughout the menstrual cycle [188]. Proteobacteria were also identified, but their relative abundance decreased in the luteal stage and during ovulation [188]. Thus, there is no defined composition of the endometrial microbiome to date, but the presence of *Lactobacillus* is generally considered beneficial.

1.3.6 The microbiome throughout pregnancy

Hormonal changes during pregnancy drive unique changes in the body and in the microbiome. In the vaginal environment, it has been shown that women with *Lactobacillus*-dominated profiles have a stable composition throughout gestation with a low abundance of diverse bacteria [189-194]. Women with a profile initially dominated by diverse bacteria, such as *Gardnerella,* frequently shifted towards a *Lactobacillus*-dominated profile throughout gestation [189, 193]. Interestingly, in the post-partum period, the microbiome showed a significant decrease in *Lactobacillus* abundance and became more diverse with a CST IV-like profile [189, 190, 192, 193]. It is thought that estrogen drives these changes, as it is known that estrogen promotes the production of glycogen by vaginal tissue, providing an essential source of carbohydrates for *Lactobacillus* [119, 120]. Estrogen is produced by the placenta throughout pregnancy and may foster the dominance of *Lactobacillus* by promoting glycogen production during gestation [195, 196]. Therefore, when the placenta is removed after birth, estrogen significantly drops, leading to a decrease in *Lactobacillus* [197].

Much less is known about the endometrial microbiome during pregnancy. Most studies observe the microbiome before or during an embryo transfer, or after birth. There is currently one case report that observed the endometrial microbiome at 4 weeks of gestation. This study found that 91% of bacteria in the endometrial fluid were *Lactobacillus*, with 9% falling under Proteobacteria [182]. However, this study should be considered cautiously as this was only investigated using a single sample, which was collected intravaginally, meaning that there is the potential for contamination from the

vaginal microbiome. One study investigated the microbiome immediately after birth by taking an endometrial biopsy after removing the placenta and fetal membranes [198]. It was found that *Lactobacillus* was not present in all the patients, and its abundance, when detected, was highly variable. The patients had a greater abundance of diverse bacteria [198]. However, these results should be interpreted cautiously as this study consisted of 19 participants, and the authors reported contamination from environmental bacteria despite efforts to ensure sterile protocols [198]. Overall, little is known about the endometrial microbiome during pregnancy and it is unclear if the composition undergoes similar changes to that seen in the vaginal environment throughout gestation.

1.4 The factors involved in the outcome of IVF

1.4.1 The endometrial microbiome and IVF failure

It is well established that a dysbiotic vaginal microbiome is associated with poor outcomes of embryo transfer, including implantation failure and pre-term birth [144, 199-201]. Thus, in recent years, there has been great interest in the role of the endometrial microbiome in IVF failure. One of the first studies to investigate this association used endometrial fluid collected on the embryo transfer catheter tip during an embryo transfer procedure [179]. Using 16s rRNA gene amplicon sequencing, this study showed that several species of bacteria dominated the microbiome, yet differences between the cohort of women who achieved a pregnancy and those who experienced IVF failure were not statistically significant. This result was largely attributed to the small sample size of 33 participants, and researchers acknowledged that a larger sample size would be necessary to identify differences between the two cohorts [179]. This was followed up by a similar

investigation into the endometrial microbiome and the association between composition and the outcomes of IVF [178]. Interestingly, this study identified *Lactobacillus* as the dominant bacteria in the endometrium and classified the cohort of 35 women into two groups: *Lactobacillus*-dominated (>90%) and non-*Lactobacillus*-dominated (<90%). When the IVF outcomes of these two groups were compared, it was determined that women with a non-*Lactobacillus*-dominated microbiome had significantly lower rates of embryo implantation, pregnancy, ongoing pregnancy, and live birth [178].

Several studies have since generated similar results showing that an endometrial microbiome dominated by *Lactobacillus* is associated with favourable outcomes of IVF embryo transfer [116, 182, 202-205]. More recently, a 2022 study of 342 participants found a negative correlation between *Lactobacillus* and diverse bacteria, including *Gardnerella, Bifidobacterium*, and *Fannyhessea,* which was associated with implantation failure [180]. Interestingly, the authors concluded that what may drive IVF failure is the presence of pathogenic bacteria rather than the absence of *Lactobacillus*, as samples with no detectable *Lactobacillus* were also associated with outcomes like live birth [180]. They proposed that *Lactobacillus* in the endometrium may be important in preventing pathogenic colonisation. However, numerous studies contradict these findings, failing to identify a correlation between *Lactobacillus* and successful IVF outcomes [143, 206-208]. Several of these studies identify that the presence of vaginal *Lactobacillus* is significantly correlated with successful outcomes but failed to show a correlation between endometrial *Lactobacillus* and successful outcomes [143, 208]. Interestingly, they show that the endometrial microbiome is more diverse than the vaginal microbiome, and those who experience implantation failure have increased diverse bacteria present in the

endometrium [143, 207, 208]. This result may support the idea that the presence of diverse or pathogenic bacteria, rather than *Lactobacillus,* is what drives poor IVF outcomes.

It is also important to consider the limitations of these studies, particularly small sample sizes and the potential for contamination by vaginal and cervical fluid during sample collection. It is also important to consider the methodology used to profile the microbiome. Most studies use 16s rRNA gene amplicon sequencing, yet many use different variable regions, with some using the V2-V3 region, others using the V3-V4 region, or the V4-V5 region [143, 206-208]. Thus, this lack of consistent methodology may create differences in the profile of bacteria identified, as different regions provide lower resolution and may be unreliable [186]. Another limitation of 16s rRNA gene amplicon sequencing is that it is not able to distinguish between species due to homology between sequences [209]. Thus, many endometrial studies are limited to the genera level [178, 180]. Identifying the species present in the endometrium and their associations with the outcome of IVF is valuable as the outcome of embryo transfer may be species dependent. Recent literature has use metagenomic analysis to overcome this limitation [210]. Endometrial swabs from 142 IVF participants were collected and metagenomic analysis was used to identify 22 strains of bacteria. The authors confirmed that 57% of the strains were *Lactobacillus* with *Lactobacillus helveticus* being the most abundant species [210]. However, it is important to note that this study did not assess the association between the species and the outcome of treatment. Overall, what comprises a beneficial or detrimental profile of endometrial microbiota at the time of embryo transfer is not well-established, but *Lactobacillus* dominance is generally considered ideal in the literature.

1.4.2 The endometrial microbiome, receptivity, and the immune response

It is thought that the microbiome may affect host factors like the development of endometrial tissue receptivity, resulting in implantation failure. A study of 185 participants used the ERA to determine that those in the pre-receptive stage had a significantly lower proportion of *Lactobacillus* in the endometrium [211]. The authors suggested that *Lactobacillus* may be involved in the development of receptivity. Interestingly, another investigation compared the endometrial microbiome and ERA results from a cohort of women with repeated implantation failure to healthy non-pregnant controls and found an association between the composition and key elements of receptivity [212]. The authors highlighted the negative correlation between *Sphingomonas* and angiogenesis. Angiogenesis is essential for the development and remodelling of spiral arteries in the endometrium during receptivity and embryo implantation. Thus, the presence of *Sphingomonas* could limit this process, ultimately altering receptivity [212]. The authors also proposed that alterations in the microbiome may interfere with fat and carbohydrate metabolism, ultimately affecting the immune status and T cell function in the endometrium as a mechanism for repeated implantation failure [212]. However, these should be interpreted with caution, as this study used the ERA, which may not accurately capture endometrial receptivity. Over 3400 genes are involved in developing endometrial receptivity, and their expression rapidly changes [17]. Additionally, they used healthy non-pregnant controls rather than a cohort of participants who successfully achieved a pregnancy, which in future studies may be a more ideal comparison to investigate this mechanism.

Another study investigated the composition of the endometrial microbiome in participants with repeated implantation failure compared to those who achieved a clinical pregnancy [213]. They determined that repeated implantation failure was associated with a reduced abundance of *Lactobacillus* and a higher abundance of diverse bacteria, including *Gardnerella*. This microbial profile negatively correlated with endometrial receptivity markers, Leukemia Inhibitor Factor (LIF) and the Vascular Endothelial Growth Factor (VEGF), indicating that microbiota may disrupt the development of receptivity, leading to implantation failure [213]. Thus, it is clear that the endometrial microbiome impacts host activities and is implicated in the development of receptivity.

The balance of endometrial pro- and anti-inflammatory responses is also essential during the development of receptivity and embryo implantation. However, the endometrial microbiome may also have a role in immunomodulation. It has been shown that *Lactobacillus* abundance in the endometrium is negatively correlated to the concentration of pro-inflammatory cytokines, including IL-6 and IL-1β, and positively correlated with the concentration of anti-inflammatory cytokines like IL-10 [214]. On the other hand, the abundance of diverse bacteria like *Gardnerella* are positively correlated with the concentration of IL-6, which is a key mediator of a pro-inflammatory response in the endometrium. Thus, the authors suggested *Lactobacillus* may be essential to modulating the immune response and that an abundance of diverse bacteria could trigger a detrimental response during the development of receptivity and implantation [214]. However, it is important to consider that the cohort consisted of 26 participants, all of which experienced infertility. The authors highlighted that including a healthy, fertile cohort could improve our understanding of inflammation in the endometrium [214].

Interestingly, another study conducted RNA sequencing to assess the functionally active microbiota, revealing that participants with an unreceptive profile had an altered microbial composition compared to those with a receptive profile [215]. This composition may promote the eicosapentaenoic acid biosynthesis pathway in the host, leading to an aberrant immune response. Furthermore, they suggest that *Treponema succinifaciens* and *Fusobacterium* may have a role in the dysregulation of the immune response [215]. However, it is important to consider that the study only shows the correlation between the active pathways and bacteria; thus further investigation is required to determine a causal relationship. Likewise, additional microbes or host pathways could be involved in this process but not detected, as RNA sequencing only shows the point in time that the sample is collected for analysis. Assessing these pathways and active microbiota at different points during the receptive stage may be beneficial.

Another group showed a high abundance of *Phyllobacterium* and *Sphingomonas* in the endometrium of those with chronic endometritis [216]. By calculating the abundance of immune cells from host RNA sequencing data, they determined NK cells were positively associated with these genera, and macrophages were negatively associated, which could affect the development of receptivity controlled by innate immune cells [216]. However, it is important to consider that this cohort of participants had chronic endometritis, which is characterised by long-term inflammation. Thus, these results may not apply to all patients experiencing implantation failure or an altered endometrial microbiome. Thus, there is a connection between the endometrial microbiome and IVF outcomes, likely via host tissue responses to microbiota, which ultimately affects immune or functional components of implantation and the development of receptivity.

1.4.3 Modelling the endometrial environment and the microbiome

The female reproductive tract is complex and dynamic, making it challenging to model *in vitro.* Embryo culture has provided an opportunity to study embryo development, while the ability to take fluid samples and endometrial biopsies has enabled the study of the microbiome and the conditions at the time of embryo transfer. However, this can only provide insight into conditions prior to embryo implantation, thus limiting our understanding of the role of the microbiome and processes involved in implantation. These studies also only provide an association between the microbiome and the outcome of IVF, but do not provide mechanistic knowledge or evidence.

Murine models have been used to represent the human reproductive tract. Successful mouse models have provided insight into aspects including gene expression, cytokine, and protein expression, crosstalk between the embryo and epithelium, and the role of angiogenesis in implantation [217-221]. However, mouse models are limited as rodents have eccentric implantation, meaning the endometrial epithelium forms an invagination surrounding the embryo, whereas human implantation is invasive [222]. Furthermore, modelling the microbiome in mouse models is challenging as they cannot support the same microbiome as humans. This was demonstrated by colonising germ-free mice with samples of human vaginal fluid from healthy asymptomatic participants and participants with BV [223]. The bacterial profile isolated from the mice did not resemble that of the human samples and did not align with the BV status of the participants, meaning this model is not ideal for studying the human microbiome [223]. However, more recently, a humanised mouse model was developed to more closely represent the

human vaginal microbiome with a greater abundance of *Lactobacillus* [224]. However, there were limitations as only 25.3% of mice were dominated by *Lactobacillus,* with the rest of the mice in the study colonised with normal murine flora [224].

Alternatively, cell culture models can provide a more controlled, reproducible format. Immortalised cell lines are typically derived from tumours and can indefinitely proliferate in *in vitro* culture, rather than following natural cellular senescence [225]. Immortalised cell lines have been used extensively throughout the literature to model different tissues and are an effective method for gathering preliminary evidence. As highlighted in Table 4, there are several advantages to using immortalised cell lines, including established protocols, low cost, technical reproducibility between facilities and laboratories, and homogeneity. Cell lines such as Ishikawa and RL95-2 cells are considered appropriate models for a receptive endometrium, normal endometrial function, and endocrine signalling [226-230]. The JAR cell line has been demonstrated to be a suitable model for the trophoblast, as it expresses essential trophoblastic markers such as KRT7 and hCG, can model embryo implantation, and can be used to generate spheroids (Table 4) [231-234]. Innate immune cell lines such as THP-1 and NK-92 cells have been used extensively in the literature to model immune cells in the endometrial environment [235-237]. THP-1 cells are advantageous as they can be differentiated to represent macrophages and secrete inflammatory cytokines [238]. NK-92 cells also secrete inflammatory cytokines and express receptors consistent with NK cells [239]. Overall, these immortalised cell models provide consistency across the field to establish, compare, and contrast studies looking to explore endometrial and reproductive biology.

However, there are notable limitations and disadvantages of immortalised cell lines. As highlighted in Table 4, immortalised cell lines lack complexity, have features consistent with tumour cells, may spontaneously transform, and cannot truly represent the original tissue. When looking at specific cell lines, JAR cells were derived from a later stage in development than true trophoblast cells [240]. Cells like THP-1 are susceptible to inconsistent culture conditions and require strict adherence to protocols to maintain their characteristics [238]. While NK-92 cells are a good representation of NK cells, they also lack key killer inhibitory receptors that are present on primary NK cells [239]. These limitations should be kept in mind when interpreting the data presented in this study and in the past literature reviewed. Thus, not all findings may translate into an *in vivo* context. Nonetheless, the benefits outweigh the disadvantages of using immortalised models. The data presented here provides important preliminary findings that expand knowledge on microbiota-associated metabolites and their role in endometrial receptivity, the inflammatory response, and embryo implantation. Whereas current literature largely focuses on correlations between the microbiome composition and the outcome of IVF treatments.

Table 4. The advantages and disadvantages of different modelling formats.

	Immortalised cell lines		***Primary cells and organoids***		***Microfluidic models***	
Advantages	Low cost	[240]	Greater complexity and structures with epithelium and stroma can be formed	[241]	Control of environmental and cellular factors	[242-244]
	Well-established protocols	[226, 228, 245, 246]	Can model implantation	[247]	The platform includes sensors and electrodes for analysis	[248]
	Homogenous growth and proliferation	[249]	Can be used to model different stages of the menstrual cycle	[250]	Can model the menstrual cycle	[242]
	Effective in demonstrating cellular mechanisms	[226-230, 235-237]	Can express hormone regulated features of receptivity	[251]	Can represent vascularisation	[242]

	Can be used to form spheroids which can negate the ethical concerns around the use of embryos	[252]	Similarity to the tissue of origin	[253]		
			Can accurately replicate host-pathogen interactions	[254]		
Disadvantages	Cannot reflect some features of the primary tissue	[255]	High cost	[240]	Potential lack of biocompatibility of materials	[256]
	Lack interactions with cells within the *in vivo* environment	[257]	Challenging and complex protocols to collect and maintain the culture	[258, 259]	High cost and complex protocols	[260]
	Cell line contamination and misidentification	[261, 262]	Organoids form closed structures that limit access to oxygen and nutrients	[263]	Leeching of uncured materials	[264]

	Tumour cell features	[249]	Limited lifespan in culture	[253]
	Risk of unwanted spontaneous transformation	[249]	Risk of unwanted spontaneous transformation	[240]
			Reproducibility	[265]

Primary cells are cells that are not immortalised and are derived from tissue samples or biopsies [266]. In research, they can be collected from multiple participants, maintain the morphology of the tissue they were sourced from, and can in some culture models more accurately replicate cell function compared to immortalised cell lines (Table 4). Primary cells can be used to generate organoids, which are 3-dimensional cultures that allow for greater complexity and can represent structures like the epithelial and stromal layers of the endometrium [267]. In the literature, there are several endometrial organoids, which have advantages such as responsiveness to hormones, the ability to replicate the menstrual cycle, preserved structure and function of the endometrium, and can model embryo implantation [247, 250, 251, 253]. Additionally, primary innate immune cells can be isolated from endometrial biopsies and are used to better represent the interactions between decidual immune cells and the endometrial epithelium or trophoblast cells [268-270]. Within the literature, additional complexity can be introduced into these models by incorporating bacteria. Studies have used endometrial epithelial gland organoids, cultured with *Escherichia coli,* to successfully model endometrial infection, bacterial-host interactions, and epithelial barrier integrity [254, 271, 272].

However, primary cells and organoids are not without limitations, as shown in Table 4. Primary cells and organoids show heterogeneity and variability between samples derived from different individuals and in samples from the same participant [265]. This can reflect variation in complex systems but may compromise reproducibility. There is a high cost associated with culture, and the need for expertise and time when handling cells according to challenging protocols [263]. While endometrial organoids show the capability for longer-term culture, it is still limited compared to immortalised cell lines

and inhibits the ability to monitor post-infection changes in models incorporating bacteria [253, 272].

In terms of more complex models, microfluidic systems are becoming increasingly popular. Microfluidic models or organ-on-a-chip models combine cells with other environmental factors, such as sheer force, pH, oxygen, and available nutrients on a small cell culture platform, typically made of polydimethylsiloxane or thermoplastics [242-244]. These models are advantageous as they can replicate factors like the vascular structures and blood flow in the endometrium, the layers of the endometrium, the menstrual cycle, and embryo implantation [242, 243, 273-275]. As outlined in Table 4, the platform enables the inclusion of sensors and electrodes, which are sensitive, enable high-throughput analysis, and can directly detect analytes throughout culture [248]. However, it is important to consider the challenges of microfluidic models. As outlined in Table 4, microfluidic models have a higher cost and require specialised expertise to complete complex fabrication and culture protocols [260]. Additionally, there are challenges around the biocompatibility of the materials used; for example, polydimethylsiloxane can absorb some small molecules and may require additional coatings depending on how the platform is used [256]. While studies have shown that this issue does not impact endocrine factors, cytokines or pharmaceutical compounds in reproductive models, it is necessary to conduct the pilot studies to ensure analytes are not impacted [276-278]. There is also concern around the leeching of uncured polydimethylsiloxane into the microfluidic system, as it may interact with the cells or media used in the model [264]. It is also important to consider that microfluidic models may be most useful when investigating factors impacted by fluid dynamics or temporal changes, such as the interconnection between the endometrium and ovaries and the

kinetics of the menstrual cycle [279]. Thus, in the context of this study, microfluidic models may not be an effective method of modelling the impact of microbiota-associated metabolites to gather preliminary evidence.

Across all types of cell culture models, there have been efforts to model the reproductive microbiome. There are simple 2-dimensional or co-culture models representing the vaginal environment [160, 161, 167, 168, 280]. As well as complex organoid or microfluidic models representing the microbiome or infection in reproductive models [271, 281, 282]. Bacteria can be incorporated into the culture, but in order to directly elucidate the effect of microbiota-associated metabolites, metabolites can be added into the culture media to represent differing compositions. It is known that differing microbiome compositions have a unique metabolomic profile, thus allowing those profiles to be modelled using the corresponding metabolites [163]. This methodology has been successfully used in models of the vaginal microbial environment, enabling researchers to determine the role of metabolites like lactic, acetic and succinic acids in the inflammatory response and epithelial barrier integrity [160, 161, 167, 168]. The cells were treated with different concentrations of microbiota-associated metabolites, and their cytokine secretion, gene expression, and epithelial barrier integrity were assessed. These models successfully demonstrated that lactic acid acts directly on cervical cells to modulate the inflammatory response via IL-1RA and increased expression of proteins like Claudin-1, Claudin-4, and Tight Junction Protein 2, promoting epithelial barrier integrity [160, 161, 167, 168]. This demonstrates the effectiveness of immortalised cell culture in understanding the role of microbiota-associated metabolites. However, these studies are limited as 2-dimensional monolayers cannot replicate the layers of cervicovaginal tissue and the presence of immune cells. Similar models have not been widely used in

investigating the endometrial microbiome, although the concept was used to assess the impact of embryonic metabolites like lactic acid on endometrial epithelium [283]. This model used Ishikawa and ECC-1 cells in 2-dimensional monolayers treated with lactic acid. This study demonstrated that lactic acid can alter the expression of genes associated with receptivity, cell migration and proliferation, and epithelial barrier integrity. However, the authors acknowledge that these are simple models, and co-culture could be used to represent different cell types present in the endometrium [283].

Overall, these studies show that 2-dimensional models using immortalised cell lines can be effective in gathering preliminary evidence to understand the role of microbiota-associated metabolites. While they are not without limitations, such as a lack of complexity that can be better represented using organoids or microfluidic systems, they can be used to model the microbiome in a low-cost, controlled, and reproducible format. There is a need to better understand the role of metabolites in the endometrium, which we have aimed to address in this work using a simple immortalised cell line model. The conclusions made from this work can be translated into future, more complex models.

1.5 Knowledge gap

Although the endometrial microbiome is known to play a role in the outcomes of IVF, it remains unclear what the specific role is or the mechanism of impact. Likewise, there have been many studies demonstrating that the microbiome composition correlates with processes involved in developing receptivity and in modulating the immune response, yet it is not clear what drives this correlation. Previous studies demonstrated a correlation between vaginal metabolites, microbiome composition, and the outcome of

IVF, suggesting metabolites produced by bacteria may have a role in implantation, and a similar relationship could occur in the endometrium [284, 285]. Likewise, it has also been suggested that bacteria in the endometrial environment and their by-products may have a similar role in the modulation of the environment as they do in the vagina. Interestingly, one study showed that lactic acid can modulate key markers of receptivity in endometrial epithelial and stromal cells in culture [283]. This study showed that lactic acid could increase the expression of *VEGF* mRNA, increase the migration of stromal cells, and promote angiogenesis [283]. While this was explored in the context of lactic acid produced by the blastocyst, it may also provide some insight into lactic acid produced by *Lactobacillus*. Furthermore, primary endometrial epithelial cells co-cultured with *Lactobacillus rhamnosus* BPL005, showed decreased pro-inflammatory cytokines after the cells were exposed to diverse bacteria [286]. The authors suggested that this is due to the lactic acid and other short-chain fatty acids produced by the bacteria [286]. However, remains unclear what the role and impact of individual microbiota-metabolite has on the endometrium and without other bacterial by-products produced in a co-culture model. Therefore, there is a need to understand the role of microbiota-associated metabolites in the endometrial environment, and how these metabolites may affect the development of receptivity, the endometrial immune response, and implantation. With a greater understanding of how microbiota and their metabolites impact these processes, interventions could be developed to ultimately improve IVF treatment and outcomes by modulating the endometrial microbiome.

1.6 Endometrial model design

The concentration of endometrial microbiota-associated metabolites is currently underreported in the literature. However, a dominance of *Lactobacillus* at the time of

embryo transfer has been reported to be associated with successful outcomes [178, 180, 205, 206]. Likewise, decreased relative abundance of *Lactobacillus* and increased abundance of diverse bacteria at the time of embryo transfer has been associated with poor outcomes [178, 180, 202, 203, 206]. This study aimed to represent these two profiles using different metabolites in a cell culture model. The metabolites were designed to represent *Lactobacillus* dominance with L-lactic and D-lactic isomers. In vaginal studies, L-lactic and D-lactic acids have been shown to have differing effects, with D-lactic acid thought of as the more protective lactic acid [153]. Thus, both were used in this study to assess if they have a differing role in the endometrium. Acetic and succinic acids were used to represent diverse bacteria, including *Gardnerella*, *Prevotella*, and *Fannyhessea* [162, 168]. The concentration of metabolites used in this study was informed by the metabolomic strategies used by *Lactobacillus* and diverse bacteria. It has been shown that *Lactobacillus* uses the Embden-Meyerhof-Parnas pathway, or the phosphogluconate pathway and the phosphoketolase pathway to produce D-lactic and L-lactic acid, generating between 30-45 mM of lactic acid in culture [162]. Whereas diverse bacteria such as *Gardnerella, Prevotella,* and *Fannyhessea* in culture have been demonstrated to use the *Bifidobacterium* (Bifid) shut or mixed acid fermentation to produce up to 65 mM acetic acid, and anaerobic respiration to produce up to 18 mM succinic acid [162].

Additionally, this study was also informed by published cell culture models representing the endometrium and cervicovaginal environment [160, 161, 167, 168, 286]. An endometrial probiotic study used an *in vitro* bacterial colonisation model to demonstrate that bacteria and metabolites can modulate the immune response of endometrial epithelial cells [286]. Isolated primary cells were grown as a monolayer, and *Lactobacillus* and diverse bacteria were co-cultured with the epithelial cells to assess their

probiotic potential [286]. In culture with the primary cells, *Lactobacillus* produced up to 52 mM lactic acid, whereas diverse bacteria produced up to 20 mM acetic acid and up to 1 mM succinic acid. Using cytometric bead arrays, they determined that co-culture of epithelial cells with diverse bacteria and *Lactobacillus* resulted in up to a 5-fold decrease in IL-6 and a 3.5-fold decrease in IL-8 secreted by the epithelial cells, compared to epithelial cells cultured with diverse bacteria alone [286]. However, it is important to note that this study did not assess H_2O_2 or bacteriocins produced by *Lactobacillus*, which may have impacted the diverse bacteria investigated [286].

Furthermore, cell culture models have been developed using vaginal and cervical cell lines to represent eubiosis and dysbiosis by incorporating metabolites into media [160, 161, 167, 168]. These models have been successfully used to investigate the impact of metabolites on the inflammatory response and integrity of the epithelial barrier in the cervicovaginal environment. In these studies, cell viability when exposed to metabolites was determined using MTS assays. While *in vivo* vaginal concentrations of lactic acid can reach up to 110 mM, these models used 33 mM of lactic acid to model *Lactobacillus* dominance and to ensure the viability of cells in culture [152, 156]. Likewise, acetic acid and succinic acid can reach up to 120 mM and 22 mM *in vivo*, respectively, in a dysbiotic vaginal environment [127, 287-289]. However, 100 mM and 20 mM acetic acid and succinic acid were used to represent dysbiosis, to maintain viability. Cytometric bead arrays showed that exposure to L-lactic and D-lactic acids significantly decreased the secretion of IL-6, IL-8, and RANTES, and resulted in a 19-fold increase in IL-1RA [160]. Additionally, L-lactic acid was shown to increase claudin-1, claudin-4, and tight junction protein-2 expression, improving epithelial barrier integrity.

In this study, MTS viability assays were conducted for concentrations between 0 mM to 30 mM for L-lactic, D-lactic, acetic and succinic acids to establish the concentration at which endometrial epithelial, trophoblast, and innate immune cells would remain viable in culture. These concentrations were then used to represent a dominance of either *Lactobacillus* or diverse bacteria, akin to the aforementioned culture studies. It is important to acknowledge that the endometrium has a lower biomass of bacteria compared to the vaginal environment [176]. Therefore, the concentration of microbiota-associated metabolites may be lower than that represented in this study, but this has not been explored in the literature. The purpose of this thesis is to extend our understanding of microbial-host cell cross-talk to the endometrium. It is critical to provide insight into how microbiota-associated metabolites may affect the endometrial environment, receptivity, and inflammation, initially using cell models to determine cellular-level differences.

1.7 Hypothesis and aims

1.7.1 Hypothesis

In this study, we aimed to represent a *Lactobacillus*-dominant profile and a non-*Lactobacillus*-dominant profile using microbiota-associated metabolites in a cell culture model. L-lactic and D-lactic acid were chosen to represent *Lactobacillus*, as *Lactobacillus* (with the exception of *Lactobacillus iners*) produces both isomers via the Embden-Meyerhof-Parnas pathway or the phosphogluconate pathway and the phosphoketolase pathway [162]. In a eubiotic vaginal environment, a high concentration of lactic acid (110 mM) drives homeostasis by maintaining pH, modulating the inflammatory response, and maintaining the epithelial barrier [160, 161, 168]. Acetic and succinic acids were chosen to represent diverse bacteria, such as *Gardnerella*, *Prevotella*, and *Fannyhessea*. These bacteria produce acetic acid and succinic acid via the bifid shunt, mixed acid fermentation, or anaerobic respiration [162]. These metabolites are present in high concentrations in vaginal dysbiosis (120 mM acetic acid and 20 mM succinic acid) and drive an aberrant inflammatory response in the vaginal environment [167, 168, 288, 289].

My hypothesis was that metabolites like L-lactic and D-lactic acid produced by *Lactobacillus* create an environment conducive to successful embryo implantation by modulating the development of receptivity, the inflammatory response and embryo implantation. Metabolites produced by diverse non-*Lactobacillus* bacteria, like acetic and

succinic acids, alter receptivity, the immune response, and implantation, resulting in conditions detrimental to successful embryo implantation.

1.7.2 Aims

1. Determine the impact of microbiota-associated metabolites on receptivity markers in endometrial epithelium and innate immune cells.
2. Determine the impact of microbiota-associated metabolites on the inflammatory response of endometrial epithelium and innate immune cells.
3. Determine the impact of microbiota-associated metabolites on factors of embryo implantation.

2 Materials and Methods

2.1 Cell Culture

2.1.1 Culture and maintenance of endometrial epithelial cell lines

The Ishikawa (gifted from Prof. Deborah Marsh, ECACC; cat no. 99040201) and RL95-2 (American Type Culture Collection (ATCC), CRL-1671) cell lines were employed to model endometrial epithelium. The Ishikawa cell line was derived from a well-differentiated endometrial adenocarcinoma and has been used to model a receptive endometrium [226]. Ishikawa cells are also widely considered to closely represent normal endometrial function and have been used successfully in embryo attachment models [290, 291]. The RL95-2 cell line was derived from a moderately differentiated endometrial adenosquamous carcinoma and has also been used to represent a receptive endometrium [228-230]. RL95-2 cells are also considered a good representation of uterine glandular tissue with a tendency to form gland-like structures [228]. They have also been successfully used in embryo attachment models [292]. As Ishikawa and RL95-2 cell lines are considered receptive models of the endometrium, standard cell culture conditions were used, and hormonal priming was not incorporated into this study, in line with the literature [283, 290, 293-296].

Ishikawa cells were cultured in high glucose (4.5 g/L) Dulbecco's Modified Eagles Medium (DMEM) (Sigma-Aldrich, cat no. D6546), supplemented with 4mM L-alanyl-l-glutamine (Thermo Fisher Scientific, cat no. A2916801), 10% heat-inactivated fetal bovine serum (FBS) (Sigma-Aldrich, cat no. F9423), 100 μg/mL of streptomycin (Thermo Fisher Scientific, cat no. 11860038), and 50 μg/mL gentamycin (Thermo Fisher Scientific, cat no. 15750078). The cells were passaged when 80-90% confluency was reached. To passage cells, the spent media was removed from the monolayer and washed

twice with pre-warmed 20 mL of Dulbecco's Phosphate Buffered Saline (dPBS) (1×) (Thermo Fisher Scientific, cat no. BR0014G). The cells were then incubated for 5 minutes with 1.5 mL of 2× trypsin-EDTA (Sigma-Aldrich, cat no. T417) to detach the cells. The trypsin was deactivated with 8.5 mL of fresh complete DMEM. The cells were seeded into a Nunc EasYFlask cell culture T75 flask (Thermo Fisher Scientific, cat no. 156499) at a 1:5 subculture ratio and incubated at 37°C with 5% CO_2 until confluent.

RL95-2 cells were cultured according to ATCC guidelines in Dulbecco's Modified Eagles Medium/Nutrient Mixture F-12 (DMEM/F-12) (Thermo Fisher Scientific, cat no. 11320033), supplemented with 10% heat-inactivated FBS, 0.005 mg/mL insulin (Sigma-Aldrich, cat no. 11376497001), and 100 U/mL penicillin-streptomycin (Thermo Fisher Scientific, cat no. 15140122) [230]. Upon reaching 80-90% confluency, RL95-2 cells were passaged. The spent media was removed from the monolayer, and the cells were washed twice with 20 mL of dPBS. The cells were incubated with 1.5 mL of 2× trypsin-EDTA for 10 minutes to detach the cells, and the trypsin was deactivated with 8.5 mL of warmed complete media. The cells were seeded into a T75 flask at a 1:5 subculture ratio and incubated at 37°C with 5% CO_2 until confluent.

2.1.2 Culture and maintenance of the JAR cell line

JAR cells are a trophoblastic cell line derived from a choriocarcinoma and are known for their similarity to human trophoblast cells [297]. They express essential trophoblastic markers such as KRT7 and hCG [231, 232]. This cell line was primarily chosen as it is a good model for embryo attachment and invasion, and can be used to generate spheroids [233, 234]. Several studies have used JAR spheroids in conjunction with

Ishikawa or RL95-2 cells in spheroid attachment models [27, 229, 292, 298, 299]. The JAR cell line was purchased from the ATCC (cat no. HTB-144) and cultured according to ATCC guidelines with the addition of antibiotics [300]. The cells were cultured with Roswell Park Memorial Institute (RPMI) 1640 (Thermo Fisher Scientific, cat no. 11875119) with 10% heat-inactivated FBS and 100 U/ML penicillin-streptomycin. JAR cells were passaged when 80-90% confluency was reached. The spent media was removed from the flask, and the monolayer was washed with 20 mL of warm dPBS. To detach the cells, 1.5 mL of 2× trypsin-EDTA was added to the flask, and the cells were incubated for 5 minutes. The trypsin was deactivated with 8.5 mL of fresh complete media. The cells were seeded into a T75 flask at a 1:4 subculture ratio and incubated at 37°C with 5% CO_2 until confluent.

2.1.3 Culture and maintenance of innate immune cell lines

THP-1 (ATCC, cat no. TIB-202) and NK-92 (ATCC, cat no. CRL-2407) cell lines were used to model macrophages and natural killer cells, respectively. The THP-1 cell line was derived from acute monocytic leukemia [301]. The NK-92 line was derived from a malignant non-Hodgkin's lymphoma [302]. Both cell lines have previously been used to model immune cells in the endometrial environment [235-237]. THP-1 and NK-92 cell lines both secrete cytokines and chemokines, which play important roles in endometrial receptivity and the inflammatory response [238, 239]. Additionally, THP-1 cells can be differentiated to macrophages, which are one of the prominent cell types present in the endometrium [245, 303].

THP-1 cells were cultured in RPMI 1640 media, supplemented with 10% heat-inactivated FBS, 100 μg/mL of streptomycin and 50 μg/mL gentamycin [304]. The cells were maintained between 2×10^5 - 1×10^6 cells/mL in T75 flasks. Cells were stained with trypan blue (Thermo Fisher Scientific, cat no. 15250-061) and counted using a haemocytometer. If the cell density was above or close to 1×10^6 cells/mL, the appropriate volume of cells was transferred to a new flask with fresh, complete media to a final volume of 15 mL and incubated at 37°C with 5% CO_2. If the cells were below 1×10^6 cells/mL, they were centrifuged at 500 ×g for 5 minutes at room temperature. The spent media was removed, and the cells were resuspended with 15 mL of complete media and incubated at 37°C with 5% CO_2.

NK-92 cells were cultured in RPMI 1640 media, supplemented with 10% heat-inactivated FBS, 1 mM sodium pyruvate (Thermo Fisher Scientific, cat no. 11360070), 1× non-essential amino acids (Thermo Fisher Scientific, cat no. 11140050), 200 UI/mL interleukin (IL)-2 (Miltenyi Biotec, cat no. 130-097-745), and 100 U/mL penicillin-streptomycin [246]. The cells were maintained between 2×10^5 - 1×10^6 cells/mL in T75 flasks. The cells were centrifuged at 130 ×g for 5 minutes at room temperature every two to three days, and the spent media was removed. The cells were resuspended in 10 mL fresh media, and the concentration was determined using a haemocytometer. If the cell density was above or close to 1×10^6 cells/mL the cells were passaged, and the appropriate volume of cells was transferred to a new flask with fresh, complete media to reach a final volume of 10 mL. If the cell density was below 1×10^6 cells/mL, the cell suspension was transferred to a T75 flask and returned to the incubator. The cells were incubated at 37°C with 5% CO_2.

2.1.4 Differentiation of THP-1 cells into macrophages

THP-1 cells were differentiated into adherent macrophages before use in all experiments, as per established protocols [245, 303]. Confluent THP-1 cells were diluted to the appropriate concentration to seed well plates, and phorbol 12-myristate 13-acetate (PMA) (Sigma-Aldrich, cat no. P8139) was added to reach a final concentration of 15 ng/mL [245, 303]. Cells were seeded and incubated at 37°C with 5% CO_2 for 48 hours. The PMA media was removed and replaced with fresh, complete RMPI 1640 media without PMA. The cells were incubated for 24 hours [245, 303]. In the literature, it has been shown that THP-1 cells have limited expression of inflammatory response genes generated by PMA exposure after incubation with media lacking PMA [245]. This creates a consistent phenotype that is suitable for inflammation models [245].

2.1.5 Authentication of cell lines

All cell lines were authenticated by the Australian Genome Research Facility (AGRF). DNA was extracted from cell pellets collected from the Ishikawa, RL95-2, THP-1, NK-92, and JAR lines using the AllPrep DNA/RNA Micro kit (QIAGEN, cat no 80284). 350 μL of Buffer RLT Plus was added to the pellet and vortexed to lyse the cells. The lysate was passed through a blunt 20-gauge needle five times. The lysate was transferred to a spin column and centrifuged for 30 seconds at 8000 ×g. 500 μL of Buffer AW1 was added to the column and centrifuged for 15 seconds at 8000 ×g. 500 μL of Buffer AW2 was added to the column and centrifuged for 2 minutes at 14,000 ×g. Buffer EB was preheated to 70°C, and 50 μL was added directly to the membrane and incubated for 2 minutes at room temperature. The spin column was centrifuged for 1 minute at 8000

×g to elute the DNA. The concentration and purity of the DNA was determined using a Nanodrop One/One^{C} Microvolume UV-Vis Spectrophotometer (Thermo Fisher Scientific, cat no. ND-ONEC). The cell lines were authenticated using the AGRF's human cell line identification service, which uses the Promega GenePrint 10 system to complete short tandem repeat (STR) profiling. This method amplifies ten loci; amelogenin, CSF1PO, D13S317, D16S539, D21S11, D5S818, D7S820, TH01, TPOX, and vWA. The generated profile from each cell line was then analysed using the Cellosaurus Cell Line Authentication using STR (CLASTR) 1.4.4 program, and the cell line was identified [305]. The results are provided in Appendix 1 (Table 21).

2.1.6 Mycoplasma testing

All cell lines were routinely tested for Mycoplasma contamination to ensure the validity of all cell culture experiments [306]. The cells were cultured for two weeks in their respective media without antibiotics. A 1 mL sample of spent media was removed from the culture and tested using the MycoAlert *Mycoplasma* detection kit (Lonza Bioscience, cat no. LT07-318). All cells were confirmed to be free of *Mycoplasma* contamination.

2.2 Preparation of Metabolites

2.2.1 Stock Metabolite Solutions

The metabolites used in all assays were purchased as a concentrated stock and diluted with sterile milli-Q water, according to Table 5, to create a working stock. All solutions were filter-sterilised using 0.2 μm filters (Sartorius, cat no.S6534-FMOSK).

Table 5. Preparation of microbiota-associated metabolites from purchased stock.

Metabolite	**Supplier**	**Catalogue no.**	**Volume of H_2O (mL)**	**Amount of stock metabolite**	**Final concentration of working stock (M)**
L-lactic acid	Sigma-Aldrich	L1750	20	1.80 g	1
D-lactic acid	ChemSupply Australia	L0266	20	1.80 g	1
Glacial acetic acid	Sigma-Aldrich	A6283	18.9	1.15 mL	1
Succinic acid	Sigma-Aldrich	S9512	20	1.19 g	0.5

2.3 Viability of cells treated with microbiota-associated metabolites

2.3.1 MTS reagents

The CellTiter 96® Aqueous 3-(4,5-dimethylthiazol-2-yl)-5-(3-carboxymethoxyphenyl)-2-(4-sulfophenyl)-2H-tetrazolium (MTS) reagent powder (Promega, cat no. G1111) was dissolved in dPBS to achieve a 2 mg/mL solution with a pH between 6.0 to 6.5 [307]. The solution was sterilised using a 0.2 μm syringe filter and stored at -20°C protected from light. Phenazine methosulfate (PMS) (Sigma-Aldrich, cat no. P9625) was resuspended in dPBS to reach a concentration of 0.92 mg/mL [307]. The solution was sterilised using a 0.2 μm syringe filter and stored at -20 °C, protected from light. To create a working solution, 50 μL of PMS was added to 1 mL of the MTS solution and vortexed to mix.

2.3.2 MTS assays for cell viability

All viability assays were carried out in 96-well plates (Thermo Fisher Scientific, cat no. 167008). Ishikawa, RL95-2, and JAR cells were seeded at a density of 2×10^4 cells/well. The well plates were incubated for 24 hours at 37°C with 5% CO_2 to ensure the cells had adhered to the plate. THP-1 cells were seeded at a density of 5×10^4 cells/well and differentiated according to the outlined method (section 2.1.4). NK-92 cells were seeded at 2.5×10^4 cells/well. NK-92 cells were used immediately, as the cells are in suspension and do not adhere to the plate.

Once Ishikawa, RL95-2, JAR, and THP-1 cells had adhered to the plate, the spent media was removed and replaced with the media supplemented with microbiota-associated metabolites according to concentrations outlined in Table 6. After seeding NK-92 cells into the well plate, the appropriate volume of microbiota-associated metabolites was added directly into the wells to reach the concentrations outlined in Table 6. After the treatment was added, all well plates were incubated at 37°C with 5% CO_2 for 4, 6, and 24 hours. At each time point, 20 µL of the prepared MTS reagent was added to all wells [307]. Plates containing Ishikawa, RL95-2, or THP-1 cells were incubated at 37°C with 5% CO_2 for 2 hours and protected from light. Plates containing JAR or NK-92 cells were incubated at 37°C with 5% CO_2 for 3 hours and protected from light. After the incubation, the absorbance was read using the Tecan Infinite M200 Plate reader at 490 nm. To determine the percentage of viable cells, the following equation was used [308];

$$\%\, Viable\ Cells = \frac{Treated\ Cells - Background\ Absorbance}{Control\ Cells - Background\ Absorbance} \times 100$$

Concentrations at which cells maintained a ≥ 80% viability over the three time points were used in further experiments [309]. This cutoff aligns with ISO 10993-5 and ensures the cells are not exposed to a weakly cytotoxic dose of the microbiota-associated metabolites in all experiments [309, 310]. Initial MTS assays were conducted across a broad range of concentrations to determine the concentrations used in this study. Prior to the use of the determined concentrations, the pH was tested after culturing in standard cell culture conditions, and confirmed to remain at 7.4. This was also visually confirmed throughout all experiments by the observation of the phenol red pH indicator used in media.

Table 6. Concentration range of individual microbiota-associated metabolites used in MTS Viability Assays.

Cell line	Media	Metabolite	Concentration range
Ishikawa	DMEM	L-Lactic Acid	5-30 mM
		D-Lactic Acid	
		Acetic Acid	
		Succinic Acid	
RL95-2	DMEM/F-12	L-Lactic Acid	5-30 mM
		D-Lactic Acid	
		Acetic Acid	
		Succinic Acid	
JAR	RPMI 1640	L-Lactic Acid	5-30 mM
		D-Lactic Acid	
		Acetic Acid	
		Succinic Acid	
THP-1	RPMI 1640	L-Lactic Acid	5-30 mM
		D-Lactic Acid	
		Acetic Acid	
		Succinic Acid	
NK-92	RPMI 1640	L-Lactic Acid	1-10 mM
		D-Lactic Acid	
		Acetic Acid	
		Succinic Acid	

2.4 Culture of cells with microbiota-associated metabolites

2.4.1 Treatment and collection of supernatant and cell samples

To examine the effects of microbiota-associated metabolites, various cell lines were treated with different metabolites, including L-lactic acid, D-lactic acid, acetic acid, and succinic acid. Upon completion of the experiments, the culture supernatants were harvested to quantify cytokine production. For these experiments, Ishikawa and RL95-2 cells were seeded into 96-well plates at 2×10^4 cells/well and incubated for 24 hours before treatment to ensure the cells adhered. THP-1 cells were seeded into 96-well plates at 5×10^4 cells/well and differentiated according to the protocol outlined in section 2.1.4. NK-92 cells were seeded into 96-well plates at 2.5×10^4 cells/well and used immediately. The cells were treated with the different metabolite concentrations within the ranges outlined in Table 7 for these experiments. To generate a pro-inflammatory response, as a control for assay and cell responses, the cells were separately treated with PMA/Ionomycin (PMA/I) (1×) (Thermo Fisher Scientific, cat no. 00-4970-93) and lipopolysaccharide (LPS) (1×) (Thermo Fisher Scientific, cat no. 00-4976-93). The cell culture supernatants were collected after 24 hours of incubation at 37°C with 5% CO_2. The media was removed from the monolayer of adherent cells and transferred to 1.5 mL tubes. The suspension of media and NK-92 cells was also transferred to 1.5 mL tubes. All samples were centrifuged at 10,000 ×g for 5 minutes to remove cells and debris. The media was stored in aliquots of 50 µL and frozen at -80°C.

The cells treated with metabolites were also harvested and used in RNA extractions and RT-qPCR to investigate the changes in the expression levels of various genes. The endometrial epithelial cells and JAR cells were seeded into 6-well plates at 3×10^5 cells/well (Thermo Fisher Scientific, cat no. 140675) and were incubated for 24 hours to ensure they had adhered. THP-1 cells were seeded at 1×10^6 cells/well and differentiated according to the protocol outlined in section 2.1.4 before use. NK-92 cells were seeded into 6-well plates at 3×10^5 cells/well and used immediately. The cells were treated with the different metabolite concentrations within the ranges outlined in Table 7. The cells were separately treated with PMA/I and LPS to generate a pro-inflammatory response as positive controls. The JAR cells were not treated with PMA/I and LPS, as this project did not evaluate their inflammatory response. For these experiments, the cells were incubated with metabolites for 4 hours at 37°C with 5% CO_2. The spent media was removed from the monolayer and washed with cold dPBS. To collect cell samples for RNA extractions and RT-qPCR, 300 µL of RNAprotect Cell Reagent (QIAGEN, cat no. 76526) was added to each well and incubated for 5 minutes at room temperature to lift the cells. The cells were transferred to 1.5 mL tubes and stored at -20°C. As NK-92 cells are not adherent, the cell suspension was transferred to 1.5 mL tubes and centrifuged at 10,000 ×g for 5 minutes. The media was removed from the cell pellet, and 300 µL of RNAprotect Cell Reagent was added to resuspend the cells. The cells were stored at stored at -20°C.

Table 7. The concentration range of microbiota-associated metabolites used to treat cells.

Cell Line	Media	Metabolite	Concentration Range [A]
Ishikawa	DMEM	L-lactic acid	0-25 mM
		D-lactic acid	0-10 mM
		Acetic acid	0-10 mM
		Succinic acid	0-5 mM
RL95-2	DMEM/F-12	L-lactic acid	0-15 mM
		D-lactic acid	0-15 mM
		Acetic acid	0-5 mM
		Succinic acid	0-5 mM
JAR	RPMI 1640	L-lactic acid	0-15 mM
		D-lactic acid	0-15 mM
		Acetic acid	0-15 mM
		Succinic acid	0-5 mM
NK-92	RPMI 1640	L-lactic acid	0-5 mM
		D-lactic acid	0-4 mM
		Acetic acid	0-5 mM
		Succinic acid	0-2 mM
THP-1	RPMI 1640	L-lactic acid	0-15 mM
		D-lactic acid	0-10 mM
		Acetic acid	0-5 mM
		Succinic acid	0-5 mM

[A] The concentration range of each metabolite was determined using MTS viability assays. Cells were considered viable if the % viability of treated cells remained ≥80% over 24 hours.

2.5 Culture of epithelial cells with conditioned media

2.5.1 Preparation of conditioned media

To determine the impact of innate immune cells on the inflammatory response of endometrial epithelial cells, innate immune cell-conditioned media was used in culture with the Ishikawa and RL95-2 cells. To produce conditioned media, THP-1 cells were initially seeded into 6-well plates 1×10^6 cells/well and differentiated according to the method outlined in section 2.1.4. NK-92 cells were seeded into 6-well plates at 3×10^5 cells/well and used immediately. The cells were incubated for 24 hours in media containing the highest concentration of each metabolite (Table 7) at 37°C with 5% CO_2. The cells were also incubated with their respective complete media without metabolites added as an untreated control. After 24 hours, the media was transferred to a 15 mL falcon tube, diluted 1:2 with fresh media, and centrifuged at 500 ×g for 5 minutes to remove cells and debris. The conditioned media was then filter sterilised using a 0.2 μm syringe filter. The prepared conditioned media was used immediately.

While the immune cells were incubated with metabolites, Ishikawa and RL95-2 cells were used to seed 6-well plates at 3×10^5 cells/well. They were incubated for 24 hours at 37°C with 5% CO_2 to ensure the cells had adhered to the plate. Once the conditioned

media had been prepared, the spent media on the epithelial cells was removed, and the monolayer was washed once with warm dPBS. To initiate the experiment, 1 mL of the conditioned media was added to the wells, and the cells were incubated for 4 hours at 37°C with 5% CO_2. After 4 hours, the media was removed from the monolayer and the cells were washed with cold dPBS. To harvest cell samples for RNA extractions and RT-qPCR, 300 µL of RNAprotect Cell Reagent was added to the wells and incubated for 5 minutes at room temperature to lift the cells. The cells were transferred to 1.5 mL tubes and stored at -20°C for use in RT-qPCR.

2.6 RNA extraction and Reverse-Transcription -quantitative (RT-q)PCR

2.6.1 RNA extraction and cDNA synthesis

The stored cell samples were thawed on ice and centrifuged at 12,000 ×g for 5 minutes. The storage buffer was removed, and the pellet was washed once with 300 µL of cold nuclease-free water. The RNA was extracted using the ReliaPrep™ RNA Cell Miniprep system (Promega, cat no. Z6012) according to the manufacturer's instructions. In brief, 100 µL of the BL Buffer containing 1-thioglycerol was added to the pellet and vortexed. Next, 35 µL of 100% molecular grade isopropanol (Sigma-Aldrich, cat no. I9516) was added and vortexed for 5 seconds. The lysate was transferred to a mini-column and centrifuged for 30 seconds at 12,000 ×g. After discarding the flow-through, 500 µL of RNA wash solution was added to the mini-column and centrifuged for 30 seconds at 12,000 ×g. The flow-through was discarded. In a separate tube, per sample, 24 µL yellow core buffer, 3 µL 0.09 M $MnCl_2$, and 3 µL DNase I enzyme were mixed. A total of 30 µL

of this solution was added directly to the membrane and incubated for 15 minutes at room temperature to digest DNA in the samples. Following this, 200 µL of the column wash was added to the mini-column and centrifuged at 12,000 ×g for 15 seconds. The flow-through was discarded. Then, 500 µL of RNA wash solution was added to the mini-column and centrifuged for 30 seconds at 12,000 ×g, and the flow-through was discarded. Finally, 300 µL of RNA wash solution was added and centrifuged at 14,000 ×g for 2 minutes. The mini-column was transferred to a 1.5 mL elution tube. To elute the RNA, 15 µL of nuclease-free water was added to the membrane and was centrifuged for 1 minute at 12,000 ×g. The concentration and purity of the RNA were determined using the Nanodrop One/One^{C} Microvolume UV-Vis Spectrophotometer.

cDNA was synthesised using the Promega GoTaq® 2-Step RT-qPCR System (Cat no. A6010). The RNA was diluted with nuclease-free water to reach a concentration of 100 ng/µL. The reaction components outlined in Table 8 were combined and placed on a heating block at 70°C for 5 minutes. The samples were transferred immediately from the heat block and chilled on ice for 5 minutes. The reverse transcriptase reaction mix was prepared per reaction using the components outlined in Table 9. A total of 10 µL of the reaction mix was added to the prepared RNA/primer solution to reach a final volume of 20 µL. The samples were placed in the Rotor-Gene Q MDx 5plex HRM (QIAGEN, cat no. 9002033) and incubated according to conditions outlined in Table 10 to synthesise cDNA. cDNA was stored at -20°C until use.

Table 8. cDNA synthesis reaction components.

Component	**Volume (µL) per reaction**
RNA Template (100 ng/µL)	1
Oligo $(dT)_{15}$ Primer (0.5ug/ul)	1
Random Primers (0.5ug/ul)	1
Nuclease-free water	7
Total Volume	10

Table 9. Reverse Transcriptase reaction components.

Reaction Component	**Volume (µL) per reaction**
Nuclease-Free Water	1.5
GoScript™ 5X Reaction Buffer	4
$MgCl_2$ (25 mM)	2
PCR Nucleotide Mix (10 mM)	1
Recombinant RNasin® Ribonuclease Inhibitor	0.5
GoScript™ Reverse Transcriptase	1
Total Volume	10

Table 10. Thermal cycling conditions used to synthesise cDNA.

	Temperature (°C)	Time (minutes)
Anneal	25	5
Activation	42	60
Inactivation	70	15

2.6.2 Reverse Transcription-quantitative (RT-q) PCR

The Promega GoTaq® 2-Step RT-qPCR system and custom primer pairs (Integrated DNA Technologies) were used to complete RT-qPCR. Table 13 outlines the reference genes used for each cell line. The master mix was prepared according to Table 11. A total of 20 µL of the master mix was added to each well in a 96-well plate (Thermo Fisher Scientific; cat no. 4346907) and sealed. The plate was run in the QuantStudio™ 6K Flex Real-time PCR System (Thermo Fisher Scientific, cat no. 4485689) according to the cycling conditions in Table 12. The cycle threshold (C_t) values were determined using the Design and Analysis Software, Version 2.6 for MAC. The comparative C_t method was used to determine the effect of the metabolites on gene expression compared to untreated cells [311]. The significance was determined using an unequal variances T-test. The results were also analysed using a two-way ANOVA as there are two independent variables; metabolite treatment and concentration. Dunnett's multiple comparisons tests were completed to determine if the treatments resulted in statistically significant changes in gene expression compared to the untreated control [312-314]. A $\log_2$ fold change was considered significant if it was ≥1 or ≤-1 and the *p* value was $p \leq 0.05$ [315]. The fold

change values are represented as the normalised values, and the full data set can be found in appendices 2, 3, and 4.

Table 11. RT-qPCR master mix components.

Component	**Volume (μL) per reaction**	**Final Concentration**
GoTaq® qPCR Master Mix (2×)	10	1×
Forward Primer (20×)	1	200nM – 1μM
Reverse Primer (20×)	1	200nM – 1μM
cDNA Template	2-5	≤100ng
Nuclease-free Water	To reach a final volume of 20 μL	

Table 12. Thermal cycling conditions used to conduct RT-qPCR reactions.

Step	**Cycles**	**Temperature (°C)**	**Time (Seconds)**
DNA polymerase activation	1	95	120
Denaturation	40	95	15
Annealing and extension		60	60

Table 13. Reference gene primer sequences. All primer pairs were ordered from Integrated DNA Technologies (IDT, Singapore).

Gene	**Role**		**Sequence (5'-3')**	**Reference**
Glyceraldehyde 3-phosphate dehydrogenase (*GAPDH*)	Reference gene for JAR and NK-92 cells	Forward	TGGTATCGTGGAAGGACTCATGAC	[160]
		Reverse	ATGCCAGTGAGCTTCCCGTTCAGC	
β-Actin (*ACTB*)	Reference gene for THP-1 cells	Forward	ATTGCCGACAGGATGCAGAA	[316]
		Reverse	GCTGATCCACATCTGCTGGAA	
Hypoxanthine-guanine phosphoribosyltransferase (*HPRT1*)	Reference gene for Ishikawa, and RL95-2.	Forward	TGACACTGGCAAAACAATGCA	[317]
		Reverse	GGTCCTTTTCACCAGCAAGCT	

2.7 Glucose-uptake assay

2.7.1 Seeding and treatment of cells

Ishikawa, RL95-2, and JAR cells were seeded into white, clear bottom 96-well plates at 2×10^4 cells/well (Sigma-Aldrich, cat no. CLS3610) and incubated for 24 hours. THP-1 cells were seeded into 96-well plates at 5×10^4 cells/well and differentiated according to the protocol outlined in section 2.1.4. NK-92 cells were seeded into 96-well plates at 2.5×10^4 cells/well and used immediately. After the cells were seeded, they were treated with the highest concentration of L-lactic, D-lactic, acetic, and succinic acid they could tolerate, as outlined in Table 7. The cells were incubated for 24 hours at 37°C at 5% CO_2.

2.7.2 Glucose-uptake assay

The Glucose Uptake-Glo™ Assay kit (Promega, cat no. J1342) was used to conduct this assay according to the manufacturer's instructions. Before beginning the assay, the 2DG6P detection reagent was prepared according to Table 14. It was allowed to equilibrate at room temperature for one hour to minimise background. Additionally, 100 mM 2-deoxyglucose (2DG) (100 mM) was diluted to reach a final concentration of 1 mM in dPBS.

Table 14. 2DG6P Detection Reagent.

Component	Per Reaction (µL)
Luciferase Reagent	100
$NADP^+$ (20 mM)	1
G6PDH	2.5
Reductase	0.5
Reductase Substrate	0.0625

The media was removed from the treated cells, and the monolayer was washed once with warmed dPBS to remove any remaining glucose. A volume of 50 µL of 1 mM 2DG was added to each well. As a negative control, 50 L of dPBS was added to three wells of untreated cells instead of 2DG. The plate was gently swirled and incubated for 10 minutes at room temperature. After the incubation, 25 µL of stop buffer was added to each well, and the plate was gently swirled. Then, 25 µL of neutralisation buffer was added to each well, and the plate was gently swirled. Finally, 100 µL of the prepared 2DG6P detection reagent was added to each well, and the plate was gently swirled. The plate was then incubated for 90 minutes at room temperature, and the luminescence was measured using the Tecan Infinite M200 Plate reader with a one-second integration.

2.7.3 Analysis and figure generation for glucose-uptake assays

The background luminescence was subtracted from the luminescence readings from treated wells according to the assay protocol. The luminescence readings were reported in relative light units (RLU). The figures were generated using GraphPad Prism 9.3.0 for Windows (GraphPad Software, Boston, Massachusetts, USA www.graphpad.com), and unpaired T-tests with Welch's correction were performed to determine significance. The results were also analysed using a one-way ANOVA and Dunnett's multiple comparison tests.

3 Microbiota-associated metabolites impact the functionality of the endometrial environment

3.1 Introduction

Infertility is a common reproductive disease estimated to impact one in six people globally [67]. *In vitro* fertilisation (IVF) is a readily used treatment for infertility, with over 65,000 initiated cycles in Australia and New Zealand in 2022 [70]. The clinical pregnancy rate per fresh embryo transferred is 33.1% and has not greatly improved over the last five years [70]. This is concerning due to the cost of treatment and the physical and mental burden on patients [96, 98, 99]. Endometrial receptivity is when endometrial tissue is in the correct condition to enable the attachment and invasion of an embryo and establish a pregnancy [6]. It occurs during the window of implantation (WOI), which occurs during days 19 to 21 of the menstrual cycle [318]. Receptivity development is driven by hormonal regulation and involves the maintenance of endometrial integrity and function. The development of receptivity is essential to the success of IVF, and embryo transfer failure is often attributed to poor receptivity.

The development of receptivity is a highly controlled process, and the tissue undergoes many alterations, such as decidualisation, the development of pinopodes, endometrial thickening, and changes to gene expression [8, 17, 319]. Of particular interest in this chapter was the epithelial-to-mesenchymal transition (EMT) and mesenchymal-to-epithelial transition (MET) that occurs to prepare the endometrium and enable implantation. After menstruation, the tissue undergoes MET, rapidly migrating and restoring the epithelial layer [320]. During receptivity, the cells undergo EMT, losing their polarity, increasing motility and reorganising adhesion molecules, which are critical changes to enable embryo implantation [27, 321]. As the embryo implants, it has been suggested that the epithelium migrates away from the implantation site and undergoes

apoptosis [27]. This is thought to enable the embryo to invade and proliferate. Then, redistribution and upregulation of N-cadherin promotes the epithelial cells to migrate over the invaded embryo and cover it [27]. Furthermore, during receptivity and EMT, there is a reorganisation of desmosomal proteins and adherens junctions, but tight junction proteins like Zonula Occludens-1 (ZO-1) do not change position or expression to maintain cell-cell junctions, creating a permeability barrier around the embryo in the stromal tissue [322, 323]. Transcriptional factors like Homoebox A10 (*HOXA10)* are also involved in the development of receptivity, promoting the expression of E-cadherin, a classic marker of EMT [295]. Furthermore, receptors like Transforming Growth Factor Beta Receptor-1 *(TGFBR1)* are also essential for the control of epithelial proliferation during EMT [324, 325].

The development of receptivity also involves the regulation of several genes to promote structural and vascular development. During the receptive stage, Leukemia Inhibitory Factor (LIF) is expressed by endometrial epithelium, promoting LIF expression in the stroma [326]. LIF activates the Signal Transducer and Activator of Transcription 3 (STAT3) pathway in epithelial cells, increasing receptivity and facilitating embryo implantation [326]. Decreased LIF expression or knockout of LIF results in embryo implantation failure [326-329]. Growth factors like Vascular Endothelial Growth Factor (*VEGFA)* are expressed to promote angiogenesis, repair, and re-epithelisation of the endometrium after menstruation [330]. Additionally, the epithelium produces mucin-1 (*MUC1)*. *MUC1* is expressed on the endometrial epithelial cell surface and is regulated by the expression of progesterone, but the embryo is able to significantly decrease its expression at the implantation site [331, 332].Nuclear Factor Kappa B (NF-κB) is a transcription factor known to be involved in the expression and regulation of cytokines like

LIF and IL-6 during the receptivity stage and is inhibited to promote immune tolerance during early pregnancy [333, 334]. NK-κB consists of heterodimers and homodimers, including NF-κB1. It has been previously shown that women experiencing repeated implantation failure (RIF) have a high concentration of NF-κB1 compared to healthy controls [335]

There is now substantial evidence that the composition of the endometrial bacterial microbiome is correlated with the outcome of embryo transfer. To date, there is no defined profile of bacteria in the endometrium. However, the dominance of *Lactobacillus* and a lack of or low abundance of non-*Lactobacillus* bacteria have been associated with successful outcomes of IVF, such as clinical pregnancy, ongoing pregnancy, and live birth [178, 180]. In contrast, an environment with increased diverse bacteria such as *Fannyhessea*, *Bifidobacterium*, *Gardenerella*, *Prevotella,* and *Streptococcus,* and decreased *Lactobacillus* is associated with poor outcomes such as implantation failure and miscarriage [116, 178, 180]. There is also emerging evidence that the microbiome composition may affect processes such as angiogenesis, cell adhesion, and immunomodulation, all of which are needed for successful implantation and receptivity [212, 215].

Conversely, in the vaginal environment, it is well established that the microbiome maintains homeostasis and modulates the immune response through the production of metabolites. In a eubiotic vaginal environment, *Lactobacillus* produces up to 110 mM of lactic acid [156]. This lowers the pH, preventing pathogenic colonisation, maintaining the integrity of the epithelium, and promoting an anti-inflammatory response [160, 161, 336]. High concentrations of acetic acid (120 mM) and succinic acid (20 mM) are produced in

a dysbiotic vaginal microbiome with a low abundance of *Lactobacillus* and a high relative abundance of strict and facultative anaerobes such as *Gardnerella*, *Prevotella*, and *Fannyhessea* [162, 163, 287, 289]. These metabolites and higher pH stimulate the host response towards a pro-inflammatory profile and compromises the vaginal environment.

It is known that *Lactobacillus* and diverse bacteria such as *Gardnerella*, *Prevotella*, and *Fannyhessea* are present in the endometrium. However, little is known about the metabolites they produce, how they interact with endometrial receptivity, and if they have a similar regulatory role as microbiota-associated metabolites in the vaginal environment. Based on past vaginal and endometrial models, L-lactic, D-lactic, acetic, and succinic acids were used to represent different microbial profiles and investigated their impact on receptivity biomarkers [160, 161, 168, 286]. It is important to acknowledge that the concentration of metabolites in the endometrium may be lower than that used in this study due to the low biomass of bacteria [176]. However, this study still provides insight into the role of microbiota-associated metabolites in the endometrium.

3.2 Hypothesis and aims

3.2.1 Hypothesis

Metabolites produced by *Lactobacillus* create an environment conducive to successful embryo implantation by modulating the development of receptivity. The metabolites may modulate the regulation of EMT, the epithelial barrier integrity, and the expression of genes involved in receptivity. Metabolites produced by diverse bacteria will

adversely alter the development of receptivity, resulting in conditions detrimental to embryo implantation.

3.2.2 Aims

Determine the impact of microbiota-associated metabolites on receptivity markers in endometrial epithelium and innate immune cells.

3.3 Methods

3.3.1 Cell culture

Cells were cultured according to the methods outlined in sections 2.1.1 and 2.1.3. THP-1 cells were differentiated before use in experiments according to section 2.1.4.

3.3.2 MTS assays and the concentration of metabolites used in culture

MTS assays were conducted according to section 2.3.2 to determine the viability of cells exposed to different concentrations of metabolites in culture. Table 7 outlines the concentration range at which the cells were viable at over three time points; 4, 6, and 24 hours. The highest concentration was used to treat the cells in all experiments, representing the dominance of either *Lactobacillus* or diverse non-*Lactobacillus* bacteria. Lower concentrations were used in RT-qPCR experiments in addition to the highest concentrations.

3.3.3 Glucose-uptake assay:

The Promega Glucose Uptake-Glo™ Assay kit was used to assess the cell's glucose uptake after treatment with metabolites. This was completed according to the methods outlined in section 2.7.

3.3.4 Transepithelial Electrical Resistance (TEER):

3.3.4.1 Preparation of transwell plates:

Before using the transwell plates (Sigma-Aldrich, cat no. CLS3470), the inserts were coated with fibronectin [337]. Lyophilised human fibronectin (Thermo Fisher Scientific, cat no. 33016015) was resuspended with 5 mL sterile Milli-Q water to reach a 1 mg/mL concentration. To prepare a final concentration of 10 μg/mL, 25 μL of this solution was diluted into 2.475 mL of sterile dPBS. To coat the inserts, 50 μL of the diluted fibronectin was added to each insert, and the plate was gently swirled to ensure the membrane was covered. The inserts were incubated at room temperature for 1 hour. The excess coating solution was removed, and the inserts were washed once with 100 μL of sterile dPBS. The plates were stored at 4°C until use.

3.3.4.2 Optimisation of polarisation and TEER:

Ishikawa and RL95-2 cells were seeded in the coated transwell plates. Before seeding, the basal chamber of the transwell plates was filled with 700 μL of media and

prewarmed at 37°C with 5% CO_2 until needed. Confluent Ishikawa and RL95-2 cells were lifted, and the suspensions were filtered using a 70 μm cell strainer (Sigma-Aldrich, cat no. CLS431751) to remove cell clumps. TEER was tested using two different seeding densities for each cell line. RL95-2 cells were diluted to reach 1×10^5 cells/well and 1.5×10^5 cells/well. Ishikawa cells were diluted to reach 2×10^4 cells/well and 4×10^4 cells/well. 200 μL of each cell suspension was added to the insert. The wells were seeded in triplicates for each seeding density. The cells were incubated at 37°C at 5% CO_2 for 72 hours before beginning TEER measurements. Media in the basal chamber was refreshed every two to three days. Additionally, three wells were filled with media without cells as a blank.

The Millicell® ERS-2 voltohmmeter (Sigma-Aldrich, cat no. MERS00002) was used to measure the resistance across the membrane over 7 days. The meter was calibrated using the STX04 electrode to ensure the meter read 1000 Ω with the electrode connected. The STX01 electrode was sterilised using 80% ethanol and rinsed with dPBS before use. Before measurements were taken, the cells were removed from the incubator and allowed to come to room temperature for 10 minutes. The STX01 electrode was inserted into the well with the long arm in the basal chamber and the short arm inside the insert. The electrode was held at a 90° angle, and the reading was recorded in ohms. The readings were taken in technical triplicates for each well, and the electrode was rinsed with fresh media to prevent carryover.

3.3.4.3 TEER analysis:

The cell monolayer must polarise and form tight junctions between the cells before they are used in further experimentation. To determine if the cells have polarised, the cell-specific resistance was calculated with the following calculation [338];

$$R_{Tissue}\,(\Omega) = R_{Total} - R_{Blank}$$

To determine the TEER values at each time, the following equation was used [339];

$$M_{Area} = Area\ of\ semipermeable\ membrane$$

$$TEER\ (\Omega.cm^2) = R_{Tissue}(\Omega) \times M_{Area}(cm^2)$$

The monolayer was determined to be polarised if the TEER values reached 150 Ω.cm^2. RL95-2 cells failed to polarise after 7 days, and the Ishikawa cells moderately polarised over 7 days but failed to reach the threshold. Thus, further experiments using transwell plates were not conducted.

3.3.5 Wound Healing Assay

3.3.5.1 Wound healing assay and metabolite treatment:

Wound healing assays were completed using the endometrial epithelial cells. Ishikawa and RL95-2 cells were seeded into 6-well plates at 3×10^5 cells/well and incubated at 37°C with 5% CO_2 for 24 hours or until confluent. A wound was created in the monolayer using a 200 μL pipette tip (Neptune, cat no. BT200) and was washed twice with warm dPBS to remove debris and cells [340]. The media was replaced with 2 mL of complete media, including 10% FBS, supplemented with a metabolite. The metabolites were diluted into the media to reach the highest concentration at which the cells were determined viable, as outlined in Table 7. Immediately after the wound was created, the plates were imaged using the EVOS™ FL Colour Imaging system (Thermo Fisher Scientific, cat no. AMF4300). At 24, 48, and 72 hours, the monolayer was washed once with warm dPBS, and the media was replaced with fresh media supplemented with metabolites [341]. At each time point, the plates were imaged.

3.3.5.2 Data analysis and figure generation for wound healing assays:

All images were analysed using ImageJ and the wound healing size tool plugin [342, 343]. The area of the wound was determined, and this was used to calculate wound closure using the following equation [344, 345]:

$$Wound\ Closure\ \% = \left[\frac{A_{t=0h} - A_{t=\Delta h}}{A_{t=0h}}\right] \times 100\%$$

$$A_{t=oh}\ is\ the\ area\ of\ the\ wound\ at\ 0\ hours$$

$$A_{t=\Delta h}\ is\ the\ area\ of\ the\ wound\ after\ h\ hours$$

A two-way ANOVA and Dunnett's tests were performed in GraphPad Prism 9.3.0 for Windows (GraphPad Software, Boston, Massachusetts USA www.graphpad.com) to determine if there was a significant difference between cells cultured with metabolites and untreated cells [345-347].

3.3.6 Immunohistochemical staining for Zonula Occludens (ZO-1)

3.3.6.1 Preparation of coverslips

Immunohistochemical staining was performed using Ishikawa cell lines. RL95-2 cells were not used as they have limited expression of ZO-1 [348]. To ensure the cells adhered adequately to the glass coverslips, 13 mm glass coverslips (Australian Scientific, cat no. 0117580) were coated for one hour with a 50 µg/mL poly-D-lysine solution (Thermo Fisher Scientific, cat no. A3890401). The coverslips were washed three times with sterile Milli-Q water and dried for two hours. The coverslips were stored at 4°C until use.

3.3.6.2 Treatment of cells

The coverslips were placed into 24-well plates using tweezers and seeded with Ishikawa cells at 3×10^5 cells/well. The cells were incubated for 24 hours at 37°C with 5% CO_2 to ensure the cells had adhered to the slides. After 24 hours, the media was removed, and cells were treated with media containing metabolites at the highest concentration the cells were viable, as outlined in Table 7. The cells were cultured for 24 hours at 37°C with 5% CO_2.

3.3.6.3 Fixing and staining

After 24 hours of incubation with the metabolites, the cells were fixed and stained. The media containing metabolites was removed, and the monolayer was washed once with dPBS. Then, 1 mL of cold methanol was added to the wells, ensuring the monolayer was completely covered, and incubated for five minutes at room temperature [349]. The methanol was removed, and the cells were washed five times with dPBS. Non-specific binding sites were blocked with a 3% bovine serum albumin (BSA) (Sigma-Aldrich, cat no. A7906) solution for one hour at room temperature. The blocking solution was removed after the incubation. The primary antibody buffer was prepared using a 0.3% BSA solution with ZO-1 polyclonal antibody (Thermo Fisher Scientific, cat no. 40-2200) diluted at 1:200 [348]. The coverslips were incubated for one hour at room temperature and protected from light. After the incubation, the coverslips were washed five times with dPBS. The secondary antibody solution was prepared using a 0.3% BSA solution with Goat anti-Rabbit IgG (H+L) Cross-Adsorbed Secondary Antibody (Thermo Fisher

Scientific, cat no. A11008) diluted 1:1000 and 2,4-diamidino-2-phenylindole dihydrochloride (DAPI) (Sigma-Aldrich, cat no. 32670) diluted 1:5000 [350]. The secondary solution was added to the wells, and the coverslips were incubated at room temperature for one hour, protected from light. After the incubation, the coverslips were washed with dPBS five times. One drop of ProLong™ Glass Antifade mountant (Thermo Fisher Scientific, cat no. P36982) was placed on a glass microscope slide (ProSciTech, cat no. G300T1), and the coverslip was placed on top to mount the cells. Mounted slides were allowed to cure for 30 minutes at room temperature and stored protected from light at 4°C until confocal microscopy could be performed.

3.3.6.4 Confocal microscopy and data analysis

The fixed slides were imaged using the Nikon A1R inverted confocal microscope. Z-stacks were captured at 20× magnification, with 14 optical sections taken at 0.925 µm intervals per stack. At least three Z-stacks were taken from each slide. The images were analysed using ImageJ. The files were imported using the Bio-Formats plugin, and a Z-projection of the sum fluorescence was generated [351]. This was used to generate the mean fluorescence intensity (MFI). Background fluorescence was determined using cells stained with only the secondary antibody, and the background signal was subtracted from the MFI for the final MFI values [161, 352]. The figures were generated using GraphPad Prism, and unpaired T-tests with Welch's correction were performed to determine significance. The results were also analysed using a one-way ANOVA and Dunnett's multiple comparison tests.

3.3.7 RNA extraction and Real-Time- Quantitative PCR (RT-qPCR)

The cells were cultured according to section 2.4.1 and treated with the concentrations of metabolites outlined in Table 15. RNA extraction and cDNA synthesis were completed using the methods stated in section 2.6.1. cDNA was used to conduct RT-qPCR (section 2.6.2) using the primers listed in Table 16. *LIF* and *MUC1* primers were only used for epithelial cells as they are primarily expressed by those cells in the endometrium.

Table 15. The concentration range of microbiota-associated metabolites used to treat cells in RT-qPCR experiments.

Cell Line	Metabolites	Concentrations (mM)
Ishikawa	L-Lactic acid	0, 5, 10, 25
	D-Lactic acid	0, 5, 10
	Acetic acid	0, 5, 10
	Succinic acid	0, 2.5, 5
RL95-2	L-Lactic acid	0, 5, 10, 15
	D-Lactic acid	0, 5, 10
	Acetic acid	0, 2.5, 5
	Succinic acid	0, 2.5, 5
NK-92	L-Lactic acid	0, 2.5, 5
	D-Lactic acid	0, 2, 4
	Acetic acid	0, 2.5, 5
	Succinic acid	0, 1, 2
THP-1	L-Lactic acid	0, 5, 10, 15
	D-Lactic acid	0, 5, 10
	Acetic acid	0, 2.5, 5
	Succinic acid	0, 2.5, 5

Table 16. Primer sequences for markers of receptivity and cellular function. All primer pairs were ordered from Integrated DNA Technologies (IDT, Singapore).

Gene	**Role**		**Sequence (5'-3')**	**Reference**
Leukemia Inhibitory Factor (*LIF*)	Embryo attachment and invasion	Forward	TCTGAAGTGCAGCCCATAATGAAG	[353]
		Reverse	TATGGCACAGGTGGCGTTG	
Vascular Endothelial Growth Factor A (*VEGFA*)	Regulation of implantation and vascular changes	Forward	GCCTTCGCTTACTCTCAC	[283]
		Reverse	GCTGCTTCTTCCAACAATG	
Nuclear Factor Kappa B Subunit 1 (*NFKB1)*	Control of immune cells accumulation	Forward	AACTCTCAACAAAATGCCCCA	[354]
		Reverse	CTGAGCACCTTTGGATGCACT	
Mucin Short Variant S1 (*MUC1*)	Embryo apposition and adhesion	Forward	GTGCCCCCTAGCAGTACCG	[355]
		Reverse	GACGTGCCCCTACAAGTTGG	
Homeobox A10 (*HOXA10*)	Endometrial receptivity	Forward	GCCCTTCCGAGAGCAGCAAAG	[356]
		Reverse	AGGTGGACGCTGCGGCTAATCTCTA	
Transforming Growth Factor Beta Receptor 1 (*TGFBR1*)	Cell proliferation and apoptosis	Forward	GGCTTTTCTCCACATGCTTAGG	[357]
		Reverse	GGCAACAGAGATCACCTGTAGACA	

3.4 Results:

3.4.1 Endometrial epithelial cells and innate immune cells are viable when cultured with microbiota-associated metabolites

This study aimed to represent the endometrial environment and microbiome using an *in vitro* model. Microbiota-associated metabolites, rather than bacteria, were used to mimic the microbiome and aimed to determine the impact of bacterial metabolites on receptivity. MTS assays were conducted to determine each cell lines' viability within a biologically relevant range of L-lactic, D-lactic, acetic, and succinic acids [162]. The metabolites were considered non-cytotoxic if the treated cells remained ≥80% viable, over the three time points (4, 6, and 24 hours). This was completed for each cell line prior to carrying out further experimentation. In culture, Ishikawa cells were viable at ≤ 25 mM L-lactic acid, ≤ 10 mM D-lactic acid and acetic acid, and ≤ 5 mM succinic acid (Figure 5a). Unlike Ishikawa cells, RL95-2 cells were viable at ≤ 15 mM L-lactic acid, ≤ 10 mM D-lactic acid, and ≤ 5 mM acetic and succinic acid (Figure 5b). As for the innate immune cells, NK-92 cells were viable at much lower concentrations than epithelial cells. NK-92 cells were viable at ≤ 5 mM L-lactic acid, ≤ 4 mM D-lactic acid, ≤ 5 mM acetic acid, and ≤ 2 mM succinic acid (Figure 5c). Differentiated THP-1 cells were viable at ≤ 15 mM L-lactic acid, ≤ 10 mM D-lactic acid, ≤ 5 mM acetic acid, and ≤ 5 mM succinic acid (Figure 5d). These concentrations were chosen and used in all other experiments. Lower concentrations of metabolites were also included in RT-qPCR experiments. The data from these experiments is shown in Appendix 2.

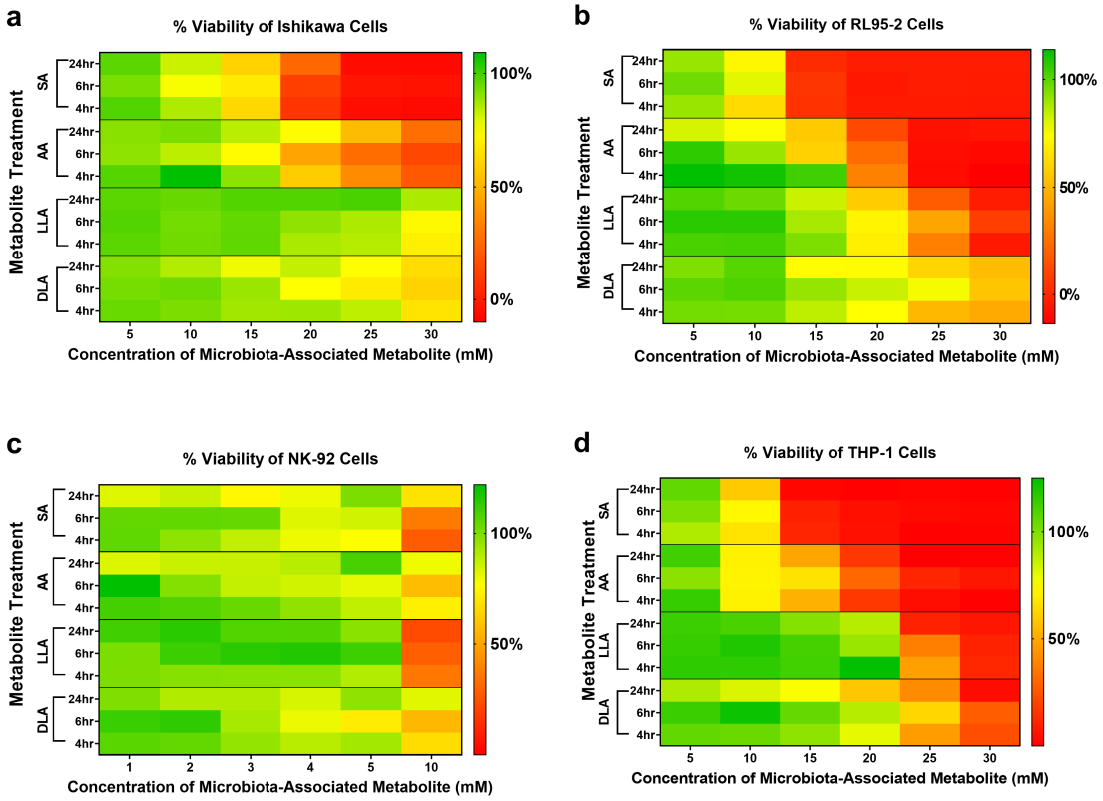


Figure 5. The viability (%) of endometrial epithelial cells and innate immune cells treated with microbiota-associated metabolites. (a) Mean viability of Ishikawa cells. (b) Mean viability of RL95-2 cells. (c) Mean viability of NK-92 cells. (d) Mean viability of THP-1 cells. Metabolites are listed on the left y-axis; DLA represents D-lactic acid, LLA represents L-lactic acid, AA represents acetic acid, and SA represents succinic acid. The incubation period in hours is indicated on the left y-axis. The viability of the cells is represented by a gradient from 0% viability (red) to ≥100% viable (green). The concentrations of each metabolite are indicated on the x-axis. n = 3.

3.4.2 Succinic acid decreases glucose uptake in NK-92 cells

Glucose metabolism is essential for the decidualisation of the endometrium and its ability to facilitate attachment [358]. Accordingly, how microbiota-associated metabolites impact the cells' glucose uptake was assessed. The cells were cultured for 24 hours with either L-lactic, D-lactic, acetic or succinic acid using the highest viable concentrations as reported in Table 7. NK-92 cells cultured with 2 mM succinic acid significantly decreased the glucose uptake ($p=0.021$) ($p=0.99$ with Dunnett's multiple comparisons test) compared to untreated control cells by -1.6 fold (Figure 6c). No significant change was observed with the other metabolites. Likewise, Ishikawa, RL95-2, and THP-1 cells cultured with the metabolites did not show significant changes in glucose uptake (Figure 6).

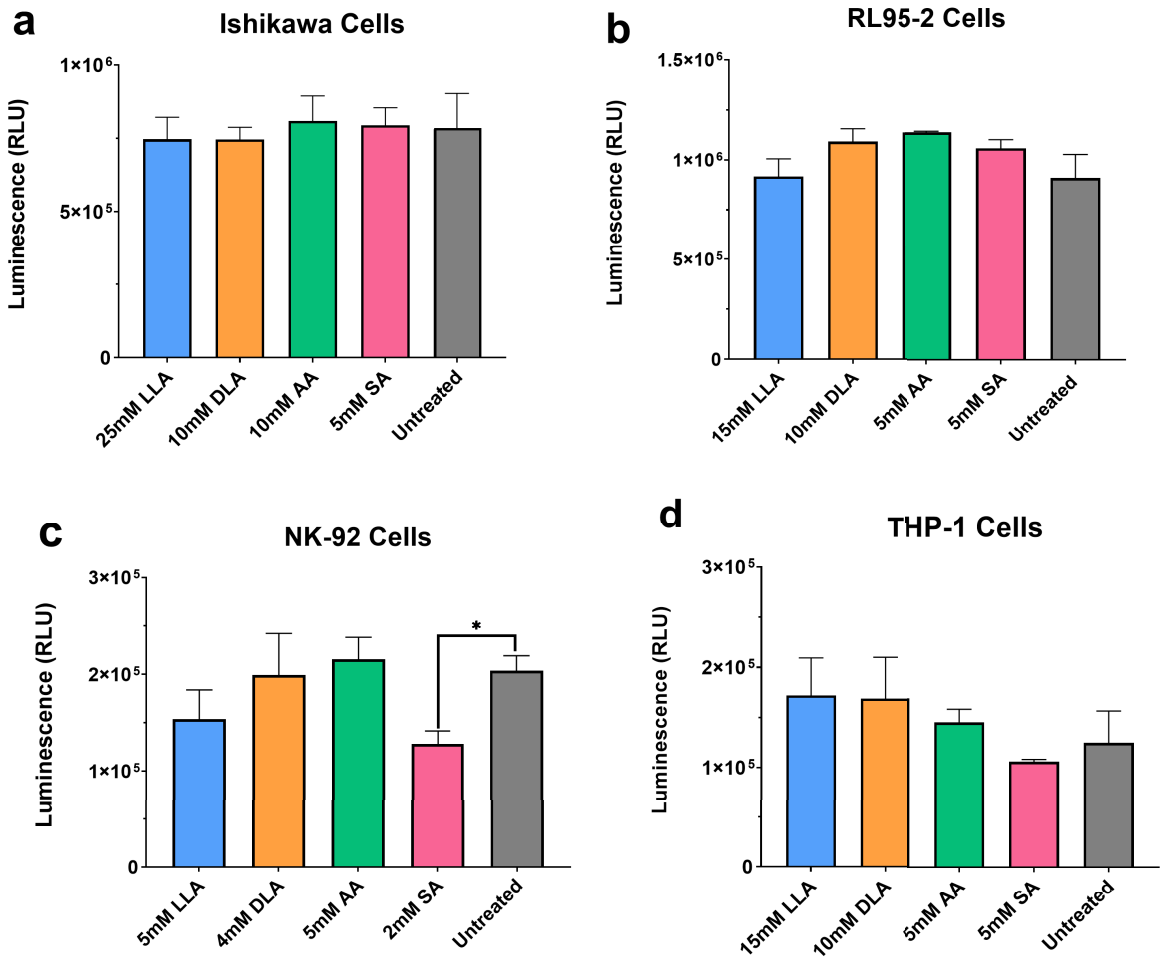


Figure 6. The glucose uptake of endometrial epithelial cells and innate immune cells after treatment with microbiota-associated metabolites. (a) Glucose uptake of Ishikawa cells. (b) Glucose uptake of RL95-2 cells. (c) Glucose uptake of NK-92 cells. (d) Glucose uptake of THP-1 cells. Glucose uptake was determined using the Promega glucose uptake-Glo™ assay. DLA represents D-lactic acid, LLA represents L-lactic acid, AA represents acetic acid, and SA represents succinic acid. The y-axis shows luminescence, and the scale of each y-axis is different. Luminescence is proportional to glucose uptake and is measured in relative light units (RLU). The data presented shows the mean ± SEM (n=3). * represents $p \leq 0.05$, analysed by unpaired T-tests with Welch's correction.

3.4.3 L-lactic acid decreases epithelial migration in Ishikawa and RL95-2 cells

Migration and the EMT/MET are essential for developing the endometrium through the menstrual cycle and during implantation [27]. Thus, a wound-healing assay was used to assess the migration of endometrial epithelial cells when cultured with microbiota-associated metabolites. The epithelial cells were grown to confluency, and a wound was created and allowed to heal over 72 hours while the cells were exposed to L-lactic, D-lactic, acetic, and succinic acids. At 48 hours, Ishikawa cells cultured with 25 mM of L-lactic acid showed significantly less wound closure at 38.1% compared to the 56% wound closure of untreated cells ($p=0.037$) (Figure *7*a). Interestingly, at 72 hours, RL95-2 cells cultured with 15 mM of L-lactic acid showed significantly less wound closure at 36.8% compared to the 68% wound closure of untreated cells ($p=0.026$) (Figure *7*c). In both cell lines, there was a trend of decreased wound closure when treated with D-lactic acid, but this was not statistically significant. Acetic and succinic acids did not significantly impact wound healing in either cell line.

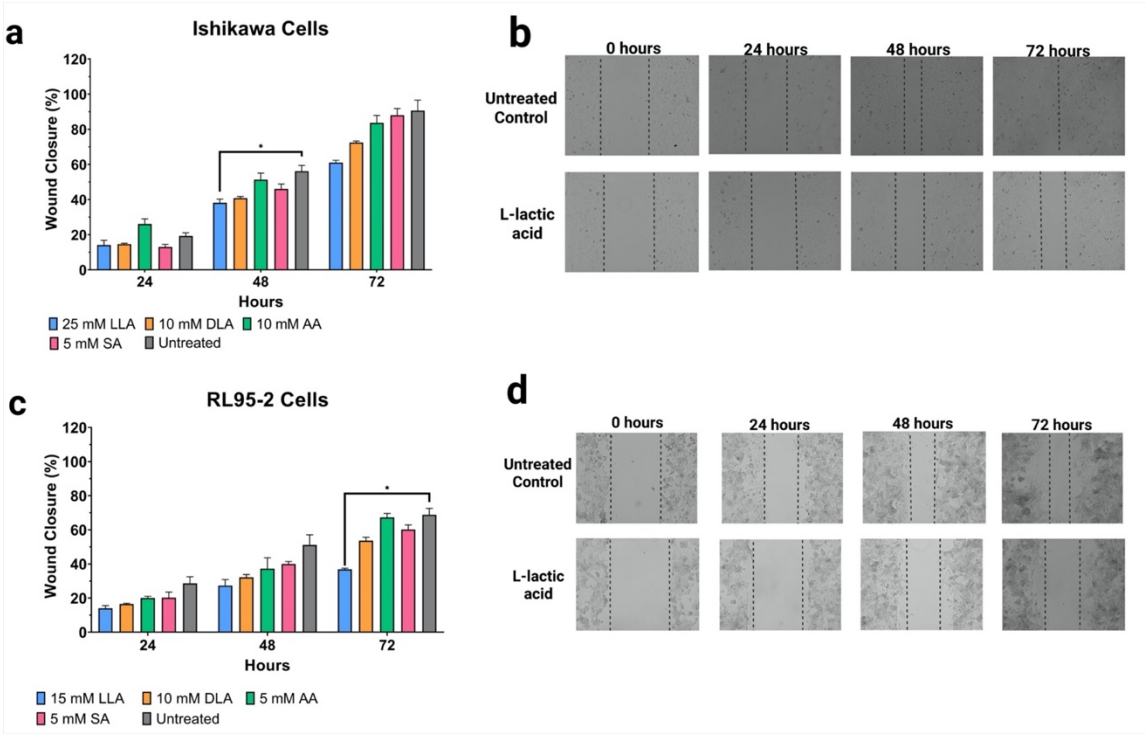


Figure 7. The wound closure of endometrial epithelial cells treated with microbiota-associated metabolites. (a) Percentage wound closure of Ishikawa cells treated with metabolites. (b) Representative images of wound closure in Ishikawa cells treated with L-lactic acid and the untreated control. (c) Percentage wound closure of RL95-2 cells treated with metabolites. (d) Representative images of wound closure in RL95-2 cells treated with L-lactic acid and the untreated control. DLA represents D-lactic acid, LLA represents L-lactic acid, AA represents acetic acid, and SA represents succinic acid. Images were taken 24, 48, and 72 hours after the wound was made. The graphs represent the mean percentage of wound closure ± SEM. * represents $p \leq 0.05$, analysed by Dunnett's multiple comparisons tests. n = 3. Created using BioRender.com.

3.4.4 D-lactic acid and acetic acid decrease the expression of ZO-1 in Ishikawa cells

ZO-1 is an important, stably expressed protein in the endometrium; its expression is necessary for tissue integrity and receptivity. RL95-2 cells have limited expression of ZO-1 [348]. Therefore, only Ishikawa cells were used in this experiment. The cells were cultured for 24 hours with microbiota-associated metabolites, and ZO-1 expression was evaluated using confocal microscopy. The expression of ZO-1 was significantly decreased when Ishikawa cells were cultured with 10 mM D-lactic acid (-2.1 fold) ($p=0.0038$) ($p=0.014$ with Dunnett's multiple comparisons test) and 10 mM acetic acid (-1.93 fold) ($p=0.0045$) ($p=0.02$) (Figure 8a). L-lactic acid did not significantly decrease ZO-1 expression when compared to untreated controls (Figure 8a). There was no significant change in the expression of ZO-1 levels in Ishikawa cells cultured with succinic acid (Figure 8a).

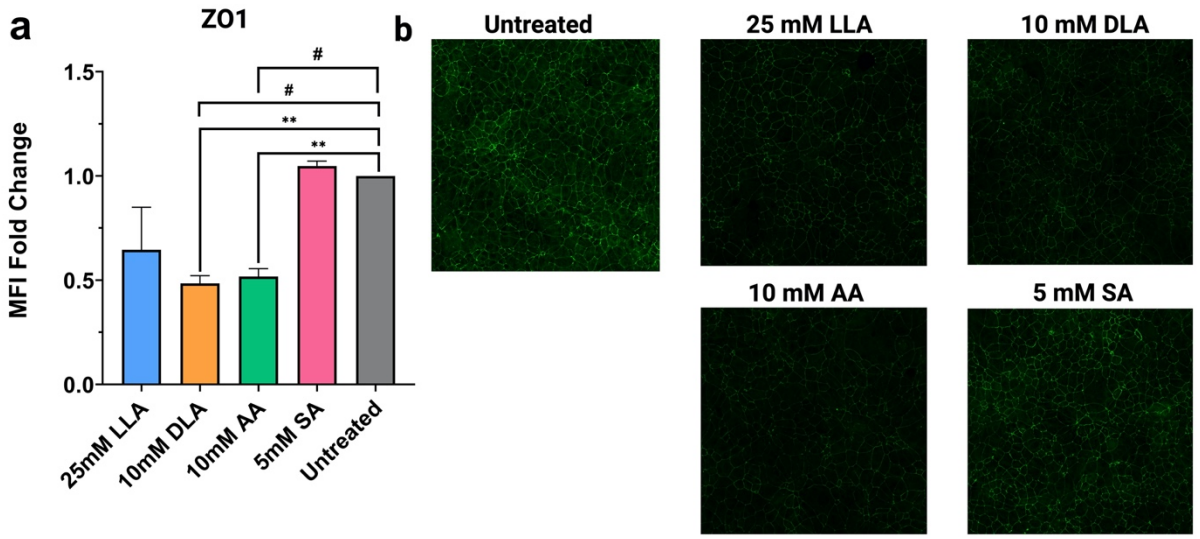


Figure 8. The decreased expression of ZO-1 in Ishikawa cells after treatment with microbiota-associated metabolites. (a) The mean fluorescence intensity (MFI) is represented as a fold change comparing treated cells to untreated cells. (b) Expression of ZO-1 by Ishikawa cells was visualised using confocal microscopy. DLA represents D-lactic acid, LLA represents L-lactic acid, AA represents acetic acid, and SA represents succinic acid. Representative images show untreated cells and cells treated with D-lactic and acetic acid. The data shows mean ± SEM (n = 3). ** represents $p \leq 0.01$, analysed by unpaired T-tests with Welch's correction . # represents $p \leq 0.05$, analysed by Dunnett's multiple comparisons test. Created using Biorender.com.

3.4.5 Ishikawa and RL95-2 cells do not polarise

During the development of receptivity, when endometrial epithelium undergoes EMT, there is a loss of tight junctions. Thus, this study aimed to determine if microbiota-associated metabolites impact polarisation. However, as shown in Figure 9, Ishikawa cells only moderately polarised, failing to reach higher TEER values, and RL95-2 cells did not polarise. As a result of this, further TEER experiments were not completed.

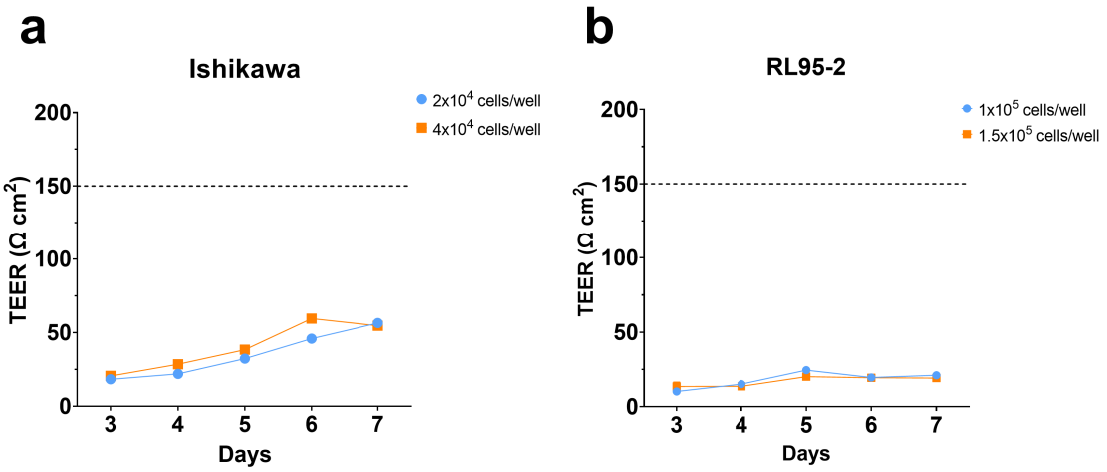


Figure 9. Transepithelial electrical resistance of endometrial epithelial cells. (a) TEER values from Ishikawa cells seeded at 2×10^4 cells/well and 4×10^4 cells/well. (b) TEER values from RL95-2 cells seeded at 1×10^5 cells/well and 1.5×10^5 cells/well. TEER readings were initially taken three days after seeding and then every day until seven days after seeding.

3.4.6 Microbiota-associated metabolites downregulate the expression of involved in receptivity in both endometrial epithelial and innate immune cell lines.

There are several key genes involved in the development of receptivity. In this study, the expression of *TGFBR1, HOXA10, NFKB1, VEGFA, LIF,* and *MUC1* was assessed. All cells were cultured with L-lactic, D-lactic, acetic, and succinic acids in a range of doses at which they were viable in culture, as outlined in Table 15. RL95-2 cells showed a significant -3.6 log_2 fold decrease in *TGFBR1* mRNA when treated with 15 mM L-lactic acid (p=0.011) (p=0.0125 with Dunnett's multiple comparisons test) (Figure 10a). At 10 mM L-lactic acid, a -2.9 log_2 fold decrease was also observed (p= 0.013) (p=0.058) (Figure 10a). There was no significant change in the expression of *TGFBR1* mRNA in Ishikawa cells (Appendix 2, Figure 31). However, Ishikawa cells treated with 10 mM of D-lactic acid showed a significant -2.3 log_2 fold decrease in *VEGFA* mRNA expression (p=0.013) (p=0.044) (Figure 10d). Additionally, when Ishikawa cells were cultured with 10 mM of acetic acid, there was a significant -2.5 log_2 fold decrease in *LIF* mRNA (p=0.0050) (p=0.063) (Figure 10e). Interestingly, when analysed with Dunnett's multiple comparisons test, Ishikawa cells treated with 5 mM LLA showed a significant decrease in *LIF* expression, with a -3.1-log_2 fold change (p=0.012). This was not significant when analysed by an unpaired T-test with Welch's correction (p=0.075). Dunnett's multiple comparisons test also found a significant log_2 -2.5 fold change (p=0.026) in *LIF* expression by Ishikawa cells treated with 10 mM D-lactic acid compared to untreated controls. This was not significant when analysed using a t-test (p=0.10).

There was no significant difference in the expression of *LIF* and *VEGFA* in RL95-2. Compared to untreated controls, there was no significant difference in *NFKB1*, *HOXA10* and *MUC1* expression in Ishikawa or RL95-2 cells treated with metabolites (Appendix 2, Figure 31 and Figure 32).

Similar to RL95-2, NK-92 and THP-1 cells showed significant downregulation of *TGFBR1* (Figure 10a and b). Treatment with 2.5 mM acetic acid resulted in a -1.6 $\log_2$ fold decrease in *TGFBR1* mRNA expression in NK-92 cells (p=0.018) (p=0.55 with Dunnett's multiple comparisons test). Additionally, a -2.6 $\log_2$ fold decrease in *TGFBR1* mRNA in THP-1 cells was seen when cultured with 2.5 mM succinic acid (p=0.015) (p=0.081). NK-92 cells also showed a -1.4 $\log_2$ fold downregulation of *NFKB1* when cultured with 2.5 mM acetic acid (p=0.012) (p=0.66) (Figure 10f). There was no significant difference in mRNA expression of *NFKB1* in THP-1 cells compared to untreated controls (Appendix 2, Figure 34). Likewise, compared to untreated controls, there was no significant difference in the expression of VEGFA and HOXA10 in NK-92 or THP-1 cells treated with metabolites (Appendix 2, Figure 33 and 33).

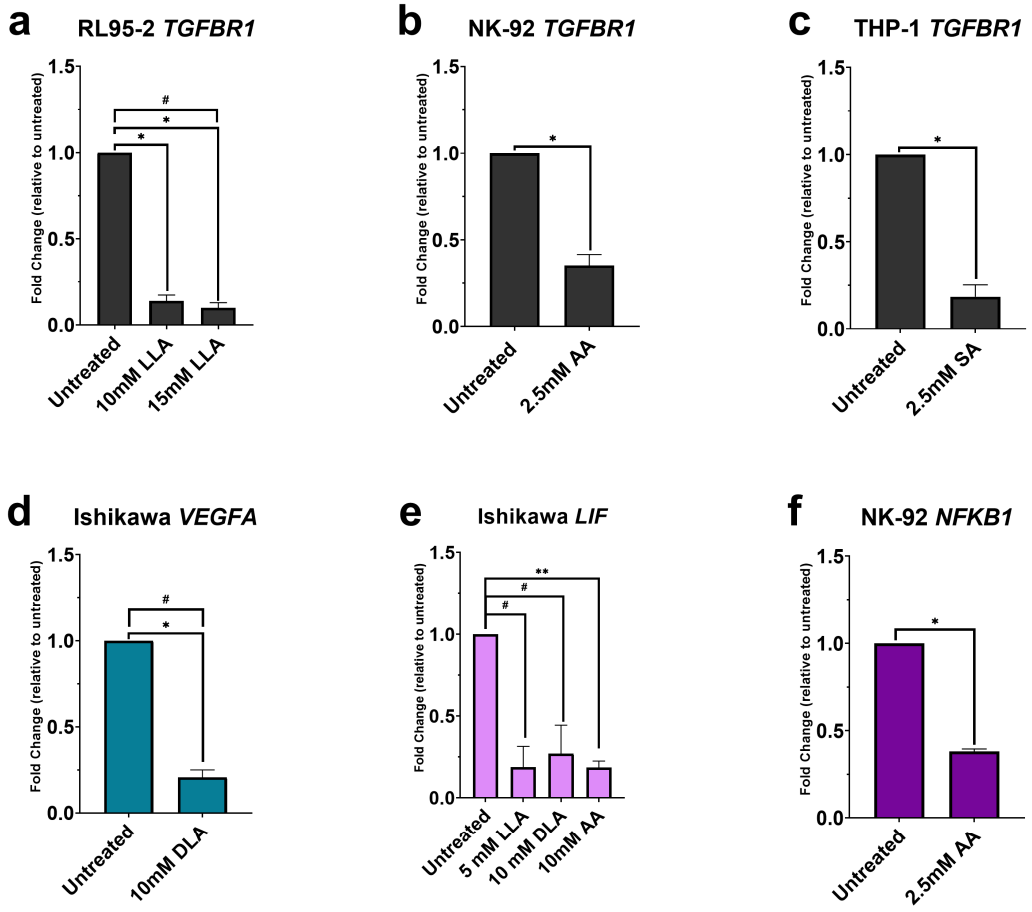


Figure 10. Relative gene expression of genes involved in receptivity compared to untreated cells. DLA represents D-lactic acid, LLA represents L-lactic acid, AA represents acetic acid, and SA represents succinic acid. (a) Fold change of *TGFBR1* in RL95-2 cells treated with LLA. (b) Fold change of *TGFBR*1 in NK-92 cells treated with AA. (c) Fold change of TGFBR1 in THP-1 cells treated with SA. (d) Fold change of *VEGFA* in Ishikawa cells treated with DLA. (e) Fold change of *LIF* in Ishikawa cells treated with AA. (f) Fold change of *NFKB1* in NK-92 cells treated with AA. Gene expression was normalised to the reference genes and expressed as fold change compared to the untreated cells using the comparative C_t method. The data shows the mean ± SEM (n = 3). * represents $p \leq 0.05$, ** represents $p \leq 0.01$, analysed by unpaired T-tests with Welch's correction. # represents $p \leq 0.05$, analysed by Dunnett's multiple comparisons test.

3.5 Discussion:

Endometrial receptivity occurs during the luteal stage of menstrual cycle and is the period of time when the endometrium has developed adequately enough to allow the successful attachment and implantation of the blastocyst [6]. A lack of endometrial receptivity is thought to contribute to the failure of IVF treatment. Current evidence in the literature suggests that abnormalities in the development of receptivity are associated with the endometrial microbiome [212, 215]. In the vaginal environment, it has been established that microbiota-associated metabolites have an important role in maintaining homeostasis [161, 359]. Thus, this study aimed to investigate the role of microbiota-associated metabolites in developing receptivity using a cell culture model incorporating metabolites rather than bacteria.

This study investigated the viability of endometrial epithelial cell lines and innate immune cell lines in the presence of L-lactic, D-lactic, acetic, and succinic acids. *Lactobacillus* was represented using L-lactic and D-lactic acid, whilst acetic and succinic acids were used to represent diverse bacteria. There is somewhat limited knowledge on the concentration of microbiota-associated metabolites in the endometrium. However, the concentration range based on the metabolomic profiles of bacteria found in the endometrium. *Lactobacillus* can produce up to 30-45 mM of lactic acid in culture [162]. Whereas, diverse bacteria can produce up to 65 mM acetic acid and 18 mM acetic acid [162]. In line with other cell culture models of the cervicovaginal environment, MTS assays were used to determine non-cytotoxic concentrations of the metabolites, which could then be used to represent differing microbiome profiles [160, 168]. If the treated

cells showed ≥80% viability compared to the untreated cells, the concentration used was considered to be non-cytotoxic and the highest viable concentration was used in further experiments to represent microbiota [309, 310]. It was confirmed that the concentrations used in this study did not decrease the pH of cell culture media in standard cell culture conditions. The Ishikawa, RL95-2, and THP-1 cells remained viable at higher L-lactic and D-lactic acid concentrations between 10-25 mM (Figure 5). This result for THP-1 cells was consistent with the literature as they have been shown to tolerate a similar concentration of lactic acid in culture [360]. As for Ishikawa and RL95-2 cells, both are derived from adenocarcinomas and may be able to tolerate a high concentration of lactic acid, as tumours create a high lactic acid environment through aerobic glycolysis [361]. Additionally, endometrial epithelial cell lines may tolerate a high lactic acid concentration, as the blastocyst also creates a high lactic acid environment through aerobic glycolysis [362]. NK-92 cells tolerated lower concentrations of both lactic acids between 4-5 mM. This is consistent with past research, in which L-lactic acid significantly decreased the viability of NK cells in increasing concentrations, and exposure to lactic acid resulted in apoptosis [363, 364]. All cell lines were viable in lower concentrations of acetic acid (5-10 mM) compared to L-lactic and D-lactic acid (Figure 5). This was not unexpected as acetic acid has been shown previously to induce cell death in a concentration-dependent manner [365]. Similarly, when exposed to succinic acid, all cell lines were only viable between 2-5 mM (Figure 5). Succinic acid has been proposed as a treatment for endometrial cancer due to its ability to induce apoptosis, and it has also been shown to induce apoptosis in immune cell lines; thus, this result was not unexpected [366, 367]. This could also provide insight into the potential detrimental effect of metabolites produced by diverse microbiota in the endometrium. Increased apoptosis and cell death in the endometrium are associated with out-of-phase endometrial tissue, where

the tissue has not developed at the expected rate and is associated with implantation failure [368].

Glucose is essential in the endometrium, and glucose metabolism is known to be enhanced during receptivity and in decidualisation of the stromal tissue [369]. Additionally, endometrial cells store glycogen during the receptivity stage, with decreased stored glycogen seen in women experiencing infertility [370]. Glucose transporters (*GLUT*) are expressed throughout the endometrium, and down-regulation of *GLUT4* has been reported when epithelial cells are exposed to lactic acid in an acidic environment [283, 369]. Thus, this study investigated the impact of microbiota-associated metabolites on the glucose uptake of endometrial epithelial cells and innate immune cells. The glucose uptake of the Ishikawa, RL95-2, and THP-1 cells did not significantly differ from untreated controls when treated with L-lactic, D-lactic, acetic or succinic acids (Figure 6). There was a significant decrease in the glucose uptake of NK-92 cultured with succinic acid (Figure 6). However, this result was not seen when the data was analysed using Dunnett's multiple comparisons test. NK cells are primarily fuelled by glucose, and NK cell function is impaired in low-glucose environments like the tumour microenvironment [371]. Yan et al. (2022) determined that in the endometrium, glucose metabolism is a driving force in the regulatory role of NK cells, with the restriction of glycolysis increasing the expression of VEGFA [372]. However, in the analysis of mRNA expression, NK-92 cells exposed to succinic acid did not show significantly different expression of *VEGFA* compared to untreated controls in this study (Appendix 2, Figure 33). This may show that succinic acid produced by diverse bacteria in the endometrium can decrease glucose uptake in NK cells without increasing *VEGFA* expression. It may

indicate that the cells can still take up enough glucose for glycolysis, not affecting *VEGFA* expression, but could instead affect gluconeogenesis.

Further investigation, such as examining genes involved in glucose uptake or gluconeogenesis, such as glucose transporters and gluconeogenic enzymes like glucose-6-phophatase could provide more insight [373]. Additionally, analysis of secreted *VEGFA* by NK cells is necessary, as only mRNA expression was assessed in this study. It is important to note that Yan et al. (2022) used decidual NK cells collected from primary tissues to demonstrate the increased expression of VEGFA when glycolysis was inhibited [372]. Decidual NK cells are the largest population of maternal immune cells in the endometrium and have distinct phenotypic differences from peripheral NK cells [40]. Whereas the NK-92 cells used in this study are more cytotoxic, displaying characteristics of activated NK cells [302]. Thus, these cell type differences could explain the difference between this study and Yan et al. (2022), and future studies may benefit from using primary cells.

During the development of receptivity and implantation, the endometrial epithelium is thought to undergo EMT to enable migration around an implanting embryo [27]. Given the importance of migration during implantation, this study aimed to determine the impact of microbiota-associated metabolites on the endometrial epithelium's migratory capacity. Ishikawa and RL95-2 cells showed significantly lower wound healing rates when exposed to L-lactic acid (Figure *7*). It is possible that L-lactic acid produced by *Lactobacillus* in the endometrium may not aid in the migration or can potentially prevent the migration of epithelial cells. This could also provide some insight into the association between *Bifidobacterium,* another L-lactic acid-producing bacteria*,*

and adverse outcomes of IVF [178, 180, 374]. This result was unexpected, as it has been demonstrated that exposure to the soluble products of *Gardnerella vaginalis* decreases wound healing significantly, and the soluble products of *Lactobacillus iners* do not generate a significant change in cell migration [375]. However, it should be considered that bacteria-produced soluble products include additional metabolites and other by-products that could have also impacted this result. Additionally, the same effect was not seen in cells treated with D-lactic acid, which is exclusively produced by bacteria. Thus, this should be interpreted cautiously. Furthermore, lactic acid spheres have been used as a model embryo, and their use in culture has shown that decidualised stroma migrates towards the source of lactic acid [283]. In the same study, Ishikawa cells treated with lactic acid and cultured in an acidic environment showed increased expression of Snail Family Transcriptional Repressor 1 (*SNAI1)*, a marker of EMT [283]. Thus, it was proposed that lactic acid may aid in receptivity to an embryo and in EMT. While this result differs from what was observed in this study, it may be due to methodological differences. Gurner et al. (2022) created a gradient of lactic acid and a low pH using the lactic acid spheres, whereas lactic acid was evenly dispersed in the culture media in this wound healing assay [283]. Thus, migration may be affected differently at lower or different concentrations of lactic acid and in combination with a low pH. It may be beneficial to investigate additional concentrations of L- and D-lactic acids in the future, in conjunction with a decreased pH.

Furthermore, this study investigated the mRNA expression of *HOXA10* in RT-qPCR experiments, as it is a key factor in EMT regulating E-cadherin. However, L-lactic acid treatment of Ishikawa or RL95-2 cells did not change their expression compared to untreated controls (Appendix 2, Figure 31 and 31). It is not the only marker of EMT/MET,

and it may be beneficial to assess additional markers of EMT, like *SNAI1,* to gain a broader understanding of the effect of lactic acid [283]. Additionally, unlike previous wound healing assay methods, the Ishikawa and RL95-2 cells were not serum-starved [340, 341, 344]. As this prevents proliferation, serum-starving could improve the results seen in this assay and may more clearly demonstrate the effect of D-lactic acid, which did not reach significance in this study.

During the development of receptivity and EMT, important changes occur in tight junction proteins, adherens junctions, and cell polarity. However, ZO-1 is stably expressed, which is thought to have a role in maintaining cell-cell linkages during receptivity and implantation [376]. Thus, this study aimed to investigate the impact of microbiota-associated metabolites on ZO-1 expression by Ishikawa cells. RL95-2 cells were not used for this, as they have limited ZO-1 expression [348]. Treatment with D-lactic acid and acetic acid significantly decreased the expression of ZO-1 in Ishikawa cells (Figure 8). L-lactic acid showed a trend towards decreased ZO-1 expression, but this was not significant. There was no change in ZO-1 expression when treated with succinic acid (Figure 8). This was surprising as in the vaginal environment, L-lactic acid has been demonstrated to upregulate the expression of tight junction proteins like claudin-1 and claudin-4, and ZO-1 is associated with L-lactate dehydrogenase abundance (the enzyme used by *Lactobacillus* to make L-lactic acid) [161]. However, this difference could be due to the differences in vaginal and endometrial tissue. The down-regulation observed when cells were treated with D-lactic and acetic acids may indicate that microbiota-associated metabolites can impact the stability of the endometrial epithelium during receptivity and implantation. Furthermore, various infection models with *Escherichia coli*, *Neisseria gonorrhoea,* and *Chlamydia trachomatis* resulted in the down-regulation and

reorganisation of ZO-1 [271, 377, 378]. This suggests that bacteria and their metabolites could adversely impact the development of receptivity and implantation. However, this should be interpreted cautiously as TEER experiments using Ishikawa cells could not be completed (Figure 9). TEER measures the electrical resistance across a membrane and can provide insight into the function and permeability of the epithelial layer as a barrier. Western blotting should also be used to quantify ZO-1 expression in the treated cells compared to the untreated cells. This could also provide a better understanding of how metabolites can affect the stability of the barrier and the expression of ZO-1. Additionally, endometrial epithelial cells can be treated with estrogen or progesterone to mimic the menstrual cycle. This has been shown to alter the polarity of the cells via desmosomes [379-381]. In future, the impact of microbiota-associated metabolites on the organisation of desmosomes could be investigated alongside ZO-1. However, it is important to acknowledge that, hormone treatment replicating the secretory phase, decreases the polarity of Ishikawa cells [379-381]. Likewise, the development of endometrial organoid models could be used in future experiments to replicate a more accurate representation of the endometrium [382].

In the endometrium, TGF-β signalling is involved in elements of receptivity, including the regulation of epithelial proliferation and decidualisation [383, 384]. Microarray analysis showed that the down-regulation of *TGFBR1* expression is associated with dysregulated decidualisation and endometrial disorders, including implantation failure [324]. Thus, this study investigated the impact of metabolites on the expression of *TGFBR1*. The results showed a significant decrease in mRNA expression of *TGFBR1* by RL95-2 cells treated with L-lactic acid (Figure 10). Interestingly, in mice models, the conditional knockout of *TGFBR1* caused mice to develop oviductal

diverticula, defective development of uterine smooth muscle, and enhanced endometrial epithelial cell proliferation [325, 384]. Further, the conditional knockout of *TGFBR1* has also been implicated in defects of uterine vascularisation, implantation, and the recruitment of NK cells to the uterus [385]. Thus, with this downregulation in epithelial cells, it is possible that microbiota-associated metabolites may adversely alter the structure of the endometrium and could detrimentally impact the development of receptivity. This was surprising because this result was only seen in RL95-2 cells treated with L-lactic acid rather than metabolites representing diverse bacteria. However, a mouse model of colorectal cancer demonstrated increased *Lactobacillus* species in mice with dysfunctional TGF-β signalling [386]. This should be interpreted cautiously as this study used heterozygous transgenic mice for downstream targets of *TGFB,* Suppressor of Mothers against Decapentaplegic *(SMAD)* and Spectrin Beta, Non-Erythrocytic 1 *(SPTBN1)* rather than *TGFBR1* [386].

Furthermore, there was a decrease in the mRNA of *TGFBR1* in NK-92 cells treated with acetic acid and THP-1 cells treated with succinic acid (Figure 10). However, this was not significant when the data was analysed with Dunnett's multiple comparison tests. *TGFBR1* is an important cytokine in the function of NK cells and macrophages, with an immunosuppressive effect on both cell types [387]. Thus, the downregulation of *TGFBR1* mRNA could indicate that acetic acid and succinic acid may affect the immunomodulation of the endometrium during receptivity. Overall, it is clear that microbiota-associated metabolites impact *TGFBR1* and could impact the signalling pathway, having detrimental impacts on the endometrial epithelium and receptivity. However, further investigation of downstream factors involved in the TGF-β pathway is required.

VEGFA and *LIF* are two important genes in the development of receptivity. *VEGFA* is primarily thought to promote angiogenesis and regulation of implantation [330]. *LIF* has a role in inducing implantation and developing the endometrial structure [328, 329]. The aberrant expression of both genes and their proteins has been associated with implantation failure [213, 327, 388-390]. Thus, this study investigated the impact of the metabolites on the expression of these genes in endometrial epithelial cells and innate immune cells. Ishikawa cells treated with D-lactic acid had a significant downregulation of *VEGFA* mRNA levels when compared to untreated controls (Figure 10). This suggests that D-lactic acid produced by bacteria can adversely impact its expression. This result was unexpected as *Lactobacillus* abundance is positively correlated with the expression of *VEGFA* [213]. Additionally, Gurner et al. (2021), exposed Ishikawa cells to lactic acid and an acidic pH which subsequently increased the expression of *VEGFA* mRNA [283]. Furthermore, Ishikawa cells treated with L-lactic, D-lactic, and acetic acids showed significant downregulation in the expression of *LIF* compared to the untreated controls (Figure 10). Decreased expression of *LIF* in the presence of acetic acid was not unexpected as *LIF* has been shown to negatively correlate with *Acinetobacter* and *Gardnerella*, both of which produce acetic acid [213]. But decreased expression of *LIF* in the presence of L-lactic and D-lactic acid was unexpected. Otsugu et al. (2025) demonstrated that lactic acid can induce *LIF* expression in endometrial epithelial cells [391]. These results may indicate that metabolites produced by diverse bacteria in the endometrium could adversely impact the development receptivity by downregulating expression of *VEGFA* and *LIF*. But it is important to consider methodological differences in this study compared to the literature. Gurner et al. (2021) were treated with hormones before use. Both *VEGFA* and *LIF* are regulated by the expression of estrogen and

progesterone [392-394]. In this study, Ishikawa cells were not hormonally primed prior to their use, which may have impacted their response to treatment with microbiota-associated metabolites. Additionally, increased *LIF* expression in Otsugu et al. (2025) was observed in cells cultured at a low pH of 5.6, and not at higher pH values such as 6.6 and 7.4 [391]. Thus, as Ishikawa cells in this study were maintained at a pH of 7.4 in standard cell culture conditions, this may have impacted their response to lactic acids and *LIF* expression.

NF-κB is an essential transcription factor expressed in the endometrium and is involved in expressing and regulating cytokines like *LIF* during the receptivity stage [333, 334]. It has been previously shown that those who experience repeated implantation failure have altered expression of NF-κB1, compared to controls, suggesting that dysregulated inflammation has a role in implantation failure [335, 395]. Therefore, this study assessed the impact of microbiota-associated metabolites on *NFKB1* mRNA expression. There was no significant change in the expression of *NFKB1* in Ishikawa cells, which also had a downregulation of *LIF,* suggesting that LIF could be downregulated via an alternative method such as via the p53 [396, 397]. Interestingly, NK-92 cells showed a significant decrease in the mRNA expression of *NFKB1* when exposed to acetic acid (Figure 10). However, this was not significant when the data was analysed with Dunnett's multiple comparison tests. This was unexpected as *Lactobacillus* in the endometrium has been shown to decrease inflammation and NF-κB1 expression, yet no significant decrease was observed in the cells treated with lactic acids [398]. On the other hand, diverse microbiota in the endometrium is associated with cytokines that activate the NF-κB pathway [399]. However, interestingly, short-chain fatty acids like butyric acid have been shown to reduce the inflammatory function of NK cells in a model

of the gut microbiome [400]. In future, to better understand the impact of acetic acid on NK-92 cells NF-κB activity should be assessed, as transcriptional changes may not be reflected in changes in activity. This can be done using electrophoretic mobility shift analysis (EMSA), which detects the DNA-protein binding activities of NF-κB [401, 402]. Additionally, western blotting can be done in conjunction with EMSAs, to assess the phosphorylation of NK-κB subunits [401, 402]

3.6 Conclusion and future directions

In conclusion, the data presented demonstrates that microbiota-associated metabolites have the capability to impact key factors involved in the development of receptivity. The effect of these metabolites on factors like migration, tight junction protein expression, glucose uptake and gene expression may not be conducive to ideal conditions for embryo implantation. It is unclear if there is a distinct difference between the conditions created by metabolites representing *Lactobacillus* dominance and metabolites representing diverse bacteria. Thus, it cannot be concluded whether or not metabolites underpin the relationship between the composition of the endometrial microbiome and the outcome of IVF embryo transfer. In future experiments, a complete dose-range should be completed to determine if similar results are seen at lower concentrations of L-lactic, D-lactic, acetic and succinic acids. This is necessary to determine if the results are concertation-dependent. Hormonal priming of cells could also be used to create conditions more representative of a receptive endometrium. Additionally, endometrial organoid models could be used to better understand metabolites' role, as they have been shown to represent the endometrium more accurately [403]. Analysis could be taken further

through techniques like RNA sequencing and shot-gun proteomic analysis to better understand global gene expression changes in the endometrial environment, rather than looking at selected factors.

4 The immunomodulatory effect of microbiota-associated metabolites in the endometrial environment

4.1 Introduction

Infertility can be due to various causes; however, one of the proposed explanations for unexplained infertility is the dysregulation of the immune response, as it is essential for the modulation of the fetal-maternal interface, the development of the endometrium, and the maintenance of pregnancy. Various studies have now demonstrated that an aberrant immune response in the endometrium is associated with poor *in vitro* fertilisation (IVF) outcomes, such as repeated implantation failure [395, 404, 405].

During implantation and in early pregnancy, the endometrium is considered an inflammatory environment. This is characterised by the expression of both pro- and anti-inflammatory cytokines and chemokines, such as tumour necrosis factor (TNF), interleukin (IL)-1β, IL-6, IL-8, IL-10, IL-4, Regulated on Activation, Normal T-cell Expressed and Secreted (RANTES), and interferon gamma (IFNγ) [53, 406-409]. Endometrial epithelial cells produce a variety of cytokines and chemokines, mainly TNF, IL-8, IL-6, and RANTES. As the first cells to come into contact with the embryo and the endometrial microbiome, the epithelium plays a key role in controlling implantation and modulating the local inflammatory environment. IL-8 is an important cytokine expressed by the epithelium that is thought to be involved in the recruitment of immune cells to the endometrium [46, 47]. While the blastocyst does not produce IL-8, *IL8* mRNA expression and peptide production in the epithelium are upregulated when exposed to the blastocyst, suggesting a role in cross-talk at the fetal-maternal interface [46]. Similarly, the expression of cytokines like IL-6 and RANTES by endometrial epithelium is associated with inflammation, chemotaxis, and cellular proliferation [48, 409]. The endometrial epithelium also produces TNF, which has been shown to promote the expression of matrix

metalloproteinases (MMPs) that aid in angiogenesis [410, 411]. The embryo also produces TNF, inducing immunoglobulin-like cell adhesion molecule (ICAM)-1 expression in the epithelium, enhancing adhesion, thus making it an important cytokine in cross-talk at the fetal-maternal interface [412]. TNF and IL-1β are also involved in promoting the expression of RANTES [413]. IL-1β is one of the forms of IL-1, and stimulating epithelial and stromal cells with IL-1β can promote the expression of various inflammatory cytokines and chemokines, including IL-8 and IL-6, which are necessary during implantation [414, 415].

During implantation and early pregnancy, the endometrium contains a unique innate immune cell population, with around 75% of those cells being natural killer (NK) cells [416]. Decidual NK (dNK) differ greatly from peripheral NK cells regarding gene expression and cytokine secretion [40, 417]. The majority have a $CD56^{bright}$ $CD16^{-}$ phenotype, and there are several subsets of dNK cells that have been reviewed extensively in the literature [418]. dNK cells can be further divided into dNK1, dNK2, and dNK3. dNK1 cells primarily interact with the extravillous trophoblast, and dNK2 and dNK3 are involved in cytokine and chemokine production more so than dNK1 cells [418]. dNK cells express IL-8 and RANTES, but mainly IL-8 is thought to support the invasion of the embryo by promoting trophoblast migration [49]. Furthermore, dNK cells also express IFNγ, which has been demonstrated in *in vitro* primary cell culture and murine models to aid in the remodelling of spiral arteries and control the differentiation of the cytotrophoblast [53, 419, 420]. Additionally, dNK cells express receptors for human leukocyte antigen (HLA)-G, which can interact with HLA-G expressed on the extravillous trophoblast and promote the expression of IL-6 [41]. IL-6 has been shown in culture to regulate angiogenesis and migration of the trophoblast [50-52]. Interestingly,

NK cells also express IL-10, which is thought to be necessary for promoting tolerance at the fetal-maternal interface [57-59]. dNK cells also express toll-like receptors (TLR) that respond to pathogen-associated molecular patterns (PAMPs), suggesting they also have a role in responding to pathogens at the fetal-maternal interface [421]. When dNK cells are stimulated with TLR agonists, they upregulate the expression of cytokines like IL-8, IL-6, and IFNγ, all of which are necessary at the fetal-maternal interface [421].

Alongside dNK cells, macrophages are another dominant immune cell in the endometrium. Decidual macrophages are thought to make up approximately 20% of the immune cells in the endometrium [43]. Decidual macrophages were previously thought of as either M1 or M2 macrophages, but it is now known that several subtypes can produce both pro- and anti-inflammatory cytokines and do not fit into the M1/M2 classification [44, 422, 423]. Decidual macrophages express cytokines and chemokines like IL-6, IL-8, IL-10, TNF, and IL-1β, which have been shown to regulate trophoblast invasion [54, 55]. Furthermore, decidual macrophages also secrete angiogenic factors and MMPs that indicate their role in the remodelling of arteries [56]. Macrophages also serve an important immunoregulatory role in the endometrium [424, 425]. Decidual macrophages express IL-4, is regulated by decidual stromal cells, promoting maternal tolerance to the embryo [60]. Much like dNK cells, decidual macrophages also express TLRs that respond to PAMPs, thus similarly having a role in responding to pathogens [421]. Likewise, the stimulation of TLRs results in the expression of cytokines required at the fetal-maternal interface [421].

It is suspected that an aberrant immune response in the endometrium could be due to the composition of the endometrial microbiome. In patients with chronic endometritis,

there was an association between *Phyllobacterium* and *Sphingomonas,* and abnormally differentiated uNK cells. These bacteria also negatively correlated with macrophages, suggesting this may affect receptivity and implantation [216]. It has also been shown that patients with repeated implantation failure had a decreased abundance of *Lactobacillus* with a great abundance of diverse bacteria and abnormalities in their T-cell response, suggesting the microbiome may play a role in this [212]. Similarly, in patients with a shifted window of implantation, transcriptomic data revealed enriched microbial-derived modules, inflammatory pathways and immune regulatory pathways [215]. Additionally, it is well-established that in the vaginal environment, bacteria modulate the inflammatory response via metabolites like lactic acid and short-chain fatty acids [160, 168]. Similarly, lactic acid is known to regulate the immune response in the tumour microenvironment, and short-chain fatty acids can modulate the inflammatory response in the gut [363, 364, 426]. Thus, I aimed to investigate the impact of microbiota-associated metabolites on endometrial epithelium and innate immune cells.

4.2 Hypothesis and Aim

4.2.1 Hypothesis

Metabolites produced by *Lactobacillus* create an environment conducive to successful embryo implantation by modulating the immune response and receptivity. Metabolites produced by diverse bacteria will adversely alter the inflammatory profile and the expression of cytokines, resulting in conditions detrimental to embryo implantation.

4.2.2 Aim

Determine the impact of microbiota-associated metabolites on the immune response of endometrial epithelium and innate immune cells.

4.3 Methods

4.3.1 Cell culture

All cells used in experiments were cultured and maintained according to the methodology outlined in sections 2.1.1 and 2.1.3. Before use, THP-1 cells were differentiated using PMA as outlined in section 2.1.4.

4.1.1 Treatment of cells and sample collection

The cells were treated with the highest concentration of each metabolite that they remained viable at in culture. Table 7 outlines the concentration range for each cell line and the microbiota-associated metabolites. The methodology for collecting cell culture supernatant and cell samples for cytometric bead arrays (CBA) and RT-qPCR is outlined in section 2.4.1. A range of concentrations was used to treat the cells, but not all results have been shown in this chapter. The results for all concentrations used in experiments can be found in Appendix 3.

4.1.2 Generation of conditioned media

Section 2.5.1 outlines the generation of media conditioned with innate immune cells. The methodology used to treat endometrial epithelial cells with the condition media and methods used to collect cell samples are also outlined in section 2.5.1.

4.1.3 Quantification of cytokines and chemokines using a cytometric bead array

4.1.3.1 Preparation of CBA assay

The concentration of cytokines produced by treated cells was quantified using the BD CBA kits (Table 17). The stored supernatant collected from experiments outlined in

section 2.4.1 was thawed to room temperature, and 10 µL of each sample was added to a 96-well plate. If necessary, samples were diluted using the assay diluent supplied before being added to the plate. Human flex sets outlined in Table 17 were resuspended in capture bead diluent, and 10 µL of the suspension was added to all wells. The plate was incubated at room temperature for one hour. The detection reagent from each flex set was resuspended in the detection reagent diluent, and 10 µL of the suspension was added to each well. The plate was incubated at room temperature for two hours. 100 µL of the wash buffer was added to all wells, and the plate was stored at 4°C, protected from light, until use. The BD LSR Fortessa X20 flow cytometer was used to analyse the samples. The flow cytometer was calibrated using the A9 and PE-F1 beads supplied in the human soluble master buffer kit (Table 17). Compensation was calculated using the A1, F1, and F9 beads supplied according to the manufacturer's instructions.

Table 17. Products purchased from BD to conduct CBA experiments.

Product	**Catalogue number**
Human soluble master buffer kit	558264
Human flex set IL-6 (A7)	558276
Human flex set IL-8 (A9)	558277
Human flex set IL-10 (B7)	558274
Human flex set IL-4 (A5)	558272
Human flex set IL-1 beta (B4)	558279
Human flex set RANTES (D4)	558324
Human flex set TNF (C4)	560112

4.1.3.2 Data Analysis and Figure Generation for CBA assay

The results generated by the BD LSR Fortessa X20 flow cytometer were exported as FCS3.0 files and analysed using FCAP Array software v3.0 (BD, cat no. 652099). A standard curve was generated for each analyte, with a working concentration of 2.5 pg/mL to 2500 pg/mL. The concentration of each cytokine in the samples was determined using these curves. An unpaired T-test with Welch's correction was used to determine if cells treated with metabolites generated significantly different secreted cytokines compared to untreated cells [427]. The results were also analysed using a two-way ANOVA and Dunnett's multiple comparison tests. All figures were generated using GraphPad Prism 9.3.0 for Windows (GraphPad Software, Boston, Massachusetts USA www.graphpad.com)

4.1.4 RT-qPCR

All RT-qPCR experiments were conducted according to the methods outlined in section 2.6.2. To assess the expression of key genes involved in the endometrial immune response, the primers outlined in Table 13 (reference genes) and Table 18 were used. Fold change values presented in the results are the $\log_2$ fold change values.

Table 18. Inflammatory marker primer sequences. All primer pairs were ordered from Integrated DNA Technologies (IDT, Singapore).

Gene	Role		Sequence (5'-3')	Reference
Interleukin-6 (*IL6*)	Immune response	Forward	CAATCTGGATTCAATGAGGAGAC	[160]
		Reverse	CTCTGGCTTGTTCCTCACTACTC	
Interleukin-8 (*IL8*)	Immune response	Forward	GCTCTGTGTGAAGGTGCAGTTTTG	[428]
		Reverse	ACCCAGTTTTCCTTGGGGTCCAG	
Interferon-γ (*IFNG*)	Immune response	Forward	CTGTTACTGCCAGGACCCAT	[428]
		Reverse	TTTCTGTCACTCTCCTCTTTCC	
Tumour Necrosis Factor (*TNF)*	Immune response	Forward	CCCCAGGGACCTCTCTCTAATC	[160]
		Reverse	GGTTTGCTACAACATGGGCTACA	
Regulated upon Activation, Normal T Cell Expressed and Presumably Secreted (*RANTES*)	Immune response	Forward	ATGGGTTCGGGAGTACATCA	[160]
		Reverse	GCAAGCAGAAACAGGCAAAT	
Indoleamine 2,3-dioxygenase 1 (*IDO1*)	Immune response	Forward	TTCAGTGCTTTGACGTCCTG	[429]
		Reverse	TGGAGGAACTGAGCAGCAT	

4.4 Results

4.4.1 L-lactic acid and acetic acid induce decreased secretion of pro-inflammatory cytokines by endometrial epithelial cells

Cytokines and chemokines are readily expressed by endometrial epithelium and immune cells and are involved in the coordinated immune response during implantation, the development of receptivity, and the maintenance of pregnancy. This study aimed to determine the impact of microbiota-associated metabolites on the expression of cytokines by endometrial epithelium. Key cytokines, including IL-6, IL-8, IL-4, IL-10, IL-1β, TNF, and RANTES, as all have a role in the immune status and fetal-maternal cross-talk. Ishikawa and RL95-2 cells were cultured for 24 hours with L-lactic, D-lactic, acetic and succinic acids, and the supernatant was analysed using CBA assays to determine the concentration of the cytokines secreted. Both cell lines produced IL-6, IL-8, RANTES, and TNF (Appendix 3). However, they showed little to no production of IL-4, IL-10, and IL-1β (Appendix 3). Ishikawa cells treated with 5 mM and 2.5 mM of acetic acid showed a decreased concentration of IL-8 ($p=0.03$, $p=0.047$, respectively) ($p=0.99$, $p=0.099$ respectively with Dunnett's multiple comparisons tests) and RANTES ($p=0.029$) ($p=0.99$), in the cell culture supernatant (Figure 11a and b). When treated with 15 mM L-lactic acid, RL95-2 cells significantly decreased the concentration of IL-8 secreted ($p=0.030$) ($p=0.99$) (Figure 11c). The microbiota-associated metabolites did not

significantly affect the secretion of any other cytokines tested in Ishikawa or RL95-2 cells (Appendix 3).

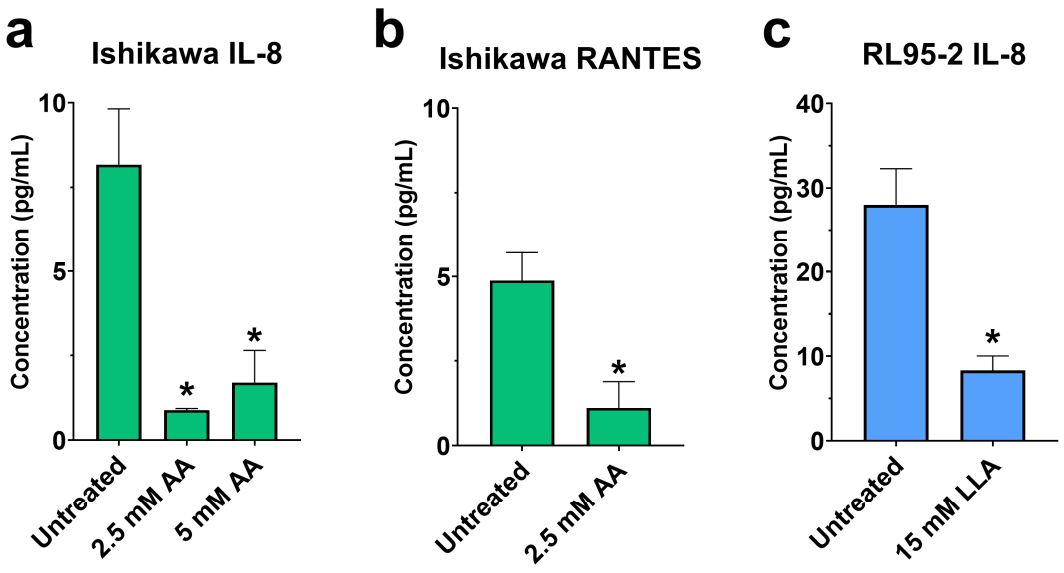


Figure 11. Ishikawa and RL95-2 cells cytokine response to microbiota-associated metabolites. Cells were seeded and treated for 24 hours with the microbiota-associated metabolite. Acetic acid is represented as AA, and L-lactic acid is represented as LLA. A cytometric bead array was used to quantify the concentration of IL-8 and RANTES represented in pg/mL. a) Concentration of secreted IL-8 by Ishikawa cells treated with AA. b) Concentration of secreted RANTES by Ishikawa cells treated with AA. c) Concentration of IL-8 by RL95-2 cells treated with LLA. The figures show the mean ± SEM (n=3). * representing $p \leq 0.05$, analysed by unpaired T-tests with Welch's correction.

4.4.2 Microbiota-associated metabolites modulate NK-92 secretion of IL-6, IL-8, and IL-10

Throughout implantation and early pregnancy, the endometrial immune cell population is dominated by NK cells [39]. The presence of NK cells aids in embryo invasion, remodelling of spiral arteries, and in promoting maternal tolerance to the embryo [59, 419, 420].This study aimed to investigate the impact of microbiota-associated metabolites on NK cells using the NK-92 cell line. The cells were treated with L-lactic, D-lactic, acetic, and succinic acids for 24 hours, and the supernatant was analysed using CBA assay. NK-92 cells secreted IL-6, IL-8, RANTES, TNF, and IL-10 and with little to no secretion of IL-4 and IL-1β (Appendix 3). Interestingly, when cultured with 4 mM and 2 mM D-lactic acid, the NK-92 cells, compared to untreated cells, increased the secretion of IL-6 ($p=0.045$, $p=0.031$ respectively) ($p=0.99$, $p=0.99$ respectively with Dunnett's multiple comparisons tests), IL-8 ($p=0.0086$, $p=0.0056$ respectively) ($p=0.99$, $p=0.99$ respectively), and IL-10 ($p=0.024$, $p=0.030$ respectively) ($p=0.99$, $p=0.99$) (Figure 12d-f). However, when cultured with 5 mM L-lactic acid, NK-92 cells significantly decreased IL-6 production ($p=0.016$) ($p=0.99$) and increased IL-8 when treated with 2.5 mM L-lactic acid ($p=0.0030$) ($p=0.99$) (Figure 12a and b). There was no significant difference in IL-10 expression in cells treated with L-lactic acid (Figure 12c). Likewise, when cultured with 5 mM acetic acid, there was a decrease in IL-6 ($p=0.0027$) ($p=0.84$) and no change in IL-10 production (Figure 12g and i). Acetic acid did generate a significant increase in IL-8 when NK-92 cells were treated with 5 mM acetic acid ($p=0.0022$) and 2.5 mM acetic acid ($p=0.0022$) ($p=0.99$ and $p=0.99$, respectively) (Figure 12h). Treatment with 2 mM and 1 mM succinic acid increased the

secretion of IL-8 (p=0.049, p=0.0032, respectively) (p=0.99, p=0.99 respectively) and IL-10 (p=0.028, p=0.013 respectively) (p=0.99, p=0.99) by NK-92 cells, without a significant change in IL-6 expression compared to untreated controls (Figure 12j-l).

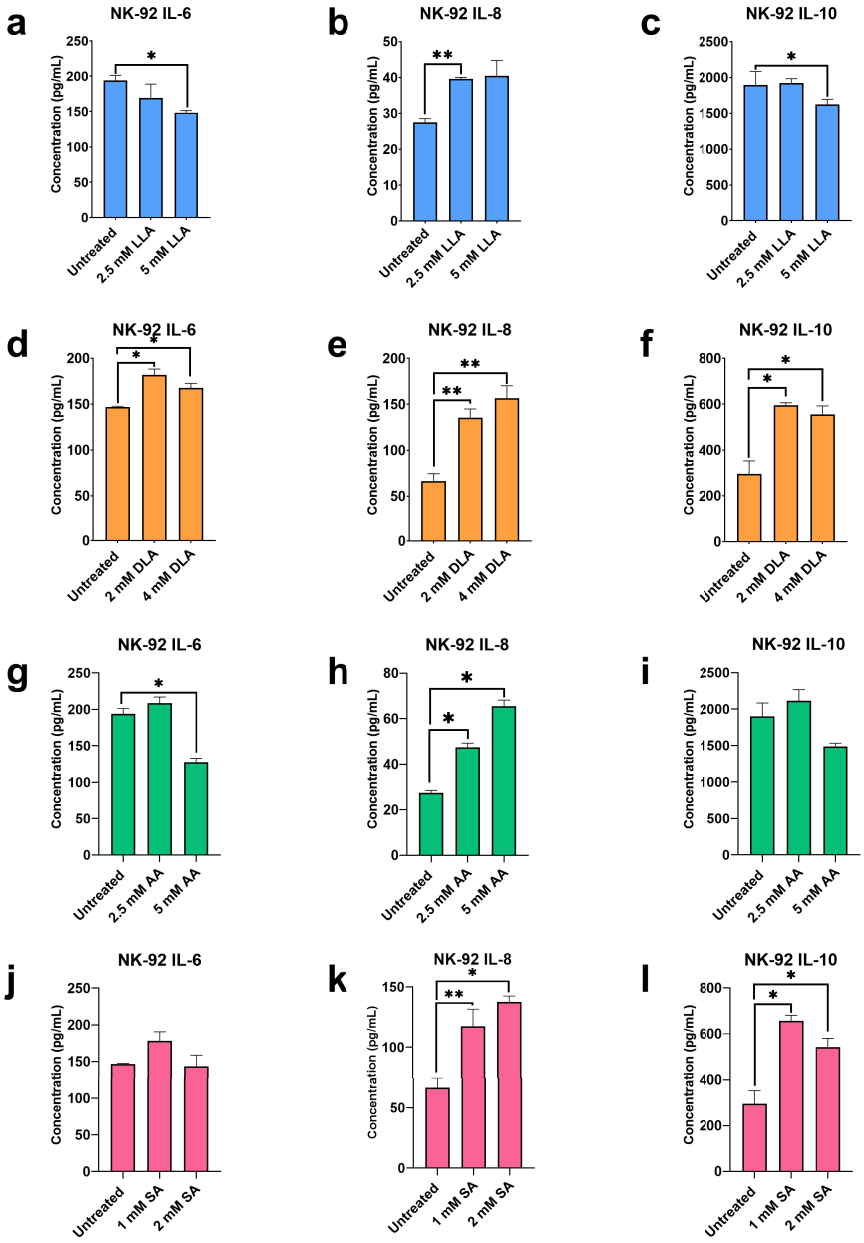


Figure 12. NK-92 cells cytokine response to microbiota-associated metabolites. Cells were seeded and treated for 24 hours with the microbiota-associated metabolites. Cytometric bead arrays were used to quantify the concentration of IL-6, IL-8, and IL-10 represented in pg/mL. Figures a-c represented NK-92 cells treated with L-lactic acid (LLA). Figures d-f represent NK-92 cells treated D-lactic acid (DLA). Figures g-i represent cells treated with acetic acid (AA). Figures j-l represent cells treated with succinic acid (SA). The figures show the mean ± SEM (n=3). * representing $p \leq 0.05$, ** representing $p \leq 0.01$, analysed by unpaired T-tests with Welch's correction.

4.4.3 L-lactic acid induces increased THP-1 secretion of IL-8 but decreases secretion of RANTES

Alongside NK cells, macrophages also comprise a significant portion of the immune cell population in the endometrium during the development of receptivity and implantation [43]. These cells express various cytokines, which aid in trophoblast invasion, angiogenesis, and immunoregulation of the endometrium [56, 424, 425]. Thus, this study aimed to investigate the impact of microbiota-associated metabolites on macrophages using differentiated THP-1 cells. The cells secreted IL-6, IL-8, RANTES, TNF, and IL-10, with little to no secretion of IL-4 and IL-1β (Appendix 3). Differentiated THP-1 cells' cytokine secretion did not significantly differ between treatment with D-lactic and succinic acids and untreated cells. However, 15 mM L-lactic acid increased IL-8 expression ($p=0.038$) ($p=0.99$ with Dunnett's multiple comparisons test) (Figure 13a). Furthermore, 10 mM and 5 mM L-lactic acid ($p= 0.014$, $p=0.045$, respectively) ($p=0.97$, $p=0.98$) resulted in decreased RANTES secretion, and 5 mM acetic acid treatment decreased the secretion of RANTES ($p=0.0065$) ($p=0.76$) (Figure 13b and c).

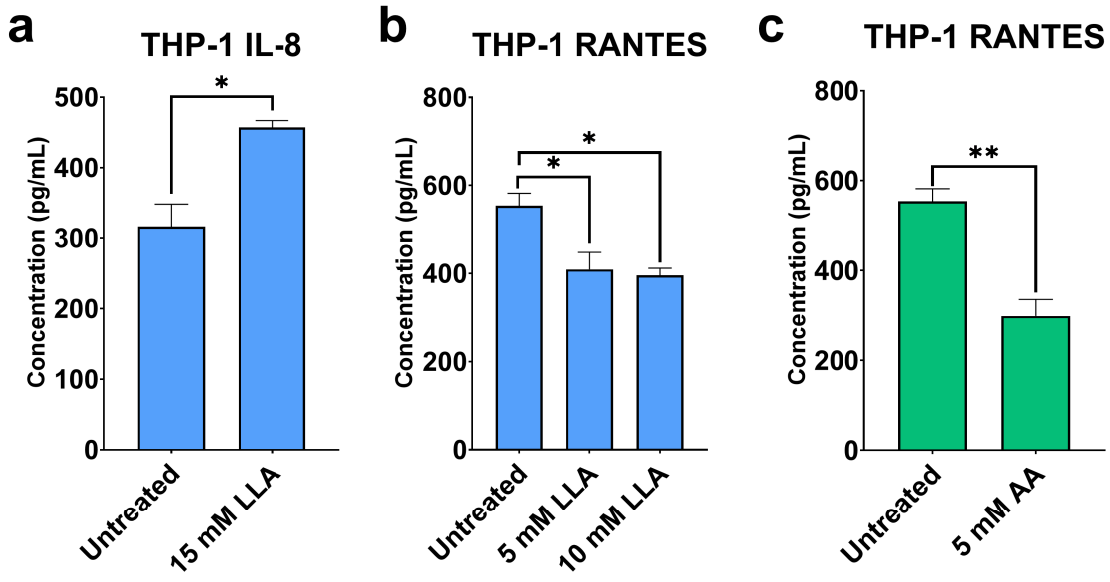


Figure 13. THP-1 cells cytokine response to microbiota-associated metabolites. Cells were seeded and treated for 24 hours with the microbiota-associated metabolite. Acetic acid is represented as AA, and L-lactic acid is represented as LLA. A cytometric bead array was used to quantify the concentration of IL-8 and RANTES represented in pg/mL. a) Concentration of secreted IL-8 by THP-1 treated with LLA. b) Concentration of secreted RANTES by THP-1 cells treated with LLA. c) Concentration of RANTES by RL95-2 cells treated with AA. The figures show the mean ± SEM (n=3). * representing $p \leq 0.05$, analysed by unpaired T-tests with Welch's correction

4.4.4 L- and D-lactic acid treatments modulate inflammatory gene expression in endometrial epithelial cells.

Alongside the secretion of cytokines in cell culture supernatant, This study also investigated changes in mRNA expression for various cytokines and chemokines in endometrial epithelial cells. Using RT-qPCR, the expression of *IL6, IL8, RANTES, TNF*,

and *IFNG* after Ishikawa and RL95-2 cells had been cultured with L-lactic, D-lactic, acetic, and succinic acids for 4 hours was assessed. Compared to untreated controls, Ishikawa cells treated with 10 mM D-lactic acid significantly downregulated *TNF* by -4 log_2 fold (p=0.010) (p=0.015 with Dunnett's multiple comparisons test) (Figure 14b). Ishikawa cells treated with 10 mM and 5 mM L-lactic acid showed a 4.5 (p=0.010) and 3.2 (p=0.036) log_2 fold increase, respectively (p=0.0080 and p=0.16, respectively, with Dunnett's multiple comparisons tests), in *IL-8* mRNA compared to untreated cells (Figure 14a). However, at 15 mM and 10 mM L-lactic acid, RL95-2 cells showed a -2.0 log_2 (p=0.036) and -2.0 (p=0.030) log_2 fold decrease in *IL8* mRNA expression, respectively, (p=0.27, p=0.29) compared to untreated controls (Figure 14c). Interestingly, when cultured with 15 mM L-lactic acid, RL95-2 cells had a -2.7 log_2 fold decrease in *RANTES* expression (p=0.025) (p=0.076) (Figure 14d). Aside from these results, the metabolite treatments did not induce significant changes in mRNA expression in *IFNG* and *IL6* (Appendix 3).

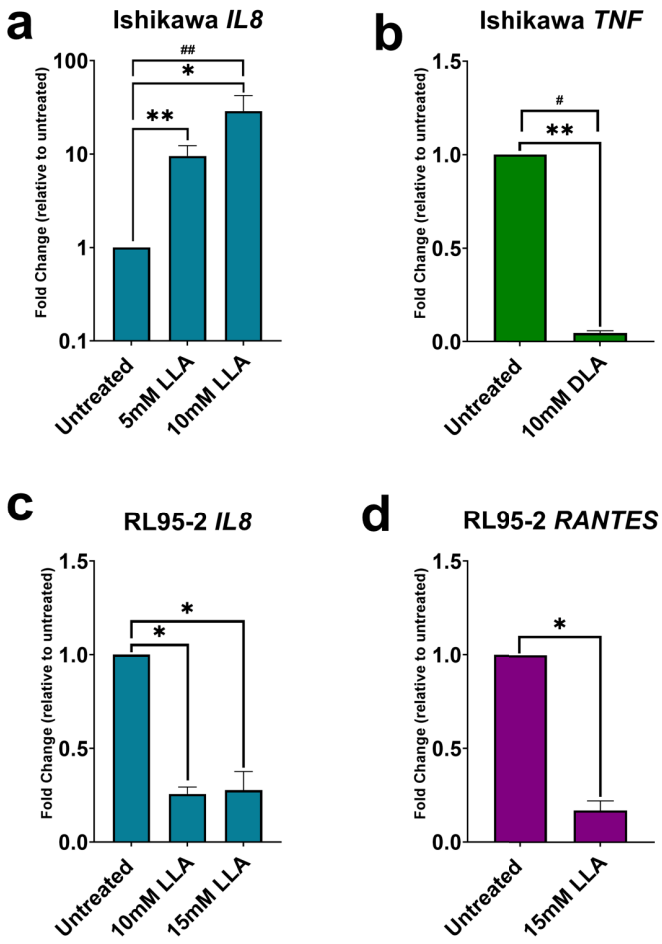


Figure 14. Relative gene expression of genes involved in the immune response in endometrial epithelial cells compared to untreated cells. DLA represents D-lactic acid, and LLA represents L-lactic acid. (a) Fold change of *IL8* in Ishikawa cells treated with LLA. (b) Fold change of *TNF* in Ishikawa cells treated with DLA. (c) Fold change of *IL8* in RL95-2 cells treated with LLA. (d) Fold change of *RANTES* in RL95-2 cells treated with LLA. Gene expression was normalised to the reference genes and expressed as fold change compared to the untreated cells using the comparative C_t method. The data shows the mean ± SEM (n = 3). * represents $p \leq 0.05$, ** represents $p \leq 0.01$, analysed by unpaired T-tests with Welch's correction. # represents $p \leq 0.05$, ## represents $p \leq 0.01$, analysed by Dunnett's multiple comparisons test.

4.4.5 L-lactic acid and acetic acid treatment was associated with downregulation of pro-inflammatory genes in natural killer cells but not in macrophages

Similarly to endometrial epithelial cells, this study assessed the expression of various cytokines and chemokines in innate immune cells. To examine the effect of metabolite treatments on NK-92 and differentiated THP-1, these cells were treated with L-lactic, D-lactic, acetic, and succinic acids for 4 hours, and *IL6, IL8, RANTES, TNF,* and *IFNG* mRNA expression levels were analysed (using RT-qPCR). When cultured with 5 mM L-lactic acid, the NK-92 cells showed significant downregulation of *IL8* and *IFNG* compared to the untreated controls. There was a -4.1 log_2 fold change (p=0.045) (p=0.0080 with Dunnett's multiple comparisons test) in the expression of IL-8 and a -2.0 log_2 fold change (p=0.020) (p=0.26) in *IFNG* (Figure 15a and b). Similarly, treatment with 5 mM and 2.5 mM acetic acid resulted in a -1.2 log_2 fold change (p=0.020) (p=0.71) and a -2.1 log_2 fold change (p=0.027) (p=0.26), respectively, in *IFNG* mRNA expression compared to untreated cells (Figure 15c). Unlike the NK-92 cells, differentiated THP-1 cells showed no significant changes in mRNA expression when treated with the metabolites (Appendix 3).

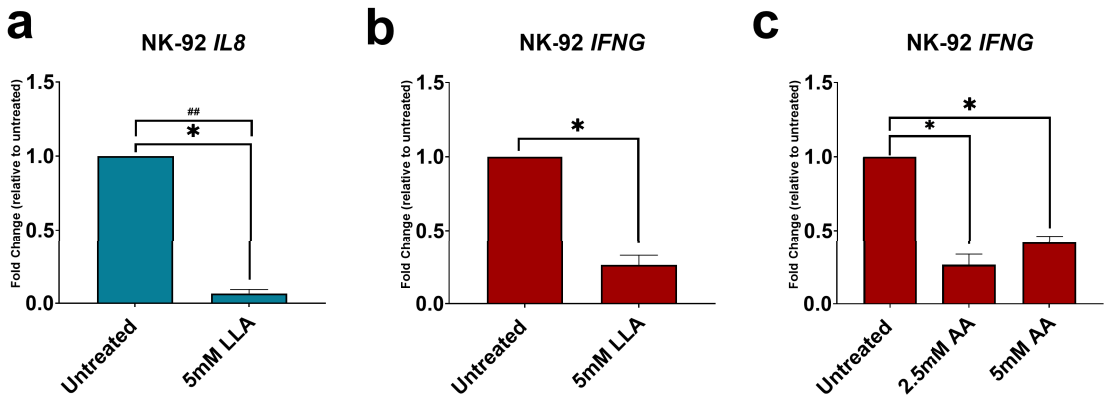


Figure 15. Relative gene expression of genes involved in the immune response in NK-92 cells compared to untreated cells. LLA represents L-lactic acid, and AA represents acetic acid. (a) Fold change of *IL8* in NK-92 cells treated with LLA. (b) Fold change of *IFNG* in NK-92 cells treated with LLA. (c) Fold change of *IFNG* in NK-92 cells treated with AA. Gene expression was normalised to the reference genes and expressed as fold change compared to the untreated cells using the comparative C_t method. The data shows the mean ± SEM (n = 3). * represents $p \leq 0.05$, analysed by unpaired T-tests with Welch's correction. ## represents $p \leq 0.01$, analysed by Dunnett's multiple comparisons test.

4.4.6 Succinic acid induces an increase in IDO1 mRNA expression in NK-92 cells

IDO1 is an important gene in immunotolerance and receptivity in the endometrial environment. It is induced by IFNγ and is thought to promote maternal tolerance through T-cell suppression [430, 431]. Since a significant downregulation of *IFNG* in the NK-92 cells treated with L-lactic and acetic acid was seen , the expression of *IDO1* in NK-92 cells treated with the microbiota-associated metabolites was investigated . Interestingly,

there was a significant 1.36 log_2 fold increase in *IDO1* mRNA expressed by NK-92 cells treated with 1 mM succinic acid (p=0.033) (p=0.46 with Dunnett's multiple comparisons test) (Figure 16). However, there was no significant change in *IDO1* compared with untreated controls when cells were treated with L-lactic, D-lactic, or acetic acids (Appendix 3).

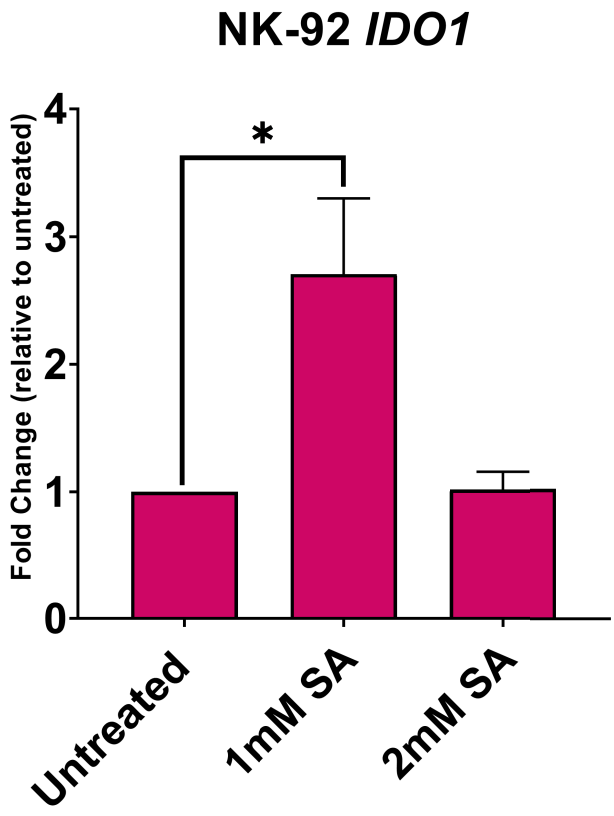


Figure 16. Relative gene expression of *IDO1* in NK-92 cells compared to untreated cells. SA represents succinic acid. The figure shows the fold change of *IDO1* in NK-92 cells treated with SA. Gene expression was normalised to the reference genes and expressed as fold change compared to the untreated cells using the comparative C_t method. The data shows the mean ± SEM (n = 3). * represents $p \leq 0.05$, analysed by unpaired T-tests with Welch's correction.

4.4.7 Conditioned media generated by THP-1 cells treated with L-lactic acid, decreases RL95-2 *IL8* expression

In the endometrial environment, NK cells and macrophages are clustered around the uterine glands during the secretory stage [432, 433]. While clustered around the glands and the epithelium, the cells may be exposed to microbiota-associated metabolites, which could impact the immune response and the immune response of the nearby epithelium. Thus, a conditioned media model was used to add complexity and replicate this interaction. NK-92 and THP-1 cells were treated with L-lactic, D-lactic, acetic, and succinic acids, and the media containing their secretome were cultured with Ishikawa and RL95-2 cells. With this model, we investigated how this affected the epithelial cells' expression of *IL6, IL8, TNF, RANTES*, and *IFNG* mRNA. Ishikawa and RL95-2 cells expressed *IL6, IL8, TNF* and *RANTES* but lacked *IFNG* expression (Figure 17). Neither cell lines express *IL8* when cultured with NK-92 conditioned media (Figure 17a and c). Interestingly, when a two-way ANOVA with Dunnett's multiple comparisons test was used to assess the expression of *IL-8* mRNA, RL95-2 cells treated with media conditioned by THP-1 cells treated with 15 mM LLA showed a significant result. There was a -4.1 $\log_2$ fold change in *IL-8* expression ($p=0.0009$) ($p=0.068$, unpaired T-tests with Welch's correction) (Figure 17d). There were no other significant changes in gene expression.

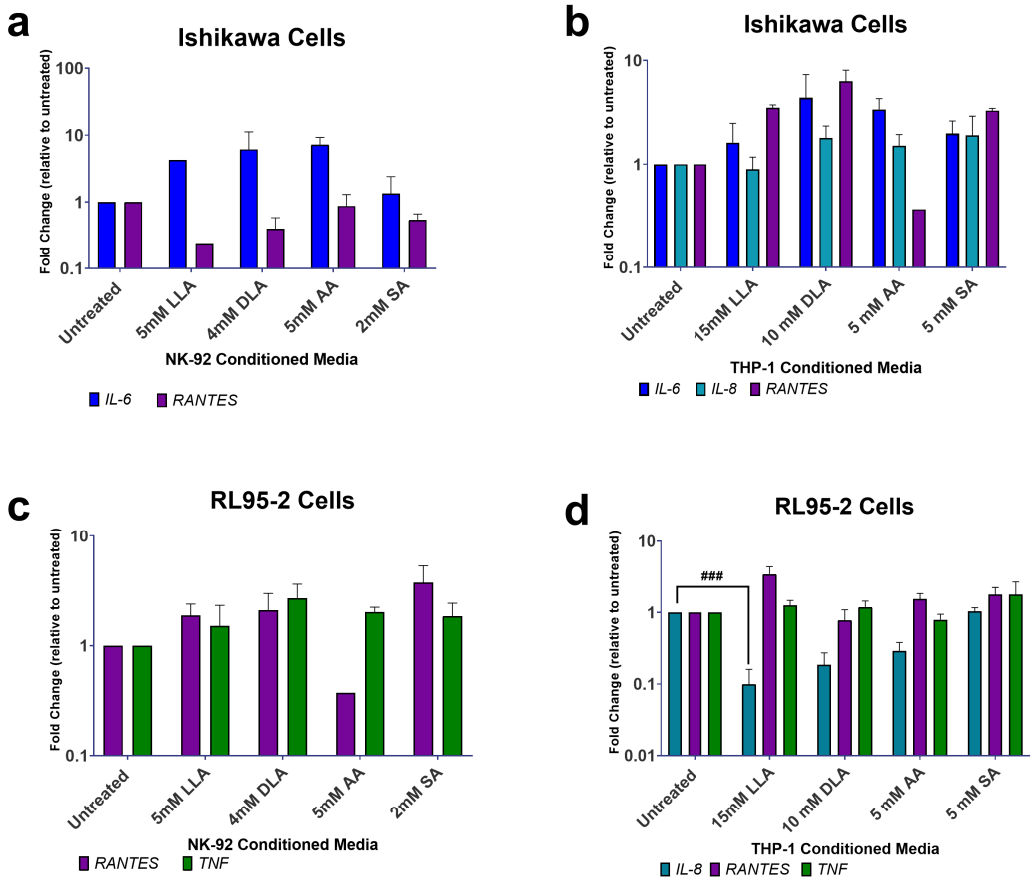


Figure 17. Relative expression of genes involved in the immune response in epithelial cells treated with conditioned media compared to untreated controls. LLA represents L-lactic acid, DLA represents D-lactic acid, AA represents acetic acid, and SA represents succinic acid. (a) Fold change of genes in Ishikawa cells treated with NK-92 conditioned media. (b) Fold change of genes in Ishikawa genes treated with THP-1 conditioned media. (c) Fold change of RL95-2 genes treated with NK-92 conditioned media. (d) Fold change of RL95-2 cells treated with THP-1 conditioned media. Gene expression was normalised to the reference genes and expressed as fold change compared to the untreated cells using the comparative C_t method. The data shows the mean ± SEM (n = 3). ### represents $p \leq 0.001$, analysed by Dunnett's multiple comparisons test.

4.5 Discussion

While there is no defined composition of the 'ideal' endometrial microbiome, the dominance of *Lactobacillus* species is considered favourable and often associated with successful IVF outcomes [178, 180, 206]. Decreased abundance of *Lactobacillus* and the presence of adverse bacteria are associated with implantation failure, biochemical pregnancy, and miscarriage [116, 178, 180, 434]. The role of the microbiome in the endometrial environment and how the tissue responds and functions is unclear. However, there is evidence that bacteria may have an immunomodulatory role, with studies demonstrating that *Lactobacillus* and diverse bacteria can induce differing cytokine and mRNA expression in the endometrium [214, 286, 435]. Yet it is unclear how microbiota drive changes in cytokine and mRNA expression in the endometrial environment. It is well-established that lactic acid in the vagina promotes an anti-inflammatory response, and short-chain fatty acids produced by adverse bacteria create a pro-inflammatory response [160, 168]. Thus, I hypothesised that microbiota-associated metabolites may have an immunomodulatory role in the endometrium similar to that seen in the vaginal environment.

The expression of IL-8 is thought to be involved in developing blood vessels, immune cell recruitment to the endometrium, and promoting trophoblast migration [46, 407, 408, 436]. Aberrant expression of IL-8 in the endometrium has been associated with implantation failure [395, 404]. Therefore, this study aimed to investigate secreted IL-8 and *IL8* mRNA expression from epithelial cells treated with microbiota-associated metabolites. In this study, Ishikawa cells showed upregulated expression of *IL8* mRNA

when exposed to L-lactic acid. However, this increase was not observed in the supernatant. This suggests that lactic acid produced by bacteria can modulate mRNA expression of *IL8* in the epithelium, and this aligns with studies showing that *Lactobacillus* can upregulate IL-8 expression in culture [437, 438]. However, these results were not consistent between the Ishikawa and RL95-2 cell lines. RL95-2 cells showed significantly reduced expression of *IL8* and decreased secretion of IL-8 when treated with L-lactic acid. This response, however, is also supported by literature demonstrating that *Lactobacillus* species can decrease IL-8 secretion in cell culture [286]. These differences could result from differing abilities to express IL-8 and toll-like receptor signalling by the cells [439].

When exposed to acetic acid, there was a significant decrease in secreted IL-8 by Ishikawa cells but not by RL95-2 cells. This decrease in IL-8 secretion was unexpected, as it has been shown that cells cultured with diverse bacteria also increased the secretion of IL-8 [286]. Likewise, in models of the vaginal environment, short-chain fatty acids, including acetic acid, increased IL-8 secretion alone and when cells were simultaneously stimulated with toll-like receptor agonists [167, 168]. However, this result was only observed at high concentrations of acetic acid (20 mM) alone or at low acetic acid concentrations in conjunction with Pam2CSK4 and imiquimod, which was not done in this study [167]. Thus, it is possible that lower concentrations like those used in this study may stimulate a different response in endometrial tissue compared to vaginal epithelium. It is also important to consider that an acidic pH can affect the secretion of IL-8, increasing or decreasing its secretion in different cell types [426, 440, 441]. Thus, pH should be considered as a variable in future studies in conjunction with the metabolites, as the embryo creates an acidic environment during implantation, which is capable of modulating

endometrial gene expression [283]. It is difficult to conclude from these results how microbiota-associated metabolites modulate endometrial epithelial immune status beyond that these metabolites can modulate IL-8 expression and secretion. Furthermore, IL-8 expression and secretion in the endometrium are under hormonal regulation [46]. The cells used in this study were not hormonally primed; thus, it is important to consider the impact this may have had on the expression of IL-8 by epithelial cells. It is also important to acknowledge that the concentration of secreted IL-8 is low. It may be beneficial in future to use a CBA kit designed to quantify low concentrations of cytokines and chemokines to elucidate concentrations that may not have been detected in the concentration range used in this assay [442].

In addition to IL-8, there were significant changes in the expression of other pro-inflammatory cytokines when the endometrial epithelial cells were treated with metabolites. This study investigated RANTES, which is expressed in a receptive endometrium and involved in immune cell recruitment to the endometrium [46, 48, 409]. Interestingly, Ishikawa cells treated with acetic acid showed decreased secretion of RANTES compared to untreated controls. RL95-2 cells also showed significant downregulation of *RANTES* mRNA when treated with L-lactic acid, but there was no difference in secreted RANTES. These results suggest that microbiota-associated metabolites could modulate the expression of RANTES and align with studies showing that lactic acid and short-chain fatty acids can reduce RANTES expression [160, 168, 443]. However, downregulated mRNA expression and decreased secretion could be detrimental as the expression of RANTES is necessary to promote a pro-inflammatory and tolerogenic response at the fetal-maternal interface [444]. It is important to note that RANTES expression in the endometrium is regulated by TNF and IL-1β secretion [413].

TNF and IL-1β are thought to have a role in implantation and the maintenance of pregnancy [214, 445]. TNF aids in invasion by creating an inflammatory environment and aids in the migration of the trophoblast [446]. Furthermore, IL-1β is involved in promoting the expression of cytokines required for successful implantation [414, 415]. Our study showed a significant downregulation of *TNF* mRNA in Ishikawa cells treated with D-lactic acid. This result could indicate that metabolites may affect TNF secretion and, therefore, RANTES expression, but there was no observed change in TNF or RANTES secretion by Ishikawa cells treated with D-lactic acid. Likewise, there was no change in TNF or IL-1β secreted by either cell line treated with L-lactic, acetic, or succinic acids. The lack of IL-1β secretion is likely due to the fact that epithelium is not the primary source of IL-1β in the endometrium [447]. It is typically expressed by endothelium and stroma. However, the epithelium expresses Interleukin-1 receptor type I (IL-1RtI), the receptor for IL-1β, which may be an ideal target for further studies [447]. Therefore, further investigation is required on the impact of the metabolites on RANTES and TNF expression from the endometrial epithelium. To my knowledge, treatment of Ishikawa and RL95-2 cells with either TNF or IL-1β in conjunction with the microbiota-associated metabolites has not been performed before. It could provide insight into how metabolites may impact the expression of RANTES in an environment more closely representing the endometrium.

dNK cells show reduced cytotoxicity compared to peripheral NK cells but express cytokines and growth factors, which enable them to regulate trophoblast implantation and the fetal-maternal interface [49, 448]. It has been shown that patients experience who recurrent miscarriage and implantation failure have greater numbers of NK cells that produce pro-inflammatory cytokines such as IFNγ and TNF [449, 450]. Additionally,

those with dysbiotic endometrial microbiomes containing less than 90% *Lactobacillus* have been shown to have a lower abundance of NK cells in the endometrium [451]. As microbiota-associated metabolites are known to regulate the vaginal immune response and microbiota can regulate the response of NK cells in other sites such as the gut, I aimed to investigate the expression of cytokines when NK-92 cells were treated with metabolites [160, 452]. In this study, NK-92 cells consistently secreted RANTES, IL-6, IL-8, and IL-10 in cell culture supernatant, which aligns with the literature [453-455]. NK-92 cells also secreted high concentrations of TNF when stimulated with PMA/I, which is consistent with the literature [454]. However, it is important to consider that there was low and inconsistent expression of IL-4 and IL-1β [453]. This result may reflect an artefact in the CBA assays as these cytokines are not typically expressed by NK-92 cells. A known limitation of multiplex CBA assays is the matrix effect, were non-specific binding and cross-reactivity can create background signal, and may have caused the detection of these cytokines [456]

Interestingly, NK-92 cells treated with D-lactic acid secreted higher concentrations of IL-6, IL-8, and IL-10 compared to untreated controls. This profile could be beneficial as IL-8 produced by NK cells regulates the invasion of trophoblast cells. This was demonstrated in a co-culture model where neutralisation of IL-8 derived from NK cells inhibited the migration of trophoblast cells [49]. IL-8 and IL-6 are upregulated by NK cell interaction with HLA-G expressed by the trophoblast, indicating their role in regulating trophoblast invasion [41, 52]. IL-8 and IL-6 have been shown in a chorionic plate artery model to induce morphological changes mimicking the remodelling of spiral arteries, further supporting their role in invasion [41, 52]. Furthermore, IL-10 produced by NK cells in murine models can modulate dendritic cells, develop maternal tolerance,

overcome early pregnancy failure, and promote angiogenesis [59]. This profile (increased IL-6, IL-8, and IL-10) was not seen when the NK-92 cells were treated with L-lactic acid, with cells showing a significant decrease in secreted IL-6, a significant increase in IL-8, and a significant decrease in secreted IL-10. This may be detrimental as both cytokines are essential to the regulation of invasion and tolerance to the embryo. Additionally, this indicates that NK cells may respond differently to lactic acid isomers, with D-lactic acid promoting a more beneficial profile. This may be similar to the role of D-lactic acid in the vaginal environment, where a higher ratio of L-lactic acid to D-lactic acid promotes EMMPRIN and MMP-8, creating an environment susceptible to infection [153]. Thus, further investigation is warranted.

Interestingly, acetic acid resulted in a significant decrease in secreted IL-6 but an increase in IL-8, while succinic acid resulted in a significant increase in secreted IL-8 and IL-10 in NK-92 cells. This could indicate that metabolites produced by diverse bacteria can beneficially alter the profile of cytokines produced by NK cells. It is important to consider that in the literature, when NK-92 cells were cultured with short-chain fatty acids, including acetic, propionic, and butyric acids, there was no change in their expression of IL-6 and IL-8 and a reduction in secreted IL-10 [457]. However, this could be due to methodological differences. NK-92 cells in Perez et al. (2024) were treated with 2-10 μM of metabolites, replicating the concentrations of short chain fatty acids in the peripheral tissue to the gut [458]. Whereas NK cells in the endometrium cluster around endometrial glands and are present throughout the stroma, and may be exposed to higher concentrations of microbiota-metabolites [459]. Thus the results of Perez et al. (2024) should be interpreted cautiously in the endometrial context. Time may also explain the difference between the supernatant and mRNA results. When NK-92 cells were cultured

with L-lactic acid, secreted IL-8 increased significantly, but *IL8* mRNA decreased. Similarly, when significant changes were observed in IL-6, IL-8, and IL-10 secreted by NK-92 when exposed to D-lactic, acetic and succinic acids, but no significant change in *IL6*, *IL8*, and *IL10* mRNA expression was seen. This could indicate that changes in gene expression may not occur within 4 hours. For example, IL-8 expression peaks at 6 hours post-treatment when cells are stimulated with IL-1β [460]. Interestingly, it has been shown that lactic acid treatment can delay changes in mRNA expression in response to LPS stimulation in human monocytes [461]. Thus, future-time course experiments could be performed to provide further insight into the NK-92 cells' response to metabolite treatment [462]. Lastly, these results should also be interpreted cautiously as the NK-92 cells are a highly cytotoxic cell line that is IL-2-dependent, which promotes their cytotoxicity [463]. NK-92 cells also display a different profile of surface receptors to that seen in dNK cells [239]. Thus, their response to microbiota-associated metabolites in this study may not completely reflect the response of dNK cells. In future studies, it may be beneficial to pre-culture NK-92 cells with trophoblastic cells to create a phenotype more aligned with dNK cells to enable a more accurate understanding of the impact of microbiota-associated metabolites [237].

NK cells in the endometrial environment express IFNγ, which is involved in migrating trophoblastic cells and remodelling spiral arteries [53, 419, 420]. Both increased and decreased mRNA expression of *IFNG* mRNA is associated with implantation failure, and has been proposed to either indicate an excessive inflammatory response or NK cell deficiency, respectively [395, 464]. Thus, this study aimed to investigate *IFNG* mRNA expression. NK-92 cells treated with L-lactic and acetic acid showed significant downregulation of *IFNG* (although not significant with Dunnett's

multiple comparisons tests). However, there was no significant difference in *IFNG* expression in endometrial epithelial cells or THP-1 cells. The downregulation of *IFNG* could be beneficial in the endometrial environment by preventing a cytotoxic immune response from NK cells but it could also be detrimental as a balance between pro- and anti-inflammatory responses is required during implantation. These results are consistent with the literature, where lactic acid has been shown to downregulate *IFNG* expression due to lactic acid's ability to prevent the upregulation of the nuclear factor of activated T cells (NFAT) [363, 364]. However, in past research, NK cells cultured with acetate showed no significant change in cytokine secretion [400]. Therefore, future studies should investigate if the secretion of IFNγ, alongside mRNA expression, is altered in NK-92 cells treated with acetic acid. It is also important to consider that NK cells produce IFNγ in response to IL-12/IL-18 stimulation, thus without stimulation, the changes in mRNA expression may not be reflected in cytokine secretion [465]

IDO1 is an immunomodulatory enzyme expressed in the endometrial environment that promotes trophoblast proliferation and migration and modulates the maternal immune response [430, 466, 467]. Aberrant expression of IDO1 in the endometrial environment is associated with recurrent miscarriage [468, 469]. IFNγ induces IDO1 expression; thus, as there was a significant downregulation in *IFNG* expression by NK-92 cells, *IDO1* expression was investigated [470]. This study showed a significant increase in *IDO1* mRNA when cells were treated with succinic acid, indicating that metabolites associated with diverse bacteria can alter *IDO1* expression. However, this should be interpreted cautiously as this was not significant in Dunnett's multiple comparisons tests, and was only seen in cells treated with 1 mM of succinic acid and not in cells treated with 2 mM succinic. Furthermore, decreased *IFNG* mRNA was only seen

in NK-92 cells treated with L-lactic and acetic acids. It is possible that this response to succinic acid could be due to a different mechanism to IFNγ-induced IDO1 expression. For example, it has been shown that butyrate can inhibit IDO1 expression by decreasing STAT1 and inhibiting histone deacetylase [471]. However, further analysis should be conducted to investigate this.

There was no significant difference in the expression of *IDO1* in the NK-92 cells treated with L-lactic, D-lactic or acetic acids. It may be possible that these metabolites do not impact *IDO1* expression. This aligns with the literature, demonstrating that IDO1 expression is not altered by exposure to acetic acid [471]. However, it is also necessary to consider that NK-92 cells in this study were only incubated with the metabolites for 4 hours. This was likely not long enough to see changes in *IDO1* expression, as it has been demonstrated that *IDO1* mRNA and protein levels reach maximum expression after cells have been stimulated for 24 hours with either TNF or IFNγ [472]. Further experiments should use longer incubation periods to assess if prolonged treatment with metabolites impacts *IDO1* mRNA expression. Additionally, protein expression should be examined in conjunction with mRNA expression. In future studies, it would also be beneficial to investigate *IDO1* expression in macrophages treated with the metabolites, as macrophages have an important role in modulating implantation via IDO1 activity [473]. Likewise, investigating *IDO1* expression in macrophages and the influence of NK cells treated with metabolites could be explored in a conditioned media model, where THP-1 derived macrophages are cultured with NK cells conditioned media to investigate the impact of decreased *IFNG* expression.

Macrophages are another dominant immune cell type in the endometrium and are thought to have a role in the development of receptivity, angiogenesis and tissue breakdown, and in modulating the immune response [56, 424, 474]. Interestingly, while decidual macrophages do not fit the traditional M1/M2 polarisation model of macrophages, it has been shown that M1-like, M2-like, or M0 profiles can affect embryo implantation. There are studies suggesting that there is a correlation between M0 and M2 macrophages and implantation failure [475, 476]. Similarly, the abundance of M1-like macrophages is associated with outcomes such as spontaneous abortion within the first 10 weeks of pregnancy [477]. Therefore, this study aimed to investigate the profile of cytokines and chemokines secreted by THP-1 derived macrophages when treated with microbiota-associated metabolites. Our data showed that THP-1-derived macrophages showed higher secretion of IL-8 when exposed to L-lactic acid. This aligns with the literature, which previously showed that L-lactic acid and co-culture with lactic acid-producing bacteria can induce increased IL-8 secretion from macrophages [478, 479]. This could be beneficial in the endometrial environment as macrophages increase IL-8 secretion via interacting with trophoblast HLA-G, which modulates trophoblast invasion and remodelling of spiral arteries [41]. However, it is important to consider that I did not observe a significant change in mRNA expression of *IL8* in THP-1 cells treated with L-lactic acid, and the results from CBA assays were not significant when analysed with Dunnett's multiple comparisons test. Additionally, other research has demonstrated that lactic acid can decrease *IL-8* expression [461].

Interestingly, when THP-1 cells were cultured with acetic acid, there was a significant decrease in secreted RANTES. This could be detrimental to embryo implantation as it has been shown that hypoxic conditions in the endometrium increase

RANTES secretion, promoting the migration and invasion of trophoblast cells [480]. However, it is also important to consider that this result was not reflected in THP-1 mRNA expression or in the results from Dunnett's multiple comparisons tests. Beyond IL-8 and RANTES, a range of other cytokines and chemokines were investigated in this study. However, there was no significant difference in their mRNA expression and secretion when THP-1 cells were exposed to metabolites. Thus, it is difficult to conclude how these metabolites may impact the inflammatory response of macrophages. In the future, polarising macrophages before their use to represent the M1-like or M2-like profiles may aid in further determining the role of microbiota-associated metabolites with macrophages in representing those found in the endometrium [481].

The final experiment of this study was a conditioned media model, where epithelial cells were cultured with media conditioned by innate immune cells. This aimed to provide insight into the interactions between epithelial cells and innate immune cells when in the presence of microbiota-associated metabolites. Interestingly, in RL95-2 cells cultured with media conditioned by THP-1 cells treated with 15 mM L-lactic acid, there was a significant decrease in *IL8* mRNA. This may indicate that macrophages are able to modulate *IL8* expression in the endometrial epithelial cells. In the literature, it has been shown that macrophage-conditioned media can significantly alter gene expression in endometrial stromal cells [482]. However, a significant increase in *IL8* mRNA was observed. The authors proposed that macrophages communicate with endometrial tissue, increasing *IL8* expression in stromal cells, promoting angiogenesis [482]. However, in this case, microbiota-associated metabolites like L-lactic acid may interfere with this communication and downregulate *IL8* expression in endometrial epithelium. However, it is important to consider that Eyster et al. (2010) used the U-973 cell line and telomerase-

immortalised human endometrial stromal cells, whereas I used THP-1 and RL95-2 cells. Therefore, the response of endometrial stromal cells to macrophages may differ from the response of epithelial cells as they have different roles in endometrial function. It would be beneficial to further investigate this interaction using a co-culture system, such as transwell plates, to directly model the interaction of THP-1 cells and RL95-2 cells. Likewise, it would be beneficial to complete cytokine analysis of epithelial cells cultured with conditioned media to determine if changes in mRNA expression are reflected in protein secretion.

There was no significant difference in cytokine mRNA expression between the Ishikawa cells cultured with media conditioned by NK-92 or THP-1 cells or in RL95-2 cells cultured with media conditioned by NK-92 cells. It is possible that changes in cytokine secretion and gene expression in the immune cells was not substantial enough to generate a response from the epithelial cells. It is also important to consider that not all changes in gene expression in innate immune cells were reflected in the cytokines secreted and, thus, may not have impacted epithelial cells. In future studies, developing a co-culture model using transwell plates to culture epithelial cells and innate immune cells within one well could ensure the cells are exposed to cytokines and other secreted products as they are produced in culture. This could more accurately represent the interactions between epithelial and innate immune cells. However, future models should take into account that the NK-92 cell line is an allogeneic cell line that displays high cytotoxicity. Their high cytotoxicity results from a high content of molecules involved in the perforin-granzyme cytolytic pathway, as well as a large number of activating receptors and few inhibitory receptors [239]. NK-92 cells also express high levels of IFNγ and IL-10, which may contribute to their cytotoxicity [453]. Thus, this should also be taken into

consideration when interpreting the results of the conditioned media models, as the expression of cytokines may create a more cytotoxic environment than what is seen in the endometrial environment.

As NK-92 cells, have a highly cytotoxic profile and the potential for an alloreactive response to endometrial epithelial cells, it is worth considering different forms of NK cell models to explore the impact of microbiota-associated metabolites in future. One method could be using primary NK cells and endometrial epithelial cells in an organoid model. While this approach has not yet been explored in the literature, similar models have been developed to model the trophoblast and NK cell interaction [268, 269, 483]. These studies generate primary trophoblast organoids from the digestion of placental villi and isolate primary uNK cells from decidual tissue [268, 269, 483]. The cells are then co-cultured to investigate their interactions. This methodology allowed researchers to determine the cytokine interactions between the trophoblast and uNK cells, that uNK cells enhance differentiation as well as aid in placentation, and that the trophoblast has a role in immunomodulation of uNK cells [268, 269, 483]. Thus, a similar approach could be taken to further investigate the interactions between uNK cells and endometrial epithelium in the presence of microbiota-associated metabolites.

4.6 Conclusion and future directions

In conclusion, the data demonstrates that microbiota-associated metabolites may affect cytokine, chemokine secretion, and mRNA expression by endometrial epithelium and innate immune cells. Microbiota-associated metabolites like L-lactic, acetic, and succinic acids, may modulate the immune response in the endometrium. This could be

detrimental to implantation, modulation of the immune response and the control of trophoblast invasion, as the downregulation of *IL8* mRNA in epithelial and NK cells and the downregulation of *RANTES* mRNA in epithelial cells was seen. Similarly, this was seen in decreased secretion of IL-8 and RANTES by epithelial cells, and THP-1 cells were also observed. However, responses generated by metabolites like D-lactic acid could also be beneficial, as demonstrated by the profile of secreted cytokines in NK-92 cells treated with D-lactic acid. Overall, considerable complexity warrants further investigation as it is difficult to conclude whether or not exposure to these metabolites creates advantageous conditions or a deleterious response from the epithelium and innate immune cells. It is also important to consider the limitations of the methodology used and how future models could be improved to provide more insight into metabolites and the immune response.

In future experiments, hormonal priming could be used to generate a receptive profile in the cells before their use, and immune cells could be differentiated to represent the phenotype present in the endometrium. Additionally, future experiments should also include a complete dose-range of the microbiota-associated metabolites to investigate if there is a dose-response. It is important to acknowledge that a limitation of this study is that *Lactobacillus* was represented using L-lactic and D-lactic acids independently. Currently, little is known about the specific species present in the endometrium due to the limited resolution of 16s rRNA gene amplicon sequencing [209]. In the vaginal environment, different species secrete differing ratios of these isomers [153]. As more information becomes available, different ratios of L-lactic and D-lactic acids can be used to better represent different *Lactobacillus* species in the endometrial environment. This may provide more insight into how NK cells respond to these metabolites and the effect this may have

on gene expression and cytokine secretion. Additionally, a co-culture system using transwell plates could be developed to enable the representation of epithelial and innate immune cell interactions. Successful models using this system have been developed for the vaginal environment and could be used to provide further insight into the endometrial environment [160].

5 Microbiota-associated metabolites and embryo implantation

5.1 Introduction

The successful implantation of an embryo is essential for the outcome of IVF treatments. Successful implantation is confirmed by the diagnosis of a clinical pregnancy, where the amniotic sac and the fetal heartbeat can be observed using an ultrasound [66]. Implantation failure is of concern, as in Australia and New Zealand, as the clinical pregnancy rate has shown marginal improvement over the last five years indicating that steps beyond embryo development need to be improved to increase positive outcomes from IVF [70]. Numerous explanations exist for why implantation failure may occur, and these have been reviewed extensively in the literature. This includes factors like endometrial receptivity, the maternal immune response, and abnormalities in embryo development [83]. There has been some emphasis on the role of the endometrial microbiome in the development of receptivity and the maternal immune response. However, less is known about the impact of the microbiome on embryonic factors, specifically cellular metabolism, adhesive and invasive properties, and how this could impact implantation. Thus, it is necessary to investigate these factors and the impact of the endometrial microbiome on essential factors involved in embryo development and implantation.

Glucose is an essential substrate for the developing embryo as it becomes the primary energy source, and glucose uptake indicates viability [484]. As the embryo rapidly develops, there is a rise in glucose consumption and an increased production of lactic acid [485]. Before the first two cell divisions, the embryo largely consumes pyruvate, which is required for the clearance of maternal mRNA and development to the 2-cell stage [486]. However, the embryo switches to consuming glucose, preventing an

arrest in development at the 2-cell stage (also known as the 2-cell block) by promoting lipid metabolism and biosynthesis [487]. This switch to consuming glucose is required for blastocyst formation and gastrulation, supporting anabolic processes such as the hexosamine biosynthetic pathway and the pentose phosphate pathway controlling trophectoderm development [488, 489]. Supporting this, it was shown that high-quality blastocysts that achieved a clinical pregnancy after transfer had significantly higher glucose uptake than embryos that failed to implant [490]. Thus, glucose uptake has been proposed as a measure of embryo viability. Furthermore, it is well-established that the embryo undergoes aerobic glycolysis, utilising glucose and producing lactic acid as a by-product [491, 492]. It has been proposed that the lactic acid produced by the embryo can act as a signalling molecule and aid in embryo implantation into the endometrium and in the development of receptivity [283]. However, it remains relatively unknown how microbiota-associated metabolites, including L-lactic, D-lactic, acetic and succinic acids, may impact the glucose uptake of an embryo in the endometrial environment.

Embryo implantation involves three main steps; apposition, adhesion and invasion. Apposition is where the embryo comes into close contact with the endometrial epithelium after moving freely within the uterine cavity [22, 493]. Adhesion follows apposition and occurs when a strong bond between the trophectoderm of the blastocyst and the epithelium forms [22]. Adhesion is mediated by cell adhesion molecules, including cadherins, integrins, mucins and immunoglobulins [24, 26-29]. The final stage of embryo implantation is invasion, where the trophectoderm proliferates into the endometrial stroma. Matrix metalloproteinase (MMP) like MMP2 and MMP9 are proteolytic enzymes that break down and remodel the extracellular matrix during invasion and are expressed by the embryo [494, 495]. MMP2 and MMP9 are gelatinases

considered the most important for trophoblast invasion [496, 497]. MMPs are regulated by tissue inhibitors of matrix metalloproteinases (TIMP) which reversibly block the active site of MMPs [498]. TIMPs are expressed by the embryo and are also thought necessary in regulating invasion [499].

Currently, there is limited knowledge of the role of the endometrial microbiome and how it impacts each of the above-described factors involved in embryo implantation. However, given the similarity in the metabolites produced by the embryo, and that several studies indicate an association between the composition of the endometrial microbiome and implantation failure, further investigation of this relationship is warranted [178-180]. Moreover, various studies have suggested that bacteria may have a role in embryo development and embryo grade, consequently affecting the outcome of the embryo transfer [500, 501]. It has been shown that *Lactobacillus* can promote the expression of trophoblast MMPs and that lactic acid produced by *Lactobacillus* regulates the expression of MMPs in the vaginal environment [153, 502]. Thus, this study aimed to investigate the impact of microbiota-associated metabolites on key factors involved in embryo development and implantation by culturing endometrial epithelial cells and innate immune cells with L-lactic, D-lactic, acetic, and succinic acids.

5.2 Hypothesis and Aim

5.2.1 Hypothesis

Metabolites produced by *Lactobacillus* create an environment conducive to successful embryo implantation by modulating factors involved in embryo development, adhesion, and invasion. Metabolites produced by diverse bacteria will adversely alter the expression of these factors and may lead to implantation failure.

5.2.2 Aim

Determine the impact of microbiota-associated metabolites on factors involved in embryo implantation.

5.3 Methods

5.3.1 Cell culture

All cells used in experiments were cultured and maintained according to the methodology outlined in sections 2.1.1, 2.1.2, and 2.1.3. In addition to the endometrial epithelial and innate immune cells used in previous chapters, JAR cells were used to investigate embryonic factors. Before use, THP-1 cells were differentiated using PMA as outlined in section 2.1.4.

5.3.2 MTS Assays

MTS assays were conducted according to section 2.3.2 to determine the viability of cells exposed to different concentrations of metabolites in culture.

5.3.3 Treatment of cells and sample collection

The cells were treated with concentrations that they remained viable at in culture. Table 7 outlines the concentration range for each cell line and the microbiota-associated metabolites. The methodology for collecting cell samples for RT-qPCR experiments is outlined in section 2.4.1. A range of concentrations was used to treat the cells. However, not all results have been included in this chapter. The results for all concentrations used in experiments can be found in Appendix 4.

5.3.4 Glucose-uptake assay

The Promega Glucose Uptake-Glo™ Assay kit was used to assess the glucose uptake of JAR cells after treatment with metabolites. This was completed according to the methods outlined in section 2.7.

5.3.5 Western blots

5.3.5.1 Preparation of protein extracts

Western blots were used to assess the protein expression of MMP2 and MMP9 in JAR cells. The cells were seeded into 12-well plates (Thermo Fisher Scientific, cat no. 150628) at a seeding density of 2×10^5 cells/well and incubated for 24 hours at 37°C at 5% CO_2. The spent media was removed and replaced with media containing metabolites, according to Table 7. The cells were incubated for 24 hours at 37°C at 5% CO_2. The monolayer was washed twice with ice-cold PBS. After washing, 1 mL of ice-cold RIPA lysis and extraction buffer (Thermo Fisher Scientific, cat no. 89900) was added to each well and incubated at room temperature for five minutes. Each well was scraped, and the lysate was transferred to a 1.5 mL tube. The samples were centrifuged at 14,000 ×g for 15 minutes to pellet the cell debris. The supernatant was aliquoted into new tubes, and the pellet was discarded. The samples were frozen at -20°C until use. An aliquot of each sample was kept on ice for use in a bicinchoninic acid (BCA) assay.

5.3.5.2 Bicinchoninic acid (BCA) assay

The Pierce™ BCA assay (Thermo Fisher Scientific, cat no. 23227) was used according to the manufacturer's instructions to determine the protein concentration of each sample. The dilution series of the BSA standard was prepared to generate a standard curve ranging from 0 μg/mL to 2000 μg/mL. The working reagent was prepared by mixing Reagent A with Reagent B in a 50:1 ratio. In a 96-well plate, 25 μL of each standard and unknown sample was added in triplicate. 200 μL of the working reagent was added to each well. The plate was incubated for 30 minutes at 37°C. The absorbance of each well was read using the Tecan Infinite M200 Plate reader at 562 nm. A standard curve was generated using the absorbance readings from the standards to determine the unknown samples' protein concentration.

5.3.5.3 Western blot

The samples used in western blots were initially thawed on ice. The protein concentrations, calculated using the BCA assay results, were adjusted to ensure 4 μg/μL was added to each lane. Once diluted, Bolt™ LDS sample buffer (4×) (Thermo Fisher Scientific, cat no. B0007) and Bolt™ Sample Reducing agent (10×) (Thermo Fisher Scientific, cat no. B0009) were added to each sample. The samples were then heated at 95°C for 5 minutes and then centrifuged for one minute at 16,000 ×g.

The Mini Gel Tank (Thermo Fisher Scientific, cat no. A25977) was used to run the samples. The tank was filled with 1× running buffer (NuPAGE™ MES SDS Running

Buffer (20×), Thermo Fisher Scientific, cat no. NP0002) and NuPAGE™ Bis-Tris Mini Protein Gels 4-12% (Thermo Fisher Scientific, cat no. NP0321BOX) were placed in the tank. Each lane was loaded with 35 µL of samples. One lane per gel was loaded with 5 µL of PageRuler™ Plus Prestained Protein ladder (Thermo Fisher Scientific, cat no. 26619) and 30 µL sample buffer. Protein separation was achieved by electrophoresis at 165 V/400-mA for 45 minutes.

The separated cellular proteins were transferred onto a Trans-Blot Turbo Mini polyvinylidene difluoride (PVDF) membrane (BioRad, cat no. 1704156) using the BioRad Trans-blot Turbo system (cat no. 1704150). Once the transfer was completed, the membranes were blocked in 5% skim milk overnight at 4°C. The membranes were incubated with the primary antibodies diluted in the blocking solution, according to Table 19, overnight at 4°C. The membranes were washed six times, for five minutes, with 1× TBST. The membranes were then incubated with the secondary antibodies diluted in blocking solution according to Table 19 for one hour at room temperature. The membranes were washed six times for five minutes in 1× TBST. Then 2 mL of Amersham™ ECL Prime Western Blotting Detection reagent (Sigma-Aldrich, cat no. GERPN2232) was added according to the manufacturer's instructions. The membranes were imaged using the Amersham™ Imager 600.

Table 19. The primary and secondary antibodies used in western blot experiments. All antibodies were ordered from Thermo Fisher Scientific.

Primary Antibody	**Dilution**	**Cat no.**	**Secondary Antibody**	**Dilution**	**Cat no.**
GAPDH polyclonal	1:10,000	PA1-987	Goat Anti-Rabbit IgG (H+L) Secondary Antibody, HRP	1:10,000	31460
MMP9 Monoclonal	1:1000	MA5-15886	Goat Anti-Mouse IgG (H+L) Secondary Antibody, HRP	1:10,000	31431
MMP2 Monoclonal	1:1000	436000			

5.3.5.4 Western blot analysis

The Western blot images were analysed using ImageJ software, and densitometry was performed. Statistical significance was determined using an unpaired T-test with Welch's correction. The results were also analysed using a one-way ANOVA and Dunnett's multiple comparison tests. The figures were generated using GraphPad Prism 9.3.0 for Windows (GraphPad Software, Boston, Massachusetts USA www.graphpad.com) and Microsoft PowerPoint 16.82 for Mac.

5.3.6 RT-qPCR

All RT-qPCR experiments were conducted according to the methods outlined in section 2.6.2. To assess the expression of MMPs and TIMPs by JAR cells, the primers outlined in Table 20 were used.

Table 20. Primer sequences for genes involved in MMP regulation by JAR cells. All primer pairs were ordered from Integrated DNA Technologies (IDT, Singapore).

Gene	**Role**		**Sequence (5'-3')**	**Reference**
Metalloproteinase 2 (*MMP2*)	Regulation of trophoblastic invasion	Forward	CAAGTGGGACAAGAACCAGA	[503]
		Reverse	CCAAAGTTGATCATGATGTC	
Metalloproteinase 9 (*MMP9*)		Forward	GTCCACCCTTGTGCTCTTCC	
		Reverse	CGACTCTCCACGCATCTCTG	
Tissue Inhibitor of metalloproteinase 1 (*TIMP1*)		Forward	GGCTTCACCAAGACCTACAC	[504]
		Reverse	TGGACACTGTGCAGGCTTCA	
Tissue Inhibitor of metalloproteinase 2 (*TIMP2*)		Forward	ACGGCAAGATGCACATCACC	
		Reverse	GCCGTCACTTCTCTTGATGC	

5.3.7 Spheroid Attachment Model

5.3.7.1 JAR Spheroid Generation and Preparation

To prepare the spheroids, JAR cells were seeded into ultra-low attachment 6-well plates (Sigma-Aldrich, cat no. CLS3471) at a concentration of 2×10^5 cells/well. The cells were incubated at 37°C at 5% CO_2 for 24 hours to allow the spheroids to form. Before use in the embryo attachment assay, the spheroids were incubated with 0.5 μg/mL calcein-AM (Thermo Fisher Scientific, cat no. 65-0853-39) for 30 minutes at 37°C at 5% CO_2 [252]. The spheroids were then passed through a 100 μm cell strainer (Sigma-Aldrich, cat no. CLS431752), followed by a 70 μm cell strainer to ensure that the spheroids were approximately the size of a blastocyst [252].

5.3.7.2 Treatment of Endometrial Epithelial Cells

The first condition tested was the treatment of the endometrial epithelial cells with microbiota-associated metabolites (Figure 18a). Ishikawa and RL95-2 cells were seeded into black, clear-bottom 96-well plates (Sigma-Aldrich, cat. no. CLS3603) at a density of 2×10^4 cells per well, 48 hours prior to the attachment assay. The cells were incubated for 24 hours at 37°C at 5% CO_2. After incubating, the spent media was removed from the cells and replaced with media containing metabolites in the concentrations outlined in Table 7. The cells were also treated 1× LPS and 1× PMA/I to determine the effect of the inflammatory controls. The cells were incubated with the metabolites for 24 hours before

use in the embryo attachment assay. The spheroids were prepared according to section 5.3.7.1.

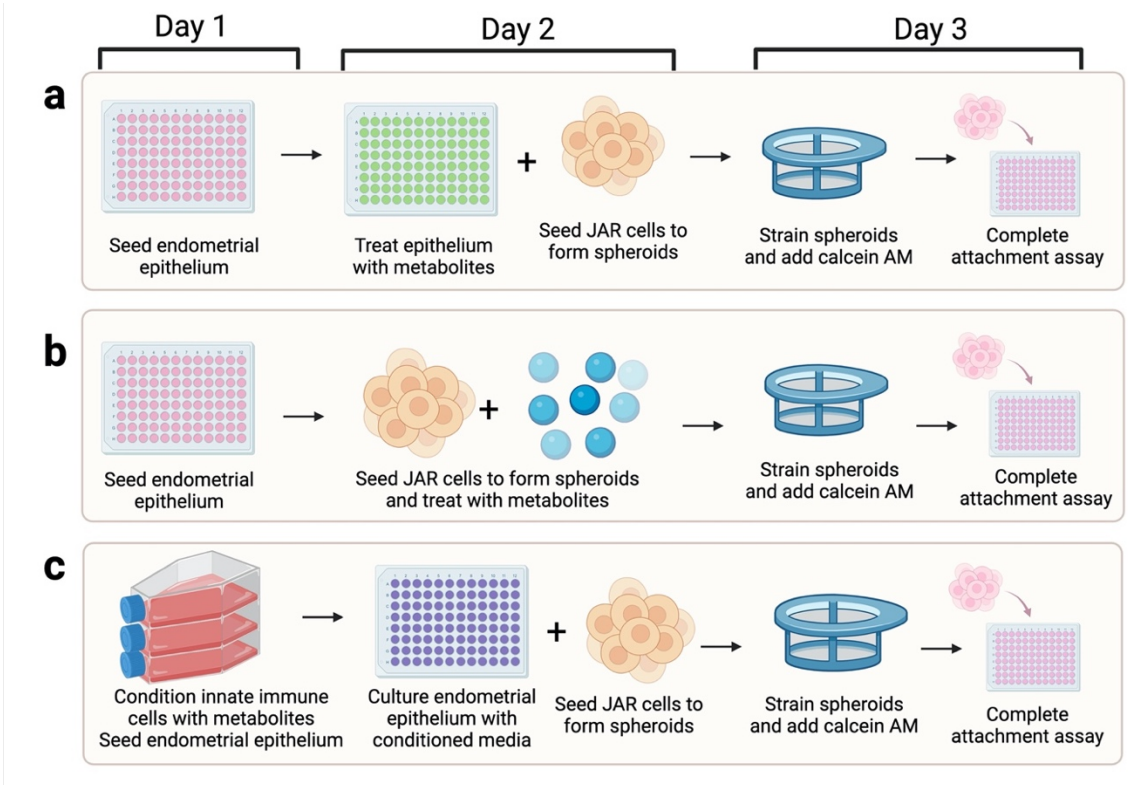


Figure 18. JAR Spheroid attachment assay workflow. (a) The JAR cell attachment assay where Ishikawa and RL95-2 cells were treated with microbiota-associated metabolites before their use in the assay. (b) The JAR cell attachment assay where JAR cells were treated with the microbiota-associated metabolites before their use in the assay. (c) The JAR cell attachment assay where NK-92 and differentiated THP-1 cells were treated with microbiota-associated metabolites to generate conditioned media. Ishikawa and RL95-2 cells were cultured with innate immune cell-conditioned media before their use in the attachment assay. Created in https://BioRender.com.

5.3.7.3 Treatment of Spheroids with Metabolites

The second condition tested was the treatment of JAR spheroids with microbiota-associated metabolites (Figure 18b). After JAR cells were seeded into ultra-low attachment plates, metabolites were added according to Table 7. As controls for these experiments, the cells were treated with 1× LPS and 1× PMA/I without microbiota-associated metabolites to determine the effect of inflammatory stimuli. Once the metabolites or inflammatory stimuli were added, the cells were cultured for 24 hours at 37°C at 5% CO_2 to allow the spheroids to form. Once the spheroids had formed, the method outlined in section 5.3.7.1 was followed. Before beginning the attachment assay, Ishikawa and RL95-2 cells were seeded into black clear-bottom 96-well plates at 2×10^4 cells/well and incubated for 24 hours at 37°C at 5% CO_2 (Sigma-Aldrich, cat no. CLS3603).

5.3.7.4 Treatment of Endometrial Epithelial Cells with Immune Cell Conditioned Media

The final condition tested was the pre-treatment of epithelial cells with innate immune cell-conditioned media (Figure 18c). The metabolite-treated conditioned media was prepared using the same method outlined in section 2.5.1. At 48 hours prior to the attachment assay, Ishikawa and RL95-2 cells were seeded into black clear-bottom 96-well plates at 2×10^4 cells/well and incubated for 24 hours at 37°C at 5% CO_2. At 24 hours, the media was removed and replaced with conditioned media. The plates were incubated

for a further 24 hours. At this point, the spheroids were prepared according to section 5.3.7.1

5.3.7.5 Spheroid Attachment Assay

Once the endometrial epithelial cells and spheroids had been prepared, the spent media was removed from 96-well plates seeded with epithelial cells and replaced with complete RPMI 1640. The cells were incubated for 30 minutes at 37°C with 5% CO_2 to ensure the media had equilibrated. Approximately 40 spheroids were added to each well and incubated with the epithelial cells for 30 minutes at 37°C with 5% CO_2 to allow attachment [252]. The fluorescence of each well was read using the Tecan Infinite M200 plate reader with the excitation at 495 nm and emission at 515 nm, with multiple readings per well to ensure the signal from all seeded spheroids was captured. To remove unattached spheroids, the media was aspirated, and the wells were washed twice with 200 µL of warm dPBS [252]. Then, 200 µL of complete RPMI 1640 was added to the wells, and the fluorescence was read again. The percentage of attached spheroids was calculated using the following equation [252];

$$\%\ Attached\ Spheroids = \frac{Attached\ spheroids}{Seeded\ spheroids} \times 100$$

The figures were generated using GraphPad Prism 9.3.0 for Windows (GraphPad Software, Boston, Massachusetts USA www.graphpad.com), and an unpaired T-test with Welch's correction was performed to determine the significance. The results were also analysed using a one-way ANOVA and Dunnett's multiple comparison tests.

5.4 Results

5.4.1 JAR cell viability at physiologically relevant concentrations of microbiota-associated metabolites

JAR cells were cultured with microbiota-associated metabolites to determine how the microbiome impacts embryo implantation. The JAR cells were used for this investigation as they are derived from a choriocarcinoma and are widely used to represent trophoblast cells and embryos in culture [252, 505]. To represent microbiota present in the endometrial environment, L-lactic, D-lactic, acetic and succinic acids were used as the bacteria are known to produce these metabolites, and have also been used successfully to represent vaginal microbiota in culture [160, 162]. MTS assays were used to determine what concentrations could be used to represent microbiota while maintaining the viability of the JAR cells in the culture. The cells were grown as a monolayer and treated with metabolite concentrations ranging from 0 mM to 30 mM. The cells were considered viable if they showed 80% or more viability over the three-time points. The JAR cells remained viable when cultured with ≤15 mM of L-lactic, D-lactic, and acetic acids (Figure 19). However, the JAR cells only remained viable when cultured with ≤5 mM succinic acid (Figure 19). These concentrations were used in all the following experiments. Lower concentrations, including 2.5 mM, 5 mM, and 10 mM of the metabolites, were used in RT-qPCR experiments to investigate a dose-dependent result, and the data for this is available in the Appendix 4.

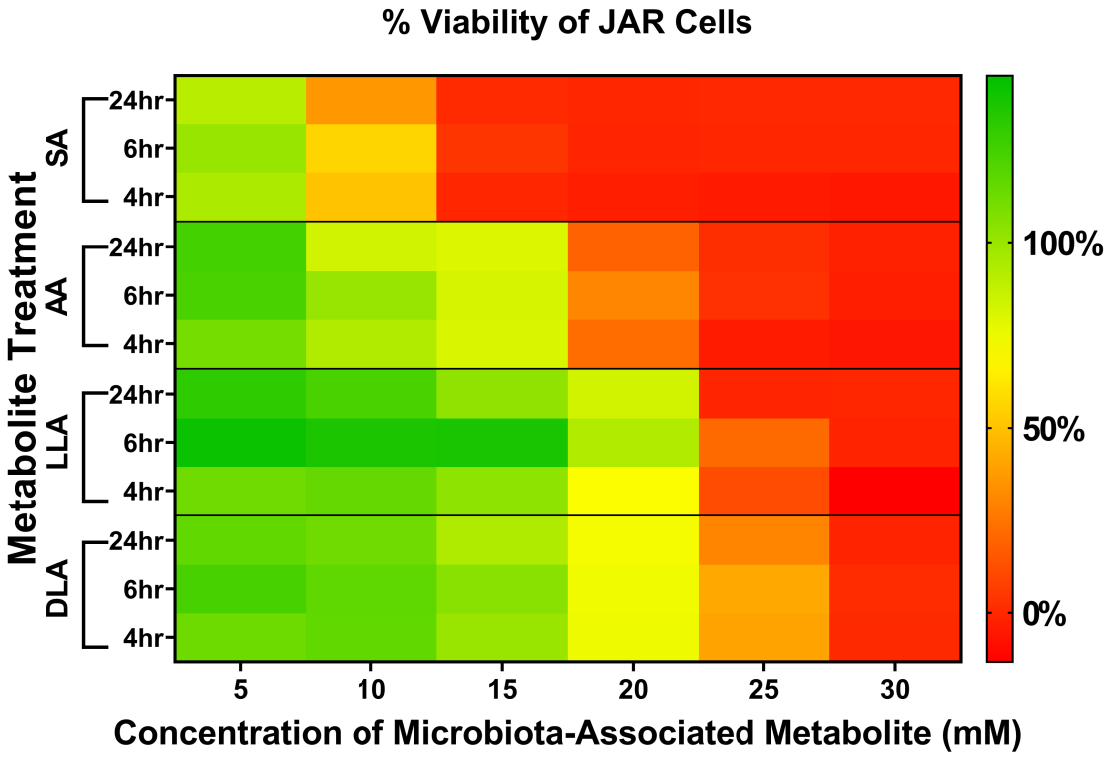


Figure 19. The viability (%) of JAR cells treated with microbiota-associated metabolites. Metabolites are listed on the left y-axis; DLA represents D-lactic acid, LLA represents L-lactic acid, AA represents acetic acid, and SA represents succinic acid. The incubation period in hours is indicated on the left y-axis. The viability of the cells is represented by a gradient from 0% viability (red) to ≥100% viable (green). The concentrations of each metabolite are indicated on the x-axis. n = 3.

5.4.2 Microbiota-associated metabolites do not impact JAR cell glucose uptake

Glucose consumption rises in the late pre-implantation period and is thought to be an important cell-signalling agent for blastocyst formation [485]. Thus, I investigated the glucose uptake of JAR cells when exposed to the microbiota-associated metabolites.

Compared to untreated controls, there was no significant difference in the glucose uptake for JAR cells when treated with the metabolites in both T-tests and Dunnett's multiple comparisons tests (Figure 20).

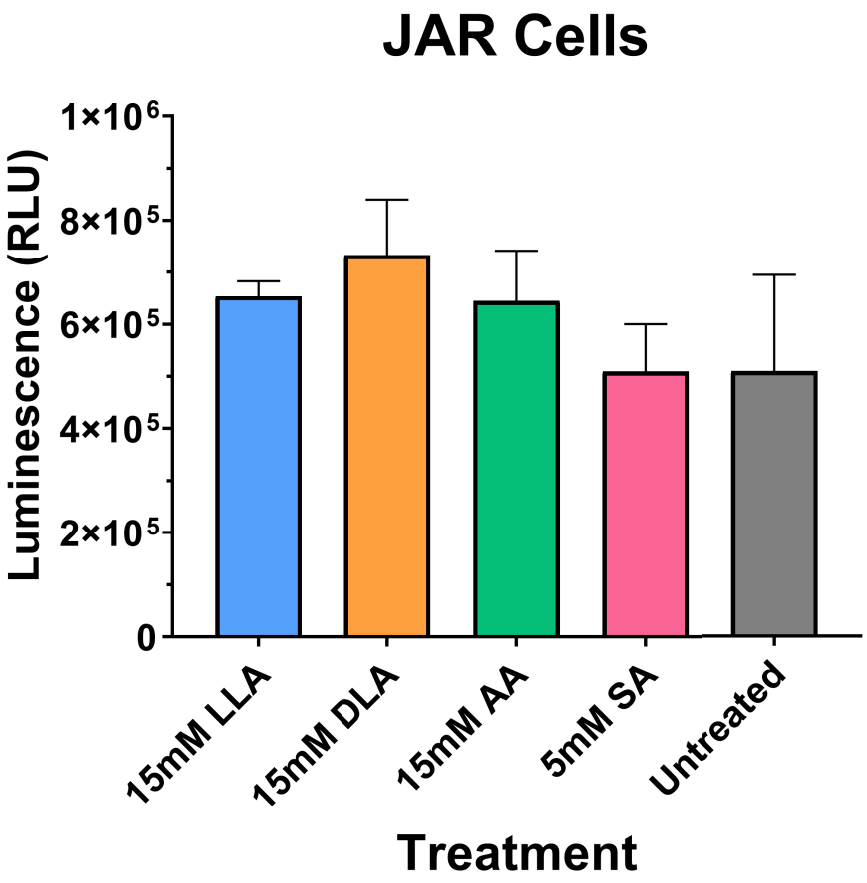


Figure 20. The glucose uptake JAR cells after treatment with microbiota-associated metabolites. Glucose uptake was determined using the Promega glucose uptake-Glo™ assay. DLA represents D-lactic acid, LLA represents L-lactic acid, AA represents acetic acid, and SA represents succinic acid. The y-axis shows luminescence, and the scale of each y-axis is different. Luminescence is proportional to glucose uptake and is measured in relative light units (RLU). The data presented shows the mean ± SEM (n=3).

5.4.3 MMP and TIMP expression is not impacted by microbiota-associated metabolites

MMP2 and MMP9 are essential in the implantation process by allowing the embryo to break down the extracellular matrix, enabling invasion [494, 495]. Tissue breakdown and implantation are regulated by inhibiting the MMP catalytic site by TIMP1 and TIMP2 [499]. Thus, I aimed to evaluate the impact of microbiota-associated metabolites on the embryo's expression of MMPs and TIMPs. JAR cells consistently expressed *MMP2*, *TIMP1*, and *TIMP2* mRNA, but the mRNA expression of *MMP9* was low. When fold change analysis was conducted relative to *GAPDH*, there was no significant difference in the expression of *MMP2, MMP9, TIMP1*, and *TIMP2* compared to the untreated controls in both T-tests and Dunnett's multiple comparisons tests (Figure 21). This was followed up by Western blot analysis of the MMP2 and MMP9 protein expressed by the JAR cells treated with the metabolites. Only MMP2 produced visible bands, and MMP9 bands were not visible (Appendix 4) (Figure 22). The western blot results were assessed using densitometry analysis relative to GAPDH, but similarly to RT-qPCR results, there was no significant difference in the MMP2 protein expressed by the cells compared to untreated controls in both T-tests and Dunnett's multiple comparisons tests (Figure 22).

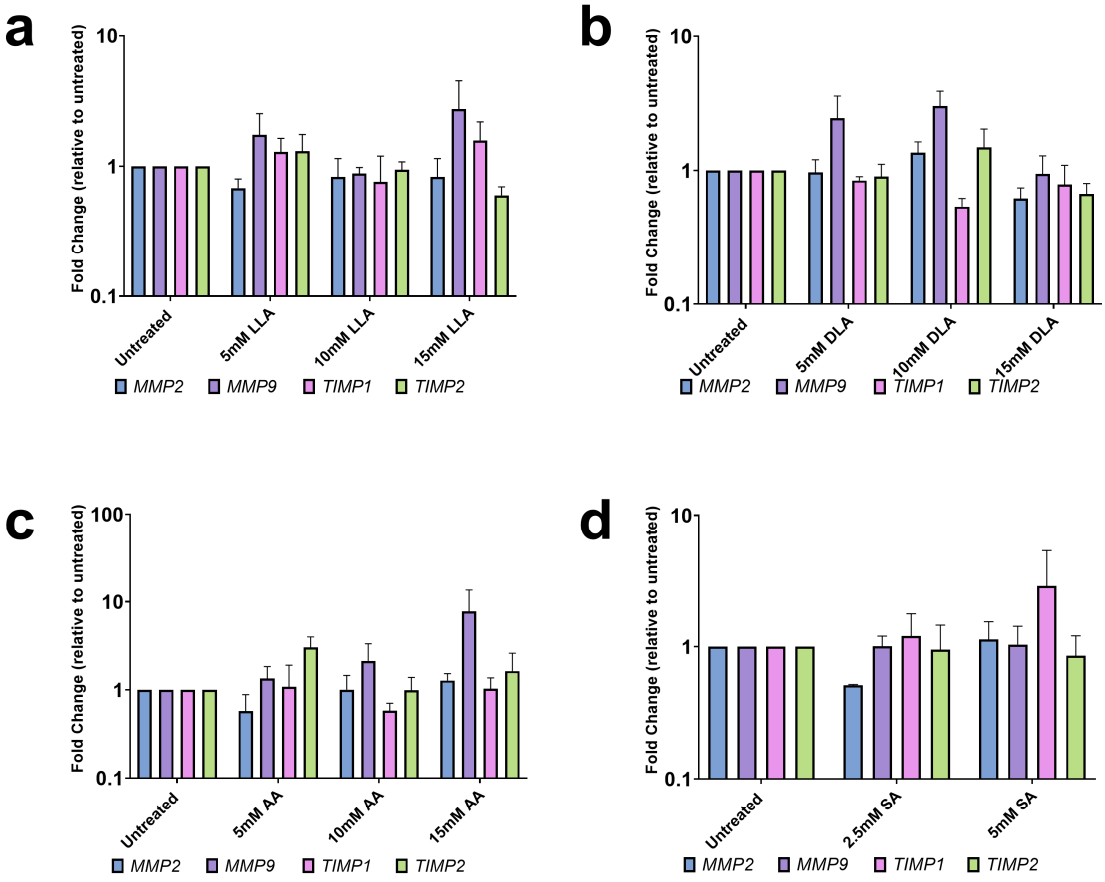


Figure 21. Relative gene expression of MMP2, MMP9, TIMP1, and TIMP2 by JAR cells treated with microbiota-associated metabolites compared to untreated cells. JAR cells were treated with L-lactic acid (LLA), D-lactic acid (DLA), acetic acid (AA), and succinic acid (SA). (a) Fold change of JAR cells treated with LLA. (b) Fold change of JAR cells treated with DLA. (c) Fold change of JAR cells treated with AA. (d) Fold change of JAR cells treated with SA. Gene expression was normalised to the reference genes and expressed as fold change compared to the untreated cells using the comparative C_t method. The data shows the mean ± SEM (n = 3).

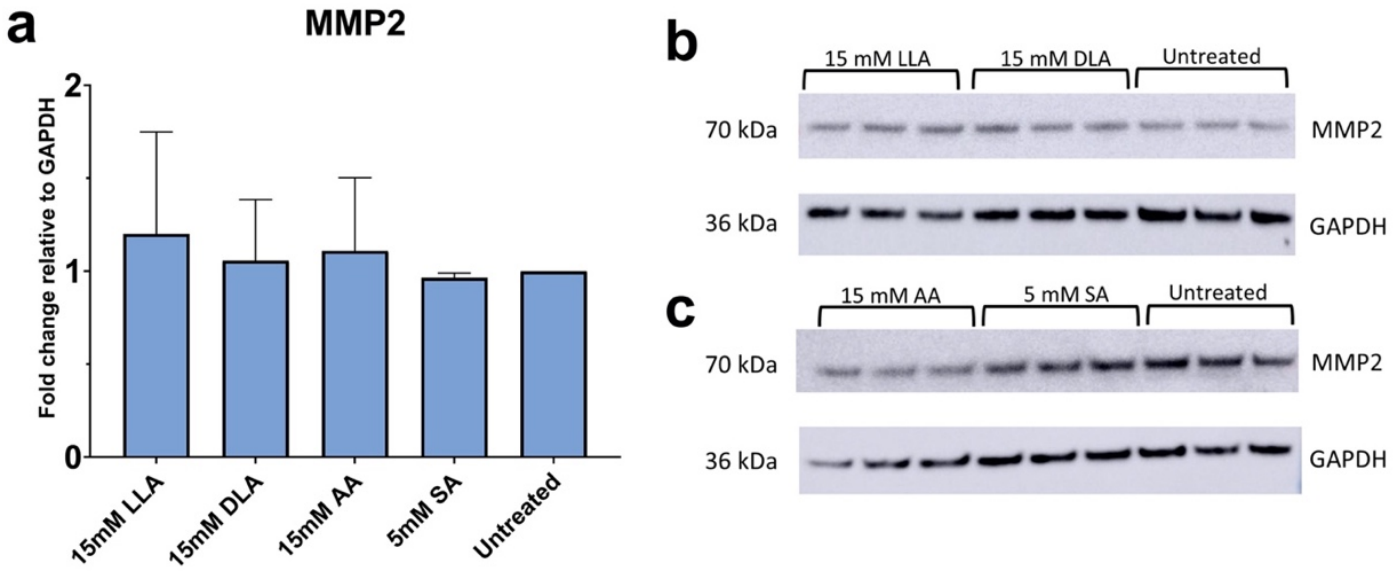


Figure 22. Protein expression of MMP2 relative to GAPDH in JAR cells treated with microbiota-associated metabolites. JAR cells were treated with L-lactic acid (LLA), D-lactic acid (DLA), acetic acid (AA), and succinic acid (SA). (a) Densitometry analysis of MMP2 expression relative to GAPDH. The data shows the mean ± SEM, (n = 3). (b) Western blots of MMP2 and GAPDH from JAR cells treated with LLA and DLA, and untreated cells. (c) Western blots of MMP2 and GAPDH from JAR cells treated with AA and SA, and untreated cells.

5.4.4 Microbiota-associated metabolites do not impact endometrial epithelium's ability to facilitate attachment

Embryo implantation involves three stages: apposition, adhesion, and invasion. Due to the practical and ethical constraints of studying implantation and embryo adhesion, spheroid attachment assays were developed to represent this process in cell culture. This study used a high-throughput model using JAR cells spheroids to model embryos and Ishikawa and RL95-2 cells to represent endometrial epithelium. To assess microbiota-associated metabolites' impact on embryo adhesion, epithelial cell monolayers were pre-treated w with L-lactic, D-lactic, acetic, and succinic acids and then carried out the attachment assay. Treating Ishikawa cells with the metabolites did not significantly affect spheroid attachment compared to untreated cells in both T-tests and Dunnett's multiple comparisons tests (Figure 23). Likewise, pre-treating RL95-2 cells did not significantly affect spheroid attachment compared to untreated controls in both T-tests and Dunnett's multiple comparisons tests (Figure 23).

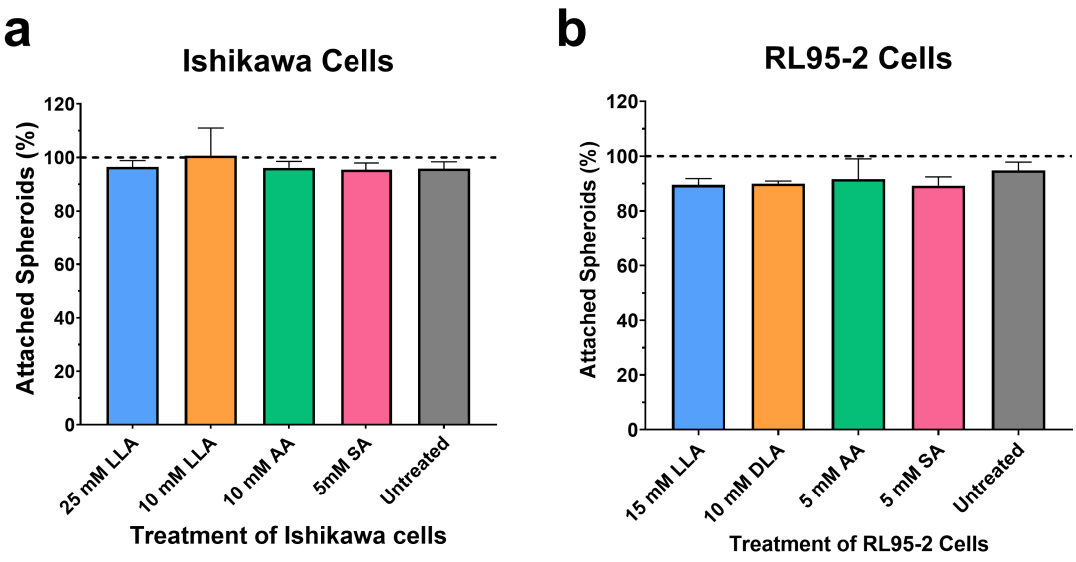


Figure 23. Spheroid attachment to endometrial epithelial cells treated with microbiota-associated metabolites. Ishikawa and RL95-2 cells were treated with L-lactic acid (LLA), D-lactic acid (DLA), acetic acid (AA), and succinic acid (SA) for 24 hours before conducting the spheroid attachment assay. (a) The percentage of attached spheroids to Ishikawa cells. (b) The percentage of attached spheroids to RL95-2 cells. The data shows the mean ± SEM (n = 3).

5.4.5 Microbiota-associated metabolites do not impact JAR spheroids' ability to attach to endometrial epithelium

As the embryo in the endometrium is also exposed to microbiota-associated metabolites during implantation, this study aimed to determine if this would impact embryo adhesion. While culturing spheroids using JAR cells, L-lactic, D-lactic, acetic, and succinic acids were added to the media. The treated spheroids were then seeded onto untreated Ishikawa or RL95-2 cell monolayers and the attachment assay was conducted.

There was no significant difference in spheroid attachment to both Ishikawa and RL95-2 monolayers compared to untreated controls in both T-tests and Dunnett's multiple comparisons tests (Figure 24).

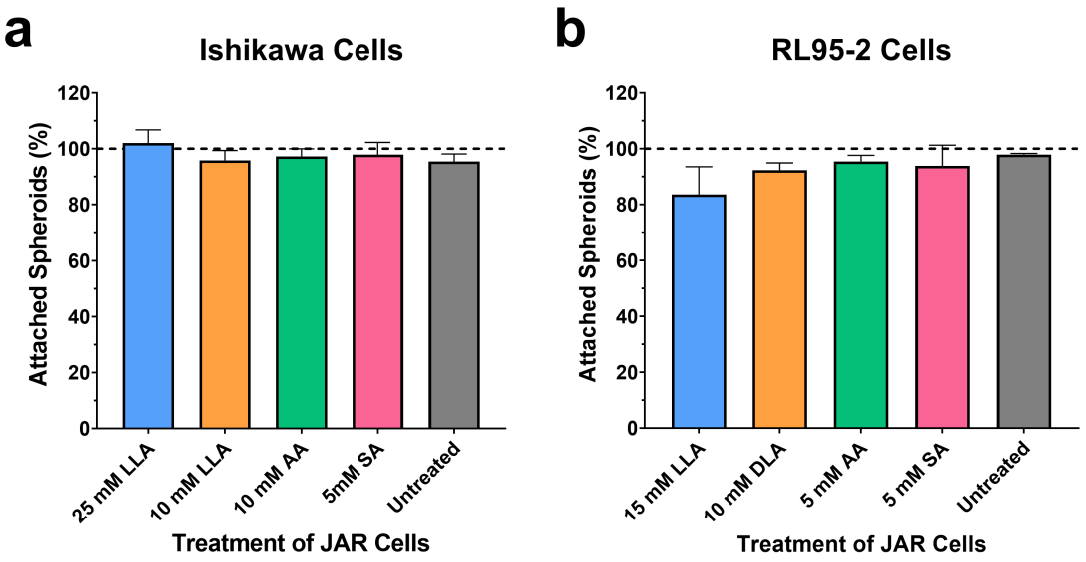


Figure 24. Attachment of JAR cells treated with microbiota-associated metabolites to untreated endometrial epithelial cells. JAR cells were treated with L-lactic acid (LLA), D-lactic acid (DLA), acetic acid (AA), and succinic acid (SA) for 24 hours before conducting the spheroid attachment assay. (a) The percentage of attached spheroids to Ishikawa cells. (b) The percentage of attached spheroids to RL95-2 cells. The data shows the mean ± SEM (n = 3).

5.4.6 The NK-92 secretome, after exposure to microbiota-associated metabolites, inhibits spheroid attachment to endometrial epithelium

Innate immune cells are important in developing receptivity in the endometrium and interact with endometrial epithelium. Thus, pre-treated Ishikawa and RL95-2 cells with media conditioned by innate immune cells were used to represent this interaction in a spheroid attachment assay. Chapters 3 and 4 demonstrated that microbiota-associated metabolites can affect mRNA expression and cytokine secretion in NK-92 and THP-1 cells. Thus, NK-92 and THP-1 cells were treated with L-lactic, D-lactic, acetic, and succinic acids for 24 hours to generate conditioned media. Ishikawa and RL95-2 monolayers were cultured with the conditioned media for 24 hours. The spheroid attachment assay was conducted using untreated JAR cell spheroids. Interestingly, when Ishikawa cells were pre-treated with media conditioned by NK-92 cells, there was a significant decrease in the attached spheroids compared to the untreated control (Figure 25a). This was seen when NK-92 cells were treated with L-lactic acid ($p=0.0093$) ($p=0.038$ with Dunnett's multiple comparisons test), D-lactic acid ($p=0.20$) ($p=0.13$), and succinic acid ($p=0.018$) ($p=0.11$) to generate conditioned media (Figure 25a). L-lactic acid treatment resulted in a 11% reduction in spheroid attachment, whereas D-lactic acid and succinic acid resulted in a 8.7% and a 9.0% decrease in spheroid attachment respectively. There was no significant impact on attachment assays using Ishikawa cells treated with THP-1 conditioned media or RL95-2 cells treated with NK-92 and THP-1 conditioned media in both T-tests and Dunnett's multiple comparisons tests (Figure 26).

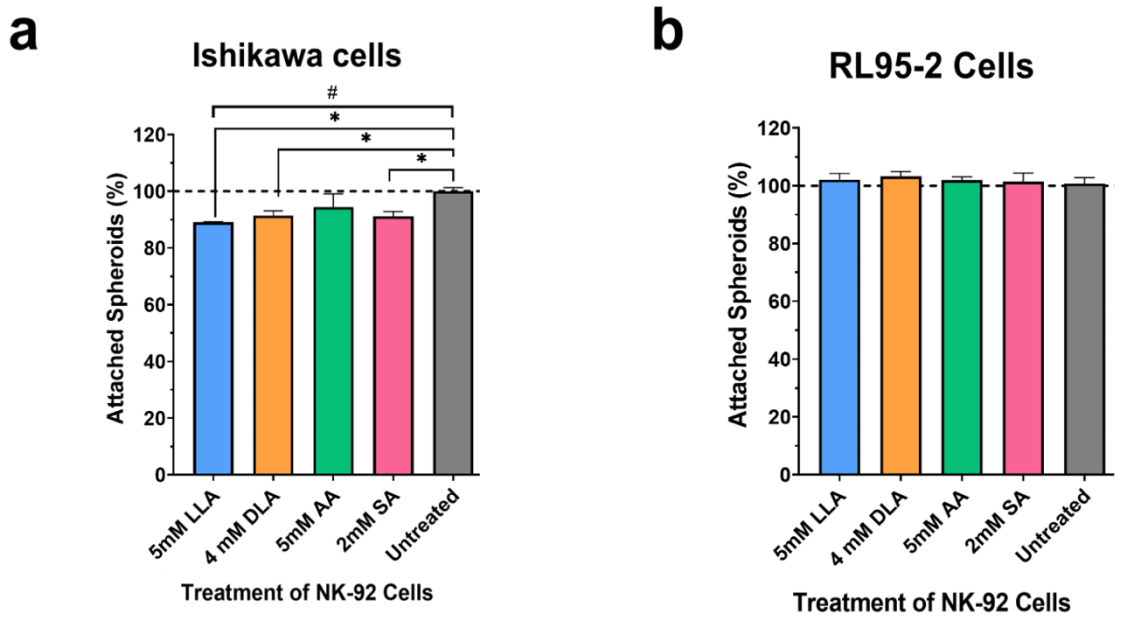


Figure 25. Spheroid attachment to endometrial epithelial cells treated with media conditioned by NK-92 cells cultured with microbiota-associated metabolites. To generate conditioned media, NK-29 cells were treated with L-lactic acid (LLA), D-lactic acid (DLA), acetic acid (AA), and succinic acid (SA) for 24 hours. Endometrial epithelial cells were treated with the conditioned media for 24 hours before conducting the spheroid attachment assay. (a) The percentage of attached spheroids to Ishikawa cells. (b) The percentage of attached spheroids to RL95-2 cells. The data shows the mean ± SEM (n = 3). * represents $p \leq 0.05$, analysed by unpaired T-tests with Welch's correction. # represents $p \leq 0.05$, analysed by Dunnett's multiple comparisons test.

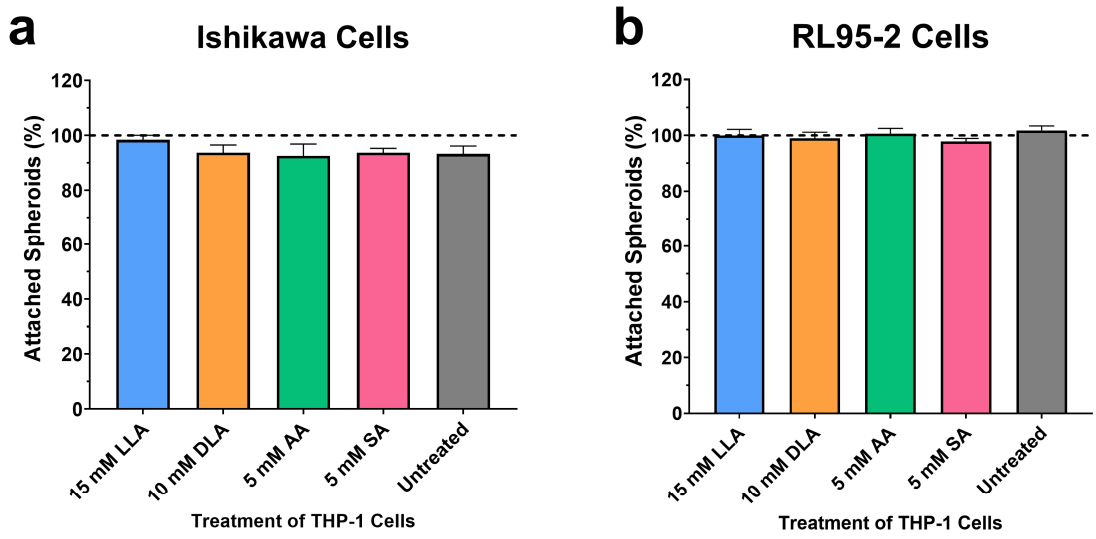


Figure 26. Spheroid attachment to endometrial epithelial cells treated with media conditioned by differentiated THP-1 cells cultured with microbiota-associated metabolites. To generate conditioned media, THP-1 cells were treated with L-lactic acid (LLA), D-lactic acid (DLA), acetic acid (AA), and succinic acid (SA) for 24 hours. Endometrial epithelial cells were treated with the conditioned media for 24 hours before conducting the spheroid attachment assay. (a) The percentage of attached spheroids to Ishikawa cells. (b) The percentage of attached spheroids to RL95-2 cells. The data shows the mean ± SEM (n = 3).

5.5 Discussion

The development of the embryo and the success of implantation are essential to successful IVF outcomes. It is widely reported in the literature that the dominance of *Lactobacillus* in the endometrium is associated with successful outcomes like clinical pregnancy and live birth [178, 180, 181]. On the other hand, diverse microbiota in the endometrium are associated with implantation failure [178, 180, 181]. However, beyond this association, little is known about the role of the endometrial microbiome and its impact on the embryo during implantation. Recent literature has demonstrated that *Lactobacillus* may aid in promoting invasion [502]. In the vaginal environment, it is known that microbiota, like *Lactobacillus*, have an important role in homeostasis by producing key metabolites, including lactic acid [506]. Likewise, it has been demonstrated that vaginal microbiota and L-lactic and D-lactic acids regulate the expression of MMPs [153]. MMPs are essential during embryo implantation in controlling trophoblast invasion [496, 497]. Thus, this study aimed to investigate the effect of microbiota-associated metabolites on embryonic factors involved in the development and implantation of an embryo using a cell culture model.

This study investigated the impact of microbiota-associated metabolites during embryo implantation in monoculture and spheroid assays using JAR cells to represent the trophoblast. L-lactic and D-lactic acids were used to represent *Lactobacillus*, and acetic and succinic acids were used to represent diverse bacteria. To model the presence of microbiota in the endometrium, concentrations at which the cells were at least 80% viable in cell culture, as 80% or greater viability in response to treatment were used [309]. The JAR cells tolerated ≤ 15 mM of L-lactic and D-lactic acid. It is well established that the

embryo undergoes aerobic glycolysis, producing a significant concentration of lactic acid while developing [485]. Likewise, it is known that the oviduct has an increased concentration of lactic acid throughout the cycle, reaching approximately 10 mM at the time of ovulation [507]. Similarly, cumulus cells also increase their glucose consumption and production of lactic acid [507]. Furthermore, it is estimated that the blastocyst may produce up to 100 mM of lactate due to its glucose consumption in the endometrium [491]. Thus, it is unsurprising that the JAR cells remained viable in ≤ 15 mM lactic acid, as the embryo can produce such high concentrations. The JAR cells remained viable when ≤ 15 mM acetic acid was added to the cell culture media. This was unsurprising as it has been shown that high concentrations of up to 50 mM of acetate can alter the morphology and trigger cell death in syncytiotrophoblast cells [508]. It has been determined that lower acetate concentrations, like 10 mM, could maintain cellular metabolism by promoting the production of acetyl-coenzyme A [508]. Additionally, JAR cells remained viable when treated ≤5 mM succinic acid. This is a much lower concentration than the other metabolites, but it has been shown that succinic acid is detrimental to other cell lines, causing cell death [366]. However, in the literature, embryos cultured in the presence of up to 5 mM succinate were beneficial to the development of the blastocyst [509]. However, it is important to note that this was done using hamster embryos, and there is limited literature on the effects of succinic acid on human embryos.

Glucose uptake is highly important in the metabolism of an embryo and increases as the embryo develops. Higher glucose uptake is a marker of viability in pre-implantation embryos and is associated with clinical pregnancy [490]. During implantation, glucose is used in glycolysis and the hexosamine biosynthetic pathway, which is essential for blastocyst formation, cell differentiation and gastrulation [488, 489]. Therefore, this study

investigated the glucose uptake of JAR cells when exposed to microbiota-associated metabolites. Compared to untreated controls, there was no significant difference in glucose uptake in cells exposed to L-lactic, D-lactic, acetic, and succinic acids. This may indicate that metabolites produced by bacteria in the endometrial environment do not affect glucose uptake in the embryo. This was unsurprising as lactate and acetate have been previously shown not to impact glucose uptake in murine embryos [510, 511]. As there was no significant difference between the untreated controls and D-lactic acid-treated cells, it may indicate that D-lactic acid, which is specifically produced by bacteria in the endometrium, also does not impact glucose uptake. Interestingly, succinic acid is enriched in the blastocyst alongside other metabolites in the citric acid cycle, and is used in culture to improve the development of hamster embryos in conjunction with glutamine, lactate, and pyruvate [509, 512]. However, it has been shown that glucose can inhibit the development of hamster blastocysts, and it is proposed that non-glucose substrates may be preferentially used [509]. However, this was not observed in the glucose uptake assay results, as succinic acid did not significantly impact glucose uptake in JAR cells. This may demonstrate that succinic acid derived from diverse bacteria may not alter glucose uptake. Overall, these results indicate that metabolites produced by bacteria in the endometrial environment may not interfere with the glucose uptake of the developing embryo. However, this should be interpreted cautiously as I used the JAR cell line, which may not adequately represent a developing embryo with a rapidly changing metabolism. In future studies, murine embryos could represent embryo development and enable analysis of the metabolism and glucose uptake over time when exposed to microbiota-associated metabolites. However, it is also important to consider that they cannot completely represent human embryos.

MMPs are proteolytic enzymes that break down the extracellular matrix, with MMP2 and MMP9 being essential for cytotrophoblast invasion into the endometrium and regulated by TIMPs [494, 495]. It is suggested that aberrant expression of MMPs and TIMPs has a role in embryo quality and implantation failure, as well as adverse outcomes such as recurrent pregnancy loss [513-515]. It has also been shown that MMP expression is influenced by microbiota-associated metabolites, like L- and D-lactic acid, in the vaginal environment [153]. Similarly, MMP-9 expression in the endometrium negatively correlated with *Acinetobacter* abundance and is associated with implantation failure [213]. Thus, this study aimed to investigate alterations in *MMP2, MMP9, TIMP1* and *TIMP2* expression by JAR cells treated with microbiota-associated metabolites. Analysis of RT-qPCR experiments showed that cells treated with the metabolites, compared to untreated controls, showed no significant difference in *MMP2, MMP9, TIMP1*, and *TIMP2* mRNA expression. This result was correlated by western blot, which also showed no significant difference in MMP2 expression. For MMP9, no visible bands were observed (Appendix 4). This may indicate that microbiota-associated metabolites do not affect trophoblast MMP and TIMP expression. However, the expression of MMPs and metabolites have been examined across sites and in multiple cell lines with differing results from what was observed in this study. Lactic acid in the tumour microenvironment has been shown in glioma cell lines to promote the expression and activation of MMP2 by inducing TGFβ2 expression [516]. Additionally, increased vaginal pH is positively associated with increased MMP3 expression in the uterosacral ligament, which was proposed to be due to a reduced abundance of *Lactobacillus* in the vaginal environment [517]. Interestingly, it has been shown in hepatocellular carcinoma and renal carcinoma cells that suppressing lactate dehydrogenase A and C results in decreased expression of MMP2 and MMP9, affecting the metastatic potential of the cells [518, 519]. Suppressing

lactate dehydrogenase also decreases lactate production, as aerobic glycolysis was inhibited [518, 519]. Additionally, short-chain fatty acids stimulated the activity of MMP9 and TIMP activity in the colon cancer cell lines when cells were cultured with media supplemented 10 mM of acetate, butyrate, or propionate [520]. However, these studies should be interpreted cautiously as the endometrium is a unique environment where embryo invasion occurs under hypoxic conditions that have been shown to inhibit the extravillous trophoblasts' invasive capabilities and activation of MMP2 and expression of TIMP2 [521].

It is important to consider the limitations of the JAR cell line when investigating MMPs and TIMPs. In the literature, JAR cells readily express MMP2, as seen in our RT-qPCR and western blot results [522]. However, JAR cells have been shown to have little to no mRNA or protein expression of MMP9, which also aligns with this study's results [522, 523]. However, studies investigating endometrial conditions affecting invasion determined that the expression and activity of MMP9 in JAR cells can be induced by stimulating the cells with TNF or through culture in hypoxic conditions [524, 525]. Thus, in future, altering culture conditions to represent the hypoxic state of the endometrium during implantation may enable a better understanding of how these metabolites impact MMP and TIMP expression. Additionally, conducting MMP activity assays may provide further insight in to MMP2 as western blotting detects both active and inactive forms of MMPs, and may not clearly indicate a difference in activity.

I modelled embryo attachment using a spheroid attachment model to investigate embryo implantation further. Spheroid models using cell lines have been developed to enable the investigation of factors involved in implantation without the ethical and

practical issues associated with *in vivo* studies [526]. Thus, I used this assay to represent embryo adhesion in the presence of microbiota-associated metabolites. The attachment assays were performed to investigate the impact of the metabolites on the epithelium and spheroids separately as both the epithelium and embryo are exposed to microbiota. In these experiments, the epithelium or spheroids were pre-treated with L-lactic, D-lactic, acetic, and succinic acids and then used in the attachment assay. Compared to untreated controls, there was no significant difference in the percentage of attached spheroids to Ishikawa or RL95-2 cells when the epithelial cells or spheroids were pre-treated. This was surprising, as it was previously shown in spheroid attachment models that lactic acid (20 mM) may induce nucleolar stress in epithelium and regulate implantation [527]. Furthermore, it has been suggested G Protein-coupled receptor 65 (GPR65) expressed by trophoblasts acts as a pH sensor and inhibits adhesion in a low pH environment such as that created by lactic acid or other metabolites [528]. This was demonstrated using both JAR cell spheroids and murine blastocysts in an attachment model using Ishikawa cells as epithelium [528]. The cells used in this study were maintained at a pH of 7.4, thus this effect mechanism may not occurred. It is also possible that microbiota-associated metabolites may not have a role in embryo adhesion and may only impact factors like endometrial migration and the endometrial immune response, as discussed in chapters three and four. Furthermore, both RL95-2 and Ishikawa cells are highly adhesive cell lines, which may mean that subtle changes in receptivity or in the adhesive properties of JAR cells that could have impacted spheroid adhesion may not have been reflected in the results of this assay [292, 505]. Interestingly, one study has developed a 3-dimensional model of spheroid attachment incorporating primary stromal cells, creating a more complex representation of endometrium [505]. This model showed the impact of stromal cells on JAR cell spheroid adhesion and provides a methodology that could be used in

future studies to closely represent this interaction in a more realistic model of the endometrium [505]. Furthermore, inclusion of an inhibitor would be a useful control in future models using highly adhesive cell lines like Ishikawa and RL95-2 cells, to demonstrate that the assay is able to model inhibition of attachment. For example, EDTA has been used successfully in past RL95-2 models as it blocks Ca^{2+} influx significantly reducing spheroid attachment to RL95-2 cells [252].

A conditioned media spheroid attachment model was developed to investigate further the interactions of innate immune cells and endometrial epithelium and its impact on embryo adhesion. In this assay, endometrial epithelium was pre-treated with media conditioned by innate immune cells cultured with microbiota-associated metabolites. When Ishikawa and RL95-2 cells were cultured with media conditioned by THP-1 cells, there was no significant difference in the percentage of attached spheroids. Likewise, RL95-2 cells cultured with media conditioned by NK-92 cells showed no significant difference in the percentage of attached spheroids compared to controls. However, when Ishikawa cells were cultured with media conditioned by NK-92 cells treated with L-lactic, D-lactic, and succinic acids there was a significant decrease in the percentage of attached spheroids. This suggests that L-lactic, D-lactic, and succinic acids produced by microbiota may adversely impact the NK cell interactions with endometrial epithelium, affecting the success of embryo implantation. As shown in chapters three and four, this could result from changes in glucose uptake or in the expression of cytokine and chemokines by NK-92 cells. However, NK-92 conditioned media did not affect endometrial epithelial expression of *IL-6, IL-8, TNF, RANTES* and *IFNG,* suggesting other genes may be affected, reducing the binding of spheroids to the epithelium. It is also important to acknowledge that the percentage reduction in spheroid attachment to the

epithelial monolayer in this model was small. Thus it should be considered that this result may not generate a biologically important result in the *in vivo* endometrial environment. Furthermore, dNK cells interact with endometrial epithelial cells via various mechanisms which could be alternative points of investigation beyond cytokine and chemokine expression. For example, dNK1 cells expression of CD39 can interact with CD73 expressed by endometrial epithelial cells to prevent activation of the inflammatory response by converting ATP to adenosine [529]. This interaction is thought to be essential in enabling implantation. Additionally, dNK cells express prokineticin 1 during the receptive stage, which acts on the endometrial epithelium, promoting the upregulation of genes involved in developing receptivity and decidualisation, including cyclooxygenase (COX)-2 [530]. Overall, the secretome of microbiota-associated metabolite-treated NK-92 cells may affect embryo adhesion. However the exact mechanism behind this requires further investigation.

It is important to acknowledge the limitations of using immortalised cell lines in these models, particularly when using the NK-92 cell line. The NK-92 cell line is an allogeneic activated cell line with a much greater killing capacity than peripheral NK cells and decidual cells [531]. They have a higher content of granzymes, resulting in increased cytotoxicity, and they lack expression of KIR receptors, which inhibit NK cell function against allogeneic cells [239]. These factors mean that these cells may not replicate NK cell function in the endometrial environment and may limit what can be interpreted from the conditioned media models used in this chapter. In future, different forms of NK cell culture models could be used to investigate the interactions between immune cells, epithelium, and trophoblast cells. As discussed in Chapter 4, organoid models have been developed to model the trophoblast and NK cell interaction [268, 269, 483]. These models

have been used to investigate processes such as uNK cell differentiation, placentation and immunomodulation [268, 269, 483]. In future, these models could be adapted to include endometrial epithelium and microbiota-associated metabolites to enable the investigation of NK cell interactions with epithelium and trophoblast cells in the presence of metabolites.

Another approach to investigating NK cells and other innate immune cells in the endometrial environment in the presence of microbiota, could be through humanised mouse models. Typically, mouse models cannot support the human reproductive microbiome, but more recently, a humanised microbiota mouse model has been developed [223]. Humanised microbiota mice were created by administering human-derived faeces to germ-free C57BL/6 mice [224, 532]. The bacteria are then passed via maternal transfer and coprophagy [224, 532]. These mice were then used to model the reproductive microbiome and demonstrated key characteristics of the human vaginal microbiome, such as a dominance of *Lactobacillus*, community state type clustering, and greater protection against pathogens [224]. Interestingly, a similar humanised microbiota mouse model with a humanised immune system has also been generated. Gnotobiotic mice undergo X-ray irradiation and receive either a bone marrow transplant, human haematopoietic stem cells, or peripheral blood mononuclear cells [533-535]. They then receive a human faecal microbiota transplant to create a human-like immune system and microbiome. These mice have been used to study gut microbiome and immune system interactions [533, 536]. These techniques have yet to be used to investigate reproduction, but they provide a new system to model a human-like microbiome and immune system for the investigation of the interactions between bacteria, metabolites, and the endometrial environment.

In order to more specifically investigate NK cells in the endometrial environment, transgenic and knockout mouse models could be used. Transgenic and knockout mice have been used in the literature to investigate the role of NK cells in the endometrium [537]. For example, knockout mice lacking NK cells were used to determine that NK cells aid in the development of the endometrium and vasculature [538]. Knockout mice, lacking IL-10, were used to determine the interactions of NK cells and dendritic cells [59]. This study found that dendritic cells promote the proliferation and differentiation of IL-10-producing NK cells, which promote immunoregulation in the endometrial environment [59]. Furthermore, TgE26 mice, which express human CD3E and lack NK cells, have been used to show the importance of NK cells in maintaining pregnancy. The implantation sites in TgE26 mice lacked lymphocytes and displayed vascular pathology associated with foetal death [539]. Thus, transgenic or knockout mouse models could be used in future studies to investigate the role of NK cells in the endometrium. They could be used in conjunction with bacteria to gain a better understanding of how NK cells and microbiota-associated metabolites interact.

5.6 Conclusion and future directions

In conclusion, the results suggest that it is unlikely that microbiota-associated metabolites directly impact embryo development and implantation. However, microbiota-associated metabolites may indirectly affect embryo adhesion via the NK cell secretome. The secretome may be able to modulate of the adhesive properties of endometrial epithelium. This was seen in spheroid attachment assays where Ishikawa cells were pre-treated with media conditioned by NK-92 cell with L-lactic, D-lactic, and succinic acids.

Further investigation is required to understand better the interactions between innate immune cells and epithelium and how this affects the implantation process. As discussed, future experiments could be conducted using murine models and murine embryos to represent the endometrial environment and a rapidly developing embryo better than an immortalised cell line, and alternative culture conditions could be used to represent the hypoxic state of the endometrium.

6 General Discussion and Future Directions

6.1 Determining the role of endometrial microbiota-associated metabolites in IVF

The endometrial microbiome has recently been characterised using next-generation sequencing techniques and is no longer considered a sterile environment. Several studies have demonstrated there is an association between the dominance of *Lactobacillus* and positive IVF outcomes, including clinical pregnancy and live birth, and an association between diverse bacteria, including *Gardnerella*, *Bifidobacterium*, *Fannyhessea*, *Streptococcus* and *Staphylococcus* and poor outcomes, including implantation failure [116, 178, 180, 181, 206, 540]. However, the mechanism behind this association is relatively unknown, with some studies implicating the microbiome's composition in aberrant development of receptivity, inflammation, and regulation of implantation [181, 213, 502]. Therefore, this project aimed determine the role of the endometrial microbiome in developing endometrial receptivity, the endometrial immune response, and embryo implantation. More specifically the study investigated the role of microbiota-associated metabolites in these factors, as metabolites in the cervicovaginal environment are essential in the integrity of the epithelium and the immune status of the environment [160, 161, 168, 169]. A cell culture model of endometrial epithelial cells and innate immune cells that incorporated physiologically relevant concentrations of L-lactic, D-lactic, acetic and succinic acids was utilised.

The first aim of this project was investigated in Chapter 3, which examined the impact of microbiota-associated metabolites on key factors involved in developing

endometrial receptivity. Ishikawa and RL95-2 cells were used to represent endometrial epithelium and NK-92 and differentiated THP-1 cells to represent innate immune cells. This chapter explored how metabolites impact cellular viability and the effect on glucose uptake, revealing that succinic acid may impact the function of NK-92 cells by decreasing glucose uptake. Further analysis showed that L-lactic acid hinders migration in both Ishikawa and RL95-2 cell lines in wound healing assays. Confocal microscopy analysis of ZO-1 (a tight junction protein) demonstrated that D-lactic and acetic acid decreased the protein expression in Ishikawa cells. RT-qPCR analysis revealed decreased mRNA expression of *TGFBR1* in RL95-2, NK-92, and THP-1, alongside decreased *LIF* and *VEGFA* expression in Ishikawa cells when treated with the metabolites. Overall, it was concluded that microbiota-associated metabolites from both *Lactobacillus* and diverse bacteria may alter the development of receptivity and may induce changes that inhibit implantation (Figure 27).

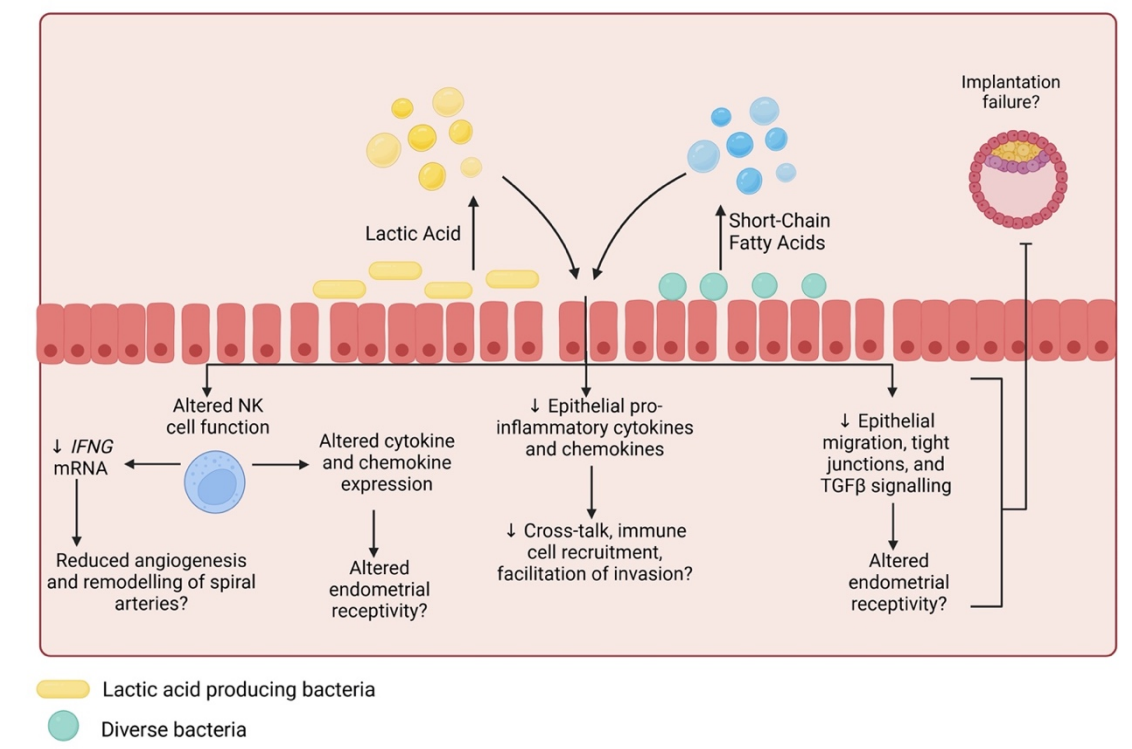


Figure 27. Proposed model of the impact of microbiota-associated metabolites on endometrial epithelium and innate immune cells. Bacteria in the endometrium produce lactic acid and short-chain fatty acids. These metabolites affect NK cell function, the expression of cytokines and chemokines, migration, and the expression of tight junctions. This may result in reduced angiogenesis, cross-talk, regulation of embryo invasion, and the development of receptivity. Ultimately, these alterations may result in implantation failure. Created in https://BioRender.com.

The second aim of this project is presented in Chapter 4, which investigated the impact of microbiota-associated metabolites on the immune response of the epithelium and innate immune cells. Analysis of cytokines secreted by treated cells found a significant decrease in secreted pro-inflammatory cytokines when treated with acetic and L-lactic acids. Interestingly, NK-92 cells treated with D-lactic acid increased secreted IL-

6, IL-8, and IL-10, which was not observed when treated with other metabolites. Interestingly, different expression of *IL8* mRNA between Ishikawa and RL95-2 cells when treated with L-lactic acid was observed. Additionally, when treated with L-lactic and acetic acids, NK-92 cells showed a significant decrease in *IFNG* and *IL8* mRNA expression. This study also investigated the impact of innate immune cell-conditioned media on epithelial cells, and determined that RL95-2 cells showed decrease *IL8* expression when cultured with media conditioned by THP-1 cells treated with L-lactic acid. Overall, it was concluded that microbiota-associated metabolites decrease the expression of pro-inflammatory cytokines and chemokines, which may detrimentally impact fetal-maternal cross-talk, angiogenesis, and the regulation of invasion (Figure ***27***). However, NK cells exposed to D-lactic acid increased the secretion of pro-inflammatory cytokines like IL-6, IL-8, and IL-10, which could aid in supporting embryo invasion and the development of maternal tolerance.

The final chapter of this project focused on the impact of metabolites on embryonic factors involved in the development and implantation of the embryo. The JAR cell line was used to represent the embryo and determined that the microbiota-associated metabolites tested here do not impact glucose uptake. Furthermore, this study investigated the expression of MMPs and TIMPs and determined that metabolites do not affect the expression of MMP2, MMP9, TIMP1 or TIMP2 by JAR cells. The final experiment of this chapter was a spheroid attachment assay using the JAR cells to generate spheroids and model embryo attachment. Through this, it was determined that the NK-92 secretome generated in response to microbiota-associated metabolites, may affect the receptivity of the endometrial epithelium and can hinder embryo attachment (Figure 27).

6.2 Do microbiota-associated metabolites in the endometrium have a similar role to metabolites in the vaginal environment?

Overall, microbiota-associated metabolites impact the development of receptivity, modulation of the endometrial inflammatory response, and the regulation of implantation. However, considering the results discussed, it is unclear whether there is a benefit or disadvantage to the response generated by the metabolites explored in this study. Likewise, it remains unclear if metabolites in the endometrial environment have a similar role in maintaining homeostasis to those in the vaginal environment. In cells treated with lactic acids, there were adverse changes in epithelial and immune cells, such as decreased secretion of cytokines like IL-8 and RANTES and decreased *IFNG* mRNA in NK-92 cells. It is well known that lactic acid in the vaginal environment can modulate the inflammatory response and reduce the expression of these cytokines, which maintains an anti-inflammatory environment [160, 168]. Yet, decreased expression in the endometrium could be detrimental due to the importance of these pro-inflammatory cytokines in developing receptivity and implantation. IL-8, expressed by both epithelial and innate immune cells, is involved in fetal-maternal cross-talk, recruiting immune cells to the endometrium and aiding trophoblast invasion during implantation [46, 49, 407]. RANTES aids in recruiting immune cells to the endometrium and develops the necessary inflammatory response during implantation [48, 444]. IFNγ expressed by dNK cells is necessary to remodel spiral arteries in the endometrium and modulate the trophoblast invasion [419, 420]. Therefore, while lactic acid may be able to reduce the expression of pro-inflammatory mediators in both the vagina and endometrium, this may not create

favourable conditions in the endometrium, unlike lactic acid in the vagina. This could also depend on timing in the menstrual cycle in the endometrium. Interestingly, a similar response in the endometrial epithelium treated with acetic acid to that of those treated with lactic acid was seen. Treatment with acetic acid decreased the expression and secretion of IL-8 and RANTES. Decreased expression of RANTES in the endometrial epithelium is a similar response to short-chain acids seen in the vaginal epithelium. However, decreased IL-8 expression contradicts past studies showing metabolites associated with diverse bacteria promote a pro-inflammatory response in the vaginal epithelium [167, 168]. Therefore, microbiota-metabolites can modulate the endometrial inflammatory response, but metabolites like acetic acid may not induce a similar response to vaginal epithelium.

Like the inflammatory response, microbiota-associated metabolites impact the integrity of the endometrium and its function during receptivity and implantation. However, this impact is different to the role of metabolites in the vaginal environment. In the vaginal environment, lactic acid promotes the formation of tight junctions by increasing expression of proteins like Claudin-1 and Claudin-4, maintaining the integrity of the vaginal epithelial layer [161]. Yet, a significant decrease in ZO-1 when treating Ishikawa cells, indicated that lactic acid may disrupt the stable expression of ZO-1 in the endometrium, compromising the integrity of the epithelium during implantation [322, 323]. Furthermore, the soluble products produced by *Lactobacillus* species have been shown to have no inhibitory effect on wound healing in cervical cells [375]. However, in our wound healing model, lactic acid significantly decreased the migration of endometrial epithelial cells, which could be detrimental to the facilitation of implantation by these cells [27]. From these results, it is possible that lactic acid does not have the same role in

the endometrium as it does in the vaginal environment. Further investigation is required to better understand the impact of lactic acid in the endometrium during the development of receptivity and early embryo implantation.

6.3 The relationship between receptivity, the immune response and implantation

In this project, the development of receptivity, the inflammatory response, and the factors involved in implantation was investigated separately. The results seen in Chapter 3 were explored in the context of the EMT and the MET and their role in implantation. Furthermore, the inflammatory response was largely discussed around angiogenesis, the development of maternal tolerance to paternal antigens, and the regulation of implantation in Chapter 4. However, endometrial receptivity, the inflammatory response, and implantation are inextricably linked. The inflammatory response is essential in developing receptivity and EMT/MET. It has been shown that under hypoxic and inflammatory stimulation with CXCL12, endometrial epithelial cells upregulate markers of EMT, including SNAI1 and ZEB1, and increase migration [541]. Furthermore, cytokines and chemokines including IL-6, IL-8, TNF, and TGF-β, can modulate the expression of markers of EMT, including SNAI1, TWIST, and N-cadherin, and can promote migratory properties when cells in culture were treated with these cytokines [542-544]. Interestingly, in this study, there was decreased secreted IL-8 and downregulation of *IL8* mRNA in RL95-2 cells when treated with L-lactic acid and decreased migration of the cells in wound healing assays. This may give us some insight into how microbiota-associated metabolites like L-lactic acid may affect the

inflammatory response of epithelium and, in turn, the EMT. Furthermore, other factors, such as the expression of tight junctions, are linked to the inflammatory response. Infection with *E. coli* has been shown to downregulate *ZO1* mRNA in organoid models, and decreased ZO-1 expression in fetal membranes has been shown in inflammatory conditions such as intrauterine infection [271, 545]. Additionally, it has been shown that ZO-1 has a role in regulating IL-8, as when ZO-1 is silenced, IL-8 expression and secretion are decreased [546]. Interestingly, in our study, I observed decreased expression of ZO-1 in Ishikawa cells treated with acetic acid and decreased secreted IL-8. There is also a similar relationship between LIF and IL-8, as LIF, like ZO-1, can induce IL-8 secretion [547]. In Ishikawa cells treated with acetic acid, there was also decreased LIF expression, which could have contributed to the decreased secreted IL-8. Overall, these results have contributed towards understanding the intersection of the inflammatory response and the development of receptivity. It is possible that the significant changes in cytokine and chemokine expression due to microbiota-associated metabolites can induce alterations in the epithelium that may be detrimental to the development of receptivity. Notably, as a selection of factors were analysed here, other factors may have also changed but were not measured in these experiments.

To explore the link between the development of receptivity, the inflammatory response, and implantation, spheroid attachment assays representing embryo adhesion were conducted. Chapter 5 investigated the impact of media conditioned by NK-92 cells treated with metabolites on spheroid adhesion. NK-92 cells treated with L-lactic, D-lactic, and succinic acids significantly reduced spheroid attachment to Ishikawa cells. It was proposed that this could result from cytokine secretion and expression changes in Chapter 4. However, it is important to note that there were no significant changes in inflammatory

gene expression in Ishikawa cells cultured in NK-92 conditioned media in these experiments. This may be due to other factors not investigated in this study. Further investigation into the expression of receptivity markers in endometrial cells cultured with innate immune cell-conditioned media is warranted and will provide a greater understanding of the complex relationship between metabolites, receptivity, inflammation, and implantation. Such experiments could also include more comprehensive target analysis, such as global transcriptomic or proteomic approaches, as there is evidence that this model can be used effectively, and changes in spheroid attachment were detected. Additionally, the genes and cytokines analysed in these studies are not the only ones involved in the development of receptivity and implantation. Thus, a transcriptomic or proteomic approach could provide a more comprehensive understanding of these factors in a cell culture model.

6.4 The limitations of modelling the endometrium and future directions

The endometrium is a complex and dynamic environment. While this study aimed to model this using endometrial epithelial and innate immune cell lines, there were several limitations. The endometrium is a low oxygen environment. There is limited literature on the oxygen concentration in the endometrium; the few studies that have investigated this have reported an intrauterine partial pressure between 15 mmHg and 21 mmHg [548-550]. This is much lower than the partial pressure of 90 mmHg in arterial blood or 40 mmHg in venous blood [551]. This is likely due to the thickness of the tissue as there is a great distance between the uterine cavity and the blood vessels supplying oxygenated

blood [552]. Interestingly, this hypoxic environment is beneficial for the development of the embryo. When exposed to hypoxic conditions, hypoxia-inducible factor (HIF) is induced. HIF is a transcriptional factor essential in controlling processes like angiogenesis via VEGF expression, embryo development through control of genome activation, and trophoblast invasion via the urokinase plasminogen receptor pathway (uPAR) [553-557]. Furthermore, HIF is essential in developing endometrial receptivity, and its expression is positively associated with *HOXA10* and controls glycolysis, migration, and EMT in epithelial cells [558, 559]. Additionally, low oxygen conditions within the first two days of embryo culture result in higher rates of top-quality and high-quality day two embryos than those cultured at atmospheric oxygen [560]. Similarly, blastocyst quality was higher in those cultured in 5% O_2 [560]. Considering the importance of a low oxygen environment in the development of receptivity and in embryo development, it is important to note that all cells in this study were cultured in standard cell culture conditions at 37°C with 5% CO_2 and atmospheric air. In future, cell-culture models could be conducted using 5% O_2 to better represent oxygen levels in the endometrium. Using these conditions could provide further insight into the aspects of receptivity and implantation are affected by hypoxia and HIF.

In future models, it would be beneficial to hormonally prime the endometrial epithelial cells before treatment with microbiota-associated metabolites. Both Ishikawa and RL95-2 cells express estrogen and progesterone receptors [227, 228]. While both cells are considered a good model of the receptive endometrium, they can be treated with these hormones before their use to replicate the hormonal changes seen in the menstrual cycle. RNA-Seq analysis of Ishikawa cells treated with estrogen and progesterone demonstrated upregulated expression of 82 biomarkers, including *MUC1* and other genes

associated with receptivity, compared to untreated cells [561]. Furthermore, in 3-dimensional models using Ishikawa cells, treatment with estrogen and progesterone resulted in glandular formations with microvilli [562]. Likewise, RL95-2 cells treated with estrogen and progesterone show changes in gene expression associated with receptivity [563]. These responses from Ishikawa and RL95-2 cells support their use as receptive models, but also demonstrate how hormonal priming can be used to promote expression of genes of interest. Hormonal priming in conjunction with metabolite treatment has been used previously to investigate the role of embryo-derived lactic acid on endometrial epithelial cells and successfully demonstrated that lactic acid can affect cellular proliferation and the expression of genes, including *VEGF* [283]. Thus, future models can incorporate hormonal priming to add complexity to models of the endometrial environment.

Another important aspect of the endometrial environment to consider is pH. It is well-established that the vaginal environment is acidic, yet there is much less known about the endometrial environment. There are mixed reports of pH in the uterine cavity, ranging from 6.6 to 8.5, with most papers reporting an average pH of 7.1 to 7.8 [178, 550, 564, 565]. However, it is proposed that the lactic acid produced by the blastocyst can decrease the pH of the endometrium during implantation in the local site [491]. Furthermore, it has been shown in models of endometrial epithelium that lactic acid, in combination with an acidic pH, significantly alters mRNA expression of genes involved in receptivity, including *VEGF, SNAI1*, and *GLUT4* [283]. Lactic acid and decreased pH also significantly decreased the proliferation and TER measurements of ECC-1 cells and increased stromal cell migration [283]. The same results were not observed in cells treated with neutralised lactic acid or acid media created by 8% CO_2 in culture. Thus, pH is also

an important factor in developing receptivity and implantation. However, it is important to consider that the low biomass of the endometrial microbiome is thought to be unable to alter endometrial pH to the same degree that the vaginal microbiome can and is not a predictor of *Lactobacillus* dominance [178]. In future, cell culture models could be cultured with 8% CO_2 to maintain an acidic environment, and pH could be assessed independently from the metabolites incorporated into the media. This methodology has been used effectively to model the endometrial environment in the past, enabling the maintenance of acidic conditions [283].

It is important to consider additional methods that better represent the endometrial environment. Standard 2-dimensional cell culture has advantages around its simplicity, cost, and straightforward maintenance [566]. But these models lack complexity. While a conditioned media model was used in this study, it still does not completely replicate the complexity of the endometrium, which consists of multiple cell types and complex interactions during implantation. Recently, several endometrial organoid models have been developed. One study developed endometrial epithelial organoids that remained genetically stable and could be cryopreserved [567]. These organoids were responsive to estrogen and progesterone, replicating changes in gene expression and protein expression seen in the proliferative and secretory stages of the menstrual cycle [567]. Likewise, organoids derived from menstrual blood showed similar responsiveness to estrogen and progesterone and altered gene expression in response to early pregnancy hormones, including hCG [568]. Furthermore, organoids have been developed to represent both a receptive and non-receptive endometrium, and the secretions of the non-receptive organoids have been shown to interfere with spheroid adhesion to primary cell monolayers [569]. Endometrial organoids have also been used to model infection and

have shown changes in receptivity markers in response to *E. coli* [271]. Thus, endometrial organoids in conjunction with microbiota-associated metabolites could be used in future studies to model a receptive and non-receptive environment and early pregnancy. This could be used to investigate the effect of the metabolites in an environment that more closely represents the endometrium and includes factors like structure, hormonal regulation, the secretions of a non-receptive profile and pathogenic organisms.

Alternatively, microfluidic models are another viable method of representing the endometrium in future models. Microfluidic models represent an organ by using microfluidics to create shear force, concentration gradients, and cell patterning, as well as incorporating sensors within the model to collect data on parameters, including oxygen and pH [570, 571]. Several have been developed for the endometrium. One model created a vascularised model of the endometrium using epithelium, stroma and endothelium. This model could represent decidualisation when treated with hormones and modelled angiogenesis [242]. Another study was able to model embryo and endometrial interactions, demonstrating that co-culture of murine embryos and stromal cells enhanced the rate of embryo development and viability and provided the stimulation of epithelial cilia via fluidics [572]. Interestingly, a vaginal organ-on-a-chip model has been developed, which incorporated microbiota and successfully replicated the epithelial inflammatory response to eubiotic and dysbiotic bacteria as well as pH and ratio of L- and D-lactic acid [281]. Specific scientific questions or hypotheses are more likely to benefit from these models due to their complexity. However, considering these models' cost and time implications, judicious selection of the methodology used, its application, and value should be considered.

Lastly, additional complexity could be added to a model of the endometrial environment by incorporating more metabolites and/or live microorganisms. This study only used L-lactic, D-lactic, acetic, and succinic acids. Yet, bacteria in the reproductive tract produce many other metabolites, including butyrate, propionate, aspartate, ethanol, and formate [162]. In vaginal models, both butyric and propionic acids have been successfully incorporated into cell culture media and have been demonstrated to play a significant role in the inflammatory response [167]. Similarly, when metabolite mixes were incorporated in cell culture, representing *Lactobacillus* dominance and dysbiosis, vaginal epithelium showed a distinct pro-inflammatory response to the dysbiotic solution [168]. Furthermore, the ratio of L- and D-lactic acid in the vaginal environment is important and is used because it is representative of the dominance of different species of *Lactobacillus* [152, 153]. Thus, additional metabolites could be included in models of the endometrial environment to represent the complex microbiome. This could also be done by incorporating live bacteria into cell culture models, as they can produce a complex mixture of metabolites and by-products that may be more representative of what endometrial epithelium and innate immune cells are exposed to *in vivo*. However, it is important to consider the challenges of incorporating bacteria into cell culture models, as they often require different conditions to what cell lines require. Diverse bacteria, such as *Gardnerella,* require anaerobic conditions and are limited to short incubation periods in cell culture, as cells require oxygen to maintain their viability [573, 574].

6.5 The microbiome and IVF in the future

The findings of this study provide valuable insight into the role of the endometrial microbiome in the endometrial environment. In an IVF context, these results may aid in

providing personalised care to IVF patients in future. Currently, additional procedures such as the ERA and endometrial microbiome metagenomics analysis (EMMA) are used to create personalised IVF treatments. The ERA involves collecting an endometrial biopsy and using a transcriptomic signature of 134 genes to determine a patient's receptive status, enabling the timing of future embryo transfers to be adjusted for the WOI [13, 14]. There is variable evidence for the use of the ERA, with literature demonstrating that its use can successfully predict the WOI and improve IVF outcomes [13, 14, 575, 576]. However, there is also evidence that it has no significant impact on IVF outcomes or may worsen live birth rates [15, 16]. The EMMA involves using 16s rRNA gene amplicon sequencing to classify the endometrial microbiome into either a *Lactobacillus*-dominated microbiome or a non-*Lactobacillus*-dominated microbiome. Based on the results, patients undergo personalised antibiotic treatment, followed by probiotic treatment to shift their microbiome to *Lactobacillus* dominance [577, 578]. In the literature, the EMMA has shown promising results, with improved clinical pregnancy and ongoing pregnancy rates in patients after treatment with antibiotics and probiotics [577, 578].

With the knowledge that microbiota-associated metabolites can impact components of endometrial receptivity and the immune response, the EMMA and ERA could be used in conjunction to personalise treatment further. This was recently explored in a prospective controlled study of 107 participants [579]. The EMMA and ERA were used to personalise treatment for 54 participants, and 53 underwent a standard IVF protocol. The participants who received personalised treatment showed significantly improved implantation, clinical pregnancy, and live birth rates compared to those undergoing the standard IVF protocol [579]. However, this study was completed using a

small sample size recruited through the same clinic, which limits what can be interpreted from these results. Thus, the use of the EMMA and ERA together should continue to be investigated.

Immunological testing can also be added to IVF procedures and is another aspect of treatment that can be personalised. There are several types of proposed immune testing that can be done, including uterine immune profiling. This involves completing histological analysis and RT-qPCR on endometrial biopsies to categorise samples into four profiles; regulated immune activation, immune overactivation, low immune activation, and a mixed immune response [580, 581]. Following this, treatment can be personalised based on the profile to promote uNK cells recruitment and activation, decrease Th1 cytokines, and hormonally support the luteal stage [580]. In a controlled matched cohort study, 193 women were treated with standard IVF protocols, and 193 women underwent uterine immune profiling and personalised IVF treatment [582]. Participants were matched based on age, method of fertilisation and embryo transfer, number of mature oocytes, and the stage of the transferred embryos. Participants who received personalised treatment based on their immune profile had a significantly higher implantation rate, live birth rate and a reduced number of miscarriages compared to the control cohort [582]. These findings were further supported by a randomised controlled open two-armed trial [583]. 484 participants enrolled, 190 women were randomised to receive conventional treatment, and 188 women were randomised to receive personalised treatment to correct immune dysregulation. Those who received personalised treatment showed significantly greater liver birth rates, ongoing pregnancy rates, and clinical pregnancy rates [583]. While these results are promising, it is important to consider that the uterine profiling performed in these studies failed to investigate all immune cell types

and focused on uNK cells [581-583]. Other cells, such as macrophages, Tregs, and dendritic cells, also have important roles in embryo implantation and pregnancy. Furthermore, this thesis has provided evidence that the microbiota-associated metabolites may have a role in regulating the endometrial immune response. Thus, future studies could use the EMMA in conjunction with uterine immune profiling to further personalise IVF treatments.

6.6 Conclusion

In this study, endometrial epithelial cell lines and innate immune cells were used to represent the endometrial environment and incorporated metabolites to represent the endometrial microbiome. It was determined that L-lactic, D-lactic, acetic, and succinic acids can alter factors in the development of receptivity, including glucose uptake, migration, the expression of tight junction proteins, and gene expression of receptivity markers. These changes may inhibit the development of receptivity and could result in decreased embryo implantation in IVF treatment. It was found that microbiota-associated metabolites also decreased the expression of pro-inflammatory cytokines in epithelial cells. This could adversely affect processes like invasion and angiogenesis, and may result in decreased embryo implantation. However, D-lactic acid may promote a beneficial pro-inflammatory response in NK cells. This could aid in controlling embryo invasion and create maternal tolerance to the embryo, promoting successful IVF outcomes. Lastly, it was established that the NK cell secretome from cells treated with microbiota-associated metabolites can adversely impact the adhesion of embryo-like spheroids. These results have provided an understanding of how microbiota-associated metabolites may impact the complex relationship between innate immune cells and endometrial epithelium.

Appendix 1

Cell line authentication

Before use in experiments, all cell lines were genotyped by the AGRF, and their authenticity was determined using the CLASTR algorithm by Cellosaurus [305]. Cell lines tested were determined to be authentic and uncontaminated.

Table 21. The results of cell line genotyping using CLASTR.

Suspected cell line	Identified cell line[A]	Accession Number	Number of Markers[B]	Score[C]
Ishikawa	Ishikawa 3-H-12-Luc	CVCL_JG52	8	96.97%
RL95-2	RL95-2	CVCL_0505	9	93.75%
JAR	JAR	CVCL_0360	9	100%
NK-92	NK-92	CVCL_2142	9	100%
THP-1	THP-1	CVCL_0006	9	100%

[A] The cell line identified by CLASTR, using the Tanable algorithm.

[B] The number of STR markers used to generate the score.

[C] The computational score generated by the pairwise comparison based on the algorithm.

Appendix 2

Wound healing assay using Ishikawa cells

These figures are representative images from wound healing assays using Ishikawa and RL95-2 cells treated with microbiota-associated metabolites. The analysis of these images is presented in Chapter 3 Section 3.4.3.

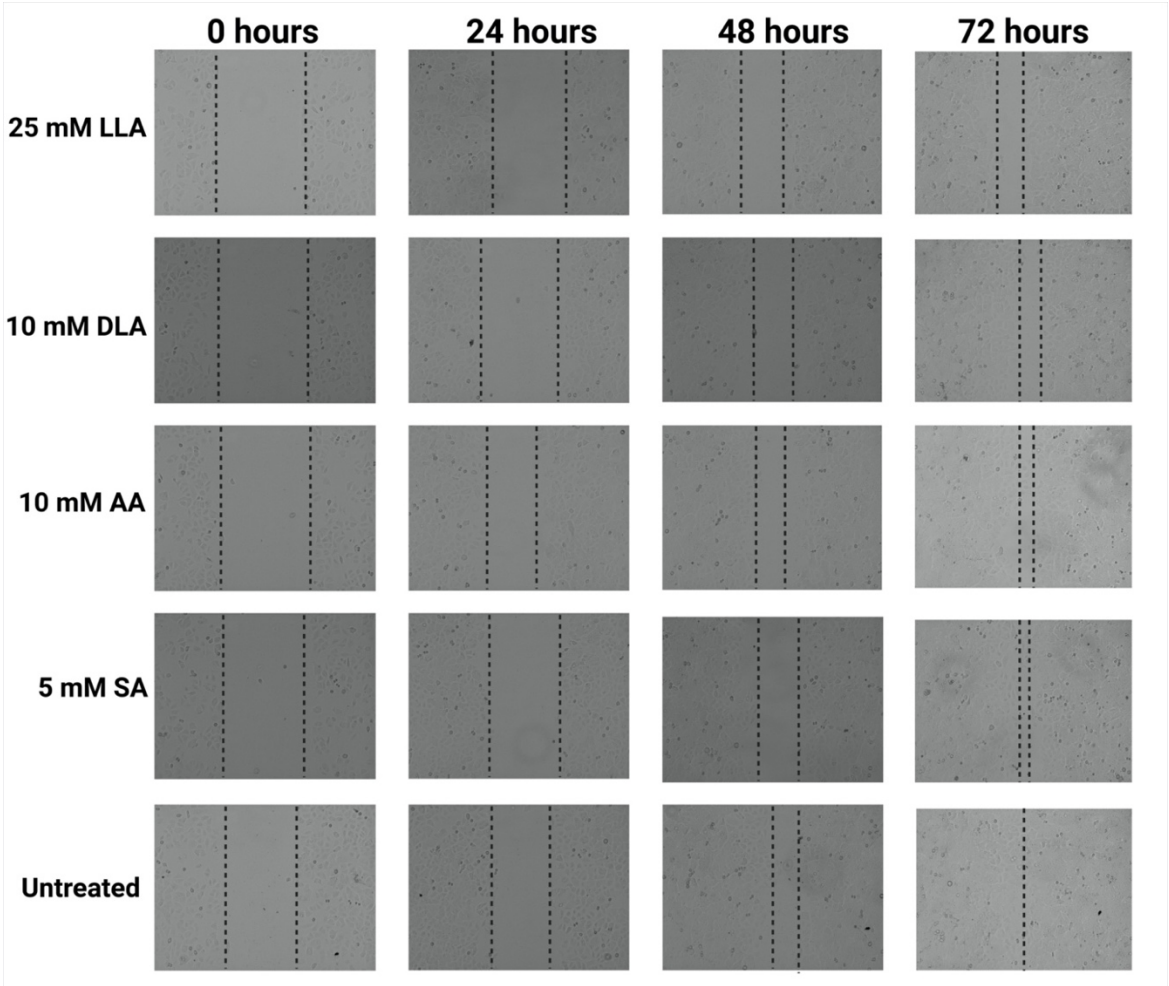


Figure 28. The impact of microbiota-associated metabolites on Ishikawa cells' wound closure. Representative images of Ishikawa cells treated with L-lactic acid (LLA), D-lactic acid (DLA), acetic acid (AA), succinic acid (SA), and untreated cells. The wound was made in the monolayer, and the cells were cultured and imaged immediately and at 24, 48, and 72 hours.

Wound healing assay using RL95-2 cells

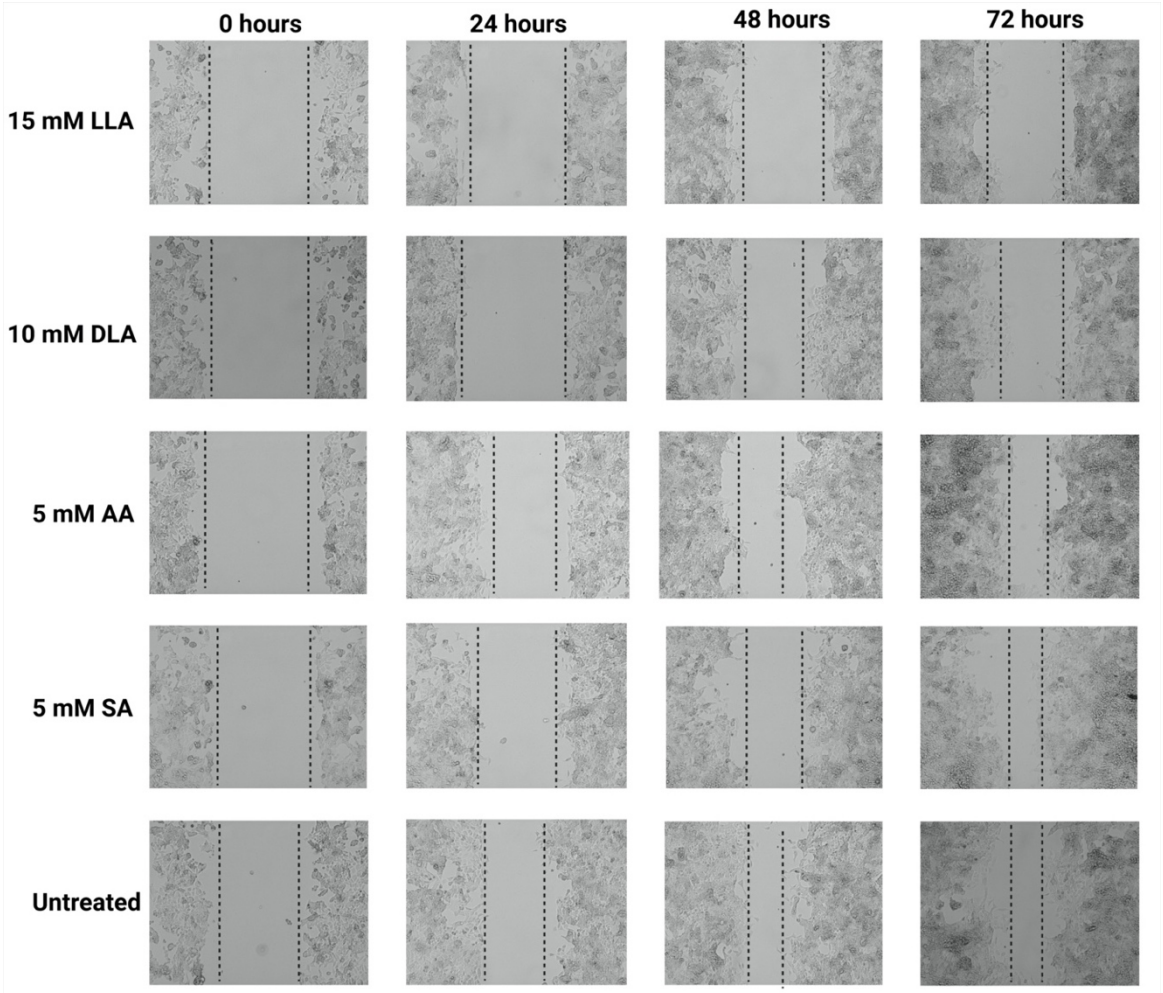


Figure 29. The impact of microbiota-associated metabolites on RL95-2 cells' wound closure. Representative images of RL95-2 cells treated with L-lactic acid (LLA), D-lactic acid (DLA), acetic acid (AA), succinic acid (SA), and untreated cells. The wound was made in the monolayer, and the cells were cultured and imaged immediately and at 24, 48, and 72 hours.

ZO-1 western blot images

This figure shows representative images of western blots completed for ZO-1 expression in Ishikawa cells treated with microbiota-metabolites. The ZO-1 band cannot be clearly observed at 230 kDa due to non-specific binding.

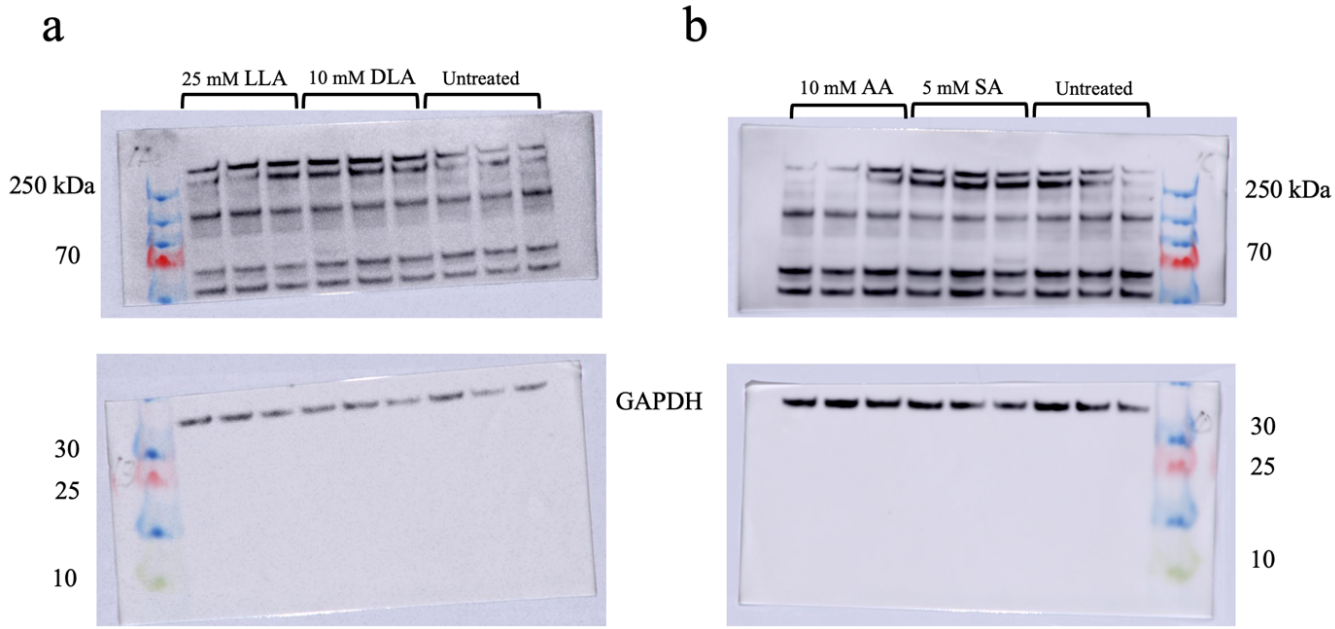


Figure 30. Representative images of protein expression of ZO-1 in Ishikawa cells treated with microbiota-associated metabolites. The cells were treated with L-lactic acid (LLA), D-lactic acid (DLA), acetic acid (AA), and succinic acid (SA). (a) Western blots of ZO-1 and GAPDH treated with LLA and DLA. (b) Western blots of ZO-1 and GAPHD treated with AA and SA.

Reference gene C_t values

The following tables show the C_t values of the reference genes as a mean ± standard deviation.

Table 22. Average C_t values of *HPRT1* in Ishikawa cells treated with microbiota-associated metabolites and controls. Mean ± SD, n=3.

Treatment	Concentration (mM)	*HPRT1* C_t ± SD
L-lactic acid	5	24.0 ± 1.2
	10	24.0 ± 0.9
	25	24.1 ± 0.7
D-lactic acid	5	25.5 ± 1.1
	10	24.6 ± 0.3
Acetic acid	5	24.5 ± 0.8
	10	24.1 ± 0.2
Succinic acid	2.5	25.9 ± 1.2
	5	24.9 ± 0.9
Untreated	0	24.6 ± 0.6
LPS	1X	25.2 ± 1.6
PMA/I	1X	25.2 ± 0.6

Table 23. Average C_t values of *HPRT1* in RL95-2 Cells treated with microbiota-associated metabolites and controls. Mean ± SD, n=3.

Treatment	Concentration (mM)	*HPRT1* C_t ± SD
L-lactic acid	5	24.5 ± 1.6
	10	24.4 ± 0.7
	15	24.0 ± 0.4
D-lactic acid	5	25.2 ± 0.3
	10	25.4 ± 0.4
Acetic acid	2.5	25.9 ± 0.6
	5	25.8 ± 0.7
Succinic acid	2.5	24.9 ± 1.3
	5	26.4 ± 1.2
Untreated	0	25.5 ± 0.4
LPS	1X	25.7 ± 0.7
PMA/I	1X	26.2 ± 1.6

Table 24. Average C_t values of *GADPH* in NK-92 cells treated with microbiota-associated metabolites and controls. Mean ± SD, n=3.

Treatment	Concentration (mM)	*GAPDH* C_t ± SD
L-lactic acid	2.5	20.0 ± 0.6
	5	19.4 ± 0.5
D-lactic acid	2	20.9 ± 2.2
	4	20.8 ± 0.5
Acetic acid	2.5	19.2 ± 0.4
	5	20.5 ± 1.2
Succinic acid	1	20.7 ± 1.3
	2	20.3 ± 0.8
Untreated	0	20.7 ± 0.6
LPS	1X	20.4 ± 1.3
PMA/I	1X	21.4 ± 0.8

Table 25. Average C_t values of *ACTB* in THP-1 cells treated with microbiota-associated metabolites. Mean ± SD, n=3.

Treatment	Concentration (mM)	*ACTB* C_t ± SD
L-lactic acid	5	18.6 ± 0.7
	10	16.9 ± 0.6
	15	17.9 ± 2.2
D-lactic acid	5	18.2 ± 1.8
	10	18.5 ± 0.4
Acetic acid	2.5	18.3 ± 0.5
	5	17.9 ± 1.4
Succinic acid	2.5	17.6 ± 0.6
	5	19.5 ± 1.8
Untreated	0	18.2 ± 0.8
LPS	1X	18.4 ± 2.2
PMA/I	1X	17.6 ± 0.7

ΔC_t values for genes associated with receptivity from cells treated with microbiota-associated metabolites

Table 26. ΔC_t values from Ishikawa cells treated with microbiota-associated metabolites. The cells were treated with L-lactic acid (LLA), D-lactic acid (DLA), acetic acid (AA), or succinic acid (SA). LPS and PMA/I were used as inflammatory controls. Mean ± SD, n=3.

Treatment	*TGFBR1*	*MUC1*	*HOXA10*	*VEGFA*	*NFKB1*	*LIF*
PMA	5.5 ± 0.2	3.7 ± 0.8	0.7 ± 0.6	-2.9 ± 0.6	0.6 ± 0.9	1.5 ± 1.1
LPS	5.9 ± 1.4	5.2 ± 1.7	-0.2 ± 0.7	-1.8 ± 0.8	2.3 ± 2.3	4.7 ± 0.6
0mM	5.8 ± 0.7	5.4 ± 1.7	1.5 ± 1.5	-0.8 ± 1.8	2.1 ± 0.2	4.7 ± 0.5
5mM AA	5.4 ± 0.5	5.3 ± 0.6	1.4 ± 0.9	-1 ± 0.5	3.3 ± 0.9	6.6 ± 1.8
10mM AA	6.1 ± 0.9	7.2 ± 0.9	1.9 ± 0.3	-0.4 ± 0.3	3.3 ± 0.9	7.2 ± 0.6
5mM LLA	5.3 ± 1.3	5.1 ± 1	1.4 ± 0.8	0.2 ± 0.9	3 ± 2	7.8 ± 1.7
10mM LLA	6.1 ± 1.6	5.8 ± 0.6	0.4 ± 1.3	-1.8 ± 1.4	2.5 ± 0.5	6 ± 2.1
25mM LLA	5.1 ± 1.1	4.9 ± 1.3	1.2 ± 0.8	-0.9 ± 1	2.2 ± 0.5	6.5 ± 2.9
PMA/I	4.3 ± 0.6	3.3 ± 0.2	0.9 ± 0.3	-0.8 ± 0.1	-0.5 ± 0	2 ± 1.4
LPS	4.9 ± 1.1	5.4 ± 0.2	2.8 ± 0.9	-1 ± 0.5	0.5 ± 0.8	-0.3 ± 1.5
0mM	4.3 ± 0.7	4.3 ± 0.7	0.9 ± 0.8	-1 ± 0.7	0.5 ± 0.8	2.3 ± 1.2
2.5mM SA	4.9 ± 1.5	4.3 ± 0.9	0.8 ± 1.2	-0.6 ± 0.7	0.5 ± 0.6	1.7 ± 0.5
5mM SA	5.5 ± 0.8	4.5 ± 0.7	2 ± 0.5	0.2 ± 0.6	1.5 ± 0.4	2.8 ± 2.5
5mM DLA	5.4 ± 1.3	5 ± 2.5	2.3 ± 1	0.8 ± 1.7	1.2 ± 0.9	4.1 ± 2.6
10mM DLA	6.4 ± 1.5	5.7 ± 1.4	2.9 ± 1.1	1.3 ± 0.5	1.6 ± 0.5	4.8 ± 1.6

Table 27. ΔC_t values from RL95-2 cells treated with microbiota-associated metabolites. The cells were treated with L-lactic acid (LLA), D-lactic acid (DLA), acetic acid (AA), or succinic acid (SA). LPS and PMA/I were used as inflammatory controls. Mean ± SD, n=3.

Treatment	*TGFBR1*	*MUC1*	*HOXA10*	*VEGFA*	*NFKB1*	*LIF*
PMA/I	2.9 ± 2.8	0.6 ± 0.8	5.8 ± 0.7	-3.5 ± 1.2	-2 ± 1	-3.2 ± 1.9
LPS	2 ± 0.2	5.1 ± 0.1	5 ± 1	-1.7 ± 0.4	0.8 ± 0.1	7.3 ± 0
0mM	3.8 ± 0.9	5.6 ± 0.6	5 ± 0.9	-1.5 ± 0.6	1 ± 1	9.9 ± 0.6
2.5mM AA	5.6 ± 2.7	6.6 ± 1.9	6.1 ± 1.8	-0.6 ± 1.6	0.5 ± 0.7	9.7 ± 3
5mM AA	4.4 ± 0.9	5.8 ± 0.7	5.6 ± 1.3	-0.6 ± 0.4	1 ± 0.8	7.3 ± 1
5mM LLA	5.3 ± 1.7	5.8 ± 1.5	5.8 ± 1.4	-0.5 ± 1.4	0.1 ± 1	9.5 ± 1
10mM LLA	6.7 ± 0.6	6.1 ± 0.1	6 ± 1.1	-0.2 ± 0.5	1.7 ± 1.2	11.3 ± 1.3
15mM LLA	7.3 ± 1	6 ± 1	5.6 ± 0.7	-0.6 ± 0.4	0.7 ± 0.3	9.3 ± 1.2
PMA/I	3.6 ± 1.1	4 ± 0.3	5.2 ± 1	-4.3 ± 1	-3.6 ± 0.9	-5.5 ± 1.2
LPS	4.1 ± 0.4	5.5 ± 0.9	5.5 ± 0.6	-1.3 ± 0.7	-0.9 ± 0.5	8.2 ± 1.4
0mM	4.6 ± 0.8	6 ± 1.1	5.4 ± 1.7	-0.7 ± 0.5	-0.6 ± 0.7	8.4 ± 1.6
2.5mM SA	4.4 ± 1.2	6.4 ± 0.8	5.8 ± 0.8	-0.2 ± 0.7	-0.3 ± 0.1	9.3 ± 1.2
5mM SA	3.9 ± 1	5.9 ± 0.5	4.8 ± 1.8	-1.4 ± 0.9	-1 ± 1	7.1 ± 0.6
5mM DLA	4.1 ± 0.3	4.7 ± 0.8	5.1 ± 2	-1.3 ± 0.2	1 ± 1.7	8.9 ± 1.3
10mM DLA	4 ± 1.2	5.3 ± 1.3	4.7 ± 0.3	-1.5 ± 0.6	-0.5 ± 0.8	7.5 ± 2.1

Table 28. ΔC_t values from NK-92 cells treated with microbiota-associated metabolites. The cells were treated with L-lactic acid (LLA), D-lactic acid (DLA), acetic acid (AA), or succinic acid (SA). LPS and PMA/I were used as inflammatory controls. Mean ± SD, n=3.

Treatment	*TGFBR1*	*HOXA10*	*VEGFA*	*NFKB1*
PMA/I	10 ± 2.7	8.4 ± 2.2	7.8 ± 3.3	5 ± 2.9
LPS	8.3 ± 0.5	6.2 ± 0.9	11.2 ± 1.8	6.4 ± 0.6
0mM	8.8 ± 0.9	6.5 ± 1.2	12.5	6.7 ± 0.5
2.5mM LLA	8.7 ± 0.6	6.8 ± 0.6	13.4 ± 0.7	6.7 ± 1.2
5mM LLA	8 ± 0.3	6.1 ± 0.6	12.9 ± 1	5.9 ± 0.3
2.5mM AA	9.5 ± 0.5	6.5 ± 0.8	12.9 ± 2.1	7.3 ± 0.1
5mM AA	8.3 ± 0.7	6.2 ± 0.8	11.3 ± 1.4	6.1 ± 0.3
PMA/I	8 ± 2.5	10.1 ± 1.9	7.1 ± 1.3	4.3 ± 1
LPS	6.6 ± 2.1	6.6 ± 1	7.8 ± 1.7	5.4 ± 1.5
0mM	7.4 ± 1	7.2 ± 0.7	8.9 ± 0.6	6.4 ± 1
1mM SA	6 ± 1.5	6.3 ± 1.1	8.8 ± 0.9	6 ± 1.1
2mM SA	7.5 ± 0.6	7 ± 0.2	11 ± 2.3	6.4 ± 0.9
2mM DLA	7.7 ± 1.1	6.6 ± 0.6	9.1 ± 1	5.8 ± 0.5
4mM DLA	7.2 ± 1.3	7.1 ± 0.4	10.7 ± 1.2	6.4 ± 0.8

Table 29. ΔC_t values from THP-1 cells treated with microbiota-associated metabolites. The cells were treated with L-lactic acid (LLA), D-lactic acid (DLA), acetic acid (AA), or succinic acid (SA). LPS and PMA/I were used as inflammatory controls. Mean ± SD, n=3.

Treatment	*TGFBR1*	*HOXA10*	*VEGFA*	*NFKB1*
PMA/I	11.2 ± 1.2	10.8 ± 0.6	10.8 ± 0.5	9 ± 1.1
LPS	11.8 ± 2.1	12.6 ± 1.4	9.3 ± 1.2	5.5 ± 1.8
0mM	10.5 ± 0.9	10.4 ± 1.4	9.7 ± 0.6	9.2 ± 0.7
2.5mM AA	9.5 ± 0.6	9.3 ± 1.1	9.1 ± 0.7	8.7 ± 0.9
5mM AA	9.9 ± 0.8	9.8 ± 0.7	10 ± 1.7	9.3 ± 0.8
5mM LLA	9.9 ± 1.8	9.2 ± 1	9.1 ± 0.9	8.7 ± 1.5
10mM LLA	10.7 ± 1.5	9.5 ± 0.6	9.2 ± 1.7	9.2 ± 0.7
15mM LLA	11.2 ± 1.9	9.6 ± 0.9	9.1 ± 1.3	9.5 ± 0.7
PMA/I	9.9 ± 0.8	11 ± 0.4	8.2 ± 0.9	7.6 ± 0.7
LPS	10.5 ± 1.5	11.6 ± 1	8.4 ± 0.5	4.8 ± 0.3
0mM	11.3 ± 0.6	11.4 ± 1.2	9.5 ± 0.1	9.8 ± 0.4
2.5mM SA	13.9 ± 0.8	11.1 ± 0.4	9.8 ± 0.2	10 ± 0.3
5mM SA	10.8 ± 2.1	9.8 ± 2.2	9.1 ± 2.7	10.2 ± 3.2
5mM DLA	10.6 ± 1.7	10.8 ± 1	10.1 ± 1.8	12.2 ± 2
10mM DLA	10.3 ± 0.4	11.1 ± 0.6	8.3 ± 0.7	9 ± 0.5

Fold change analysis of receptivity genes

These figures represent the fold change of genes associated with endometrial receptivity. The data was analysed using the comparative C_t method. The significant results are shown in Chapter 3 Section 3.4.6.

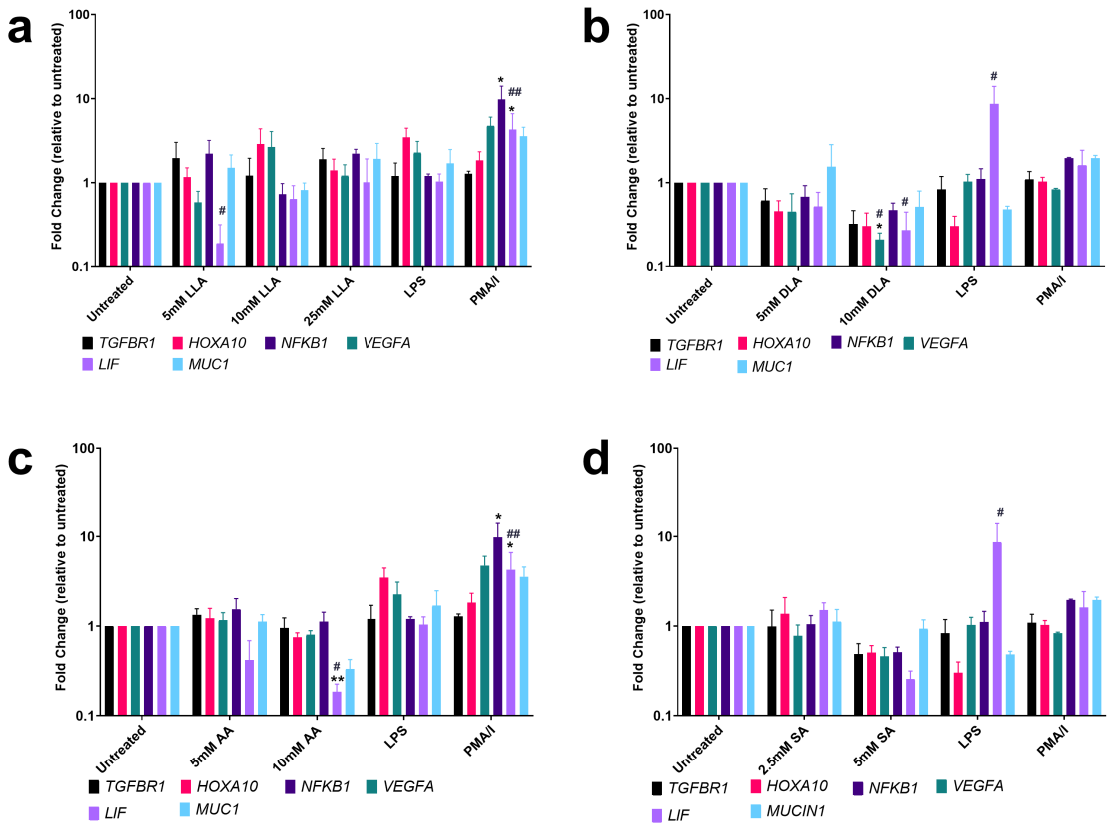


Figure 31. The relative expression of genes associated with receptivity in Ishikawa cells treated with microbiota-associated metabolites. The cells were grown to confluency and treated with microbiota-associated metabolites: a) L-lactic acid, b) D-lactic acid, c) acetic acid, and d) succinic acid. Gene expression was normalised to the reference genes and expressed as fold change compared to the untreated cells using the comparative C_t method. * representing $p \leq 0.05$, and ** representing $p \leq 0.01$, determined using an unpaired T-test with Welch's correction. # representing $p \leq 0.05$, and ## representing $p \leq 0.01$, determined using Dunnett's multiple comparisons tests. n = 3.

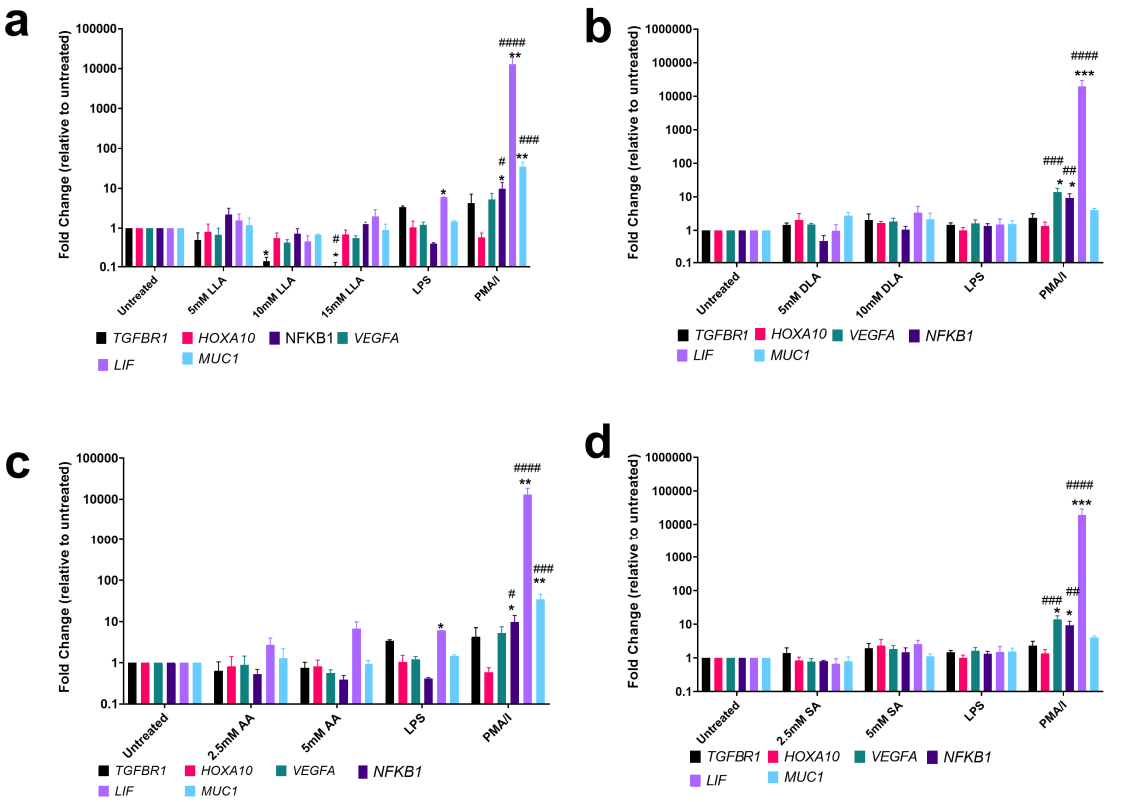


Figure 32. The relative expression of genes associated with receptivity in RL95-2 cells treated with microbiota-associated metabolites. The cells were grown to confluency and treated with microbiota-associated metabolites: a) L-lactic acid, b) D-lactic acid, c) acetic acid, and d) succinic acid. Gene expression was normalised to the reference genes and expressed as fold change compared to the untreated cells using the comparative C_t method. * representing $p \leq 0.05$, ** representing $p \leq 0.01$ and *** representing $p \leq 0.001$, determined using an unpaired T-test with Welch's correction. # representing $p \leq 0.05$, ## representing $p \leq 0.01$, ### representing $p \leq 0.001$, and #### representing $p \leq 0.0001$ determined using Dunnett's multiple comparisons tests. n = 3.

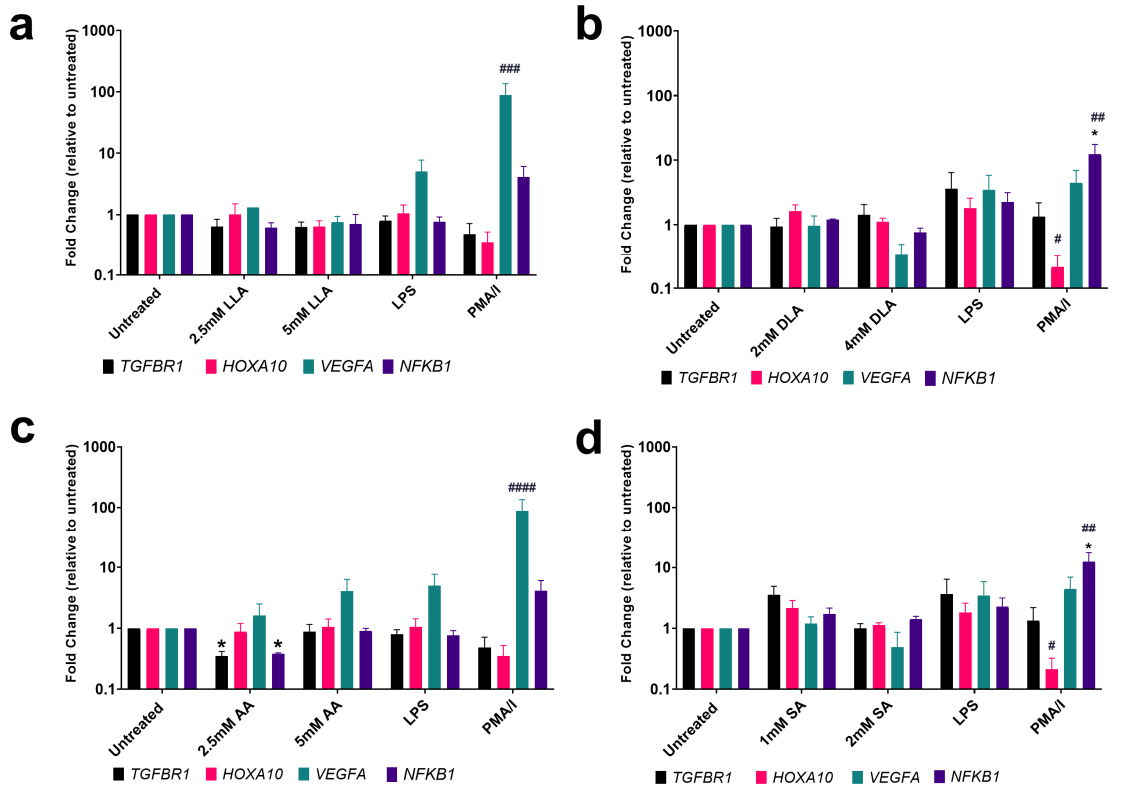


Figure 33. The relative expression of genes associated with receptivity in NK-92 cells treated with microbiota-associated metabolites. The cells were grown to confluency and treated with microbiota-associated metabolites: a) L-lactic acid, b) D-lactic acid, c) acetic acid, and d) succinic acid. Gene expression was normalised to the reference genes and expressed as fold change compared to the untreated cells using the comparative C_t method. * representing $p \leq 0.05$, determined using an unpaired T-test with Welch's correction. # representing $p \leq 0.05$, ## representing $p \leq 0.01$, ### representing $p \leq 0.001$, and #### representing $p \leq 0.0001$ determined using Dunnett's multiple comparisons tests. n = 3.

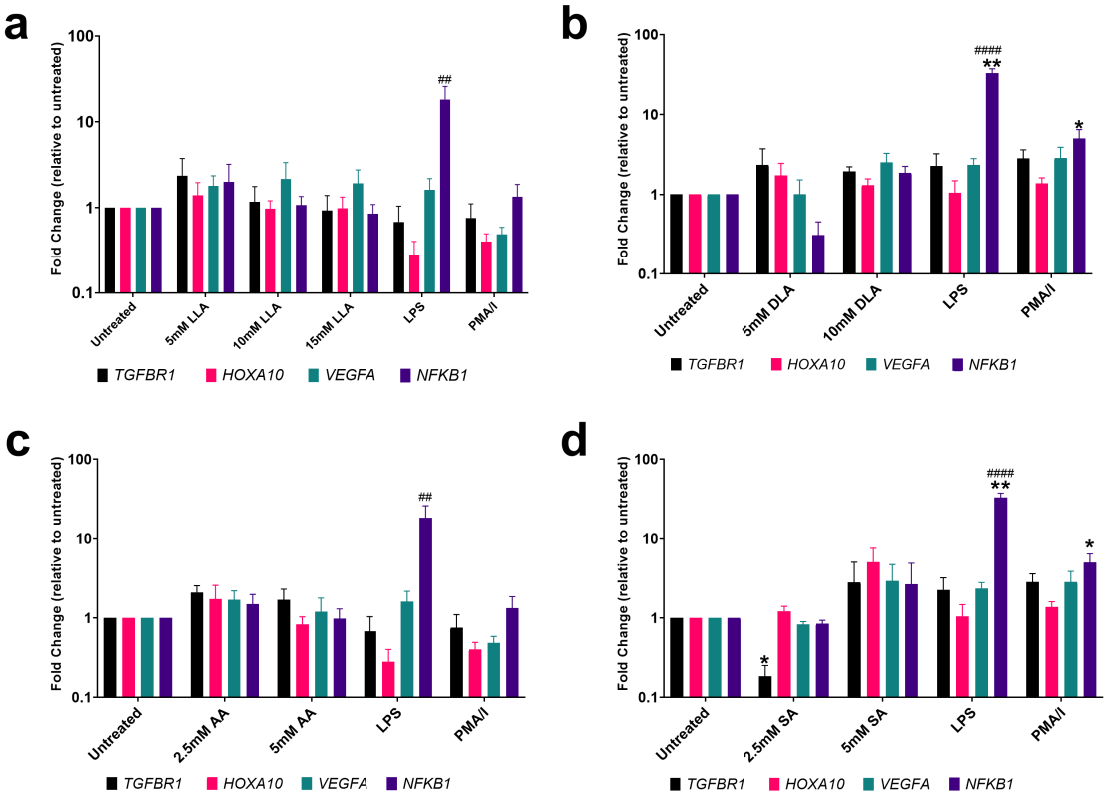


Figure 34. The relative expression of genes associated with receptivity in PMA differentiated THP-1 cells treated with microbiota-associated metabolites. The cells were differentiated and treated with microbiota-associated metabolites: a) L-lactic acid, b) D-lactic acid, c) acetic acid, and d) succinic acid. Gene expression was normalised to the reference genes and expressed as fold change compared to the untreated cells using the comparative C_t method. * representing $p \leq 0.05$, and ** representing $p \leq 0.01$, determined using an unpaired T-test with Welch's correction. ## representing $p \leq 0.01$, and #### representing $p \leq 0.0001$ determined using Dunnett's multiple comparisons tests. n = 3.

Appendix 3

Cytometric Bead Array (CBA) analysis of cytokines and chemokines

The figures show the results from CBA analysis of supernatant collected from endometrial epithelial cells and innate immune cells treated with microbiota-associated metabolites. The analysis can be found in Chapter 4, Sections 4.4.1, 4.4.2, and 4.4.3.

Cytokine and chemokine secretion by Ishikawa cells

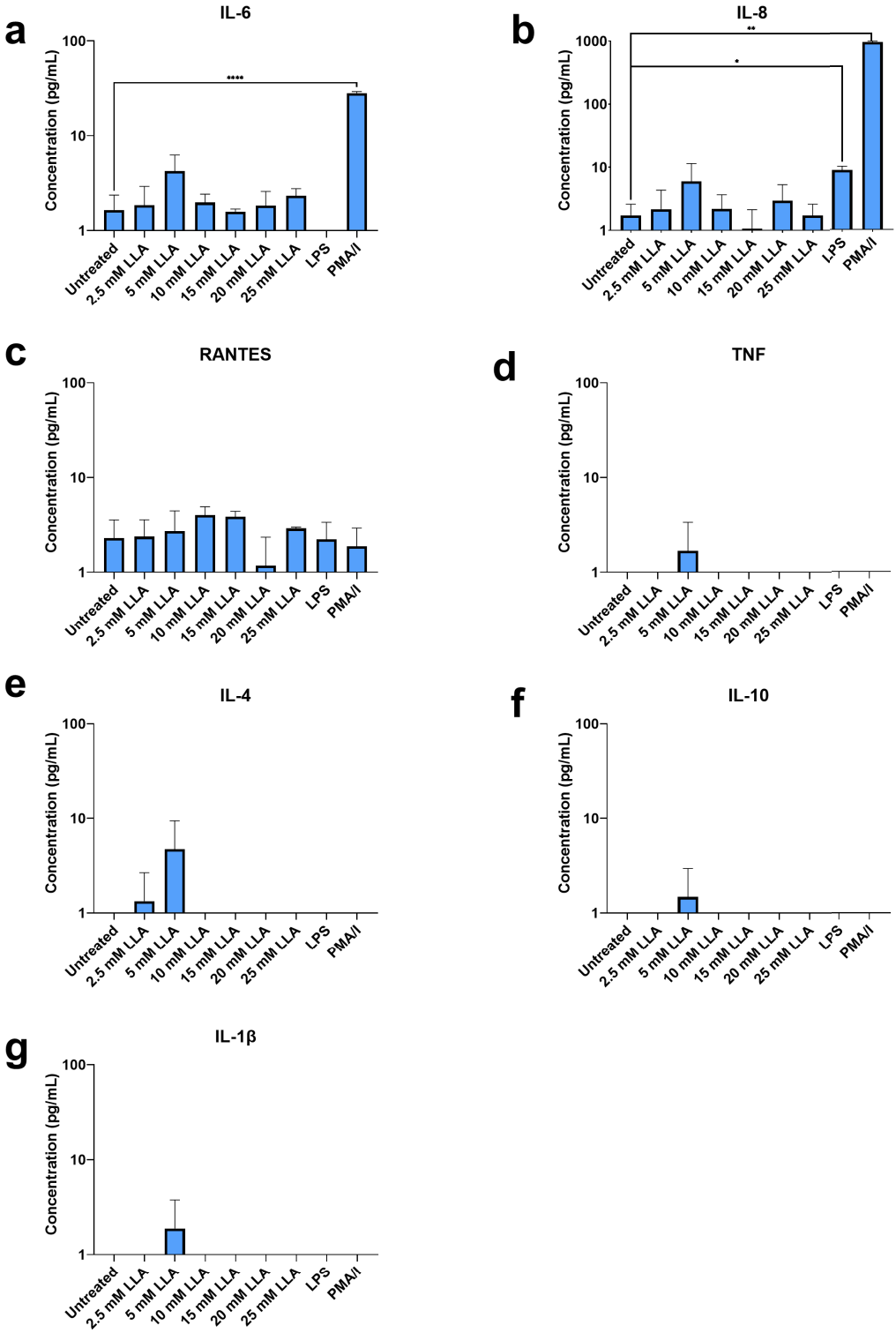


Figure 35. Cytokine expression by Ishikawa cells treated with L-lactic acid (LLA). Ishikawa cells were treated with LLA for 24 hours, and the concentration (pg/mL) of (a) IL-6, (b) IL-8, (c) RANTES, (d) TNF, (e) IL-4, (f) IL-10, and (g) IL-1β in the supernatant was determined using CBA. * representing $p \leq 0.05$, ** representing $p \leq 0.01$, *** representing $p \leq 0.001$ and **** representing $p \leq 0.0001$, determined using an unpaired T-test with Welch's correction. n = 3.

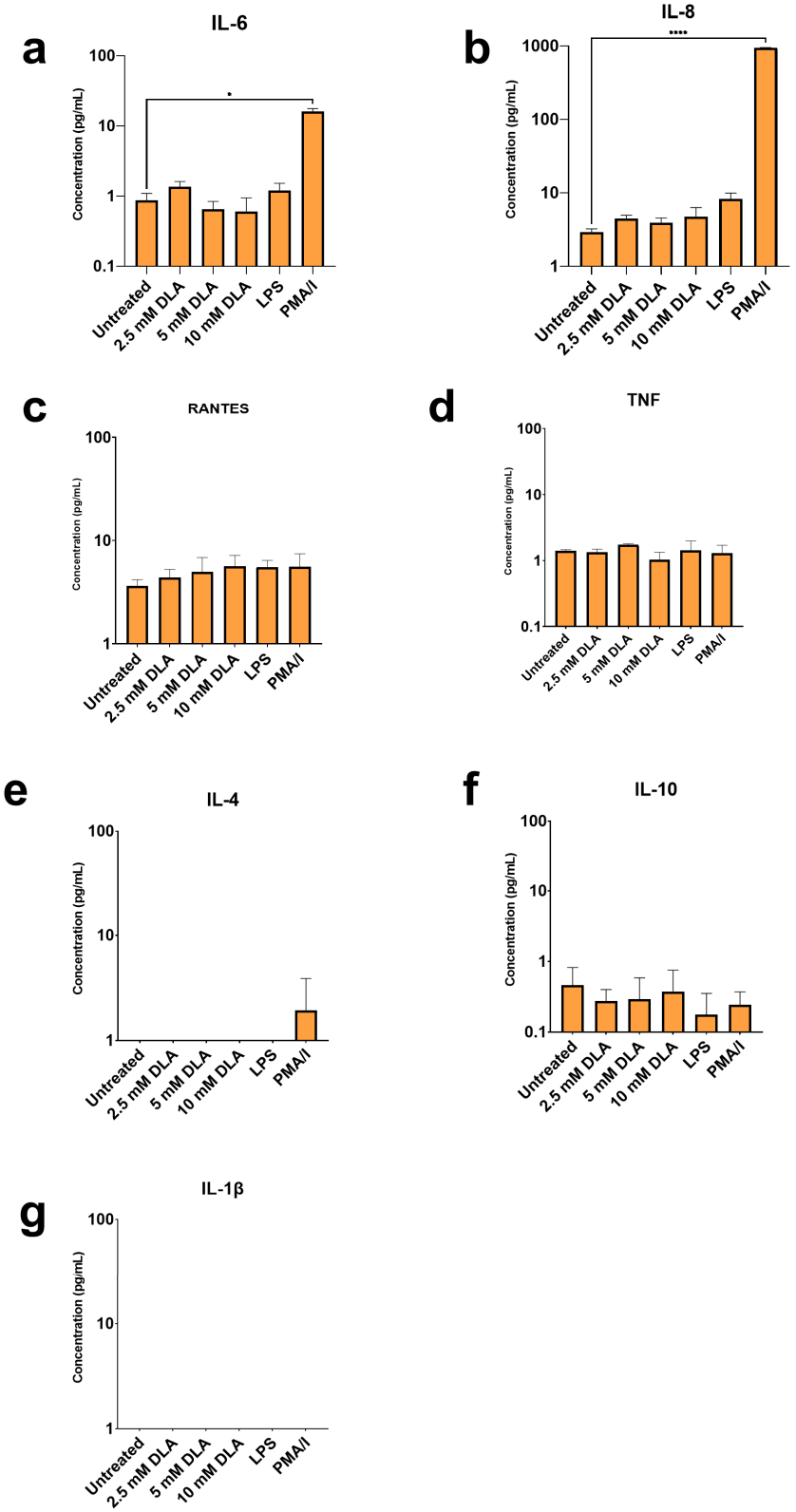


Figure 36. Cytokine expression by Ishikawa cells treated with D-lactic acid (DLA). Ishikawa cells were treated with DLA for 24 hours, and the concentration (pg/mL) of (a) IL-6, (b) IL-8, (c) RANTES, (d) TNF, (e) IL-4, (f) IL-10, and (g) IL-1β in the supernatant was determined using CBA. * representing $p \leq 0.05$, ** representing $p \leq 0.01$, *** representing $p \leq 0.001$ and **** representing $p \leq 0.0001$, determined using an unpaired T-test with Welch's correction. n = 3.

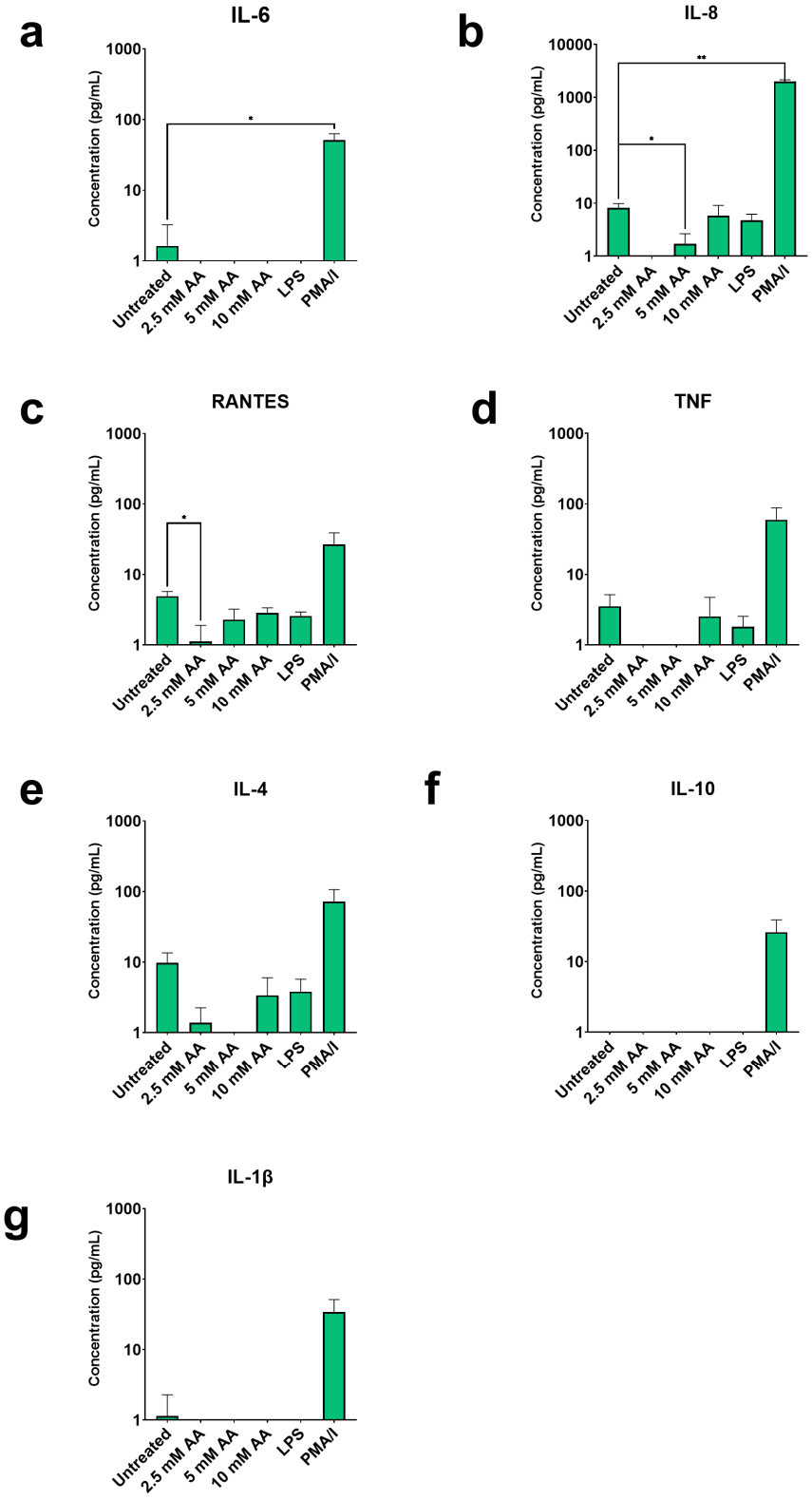


Figure 37. Cytokine expression by Ishikawa cells treated with acetic acid (AA). Ishikawa cells were treated with AA for 24 hours, and the concentration (pg/mL) of (a) IL-6, (b) IL-8, (c) RANTES, (d) TNF, (e) IL-4, (f) IL-10, and (g) IL-1β in the supernatant was determined using CBA. * representing $p \leq 0.05$, ** representing $p \leq 0.01$, *** representing $p \leq 0.001$ and **** representing $p \leq 0.0001$, determined using an unpaired T-test with Welch's correction. n = 3.

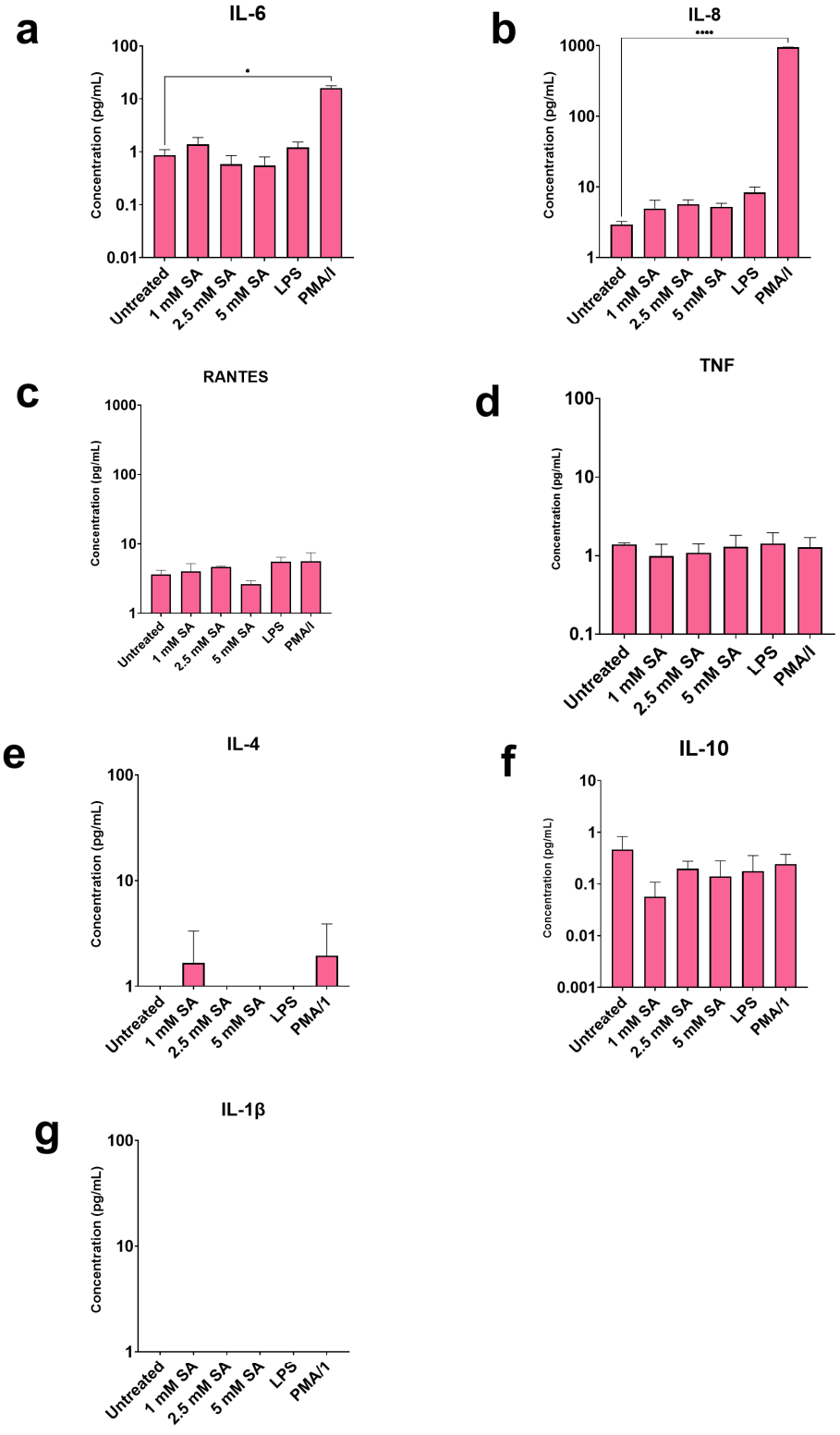


Figure 38. Cytokine expression by Ishikawa cells treated with succinic acid (SA). Ishikawa cells were treated with SA for 24 hours, and the concentration (pg/mL) of (a) IL-6, (b) IL-8, (c) RANTES, (d) TNF, (e) IL-4, (f) IL-10, and (g) IL-1β in the supernatant was determined using CBA. * representing $p \leq 0.05$, ** representing $p \leq 0.01$, *** representing $p \leq 0.001$ and **** representing $p \leq 0.0001$, determined using an unpaired T-test with Welch's correction. n = 3.

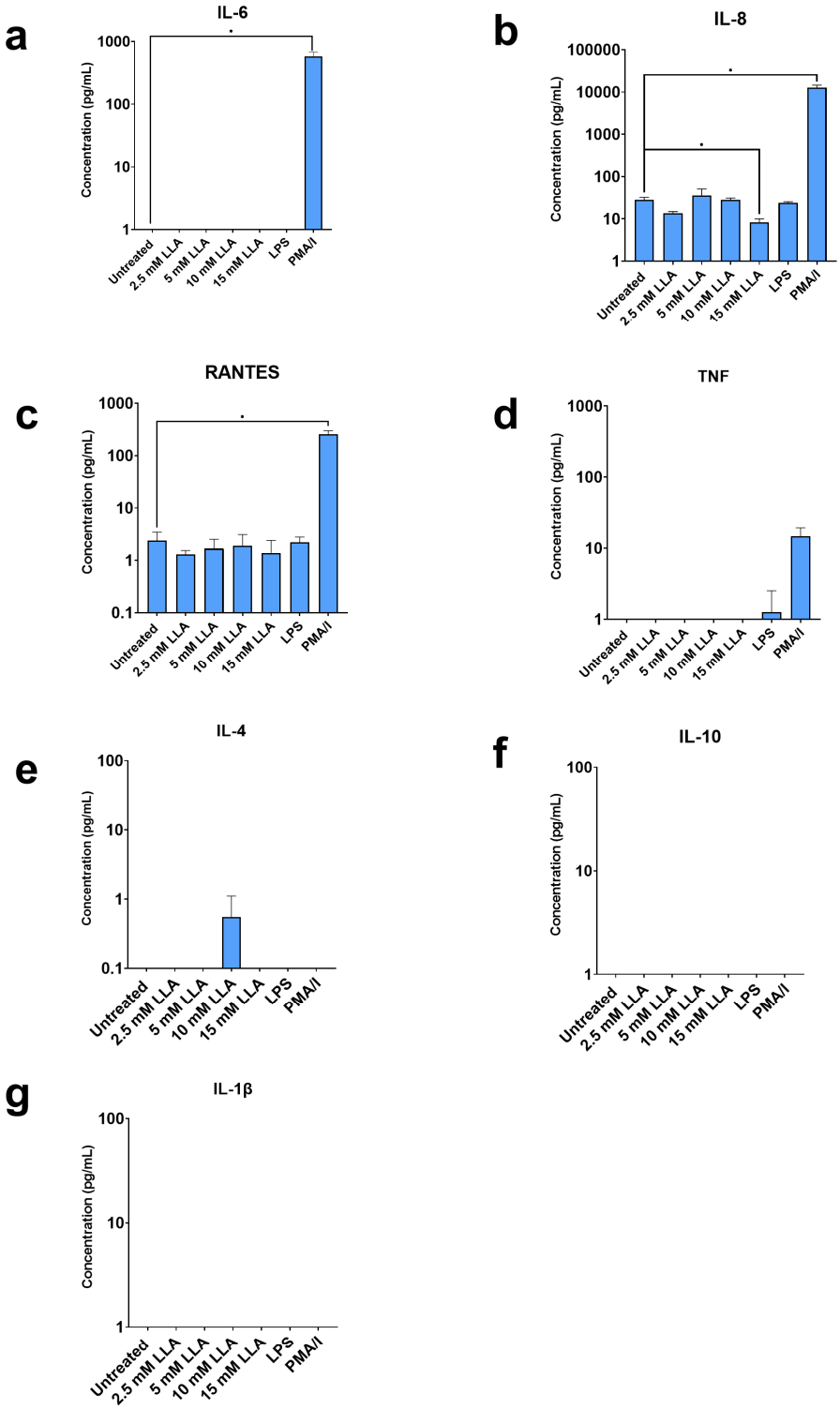


Figure 39. Cytokine expression by RL95-2 cells treated with L-lactic acid (LLA). RL95-2 cells were treated with LLA for 24 hours, and the concentration (pg/mL) of (a) IL-6, (b) IL-8, (c) RANTES, (d) TNF, (e) IL-4, (f) IL-10, and (g) IL-1β in the supernatant was determined using CBA. * representing $p \leq 0.05$, determined using an unpaired T-test with Welch's correction. n = 3.

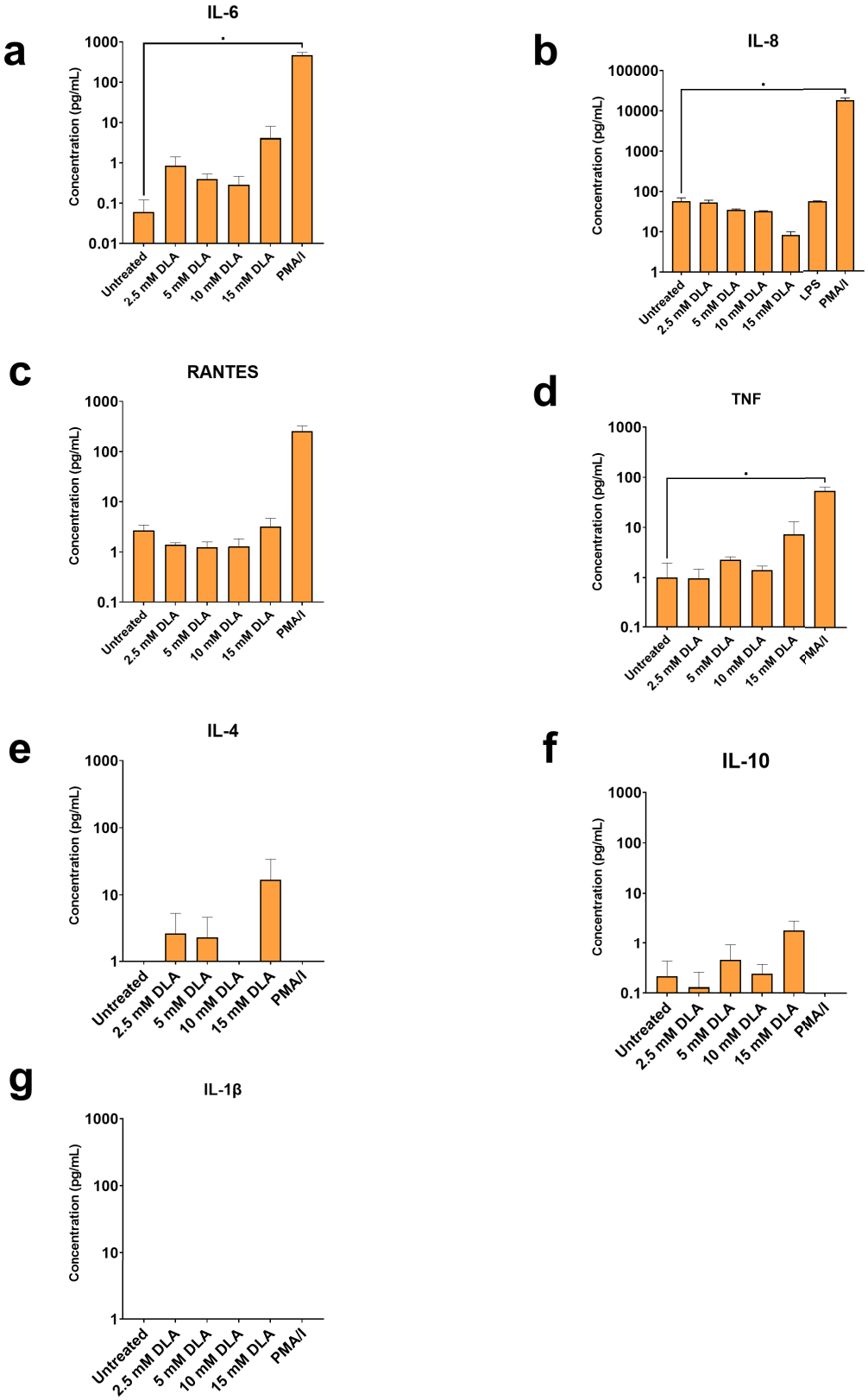


Figure 40. Cytokine expression by RL95-2 cells treated with D-lactic acid (DLA). RL95-2 cells were treated with DLA for 24 hours, and the concentration (pg/mL) of (a) IL-6, (b) IL-8, (c) RANTES, (d) TNF, (e) IL-4, (f) IL-10, and (g) IL-1β in the supernatant was determined using CBA. * representing $p \leq 0.05$, determined using an unpaired T-test with Welch's correction. n = 3.

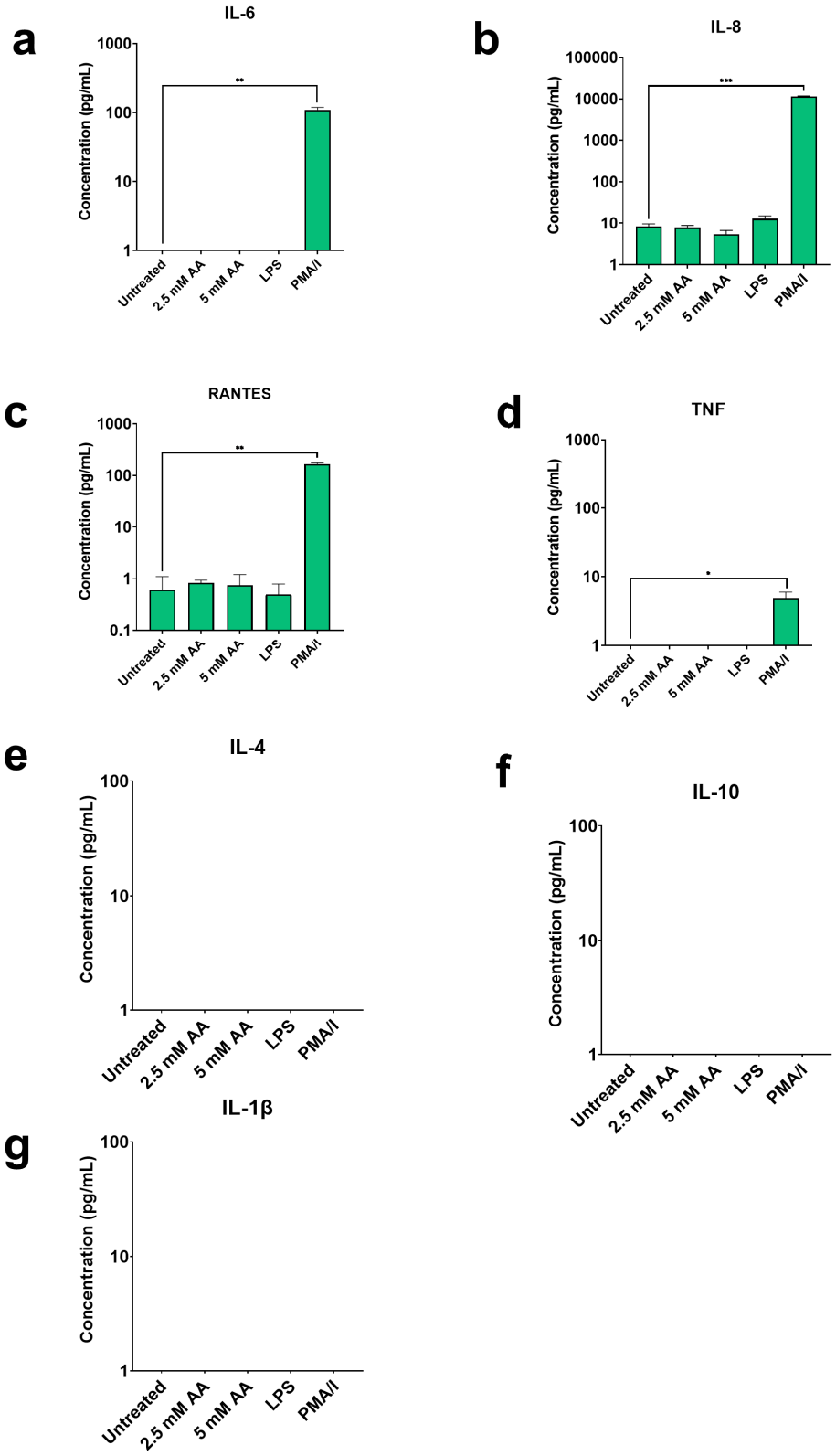


Figure 41. Cytokine expression by RL95-2 cells treated with acetic acid (AA). RL95-2 cells were treated with AA for 24 hours, and the concentration (pg/mL) of (a) IL-6, (b) IL-8, (c) RANTES, (d) TNF, (e) IL-4, (f) IL-10, and (g) IL-1β in the supernatant was determined using CBA. * representing $p \leq 0.05$, ** representing $p \leq 0.01$, and *** representing $p \leq 0.001$, determined using an unpaired T-test with Welch's correction. n = 3.

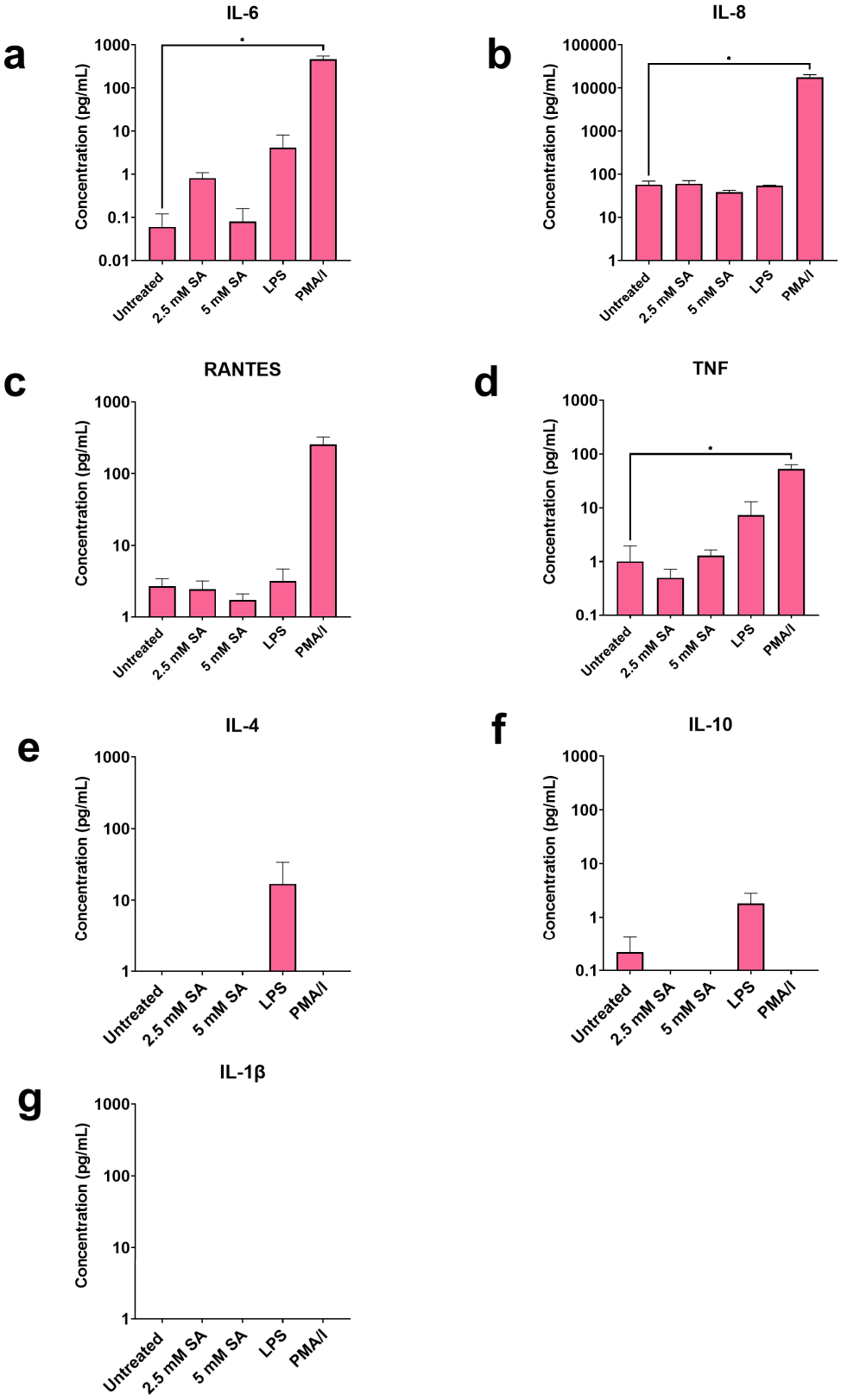


Figure 42. Cytokine expression by RL95-2 cells treated with succinic acid (SA). RL95-2 cells were treated with SA for 24 hours, and the concentration (pg/mL) of (a) IL-6, (b) IL-8, (c) RANTES, (d) TNF, (e) IL-4, (f) IL-10, and (g) IL-1β in the supernatant was determined using CBA. * representing $p \leq 0.05$, determined using an unpaired T-test with Welch's correction. n = 3.

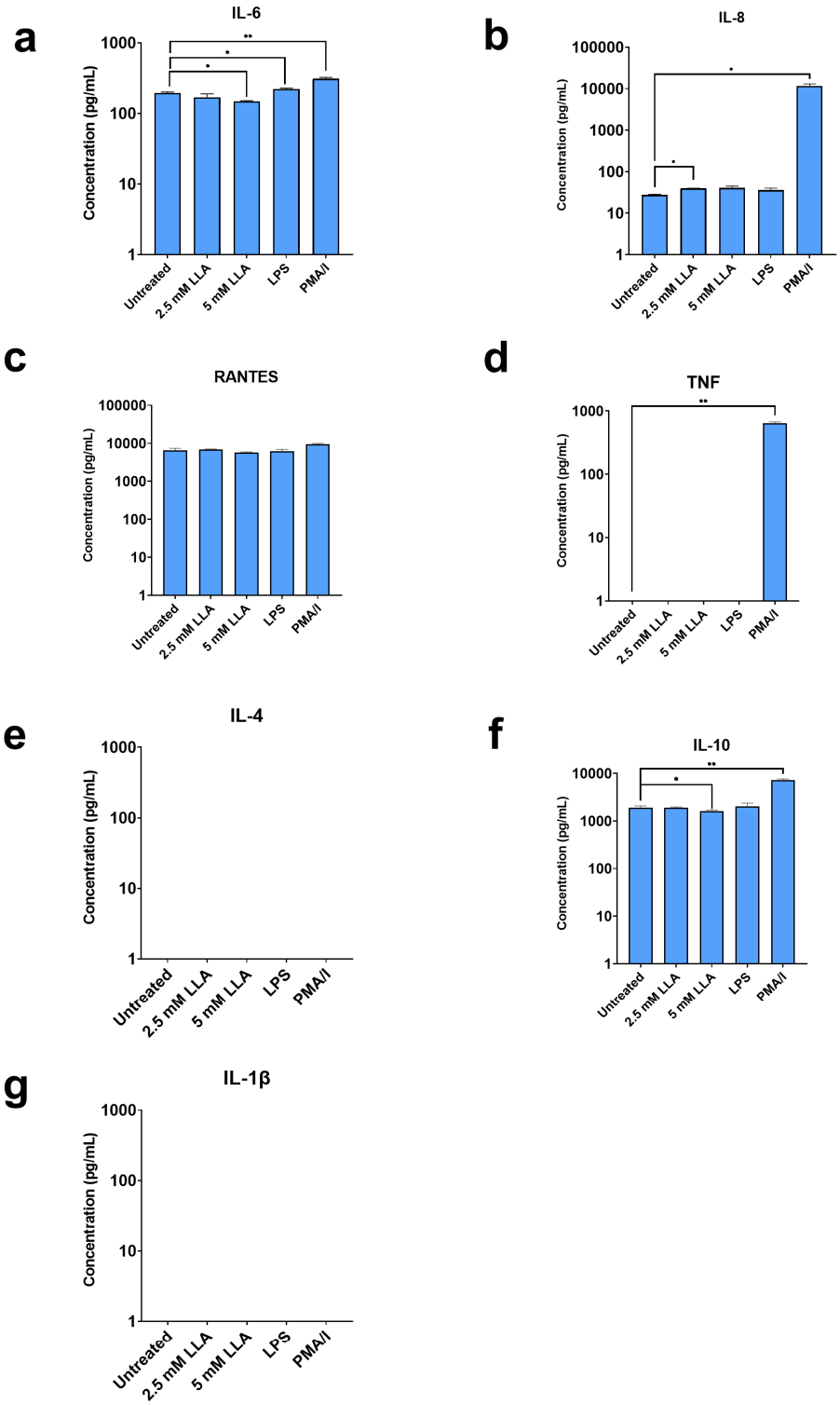


Figure 43. Cytokine expression by NK-92 cells treated with L-lactic acid (LLA). NK-92 cells were treated with LLA for 24 hours, and the concentration (pg/mL) of (a) IL-6, (b) IL-8, (c) RANTES, (d) TNF, (e) IL-4, (f) IL-10, and (g) IL-1β in the supernatant was determined using CBA. * representing $p \leq 0.05$, determined using an unpaired T-test with Welch's correction. n = 3.

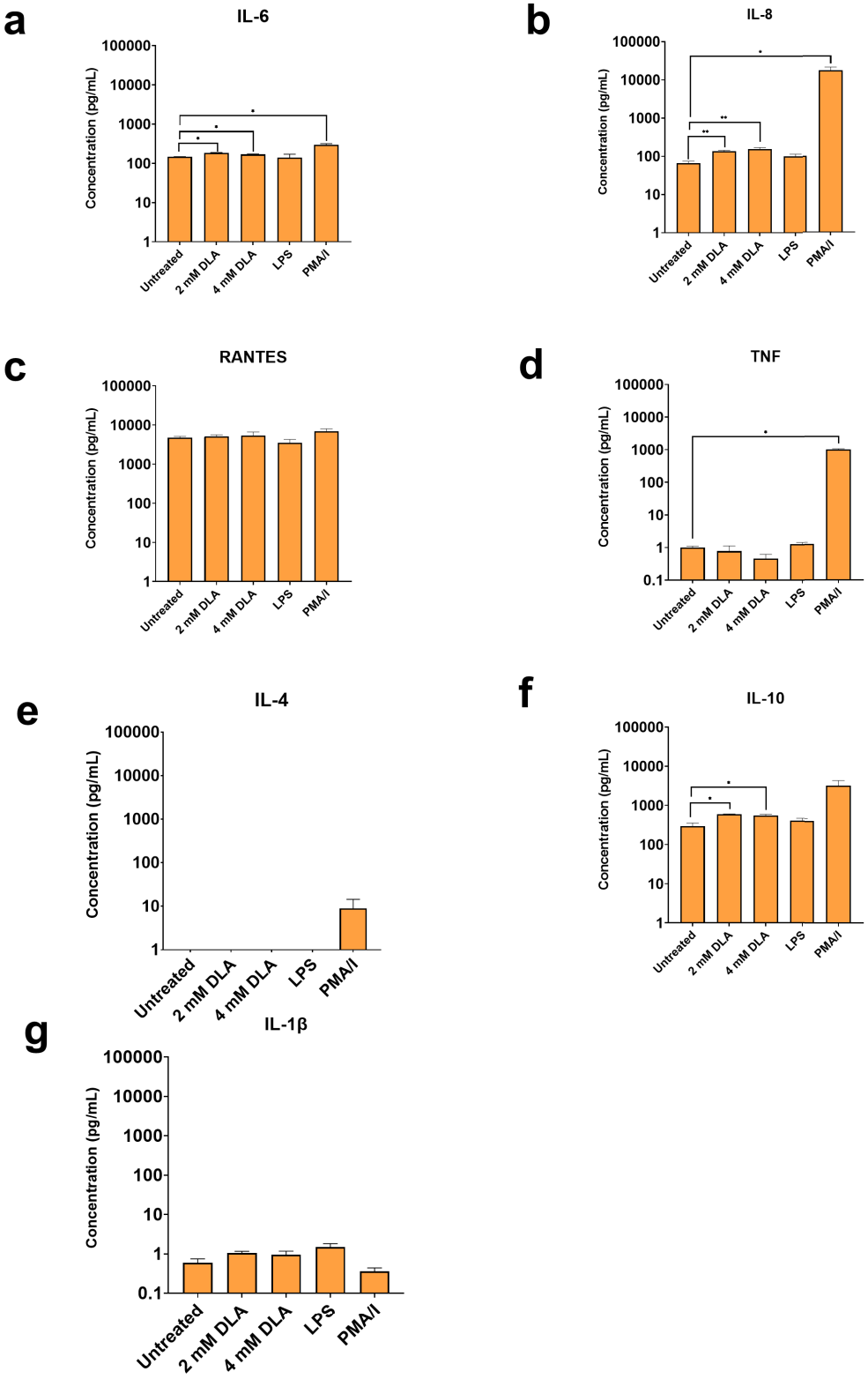


Figure 44. Cytokine expression by NK-92 cells treated with D-lactic acid (DLA). NK-92 cells were treated with DLA for 24 hours, and the concentration (pg/mL) of (a) IL-6, (b) IL-8, (c) RANTES, (d) TNF, (e) IL-4, (f) IL-10, and (g) IL-1β in the supernatant was determined using CBA. * representing $p \leq 0.05$ and ** representing $p \leq 0.01$, determined using an unpaired T-test with Welch's correction. n = 3.

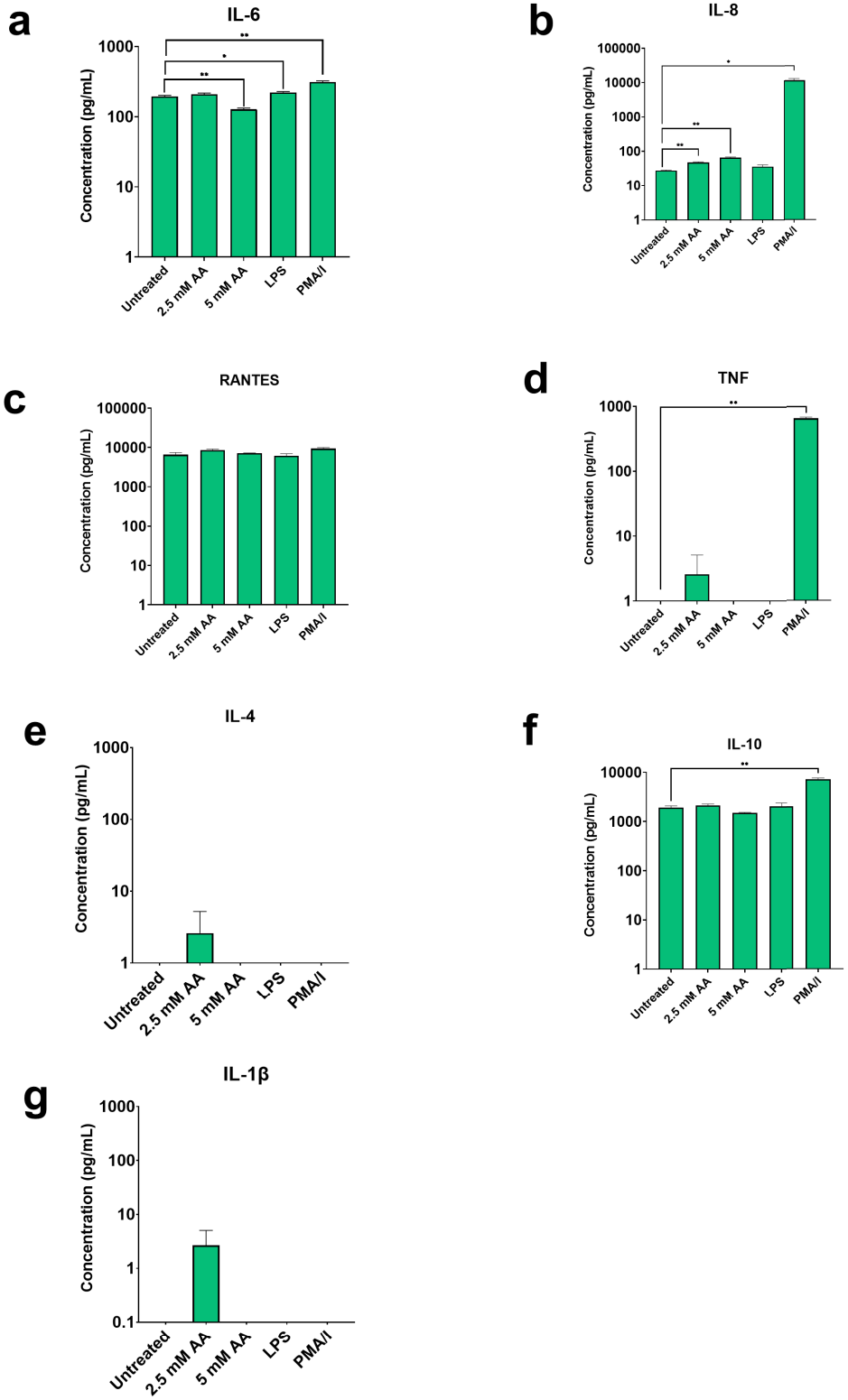


Figure 45. Cytokine expression by NK-92 cells treated with acetic acid (AA). NK-92 cells were treated with AA for 24 hours, and the concentration (pg/mL) of (a) IL-6, (b) IL-8, (c) RANTES, (d) TNF, (e) IL-4, (f) IL-10, and (g) IL-1β in the supernatant was determined using CBA. * representing $p \leq 0.05$, and ** representing $p \leq 0.01$, determined using an unpaired T-test with Welch's correction. n = 3.

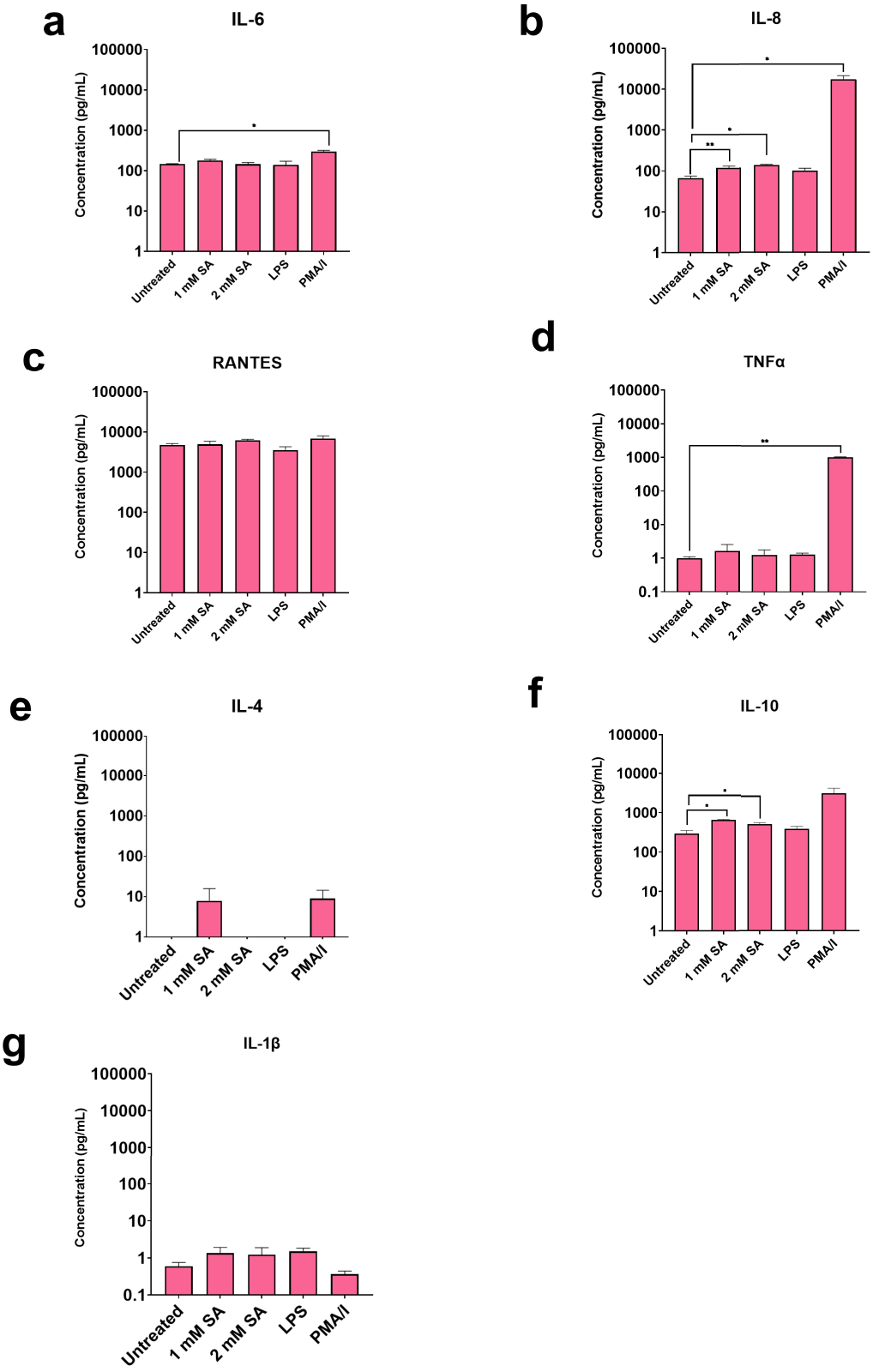


Figure 46. Cytokine expression by NK-92 cells treated with succinic acid (SA). NK-92 cells were treated with SA for 24 hours, and the concentration (pg/mL) of (a) IL-6, (b) IL-8, (c) RANTES, (d) TNF, (e) IL-4, (f) IL-10, and (g) IL-1β in the supernatant was determined using CBA. * representing $p \leq 0.05$ and ** representing $p \leq 0.01$, determined using an unpaired T-test with Welch's correction. n = 3.

Cytokine and chemokine secretion by THP-1 cells

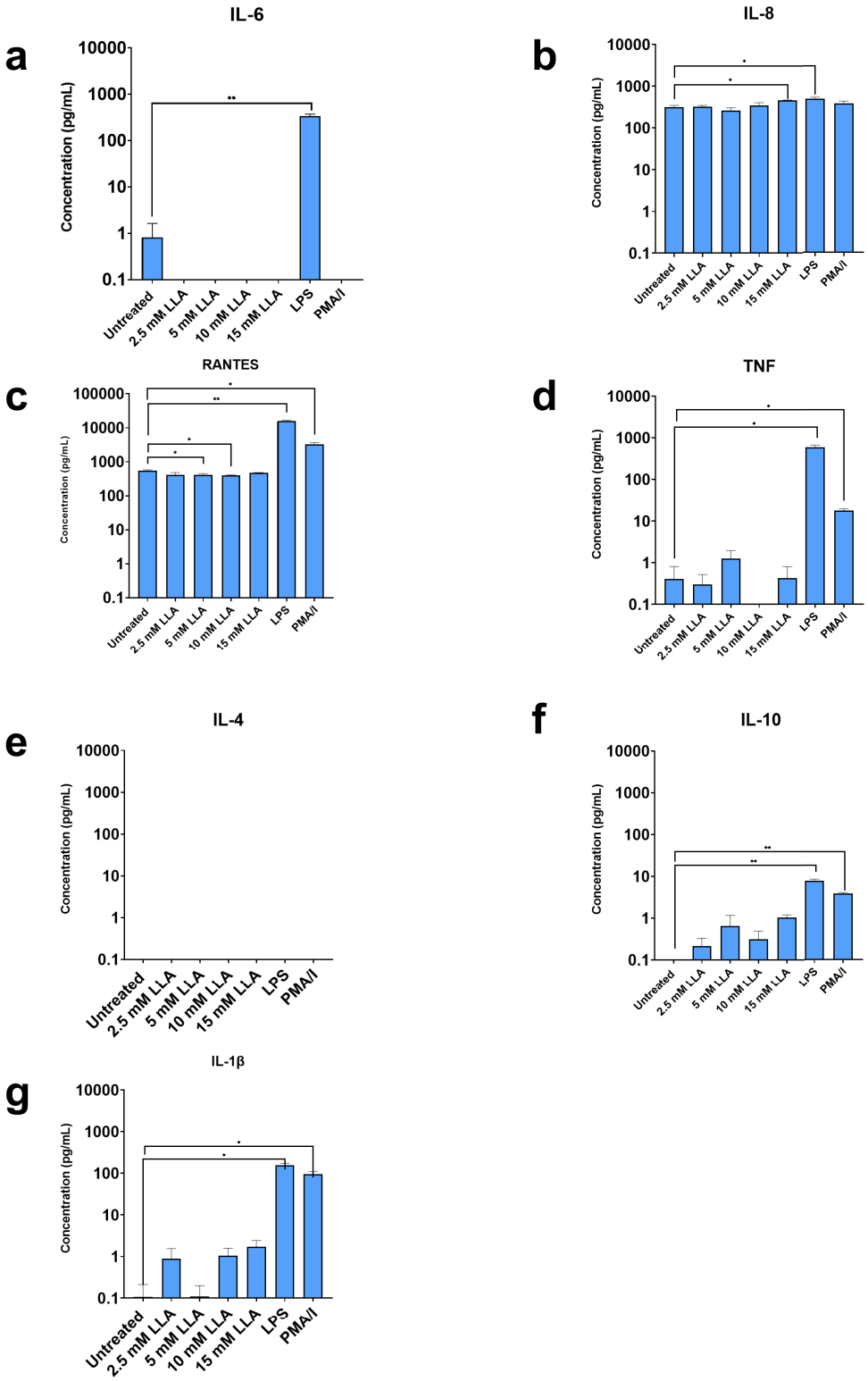


Figure 47. Cytokine expression by THP-1 cells treated with L-lactic acid (LLA). THP-1 cells were treated with LLA for 24 hours, and the concentration (pg/mL) of (a) IL-6, (b) IL-8, (c) RANTES, (d) TNF, (e) IL-4, (f) IL-10, and (g) IL-1β in the supernatant was determined using CBA. * representing $p \leq 0.05$ and ** representing $p \leq 0.01$, determined using an unpaired T-test with Welch's correction. n = 3.

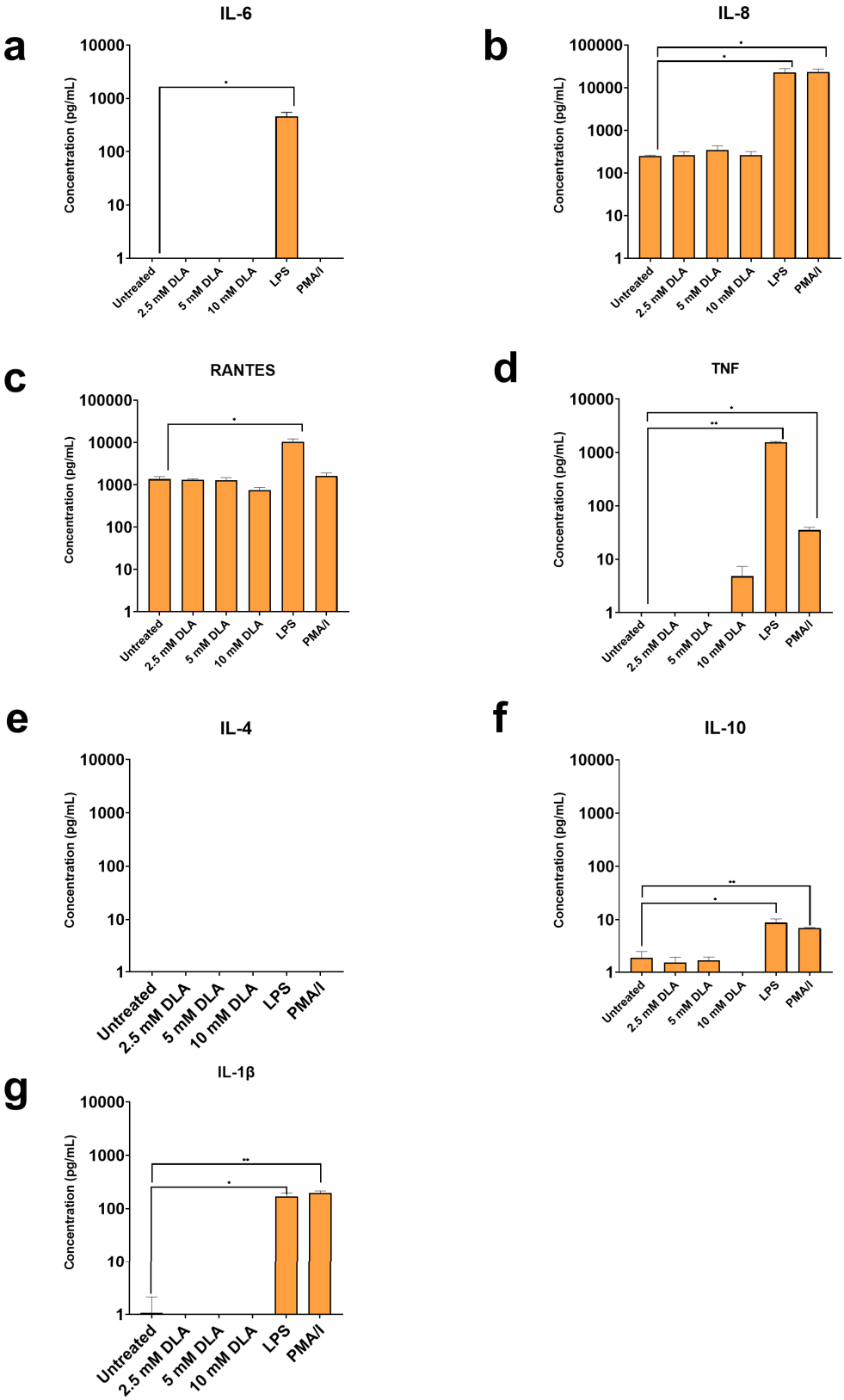


Figure 48. Cytokine expression by THP-1 cells treated with D-lactic acid (DLA). THP-1 cells were treated with DLA for 24 hours, and the concentration (pg/mL) of (a) IL-6, (b) IL-8, (c) RANTES, (d) TNF, (e) IL-4, (f) IL-10, and (g) IL-1β in the supernatant was determined using CBA. * representing $p \leq 0.05$ and ** representing $p \leq 0.01$, determined using an unpaired T-test with Welch's correction. n = 3.

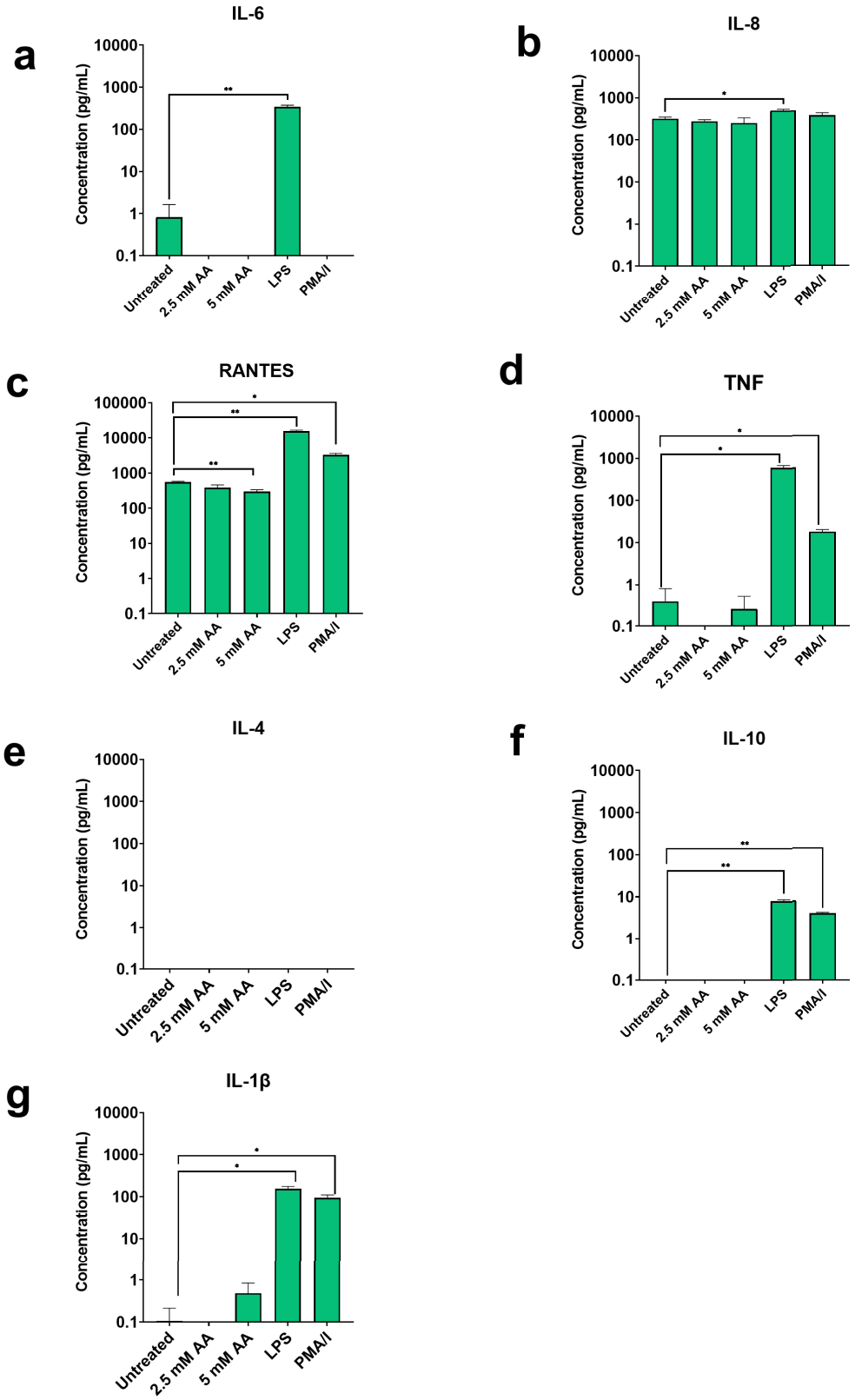


Figure 49. Cytokine expression by THP-1 cells treated with acetic acid (AA). THP-1 cells were treated with AA for 24 hours, and the concentration (pg/mL) of (a) IL-6, (b) IL-8, (c) RANTES, (d) TNF, (e) IL-4, (f) IL-10, and (g) IL-1β in the supernatant was determined using CBA. * representing $p \leq 0.05$, and ** representing $p \leq 0.01$, determined using an unpaired T-test with Welch's correction. n = 3.

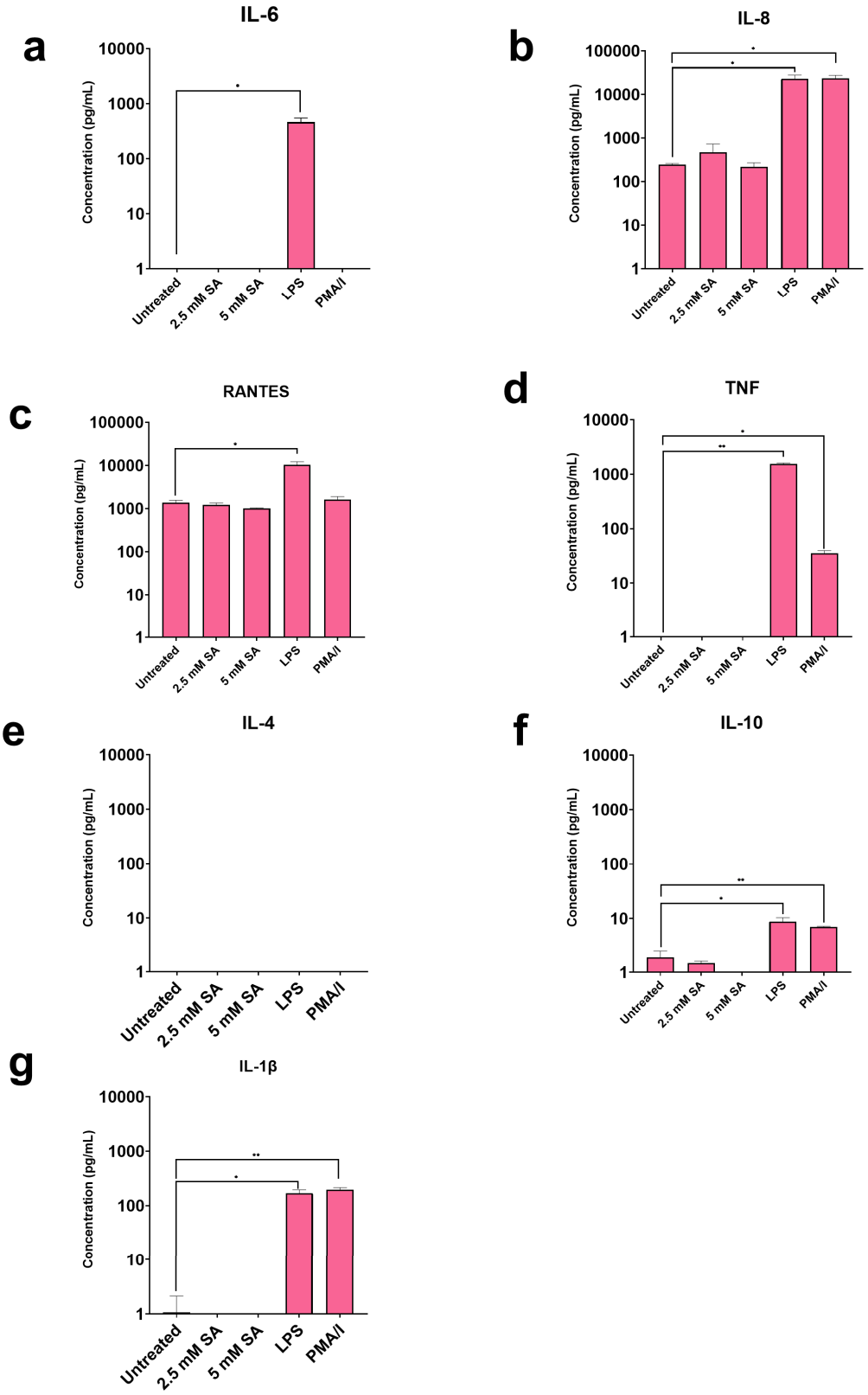


Figure 50. Cytokine expression by THP-1 cells treated with succinic acid (SA). THP-1 cells were treated with SA for 24 hours, and the concentration (pg/mL) of (a) IL-6, (b) IL-8, (c) RANTES, (d) TNF, (e) IL-4, (f) IL-10, and (g) IL-1β in the supernatant was determined using CBA. * representing $p \leq 0.05$ and ** representing $p \leq 0.01$, determined using an unpaired T-test with Welch's correction. n = 3.

C_t values of reference genes in conditioned media models

The following tables show the C_t values of the reference genes used in conditioned media models.

Table 30. Average C_t values of *HPRT1* in Ishikawa cells cultured with THP-1 conditioned media. Mean ± SD, n=3.

Treatment	Concentration (mM)	*HPRT1* C_t ± SD
L-lactic acid	15	26.2 ± 0.7
D-lactic acid	10	26.9 ± 1.0
Acetic acid	5	27.6 ± 1.5
Succinic acid	5	27.1 ± 0.5
Untreated	0	26.0 ± 0.5
LPS	1X	26.7 ± 0.3
PMA/I	1X	27.2 ± 0.7

Table 31. Average C_t values of *HPRT1* in Ishikawa cells cultured with NK-92 conditioned media. Mean ± SD, n=3.

Treatment	Concentration (mM)	*HPRT1* C_t ± SD
L-lactic acid	5	25.5 ± 0.5
D-lactic acid	4	25.1 ± 0.7
Acetic acid	5	25.3 ± 0.5
Succinic acid	2	24.3 ± 1.0
Untreated	0	25.5 ± 0.8
LPS	1X	25.7 ± 0.4
PMA/I	1X	24.6 ± 0.2

Table 32. Average C_t values of *HPRT1* in RL95-2 cells cultured with THP-1 conditioned media. Mean ± SD, n=3.

Treatment	Concentration (mM)	*HPRT1* C_t ± SD
L-lactic acid	15	26.6 ± 1.0
D-lactic acid	10	26.0 ± 0.5
Acetic acid	5	26.3 ± 0.3
Succinic acid	5	26.9 ± 0.7
Untreated	0	26.9 ± 1.0
LPS	1X	27.1 ± 1.3
PMA/I	1X	27.8 ± 1.3

Table 33. Average C_t values of *HPRT1* in RL95-2 cells cultured with NK-92 conditioned media. Mean ± SD, n=3.

Treatment	Concentration (mM)	*HPRT1* C_t ± SD
L-lactic acid	5	27.1 ± 1.1
D-lactic acid	4	28.5 ± 1.0
Acetic acid	5	26.7 ± 1.0
Succinic acid	2	27.2 ± 1.1
Untreated	0	28.2 ± 0.7
LPS	1X	27.4 ± 1.7
PMA/I	1X	28.6 ± 0.2

ΔC_t values for genes associated with the immune response from cells treated with microbiota-associated metabolites

The following tables show the ΔC_t values for genes associated with the immune response from cells treated with microbiota-associated metabolites.

Table 34. ΔC_t values from Ishikawa cells treated with microbiota-associated metabolites. The cells were treated with L-lactic acid (LLA), D-lactic acid (DLA), acetic acid (AA), or succinic acid (SA). LPS and PMA/I were used as inflammatory controls. Mean ± SD, n=3.

Treatment	*IL8*	*RANTES*	*TNF*	*IFNG*
PMA	2.1 ± 0.3	5.6 ± 1.1	7.8 ± 1.2	8.5 ± 1.6
LPS	7.7 ± 0.8	6.3 ± 1	9.1 ± 0.1	8.9 ± 0.7
0mM	12.6 ± 0.6	6.7 ± 0.3	9.5 ± 0.5	11.1 ± 4.9
5mM AA	10.1 ± 0.9	7.6 ± 0.8	11 ± 0.7	12.1 ± 0.3
10mM AA	10.9 ± 1.4	6.3 ± 1.1	8.8 ± 1.4	9.1 ± 0.4
5mM LLA	9.4 ± 0.6	8.1 ± 1.6	11 ± 1.6	11.7 ± 0.8
10mM LLA	8.1 ± 1.1	7.1 ± 2.2	9.1 ± 1.9	9.9 ± 2
25mM LLA	12.4 ± 1.8	7.5 ± 1.7	11.6 ± 1.3	10.1 ± 1
PMA/I	7.8 ± 0.6	6 ± 1.6	9.1 ± 1	10.1 ± 1
LPS	0.9 ± 0.4	6.4 ± 2.2	9.6 ± 1.4	9.7 ± 0.3
0mM	8.3 ± 0.5	6 ± 0.9	9 ± 0.7	12.0
2.5mM SA	8.9 ± 1.5	6.1 ± 0.6	8.4 ± 0.4	11.4 ± 0.1
5mM SA	8.8 ± 0.1	6.4 ± 0.3	12.4 ± 1.7	13.4
5mM DLA	8.6 ± 0.2	6.9 ± 1.5	11.2 ± 2.9	13.2
10mM DLA	10.5 ± 2.1	7.1 ± 0.4	13.6 ± 0.8	12.7 ± 0.8

Table 35. ΔC_t values from RL95-2 cells treated with microbiota-associated metabolites. The cells were treated with L-lactic acid (LLA), D-lactic acid (DLA), acetic acid (AA), or succinic acid (SA). LPS and PMA/I were used as inflammatory controls. Mean ± SD, n=3.

Treatment	*IL8*	*IL6*	*RANTES*	*TNF*	*IFNG*
PMA/I	-3.6 ± 0.3	-0.2 ± 0.4	-0.2 ± 0.8	0.8 ± 0.7	5.3 ± 1.3
LPS	5.4 ± 0.2	9.2 ± 0.7	2.3 ± 1	4.3 ± 0.3	7.9 ± 0.7
0mM	4.9 ± 0.8	10.7 ± 0.9	3.9 ± 1	5.7 ± 0.1	8.5 ± 1.1
2.5mM AA	6.4 ± 1.2	8.4 ± 1.6	5.2 ± 2.6	5.8 ± 0.9	7.8 ± 2.4
5mM AA	6.5 ± 1.2	8.9 ± 1.9	1.8 ± 1	4.8 ± 1.8	7.3 ± 1.4
5mM LLA	6.2 ± 0.9	8.5 ± 1.4	6.3 ± 1.2	6.8 ± 1.8	9.2 ± 1
10mM LLA	6.9 ± 0.4	11.6 ± 2.4	5.3 ± 0	6.8 ± 0.9	10.2 ± 2.5
15mM LLA	7 ± 0.8	10.6 ± 2.5	6.6 ± 0.7	7 ± 0.7	9.9 ± 1.9
PMA/I	-4.7 ± 0.9	0.6 ± 0.2	0.2 ± 1.4	0 ± 1	9.2 ± 0.7
LPS	5.6 ± 1	10.7 ± 1.9	4.2 ± 1.1	5.8 ± 0.4	10.8 ± 0.4
0mM	5.9 ± 1.7	8.7 ± 0.7	4.7 ± 1.6	4.6 ± 0.6	10.6 ± 0.6
2.5mM SA	6.8 ± 1.1	9.3 ± 0.2	4.8 ± 1.1	5 ± 0.6	10.6 ± 1.8
5mM SA	5.1 ± 1.3	7.6 ± 0.1	3.6 ± 1.2	4.6 ± 1.1	10.4 ± 2.7
5mM DLA	5.5 ± 0.1	8.5	4.6 ± 0.5	7.5 ± 3.6	11.5 ± 0.7
10mM DLA	6 ± 0.5	7.7 ± 0	4.8 ± 2.2	5.9 ± 1.9	10.2 ± 2.8

Table 36. ΔC_t values from NK-92 cells treated with microbiota-associated metabolites. The cells were treated with L-lactic acid (LLA), D-lactic acid (DLA), acetic acid (AA), or succinic acid (SA). LPS and PMA/I were used as inflammatory controls. Mean ± SD, n=3.

Treatment	*IL8*	*IL6*	*RANTES*	*TNF*	*IFNG*	*IDO1*
PMA/I	0.8 ± 2	8.9 ± 2.6	0.9 ± 2	5.3 ± 2.8	0.7 ± 3.2	12.1 ± 2.2
LPS	13.9 ± 1.4	8.5 ± 0.7	1.5 ± 0.5	7.1 ± 1	6.1 ± 0.4	13.4 ± 0.5
0mM	11.6 ± 0.6	8.7 ± 0.8	0.8 ± 0.7	6.1 ± 1	5.3 ± 0.5	14.2 ± 1
2.5mM LLA	12.1 ± 0.3	8.6 ± 1.7	1.4 ± 1.2	5.9 ± 0.4	6.6 ± 0.8	14 ± 0.4
5mM LLA	15.7 ± 0.9	8.4 ± 1.6	1.6 ± 0.6	6.8 ± 1.6	7.3 ± 0.7	15.6 ± 0.9
2.5mM AA	13.7 ± 1	11.2 ± 1.8	2.6 ± 1.1	8.1 ± 1.1	7.3 ± 0.8	16.2 ± 1.1
5mM AA	12.9 ± 2.1	9.5 ± 0.8	1.6 ± 0.4	7.8 ± 1.5	6.6 ± 0.3	13.9 ± 0.4
PMA/I	-2.5 ± 1	9.1 ± 1.6	-0.3 ± 0.5	4.3 ± 1	-2.6 ± 0.9	12.8 ± 1.2
LPS	14.1 ± 2.8	8.1 ± 0.7	1.1 ± 0.8	5.4 ± 1.5	5.6 ± 0.7	12 ± 2.4
0mM	10.4 ± 0.6	8.2 ± 0.9	1.6 ± 0.6	6.4 ± 1	6 ± 0.9	14.4 ± 0.3
1mM SA	11.1 ± 1.9	7.4 ± 1.1	0.5 ± 1	6 ± 1.1	5 ± 1.2	13.1 ± 0.6
2mM SA	12.8 ± 1.9	8.9 ± 0.6	1.7 ± 0.8	6.4 ± 0.9	6 ± 0.7	14.4 ± 0.3
2mM DLA	11.6 ± 1.2	7.9 ± 0	1.4 ± 0.6	5.8 ± 0.5	6 ± 0.2	13.2 ± 0.6
4mM DLA	11.2 ± 1.1	8.6 ± 1.3	1.7 ± 0.9	6.4 ± 0.8	6.5 ± 0.2	14 ± 0.4

Table 37. ΔC_t values from THP-1 cells treated with microbiota-associated metabolites. The cells were treated with L-lactic acid (LLA), D-lactic acid (DLA), acetic acid (AA), or succinic acid (SA). LPS and PMA/I were used as inflammatory controls. Mean ± SD, n=3.

Treatment	*IL8*	*RANTES*	*TNF*	*IFNG*
PMA/I	11.7 ± 0.5	6.3 ± 0.3	12 ± 1	19.8 ± 1.3
LPS	2.5 ± 0.8	2 ± 1.8	3.8 ± 1.4	18.3 ± 1.9
0mM	12.5 ± 1.2	5.9 ± 0.8	12.5 ± 1.7	19.4 ± 1.1
2.5mM AA	13.6 ± 0.5	5.4 ± 0.7	12.1 ± 0.9	19.9 ± 2.1
5mM AA	12.9 ± 0.6	5 ± 0.3	13 ± 1	17.8 ± 2.1
5mM LLA	12 ± 0.8	5.4 ± 0.8	12.7 ± 2.5	17.6 ± 1.9
10mM LLA	13 ± 0.5	5.6 ± 0.8	12.7 ± 0.9	18.6 ± 1
15mM LLA	11.5 ± 0.5	4.9 ± 0.8	12.7 ± 1.3	17.3 ± 1.7
PMA/I	4.6 ± 0.8	4.1 ± 0.1	12.3 ± 1.3	18.9 ± 0.8
LPS	1.5 ± 0.1	1.3 ± 0.8	5.6 ± 0.7	18 ± 1.9
0mM	12.8 ± 0.8	7 ± 0.5	15.3 ± 1.2	20.2 ± 1.4
2.5mM SA	14.5 ± 0.6	6.9 ± 0.7	14.6 ± 0.7	20.3 ± 1.6
5mM SA	11.6 ± 1.1	5.7 ± 1.8	12.8 ± 1.8	17.2 ± 2
5mM DLA	13.7 ± 0.9	7 ± 1.7	14.6 ± 1.6	19.7 ± 1.9
10mM DLA	12.9 ± 1.3	6.7 ± 1.2	15.2 ± 0.8	18.6 ± 1.4

ΔC_t values for genes associated with the immune response from cells treated with conditioned media

The following tables sow the ΔC_t values from cells cultured with innated immune cell conditioned media.

Table 38. ΔC_t values from Ishikawa cells cultured with NK-92 cell-conditioned media. Mean ± SD, n=3.

Treatment [a]	*RANTES*	*IL6*
PMA/I	9.9 ± 1.1	8.1 ± 0.7
LPS	9.2 ± 3.1	8.7 ± 1.6
0mM	7.6 ± 0.2	11.2 ± 3.5
2mM SA	8.6 ± 0.6	11.5 ± 2.2
5mM AA	8.1 ± 1.1	8.4 ± 0.6
4mM DLA	9.3 ± 1.4	9.5 ± 2.4
5mM LLA	9.7	9.1

[a] The concentration of metabolites used to treat NK-92 cells to generate conditioned media. The cells were treated with L-lactic acid (LLA), D-lactic acid (DLA), acetic acid (AA), or succinic acid (SA). LPS and PMA/I were used as inflammatory controls.

Table 39. ΔC_t values from Ishikawa cells cultured with THP-1 cell-conditioned media. Mean ± SD, n=3.

Treatment [a]	*RANTES*	*IL6*	*IL8*
PMA/I	10.4 ± 2.7	6.8 ± 0.1	1.9 ± 0.2
LPS	9.1 ± 2.4	4.4 ± 1.1	1.4 ± 0.5
0mM	9.9 ± 2.4	6.9 ± 0.1	6.5 ± 0.4
5mM SA	8.1 ± 0.1	6.1 ± 1	6.1 ± 1.4
5mM AA	11.3	5.2 ± 0.8	6 ± 0.7
10mM DLA	7.4 ± 0.8	5.6 ± 2.2	5.9 ± 1
15mM LLA	8.1 ± 0.2	6.6 ± 1.3	6.9 ± 1

[a] The concentration of metabolites used to treat THP-1 cells to generate conditioned media. The cells were treated with L-lactic acid (LLA), D-lactic acid (DLA), acetic acid (AA), or succinic acid (SA). LPS and PMA/I were used as inflammatory controls.

Table 40. ΔC_t values from RL95-2 cells cultured with NK-92 cell-conditioned media. Mean ± SD, n=3.

Treatment [a]	*RANTES*	*TNF*
PMA/I	-2.4 ± 0.9	3 ± 0.5
LPS	5.9 ± 0.5	9.0
0mM	7.4 ± 0.4	7.9 ± 0.7
2mM SA	5.8 ± 1	7.1 ± 0.7
5mM AA	9.8 ± 1.3	6.9 ± 0.2
4mM DLA	6.6 ± 1.1	6.5 ± 0.7
5mM LLA	6.6 ± 0.6	8.4 ± 2.9

[a] The concentration of metabolites used to treat RL95-2 cells to generate conditioned media. The cells were treated with L-lactic acid (LLA), D-lactic acid (DLA), acetic acid (AA), or succinic acid (SA). LPS and PMA/I were used as inflammatory controls.

Table 41. ΔC_t values from RL95-2 cells cultured with THP-1 cell-conditioned media.

Mean ± SD, n=3.

Treatment [a]	*RANTES*	*TNF*	*IL8*
PMA/I	-0.9 ± 0.8	-3.5 ± 0.4	1.7 ± 1.4
LPS	1.5 ± 0.3	-1.7 ± 1	2 ± 0.3
0mM	7 ± 1.4	5.3 ± 0.1	7 ± 1
5mM SA	6.3 ± 0.8	5.3 ± 0.3	7.2 ± 2.6
5mM AA	6.4 ± 0.5	7.3 ± 1	7.4 ± 0.5
10mM DLA	7.6 ± 1	7.9 ± 1	6.8 ± 0.6
15mM LLA	5.4 ± 0.9	9.4 ± 2	6.7 ± 0.5

[a] The concentration of metabolites used to treat THP-1 cells to generate conditioned media. The cells were treated with L-lactic acid (LLA), D-lactic acid (DLA), acetic acid (AA), or succinic acid (SA). LPS and PMA/I were used as inflammatory controls.

Fold change analysis of immune response genes

These figures represent the fold change of genes associated with the immune response. The data was analysed using the comparative C_t method. The significant results are shown in Chapter 4, Sections 4.4.4, 4.4.5 and 4.4.6.

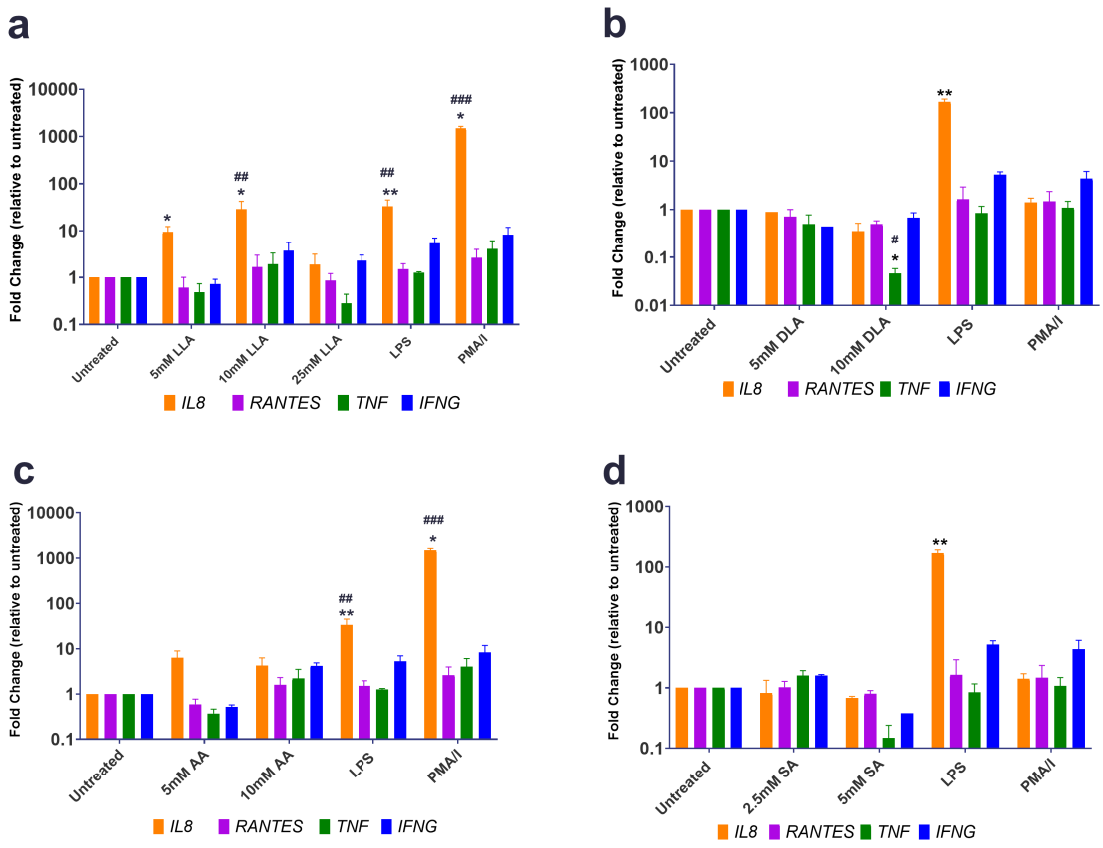


Figure 51. The relative expression of genes associated with the immune response in Ishikawa cells treated with microbiota-associated metabolites. The cells were grown to confluency and treated with microbiota-associated metabolites: a) L-lactic acid, b) D-lactic acid, c) acetic acid, and d) succinic acid. Gene expression was normalised to the reference genes and expressed as fold change compared to the untreated cells using the comparative C_t method. * representing $p \leq 0.05$, and ** representing $p \leq 0.01$, determined using an unpaired T-test with Welch's correction. # representing $p \leq 0.05$, ## representing $p \leq 0.01$,and ### representing $p \leq 0.001$, determined using Dunnett's multiple comparisons tests. n = 3.

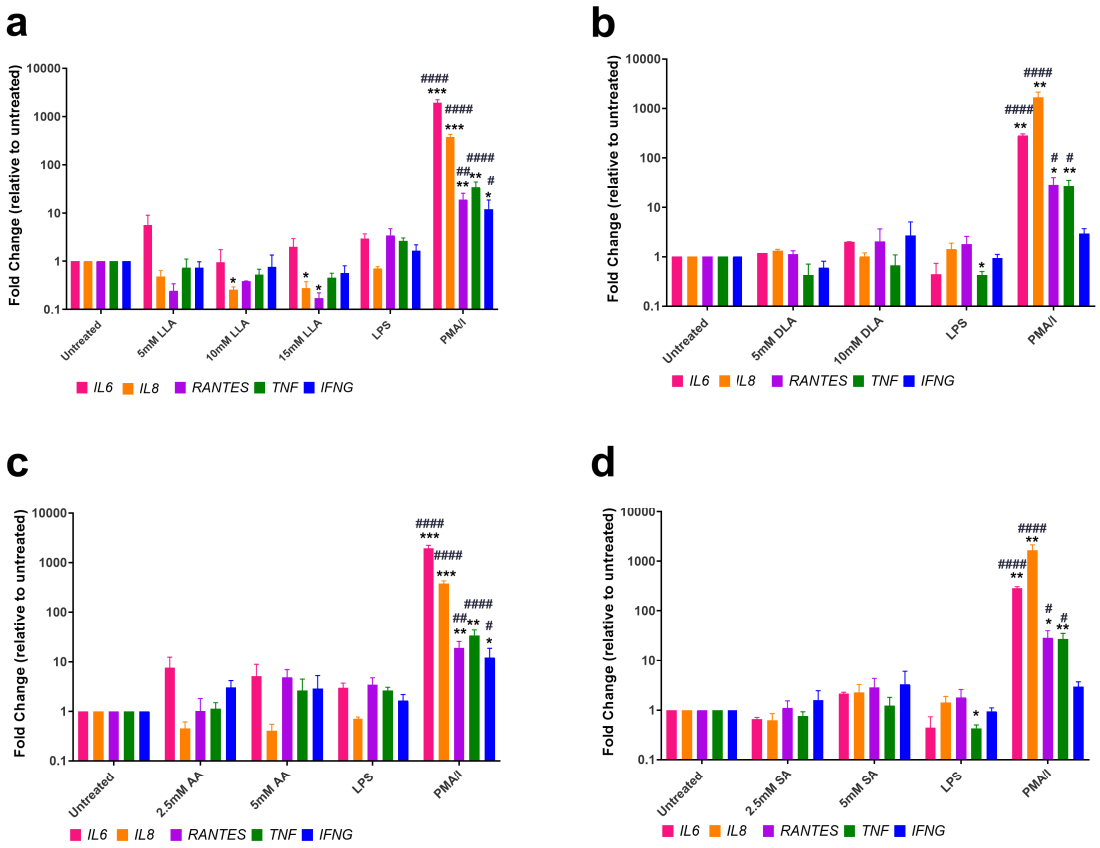


Figure 52. The relative expression of genes associated with the immune response in RL95-2 cells treated with microbiota-associated metabolites. The cells were grown to confluency and treated with microbiota-associated metabolites: a) L-lactic acid, b) D-lactic acid, c) acetic acid, and d) succinic acid. Gene expression was normalised to the reference genes and expressed as fold change compared to the untreated cells using the comparative C_t method. * representing $p \leq 0.05$, ** representing $p \leq 0.01$, and *** representing $p \leq 0.001$ determined using an unpaired T-test with Welch's correction. # representing $p \leq 0.05$, ## representing $p \leq 0.01$, ### representing $p \leq 0.001$, and #### representing $p \leq 0.0001$determined using Dunnett's multiple comparisons tests. n = 3.

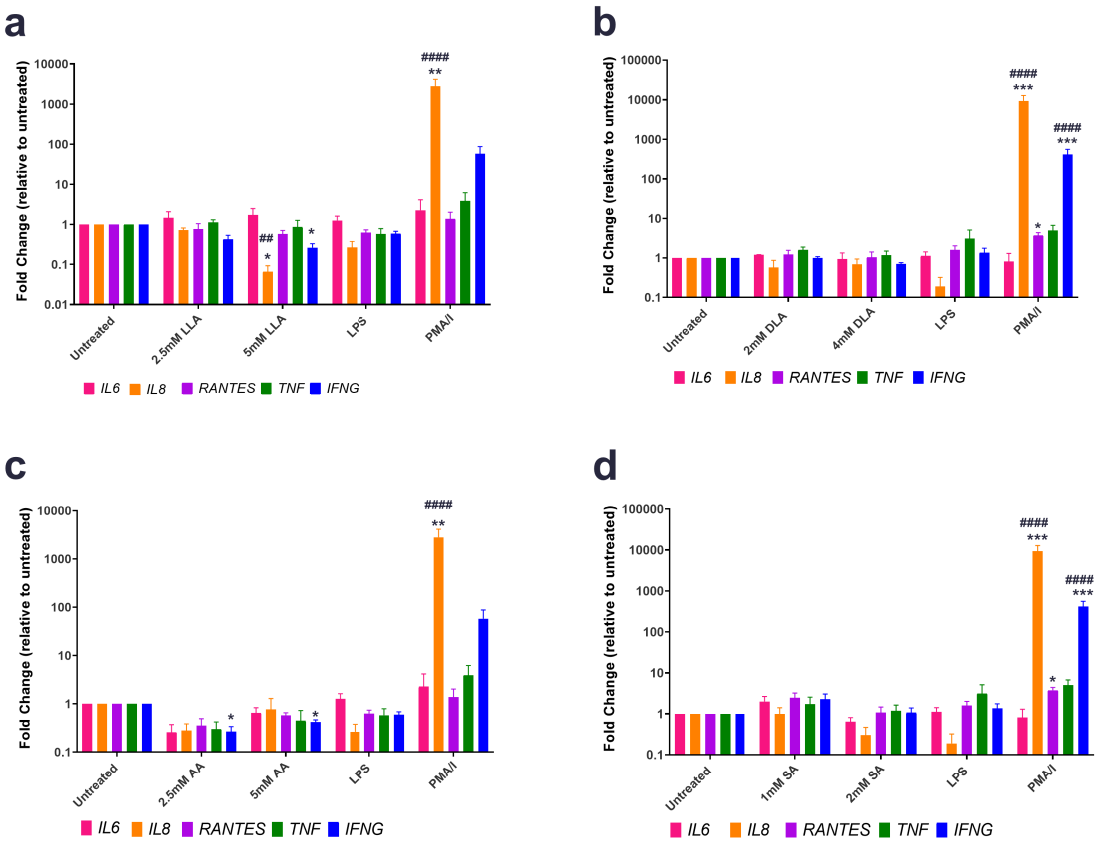


Figure 53. The relative expression of genes associated with the immune response in NK-92 cells treated with microbiota-associated metabolites. The cells were grown to confluency and treated with microbiota-associated metabolites: a) L-lactic acid, b) D-lactic acid, c) acetic acid, and d) succinic acid. Gene expression was normalised to the reference genes and expressed as fold change compared to the untreated cells using the comparative C_t method. * representing $p \leq 0.05$, ** representing $p \leq 0.01$, and *** representing $p \leq 0.001$ determined using an unpaired T-test with Welch's correction. ## representing $p \leq 0.01$, and #### representing $p \leq 0.0001$determined using Dunnett's multiple comparisons tests. n = 3.

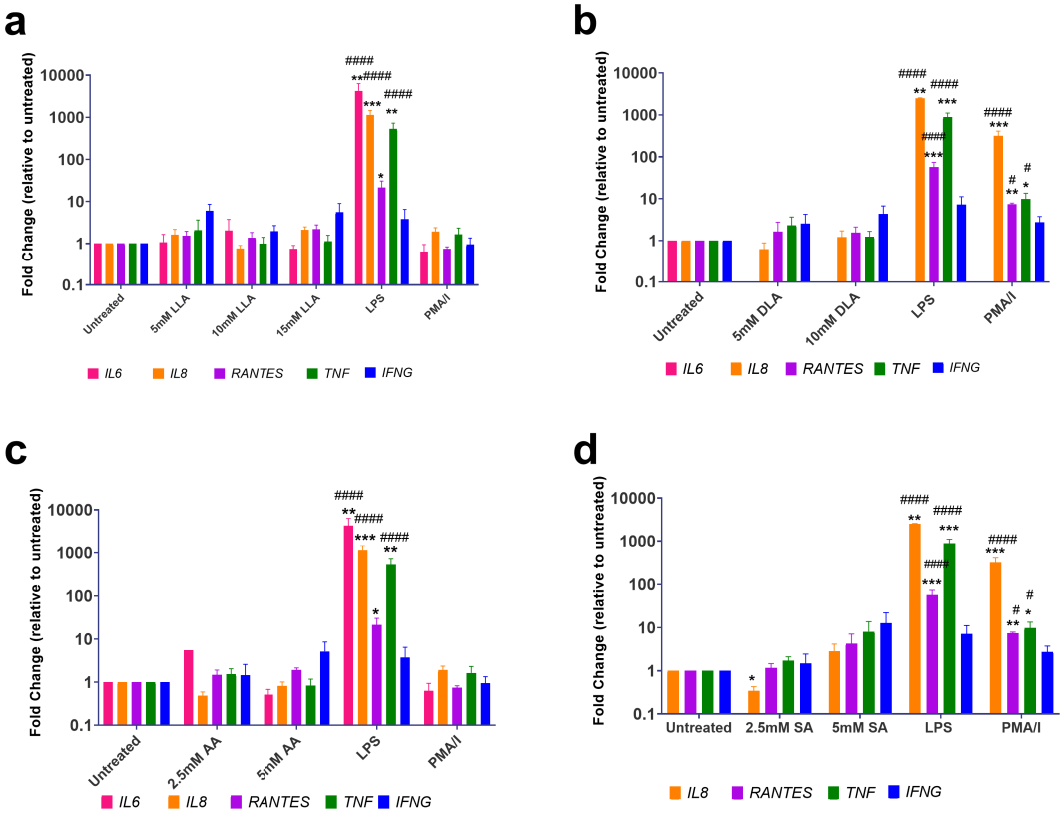


Figure 54. The relative expression of genes associated with the immune response in THP-1 cells treated with microbiota-associated metabolites. The cells were grown to confluency and treated with microbiota-associated metabolites: a) L-lactic acid, b) D-lactic acid, c) acetic acid, and d) succinic acid. Gene expression was normalised to the reference genes and expressed as fold change compared to the untreated cells using the comparative C_t method. * representing $p \leq 0.05$, ** representing $p \leq 0.01$, and *** representing $p \leq 0.001$ determined using an unpaired T-test with Welch's correction. # representing $p \leq 0.05$, ### representing $p \leq 0.001$, and #### representing $p \leq 0.0001$determined using Dunnett's multiple comparisons tests. n = 3.

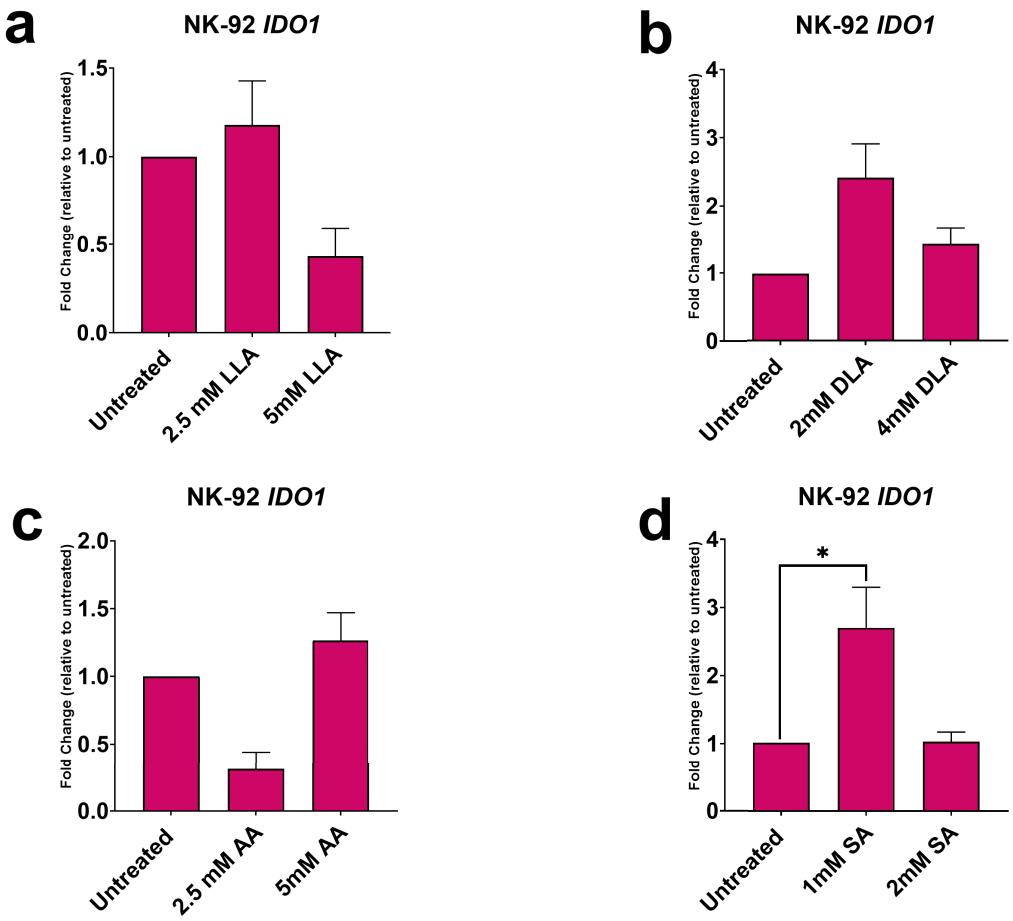


Figure 55. The relative expression of IDO1 in NK-92 cells treated with microbiota-associated metabolites. The cells were grown to confluency and treated with microbiota-associated metabolites: a) L-lactic acid, b) D-lactic acid, c) acetic acid, and d) succinic acid. Gene expression was normalised to the reference genes and expressed as fold change compared to the untreated cells using the comparative C_t method. * representing $p \leq 0.05$, determined using an unpaired T-test with Welch's correction. n = 3.

Appendix 4

C_t Values for reference genes in JAR cells

The following table shows the C_t values for *GAPDH. GAPDH* was used as the reference gene in experiments using the JAR cells.

Table 42. Average C_t values of *GAPDH* in JAR cells treated with microbiota-associated metabolites and controls. Mean ± SD, n=3.

Treatment	Concentration (mM)	*GAPDH* C_t± SD
L-lactic acid	5	20.2 ± 0.6
	10	20.1 ± 1.0
	15	20.3 ± 0.4
D-lactic acid	5	19.4 ± 0.2
	10	20.3 ± 1.3
	15	19.7 ± 0.8
Acetic acid	5	20.9 ± 1.2
	10	20.1 ± 1.0
	15	20.8 ± 0.9
Succinic acid	2.5	20.7 ± 0.6
	5	20.2 ± 1.2
Untreated	0	20.0 ± 0.9

ΔC_t Values for TIMP and MMP genes in JAR cells

The following table shows the ΔC_t values for TIMP and MMP genes.

Table 43. ΔC_t values from JAR cells treated with microbiota-associated metabolites. The cells were treated with L-lactic acid (LLA), D-lactic acid (DLA), acetic acid (AA), or succinic acid (SA). Mean ± SD, n=3.

Treatment	*TIMP1*	*TIMP2*	*MMP2*	*MMP9*
0mM	14.1 ± 1.8	4.3 ± 1.2	4.3 ± 1.2	18.2 ± 1.3
2.5mM SA	14.1 ± 1.1	4.8 ± 1.1	5.2 ± 0	18.3 ± 0.5
5mM SA	13.5 ± 2.7	4.8 ± 1.2	4.3 ± 1	18.3 ± 0.8
5mM AA	14.6 ± 2.1	4.5 ± 2.3	5.7 ± 1.8	17.9 ± 0.8
10mM AA	14.9 ± 0.6	4.6 ± 1.1	4.6 ± 1.2	17.6 ± 1.4
15mM AA	14.1 ± 0.7	2.9 ± 0.7	4 ± 0.6	16.3 ± 2.3
5mM DLA	14.3 ± 0.2	4.6 ± 0.6	4.4 ± 0.7	17.6 ± 2.1
10mM DLA	15 ± 0.4	4 ± 1	3.9 ± 0.5	16.8 ± 0.8
15mM DLA	14.6 ± 1	5 ± 0.5	5 ± 0.6	18.5 ± 0.9
5mM LLA	13.9 ± 0.8	4.1 ± 0.8	4.9 ± 0.5	17.8 ± 1.3
10mM LLA	14.8 ± 1.3	4.5 ± 0.4	5.2 ± 1.6	18.4 ± 0.2
15mM LLA	13.7 ± 1.2	5.1 ± 0.4	4.7 ± 0.9	17.2 ± 1.6

Spheroid Attachment Assay

These figures show the analysis of spheroid attachment, including cells treated with PMA/I and LPS. The analysis of this data can also be found in Chapter 5, Sections 5.4.4, 5.4.5, and 5.4.6.

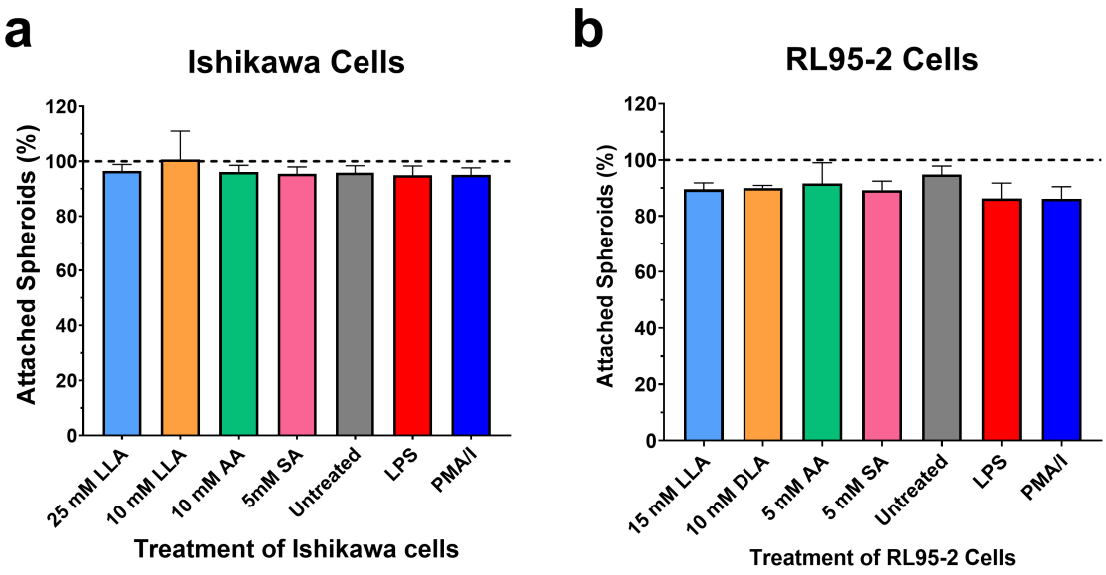


Figure 56. Spheroid attachment to endometrial epithelial cells treated with microbiota-associated metabolites. Ishikawa and RL95-2 cells were treated with L-lactic acid (LLA), D-lactic acid (DLA), acetic acid (AA), and succinic acid (SA) for 24 hours before conducting the spheroid attachment assay. (a) The percentage of attached spheroids to Ishikawa cells. (b) The percentage of attached spheroids to RL95-2 cells. The data shows mean ± SEM (n = 3).

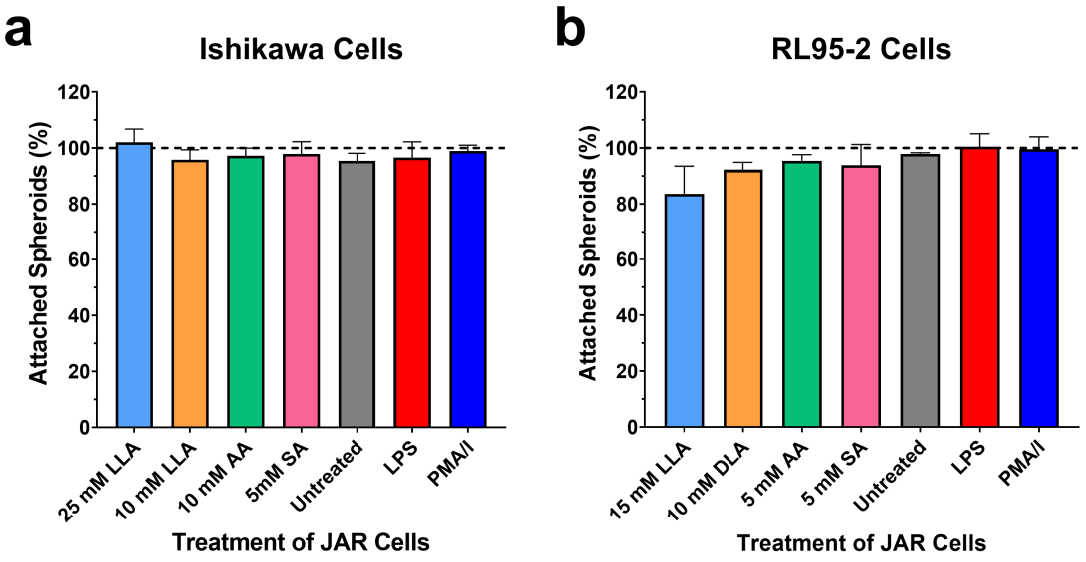


Figure 57. Attachment of JAR cells treated with microbiota-associated metabolites to untreated endometrial epithelial cells. JAR cells were treated with L-lactic acid (LLA), D-lactic acid (DLA), acetic acid (AA), and succinic acid (SA) for 24 hours before conducting the spheroid attachment assay. (a) The percentage of attached spheroids to Ishikawa cells. (b) The percentage of attached spheroids to RL95-2 cells. The data shows mean ± SEM (n = 3).

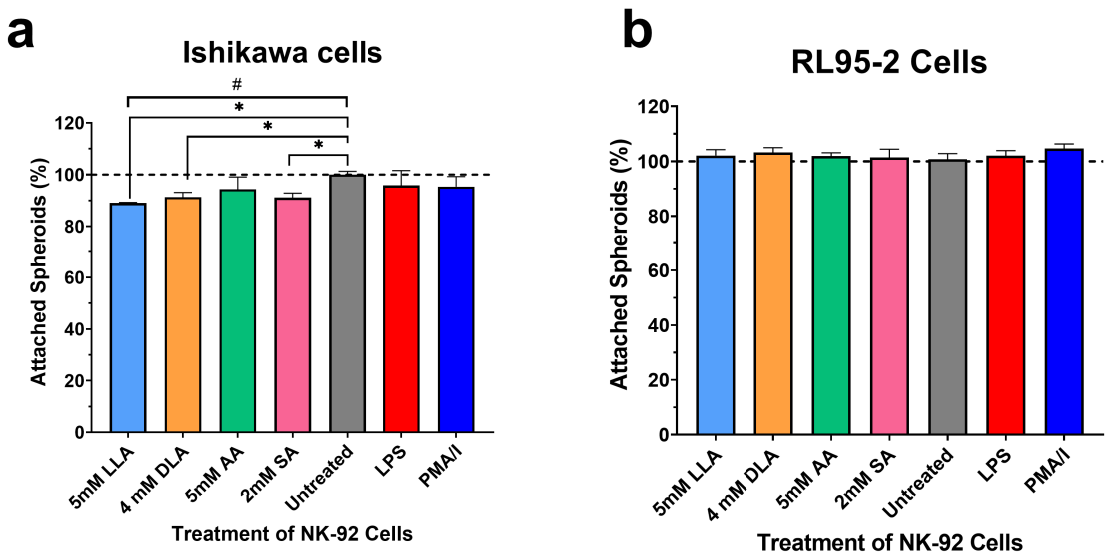


Figure 58. Spheroid attachment to endometrial epithelial cells treated with media conditioned by NK-92 cells cultured with microbiota-associated metabolites. To generate conditioned media, NK-29 cells were treated with L-lactic acid (LLA), D-lactic acid (DLA), acetic acid (AA), and succinic acid (SA) for 24 hours. Endometrial epithelial cells were treated with the conditioned media for 24 hours before conducting the spheroid attachment assay. (a) The percentage of attached spheroids to Ishikawa cells. (b) The percentage of attached spheroids to RL95-2 cells. The data shows mean ± SEM (n = 3). * represents $p \leq 0.05$, determined using an unpaired T-test with Welch's correction. # represents $p \leq 0.05$, analysed by Dunnett's multiple comparisons test.

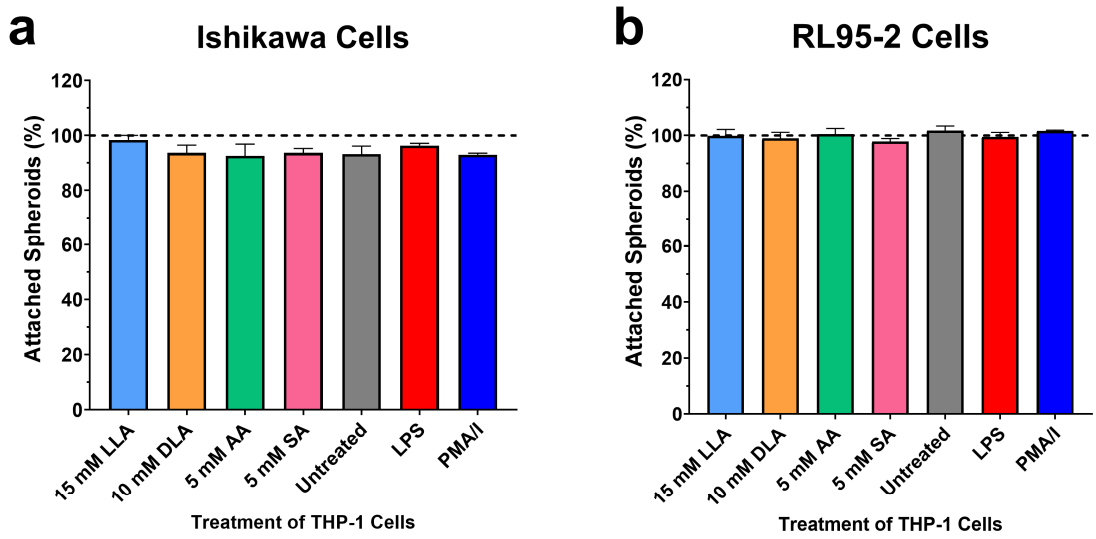


Figure 59. Spheroid attachment to endometrial epithelial cells treated with media conditioned by differentiated THP-1 cells cultured with microbiota-associated metabolites. To generate conditioned media, THP-1 cells were treated with L-lactic acid (LLA), D-lactic acid (DLA), acetic acid (AA), and succinic acid (SA) for 24 hours. Endometrial epithelial cells were treated with the conditioned media for 24 hours before conducting the spheroid attachment assay. (a) The percentage of attached spheroids to Ishikawa cells. (b) The percentage of attached spheroids to RL95-2 cells. The data shows mean ± SEM (n = 3).

Expression of MMP9 by JAR Cells

These images show the western blot images for MMP9 expression by JAR cells treated with microbiota-associated metabolites. The analysis of MMP2 western blot images can be found in Chapter 5, Section 5.4.3.

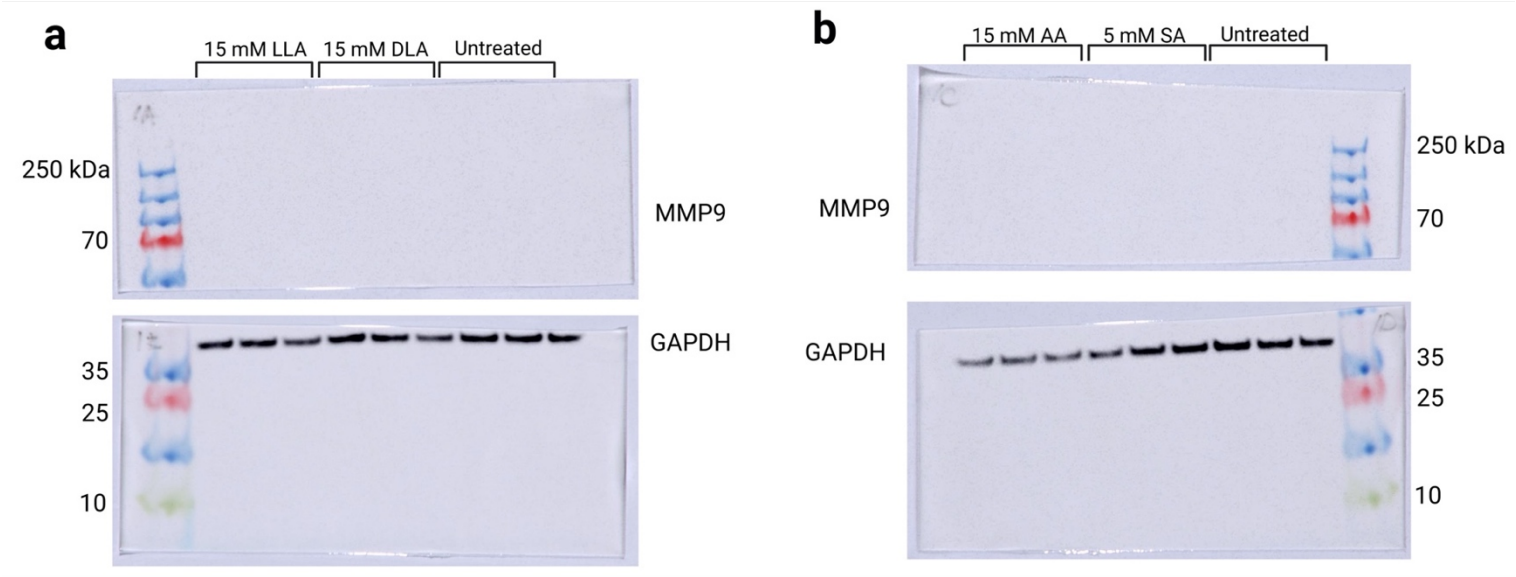


Figure 60. Protein expression of MMP9 and GAPDH in JAR cells treated with microbiota-associated metabolites. JAR cells were treated with L-lactic acid (LLA), D-lactic acid (DLA), acetic acid (AA), and succinic acid (SA). (a) Western blots of MMP9 and GAPDH from JAR cells treated with LLA and DLA, and untreated cells. (b) Western blots of MMP9 and GAPDH from JAR cells treated with AA and SA, and untreated cells

Bibliography

1. Ross, M.H. and W. Pawlina, *Female Reproductive System.*, in *Histology: A Text and Atlas: With Correlated Cell and Molecular Biology.* 2016, Wolters Kluwer Health: Philadelphia, PA, USA. p. 834-899.
2. Hoare, B.S. and Y.S. Khan, *Anatomy, Abdomen and Pelvis: Female Internal Genitals*. 2023: StatPearls Publishing, Treasure Island (FL).
3. Itriyeva, K., *The normal menstrual cycle.* Curr Probl Pediatr Adolesc Health Care, 2022. **52**(5): p. 101183.
4. Gnainsky, Y., N. Dekel, and I. Granot, *Implantation: mutual activity of sex steroid hormones and the immune system guarantee the maternal-embryo interaction.* Semin Reprod Med, 2014. **32**(5): p. 337-45.
5. McKinley MP, O'Loughlin VD, and Bidle TS, *Reproductive System*, in *Anatomy and Physiology: An Integrative Approach*. 2016, McGraw-Hill Education: New York, NY, USA. p. 1092-1132.
6. Lessey, B.A. and S.L. Young, *What exactly is endometrial receptivity?* Fertil Steril, 2019. **111**(4): p. 611-617.
7. Rock, J. and M.K. Bartlett, *Biopsy studies of human endometrium: criteria of dating and information about amenorrhea, menorrhagia, and time of ovulation.* J Am Med Assoc, 1937. **108**(24): p. 2022-8.
8. Noyes, R.W., A.T. Hertig, and J. Rock, *Dating the endometrial biopsy.* Am J Obstet Gynecol, 1975. **122**(2): p. 262-3.
9. Nikas, G., *Pinopodes as markers of endometrial receptivity in clinical practice.* Hum Reprod, 1999. **14 Suppl 2**(suppl_2): p. 99-106.
10. Whitby, S., W. Zhou, and E. Dimitriadis, *Alterations in Epithelial Cell Polarity During Endometrial Receptivity: A Systematic Review.* Front Endocrinol (Lausanne), 2020. **11**: p. 596324.
11. Craciunas, L., et al., *Conventional and modern markers of endometrial receptivity: a systematic review and meta-analysis.* Hum Reprod Update, 2019. **25**(2): p. 202-223.
12. Kao, L.C., et al., *Global gene profiling in human endometrium during the window of implantation.* Endocrinology, 2002. **143**(6): p. 2119-38.
13. Diaz-Gimeno, P., et al., *A genomic diagnostic tool for human endometrial receptivity based on the transcriptomic signature.* Fertil Steril, 2011. **95**(1): p. 50-60, 60 e1-15.
14. Diaz-Gimeno, P., et al., *The accuracy and reproducibility of the endometrial receptivity array is superior to histology as a diagnostic method for endometrial receptivity.* Fertil Steril, 2013. **99**(2): p. 508-17.
15. Cozzolino, M., et al., *Use of the endometrial receptivity array to guide personalized embryo transfer after a failed transfer attempt was associated with a lower cumulative and per transfer live birth rate during donor and autologous cycles.* Fertil Steril, 2022. **118**(4): p. 724-736.
16. Arian, S.E., et al., *Endometrial receptivity array before frozen embryo transfer cycles: a systematic review and meta-analysis.* Fertil Steril, 2023. **119**(2): p. 229-238.

17. Teh, W.T., et al., *A molecular staging model for accurately dating the endometrial biopsy.* Nat Commun, 2023. **14**(1): p. 6222.
18. Rossant, J. and P.P.L. Tam, *Early human embryonic development: Blastocyst formation to gastrulation.* Dev Cell, 2022. **57**(2): p. 152-165.
19. Stevens, A., et al., *The Human Early Maternal–Embryonic Interactome.* Reproductive Medicine, 2023. **4**(1): p. 40-56.
20. Park, J.Y., et al., *A microphysiological model of human trophoblast invasion during implantation.* Nat Commun, 2022. **13**(1): p. 1252.
21. Ruane, P.T., et al., *Apposition to endometrial epithelial cells activates mouse blastocysts for implantation.* Mol Hum Reprod, 2017. **23**(9): p. 617-627.
22. Enders, A.C. and S. Schlafke, *Cytological aspects of trophoblast-uterine interaction in early implantation.* Am J Anat, 1969. **125**(1): p. 1-29.
23. Singh, H., et al., *Early stages of implantation as revealed by an in vitro model.* Reproduction, 2010. **139**(5): p. 905-14.
24. Aberkane, A., et al., *Expression of adhesion and extracellular matrix genes in human blastocysts upon attachment in a 2D co-culture system.* Mol Hum Reprod, 2018. **24**(7): p. 375-387.
25. Kagawa, H., et al., *Human blastoids model blastocyst development and implantation.* Nature, 2022. **601**(7894): p. 600-605.
26. Tiwari, A., et al., *Modulation of E-Cadherin and N-Cadherin by ovarian steroids and embryonic stimuli.* Tissue Cell, 2021. **73**: p. 101670.
27. Uchida, H., et al., *Studies using an in vitro model show evidence of involvement of epithelial-mesenchymal transition of human endometrial epithelial cells in human embryo implantation.* J Biol Chem, 2012. **287**(7): p. 4441-50.
28. Francis, L.W., et al., *Highly glycosylated MUC1 mediates high affinity L-selectin binding at the human endometrial surface.* J Nanobiotechnology, 2021. **19**(1): p. 50.
29. Governini, L., et al., *Main actors behind the endometrial receptivity and successful implantation.* Tissue Cell, 2021. **73**: p. 101656.
30. Gauster, M., et al., *Early human trophoblast development: from morphology to function.* Cell Mol Life Sci, 2022. **79**(6): p. 345.
31. Bentin-Ley, U., et al., *Ultrastructure of human blastocyst-endometrial interactions in vitro.* J Reprod Fertil, 2000. **120**(2): p. 337-50.
32. Enders, A. *Images of human implantation*. n.d [cited 2022; Available from: https://www.trophoblast.cam.ac.uk/Resources/enders.
33. Ruane, P.T., et al., *Trophectoderm differentiation to invasive syncytiotrophoblast is promoted by endometrial epithelial cells during human embryo implantation.* Hum Reprod, 2022. **37**(4): p. 777-792.
34. Betz, D. and K. Fane, *Human chorionic gonadotropin*, in *StatPearls [Internet]*. 2023, StatPearls Publishing.
35. You, Y., et al., *Novel 3D in vitro models to evaluate trophoblast migration and invasion.* Am J Reprod Immunol, 2019. **81**(3): p. e13076.
36. Chen, X., et al., *Physiological and pathological angiogenesis in endometrium at the time of embryo implantation.* American Journal of Reproductive Immunology, 2017. **78**(2): p. e12693.
37. Craven, C.M., T. Morgan, and K. Ward, *Decidual spiral artery remodelling begins before cellular interaction with cytotrophoblasts.* Placenta, 1998. **19**(4): p. 241-52.

38. Jinno, M., et al., *Measurement of endometrial tissue blood flow: a novel way to assess uterine receptivity for implantation.* Fertility and Sterility, 2001. **76**(6): p. 1168-1174.
39. Bulmer, J.N., et al., *Granulated lymphocytes in human endometrium: histochemical and immunohistochemical studies.* Hum Reprod, 1991. **6**(6): p. 791-8.
40. Koopman, L.A., et al., *Human Decidual Natural Killer Cells Are a Unique NK Cell Subset with Immunomodulatory Potential.* Journal of Experimental Medicine, 2003. **198**(8): p. 1201-1212.
41. Li, C., et al., *HLA-G homodimer-induced cytokine secretion through HLA-G receptors on human decidual macrophages and natural killer cells.* Proc Natl Acad Sci U S A, 2009. **106**(14): p. 5767-72.
42. Hu, W.T., et al., *Decidual stromal cell-derived IL-33 contributes to Th2 bias and inhibits decidual NK cell cytotoxicity through NF-kappaB signaling in human early pregnancy.* J Reprod Immunol, 2015. **109**: p. 52-65.
43. Lessin, D.L., et al., *Antigen expression by cells near the maternal-fetal interface.* Am J Reprod Immunol Microbiol, 1988. **16**(1): p. 1-7.
44. Houser, B.L., et al., *Two unique human decidual macrophage populations.* The Journal of immunology (1950), 2011. **186**(4): p. 2633-2642.
45. Fahey, J.V., et al., *Secretion of cytokines and chemokines by polarized human epithelial cells from the female reproductive tract.* Hum Reprod, 2005. **20**(6): p. 1439-46.
46. Caballero-Campo, P., et al., *Hormonal and embryonic regulation of chemokines IL-8, MCP-1 and RANTES in the human endometrium during the window of implantation.* Molecular Human Reproduction, 2002. **8**(4): p. 375-384.
47. Arici, A., et al., *Interleukin-8 in the human endometrium.* J Clin Endocrinol Metab, 1998. **83**(5): p. 1783-7.
48. Hornung, D., et al., *Immunolocalization and Regulation of the Chemokine RANTES in Human Endometrial and Endometriosis Tissues and Cells*.* The Journal of Clinical Endocrinology & Metabolism, 1997. **82**(5): p. 1621-1628.
49. Hanna, J., et al., *Decidual NK cells regulate key developmental processes at the human fetal-maternal interface.* Nature Medicine, 2006. **12**(9): p. 1065-1074.
50. Belyakova, K.L., et al., *Interaction of NK Cells, Trophoblast, and Endothelial Cells during Angiogenesis.* Bull Exp Biol Med, 2019. **167**(1): p. 169-176.
51. Sokolov, D.I., et al., *Proliferative and Migration Activity of JEG-3 Trophoblast Cell Line in the Presence of Cytokines.* Bull Exp Biol Med, 2015. **159**(4): p. 550-6.
52. Pitman, H., et al., *Altered expression of interleukin-6, interleukin-8 and their receptors in decidua of women with sporadic miscarriage.* Hum Reprod, 2013. **28**(8): p. 2075-86.
53. Ashkar, A.A., J.P. Di Santo, and B.A. Croy, *Interferon gamma contributes to initiation of uterine vascular modification, decidual integrity, and uterine natural killer cell maturation during normal murine pregnancy.* J Exp Med, 2000. **192**(2): p. 259-70.
54. Aldo, P.B., et al., *Trophoblast induces monocyte differentiation into CD14+/CD16+ macrophages.* Am J Reprod Immunol, 2014. **72**(3): p. 270-84.
55. Lash, G.E., et al., *Interaction between uterine natural killer cells and extravillous trophoblast cells: effect on cytokine and angiogenic growth factor production.* Hum Reprod, 2011. **26**(9): p. 2289-95.

56. Lash, G.E., et al., *Decidual macrophages: key regulators of vascular remodeling in human pregnancy.* J Leukoc Biol, 2016. **100**(2): p. 315-25.
57. Viganò, P., et al., *Interleukin-10 is produced by human uterine natural killer cells but does not affect their production of interferon-γ.* Molecular Human Reproduction, 2001. **7**(10): p. 971-977.
58. Murphy, S.P., et al., *Uterine NK cells mediate inflammation-induced fetal demise in IL-10-null mice.* J Immunol, 2005. **175**(6): p. 4084-90.
59. Blois, S.M., et al., *NK cell-derived IL-10 is critical for DC-NK cell dialogue at the maternal-fetal interface.* Sci Rep, 2017. **7**(1): p. 2189.
60. Wei, C.Y., et al., *Immune status of decidual macrophages is dependent on the CCL2/CCR2/JAK2 pathway during early pregnancy.* Am J Reprod Immunol, 2021. **86**(5): p. e13480.
61. Chen, Z., et al., *Characteristics and functions of memory regulatory T cells in normal pregnancy cycle and pregnancy complications.* J Reprod Immunol, 2024. **163**: p. 104235.
62. Huang, N., H. Chi, and J. Qiao, *Role of Regulatory T Cells in Regulating Fetal-Maternal Immune Tolerance in Healthy Pregnancies and Reproductive Diseases.* Front Immunol, 2020. **11**: p. 1023.
63. Zhu, L., et al., *Treg/Th17 Cell Imbalance and IL-6 Profile in Patients With Unexplained Recurrent Spontaneous Abortion.* Reproductive Sciences, 2017. **24**(6): p. 882-890.
64. Qian, J., et al., *Distinct pattern of Th17/Treg cells in pregnant women with a history of unexplained recurrent spontaneous abortion.* Biosci Trends, 2018. **12**(2): p. 157-167.
65. Mor, G., P. Aldo, and A.B. Alvero, *The unique immunological and microbial aspects of pregnancy.* Nat Rev Immunol, 2017. **17**(8): p. 469-482.
66. Zegers-Hochschild, F., et al., *International Committee for Monitoring Assisted Reproductive Technology (ICMART) and the World Health Organization (WHO) revised glossary of ART terminology, 2009.* Fertil Steril, 2009. **92**(5): p. 1520-4.
67. *Infertility prevalence estimates, 1990–2021*. 2023, World Health Organisation: Geneva.
68. Barbieri, R.L., *Female Infertility*. 8th ed. Yen & Jaffe's Reproductive Endocrinology. 2019: Physiology, Pathophysiology, and Clinical Management.
69. Garolla, A., et al., *Practical Clinical and Diagnostic Pathway for the Investigation of the Infertile Couple.* Front Endocrinol (Lausanne), 2020. **11**: p. 591837.
70. Newman, J.E., et al., *Assisted reproductive technology in Australia and New Zealand 2022. Sydney: National Perinatal Epidemiology and Statistics Unit, the University of New South Wales*. 2024.
71. Dafopoulos, K. and B.C. Tarlatzis, *Ovarian stimulation protocols*, in *Management of Infertility*. 2023. p. 199-204.
72. Ovarian Stimulation, T., et al., *ESHRE guideline: ovarian stimulation for IVF/ICSI(dagger).* Hum Reprod Open, 2020. **2020**(2): p. hoaa009.
73. Steptoe, P.C. and R.G. Edwards, *Birth after the reimplantation of a human embryo.* Lancet, 1978. **2**(8085): p. 366.
74. Allersma, T., C. Farquhar, and A.E. Cantineau, *Natural cycle in vitro fertilisation (IVF) for subfertile couples.* Cochrane Database Syst Rev, 2013. **2013**(8): p. CD010550.

75. De Marco, M.P., et al., *Natural Cycle Results in Lower Implantation Failure than Ovarian Stimulation in Advanced-Age Poor Responders Undergoing IVF: Fertility Outcomes from 585 Patients.* Reprod Sci, 2021. **28**(7): p. 1967-1973.
76. Kumar, P., et al., *Ovarian hyperstimulation syndrome.* Journal of Human Reproductive Sciences, 2011. **4**(2): p. 70-75.
77. Wang, N., et al., *Sudden Death Due to Severe Ovarian Hyperstimulation Syndrome: An Autopsy-Centric Case Report.* Am J Forensic Med Pathol, 2021. **42**(1): p. 88-91.
78. Committee, R.T.A., *Code of Practice for Assisted Reproductive Technology Units*, F.S.o. Australia, Editor. 2021. p. 1-24.
79. Transfer, E.G.G.o.t.N.o.E.t., et al., *ESHRE guideline: number of embryos to transfer during IVF/ICSIdagger.* Hum Reprod, 2024. **39**(4): p. 647-657.
80. Newman, J.E., P.C. Repon, and C.M. Chambers, *Assisted reproductive technology in Australia and New Zealand 2021*. 2023, National Perinatal Epidemiology and Statistics Unit: Sydney.
81. Wong, K.M., et al., *Transfer of fresh or frozen embryos: a randomised controlled trial.* Hum Reprod, 2021. **36**(4): p. 998-1006.
82. Roque, M., et al., *Fresh versus elective frozen embryo transfer in IVF/ICSI cycles: a systematic review and meta-analysis of reproductive outcomes.* Hum Reprod Update, 2019. **25**(1): p. 2-14.
83. Ma, J., W. Gao, and D. Li, *Recurrent implantation failure: A comprehensive summary from etiology to treatment.* Front Endocrinol (Lausanne), 2022. **13**: p. 1061766.
84. for the participants to the Lugano, R.I.F.W., et al., *Recurrent implantation failure: reality or a statistical mirage?: Consensus statement from the July 1, 2022 Lugano Workshop on recurrent implantation failure.* Fertil Steril, 2023. **120**(1): p. 45-59.
85. Wilcox, L.S., et al., *Defining and interpreting pregnancy success rates for in vitro fertilization.* Fertility and Sterility, 1993. **60**(1): p. 18-25.
86. Maleki-Hajiagha, A., et al., *Vaginal probiotics as therapeutic adjuncts for improving embryo transfer success rates: a systematic review and meta-analysis.* BMC Pregnancy Childbirth, 2025. **25**(1): p. 262.
87. Ottun, T.A., et al., *Factors Associated with Clinical Pregnancy following Assisted Reproductive Technology: A Comparative Cross-Sectional Study.* J West Afr Coll Surg, 2025. **15**(1): p. 37-43.
88. Guzick, D.S., C. Wilkes, and H.W. Jones, Jr., *Cumulative pregnancy rates for in vitro fertilization.* Fertil Steril, 1986. **46**(4): p. 663-7.
89. Yovich, J.L., J.M. Yovich, and W.R. Edirisinghe, *The relative chance of pregnancy following tubal or uterine transfer procedures.* Fertil Steril, 1988. **49**(5): p. 858-64.
90. Wood, C., et al., *Factors influencing pregnancy rates following in vitro fertilization and embryo transfer.* Fertil Steril, 1985. **43**(2): p. 245-50.
91. Audibert, F., et al., *Results of IVF attempts in patients with unexplained infertility.* Hum Reprod, 1989. **4**(7): p. 766-71.
92. Trounson, A., *Development of in vitro fertilization in Australia.* Fertil Steril, 2018. **110**(1): p. 19-24.
93. Fitzgerald, O., et al., *Assisted reproductive technology in Australia and New Zealand in 2015*. 2017, National Perinatal Epidemiology and Statistics Unit, the University of New South Wales Sydney: Sydney.

94. Chambers, G.M., et al., *International Committee for Monitoring Assisted Reproductive Technologies world report: assisted reproductive technology, 2014dagger.* Hum Reprod, 2021. **36**(11): p. 2921-2934.
95. Zegers-Hochschild, F., et al., *International Committee for Monitoring Assisted Reproductive Technology: world report on assisted reproductive technology, 2005.* Fertil Steril, 2014. **101**(2): p. 366-78.
96. Matorras, R., et al., *Evaluation of costs associated with fertility treatment leading to a live birth after one fresh transfer: A global perspective.* Best Pract Res Clin Obstet Gynaecol, 2023. **89**: p. 102349.
97. Lensen, S., et al., *IVF add-ons in Australia and New Zealand: A systematic assessment of IVF clinic websites.* Aust N Z J Obstet Gynaecol, 2021. **61**(3): p. 430-438.
98. Assaysh-Oberg, S., C. Borneskog, and E. Ternstrom, *Women's experience of infertility & treatment - A silent grief and failed care and support.* Sex Reprod Healthc, 2023. **37**: p. 100879.
99. Ni, Y., et al., *Differences in Fertility-Related Quality of Life and Emotional Status Among Women Undergoing Different IVF Treatment Cycles.* Psychol Res Behav Manag, 2023. **16**: p. 1873-1882.
100. McMahon, C., et al., *What do women undergoing in vitro fertilization (IVF) understand about their chance of IVF success?* Hum Reprod, 2024. **39**(1): p. 130-138.
101. Volgsten, H., A.S. Svanberg, and P. Olsson, *Unresolved grief in women and men in Sweden three years after undergoing unsuccessful in vitro fertilization treatment.* Acta Obstet Gynecol Scand, 2010. **89**(10): p. 1290-7.
102. Peterson, J., et al., *The NIH Human Microbiome Project.* Genome Res, 2009. **19**(12): p. 2317-23.
103. Sola-Leyva, A., et al., *Mapping the entire functionally active endometrial microbiota.* Hum Reprod, 2021. **36**(4): p. 1021-1031.
104. Kaelin, E.A., et al., *Cervicovaginal DNA Virome Alterations Are Associated with Genital Inflammation and Microbiota Composition.* mSystems, 2022. **7**(2): p. e0006422.
105. Han, X., et al., *Endometrial microbial dysbiosis and metabolic alteration promote the development of endometrial cancer.* International journal of gynecology and obstetrics, 2024. **167**(2): p. 810-822.
106. Patel, J.B., *16S rRNA gene sequencing for bacterial pathogen identification in the clinical laboratory.* Molecular diagnosis, 2001. **6**(4): p. 313-321.
107. Caporaso, J.G., et al., *QIIME allows analysis of high-throughput community sequencing data.* Nature Methods, 2010. **7**(5): p. 335-336.
108. Estaki, M., et al., *QIIME 2 Enables Comprehensive End-to-End Analysis of Diverse Microbiome Data and Comparative Studies with Publicly Available Data.* Curr Protoc Bioinformatics, 2020. **70**(1): p. e100.
109. Cassol, I., M. Ibanez, and J.P. Bustamante, *Key features and guidelines for the application of microbial alpha diversity metrics.* Sci Rep, 2025. **15**(1): p. 622.
110. O'Callaghan, J.L., et al., *Limitations of 16S rRNA Gene Sequencing to Characterize Lactobacillus Species in the Upper Genital Tract.* Front Cell Dev Biol, 2021. **9**: p. 641921.
111. Graspeuntner, S., et al., *Selection of validated hypervariable regions is crucial in 16S-based microbiota studies of the female genital tract.* Sci Rep, 2018. **8**(1): p. 9678.

112. Berman, H.L., M.R. McLaren, and B.J. Callahan, *Understanding and interpreting community sequencing measurements of the vaginal microbiome.* BJOG, 2020. **127**(2): p. 139-146.
113. Liu, F., et al., *Comparative metagenomic analysis of the vaginal microbiome in healthy women.* Synth Syst Biotechnol, 2021. **6**(2): p. 77-84.
114. Salas-Espejo, E., et al., *Exploring the Microbiome in Human Reproductive Tract: High-Throughput Methods for the Taxonomic Characterization of Microorganisms.* Semin Reprod Med, 2023. **41**(5): p. 125-143.
115. Lagier, J.C., et al., *Culturing the human microbiota and culturomics.* Nat Rev Microbiol, 2018. **16**: p. 540-550.
116. Cariati, F., et al., *Endometrial microbiota profile in in-vitro fertilization (IVF) patients by culturomics-based analysis.* Front Endocrinol (Lausanne), 2023. **14**: p. 1204729.
117. Döderlein, A., *Das Scheidensekret und seine Bedeutung für das Puerperalfieber*. 1892, Germany: Besold, 1892.
118. Butler, B.C. and J.W. Beakley, *Bacterial flora in vaginitis: a study before and after treatment with pure cultures of Doederlein bacillus.* Am J Obstet Gynecol, 1960. **79**: p. 432-40.
119. Mirmonsef, P., et al., *Free glycogen in vaginal fluids is associated with Lactobacillus colonization and low vaginal pH.* PLoS One, 2014. **9**(7): p. e102467.
120. Navarro, S., et al., *Glycogen availability and pH variation in a medium simulating vaginal fluid influence the growth of vaginal Lactobacillus species and Gardnerella vaginalis.* BMC Microbiol, 2023. **23**(1): p. 186.
121. Miller, E.A., et al., *Lactobacilli Dominance and Vaginal pH: Why Is the Human Vaginal Microbiome Unique?* Front Microbiol, 2016. **7**: p. 1936.
122. Kaur, H., et al., *Crosstalk Between Female Gonadal Hormones and Vaginal Microbiota Across Various Phases of Women's Gynecological Lifecycle.* Front Microbiol, 2020. **11**: p. 551.
123. Shen, J., et al., *Effects of low dose estrogen therapy on the vaginal microbiomes of women with atrophic vaginitis.* Sci Rep, 2016. **6**: p. 24380.
124. Reid, G., et al., *Identification and plasmid profiles of Lactobacillus species from the vagina of 100 healthy women.* FEMS Immunol Med Microbiol, 1996. **15**(1): p. 23-6.
125. Kim, T.K., et al., *Heterogeneity of vaginal microbial communities within individuals.* J Clin Microbiol, 2009. **47**(4): p. 1181-9.
126. Ravel, J., et al., *Vaginal microbiome of reproductive-age women.* Proc Natl Acad Sci U S A, 2011. **108 Suppl 1**(Suppl 1): p. 4680-7.
127. Gajer, P., et al., *Temporal dynamics of the human vaginal microbiota.* Sci Transl Med, 2012. **4**(132): p. 132ra52.
128. France, M.T., et al., *VALENCIA: a nearest centroid classification method for vaginal microbial communities based on composition.* Microbiome, 2020. **8**(1): p. 166.
129. Lebeer, S., et al., *A citizen-science-enabled catalogue of the vaginal microbiome and associated factors.* Nat Microbiol, 2023. **8**(11): p. 2183-2195.
130. Qin, L., et al., *Population-level analyses identify host and environmental variables influencing the vaginal microbiome.* Signal Transduct Target Ther, 2025. **10**(1): p. 64.
131. Holm, J.B., et al., *Integrating compositional and functional content to describe vaginal microbiomes in health and disease.* Microbiome, 2023. **11**(1): p. 259.

132. Petersen, C. and J.L. Round, *Defining dysbiosis and its influence on host immunity and disease.* Cell Microbiol, 2014. **16**(7): p. 1024-33.
133. Lev-Sagie, A., et al., *The Vaginal Microbiome: II. Vaginal Dysbiotic Conditions.* J Low Genit Tract Dis, 2022. **26**(1): p. 79-84.
134. Nugent, R.P., M.A. Krohn, and S.L. Hillier, *Reliability of diagnosing bacterial vaginosis is improved by a standardized method of gram stain interpretation.* J Clin Microbiol, 1991. **29**(2): p. 297-301.
135. Amsel, R., et al., *Nonspecific vaginitis. Diagnostic criteria and microbial and epidemiologic associations.* Am J Med, 1983. **74**(1): p. 14-22.
136. Srinivasan, S., et al., *Bacterial communities in women with bacterial vaginosis: high resolution phylogenetic analyses reveal relationships of microbiota to clinical criteria.* PLoS One, 2012. **7**(6): p. e37818.
137. Fredricks, D.N., T.L. Fiedler, and J.M. Marrazzo, *Molecular identification of bacteria associated with bacterial vaginosis.* N Engl J Med, 2005. **353**(18): p. 1899-911.
138. Dos Santos, S.J., et al., *Vaginal metatranscriptome meta-analysis reveals functional BV subgroups and novel colonisation strategies.* Microbiome, 2024. **12**(1): p. 271.
139. Brochu, H.N., et al., *Characterization of vaginal microbiomes in clinician-collected bacterial vaginosis diagnosed samples.* Microbiol Spectr, 2025: p. e0258224.
140. Allsworth, J.E. and J.F. Peipert, *Severity of bacterial vaginosis and the risk of sexually transmitted infection.* Am J Obstet Gynecol, 2011. **205**(2): p. 113 e1-6.
141. Atashili, J., et al., *Bacterial vaginosis and HIV acquisition: a meta-analysis of published studies.* AIDS, 2008. **22**(12): p. 1493-501.
142. Turpin, R., et al., *Bacterial Vaginosis and Behavioral Factors Associated With Incident Pelvic Inflammatory Disease in the Longitudinal Study of Vaginal Flora.* J Infect Dis, 2021. **224**(12 Suppl 2): p. S137-S144.
143. Ichiyama, T., et al., *Analysis of vaginal and endometrial microbiota communities in infertile women with a history of repeated implantation failure.* Reprod Med Biol, 2021. **20**(3): p. 334-344.
144. Kong, Y., et al., *The Disordered Vaginal Microbiota Is a Potential Indicator for a Higher Failure of in vitro Fertilization.* Front Med (Lausanne), 2020. **7**: p. 217.
145. Donders, G.G., et al., *Definition of a type of abnormal vaginal flora that is distinct from bacterial vaginosis: aerobic vaginitis.* BJOG, 2002. **109**(1): p. 34-43.
146. Wang, C., et al., *Vaginal bacterial profiles of aerobic vaginitis: a case-control study.* Diagn Microbiol Infect Dis, 2020. **96**(4): p. 114981.
147. Fan, A., et al., *Aerobic vaginitis and mixed infections: comparison of clinical and laboratory findings.* Arch Gynecol Obstet, 2013. **287**(2): p. 329-35.
148. Donders, G.G., et al., *Predictive value for preterm birth of abnormal vaginal flora, bacterial vaginosis and aerobic vaginitis during the first trimester of pregnancy.* BJOG, 2009. **116**(10): p. 1315-24.
149. Hassan, M.F., et al., *Does Aerobic Vaginitis Have Adverse Pregnancy Outcomes? Prospective Observational Study.* Infect Dis Obstet Gynecol, 2020. **2020**: p. 5842150.
150. Han, C., et al., *Aerobic vaginitis in late pregnancy and outcomes of pregnancy.* Eur J Clin Microbiol Infect Dis, 2019. **38**(2): p. 233-239.

151. Nguyen, A.T.C., et al., *Aerobic vaginitis in the third trimester and its impact on pregnancy outcomes.* BMC Pregnancy Childbirth, 2022. **22**(1): p. 432.
152. Boskey, E.R., et al., *Origins of vaginal acidity: high D/L lactate ratio is consistent with bacteria being the primary source.* Hum Reprod, 2001. **16**(9): p. 1809-13.
153. Witkin, S.S., et al., *Influence of vaginal bacteria and D- and L-lactic acid isomers on vaginal extracellular matrix metalloproteinase inducer: implications for protection against upper genital tract infections.* mBio, 2013. **4**(4): p. e00460-13.
154. de Magalhães, C.C.B., et al., *Comparative measurement of D- and L-lactic acid isomers in vaginal secretions: association with high-grade cervical squamous intraepithelial lesions.* Archives of Gynecology and Obstetrics, 2022. **305**(2): p. 373-377.
155. Zalambani, C., et al., *Role of D(-)-Lactic Acid in Prevention of Chlamydia trachomatis Infection in an In Vitro Model of HeLa Cells.* Pathogens, 2023. **12**(7).
156. O'Hanlon, D.E., T.R. Moench, and R.A. Cone, *Vaginal pH and microbicidal lactic acid when lactobacilli dominate the microbiota.* PLoS One, 2013. **8**(11): p. e80074.
157. O'Hanlon, D.E., R.A. Come, and T.R. Moench, *Vaginal pH measured in vivo: lactobacilli determine pH and lactic acid concentration.* BMC Microbiol, 2019. **19**(1): p. 13.
158. Gong, Z., et al., *Lactobacilli inactivate Chlamydia trachomatis through lactic acid but not H2O2.* PLoS One, 2014. **9**(9): p. e107758.
159. Tyssen, D., et al., *Anti-HIV-1 Activity of Lactic Acid in Human Cervicovaginal Fluid.* mSphere, 2018. **3**(4).
160. Hearps, A.C., et al., *Vaginal lactic acid elicits an anti-inflammatory response from human cervicovaginal epithelial cells and inhibits production of pro-inflammatory mediators associated with HIV acquisition.* Mucosal Immunol, 2017. **10**(6): p. 1480-1490.
161. Delgado-Diaz, D.J., et al., *Lactic acid from vaginal microbiota enhances cervicovaginal epithelial barrier integrity by promoting tight junction protein expression.* Microbiome, 2022. **10**(1): p. 141.
162. Horrocks, V., et al., *Nuclear Magnetic Resonance Metabolomics of Symbioses between Bacterial Vaginosis-Associated Bacteria.* mSphere, 2022. **7**(3): p. e0016622.
163. Ceccarani, C., et al., *Diversity of vaginal microbiome and metabolome during genital infections.* Sci Rep, 2019. **9**(1): p. 14095.
164. Srinivasan, S., et al., *Metabolic signatures of bacterial vaginosis.* mBio, 2015. **6**(2): p. e00204-15.
165. Nelson, T.M., et al., *Vaginal biogenic amines: biomarkers of bacterial vaginosis or precursors to vaginal dysbiosis?* Front Physiol, 2015. **6**: p. 253.
166. Vitali, B., et al., *Vaginal microbiome and metabolome highlight specific signatures of bacterial vaginosis.* Eur J Clin Microbiol Infect Dis, 2015. **34**(12): p. 2367-76.
167. Mirmonsef, P., et al., *Short-chain fatty acids induce pro-inflammatory cytokine production alone and in combination with toll-like receptor ligands.* Am J Reprod Immunol, 2012. **67**(5): p. 391-400.
168. Delgado-Diaz, D.J., et al., *Distinct Immune Responses Elicited From Cervicovaginal Epithelial Cells by Lactic Acid and Short Chain Fatty Acids*

Associated With Optimal and Non-optimal Vaginal Microbiota. Front Cell Infect Microbiol, 2019. **9**: p. 446.
169. Schwecht, I., et al., *Lactic acid enhances vaginal epithelial barrier integrity and ameliorates inflammatory effects of dysbiotic short chain fatty acids and HIV-1.* Sci Rep, 2023. **13**(1): p. 20065.
170. Teisala, K., *Endometrial microbial flora of hysterectomy specimens.* Eur J Obstet Gynecol Reprod Biol, 1987. **26**(2): p. 151-5.
171. Sturgis, S.H., *The cervix and uterus in sterility.* Fertil Steril, 1956. **7**(5): p. 468-84.
172. Ansbacher, R., W.A. Boyson, and J.A. Morris, *Sterility of the uterine cavity.* Am J Obstet Gynecol, 1967. **99**(3): p. 394-6.
173. Moller, B.R., et al., *Sterility of the uterine cavity.* Acta Obstet Gynecol Scand, 1995. **74**(3): p. 216-9.
174. Mitchell, C.M., et al., *Colonization of the upper genital tract by vaginal bacterial species in nonpregnant women.* Am J Obstet Gynecol, 2015. **212**(5): p. 611 e1-9.
175. Verstraelen, H., et al., *Characterisation of the human uterine microbiome in non-pregnant women through deep sequencing of the V1-2 region of the 16S rRNA gene.* PeerJ, 2016. **4**: p. e1602.
176. Chen, C., et al., *The microbiota continuum along the female reproductive tract and its relation to uterine-related diseases.* Nat Commun, 2017. **8**(1): p. 875.
177. Reschini, M., et al., *Endometrial microbiome: sampling, assessment, and possible impact on embryo implantation.* Sci Rep, 2022. **12**(1): p. 8467.
178. Moreno, I., et al., *Evidence that the endometrial microbiota has an effect on implantation success or failure.* Am J Obstet Gynecol, 2016. **215**(6): p. 684-703.
179. Franasiak, J.M., et al., *Endometrial microbiome at the time of embryo transfer: next-generation sequencing of the 16S ribosomal subunit.* J Assist Reprod Genet, 2016. **33**(1): p. 129-36.
180. Moreno, I., et al., *Endometrial microbiota composition is associated with reproductive outcome in infertile patients.* Microbiome, 2022. **10**(1): p. 1.
181. Peng, S., et al., *Human embryo implantation: The complex interplay between endometrial receptivity and the microbiome.* J Reprod Immunol, 2025. **168**: p. 104440.
182. Moreno, I., et al., *The first glimpse of the endometrial microbiota in early pregnancy.* Am J Obstet Gynecol, 2020. **222**(4): p. 296-305.
183. Tao, X., et al., *Characterizing the endometrial microbiome by analyzing the ultra-low bacteria from embryo transfer catheter tips in IVF cycles: Next generation sequencing (NGS) analysis of the 16S ribosomal gene.* Human Microbiome Journal, 2017. **3**: p. 15-21.
184. Garcia-Grau, I., C. Simon, and I. Moreno, *Uterine microbiome—low biomass and high expectations.* Biology of Reproduction, 2018. **101**(6): p. 1102-1114.
185. Swidsinski, A., et al., *Presence of a polymicrobial endometrial biofilm in patients with bacterial vaginosis.* PLoS One, 2013. **8**(1): p. e53997.
186. Sirichoat, A., et al., *Comparison of different hypervariable regions of 16S rRNA for taxonomic profiling of vaginal microbiota using next-generation sequencing.* Arch Microbiol, 2021. **203**(3): p. 1159-1166.
187. Kadogami, D., Y. Nakaoka, and Y. Morimoto, *Use of a vaginal probiotic suppository and antibiotics to influence the composition of the endometrial microbiota.* Reprod Biol, 2020. **20**(3): p. 307-314.

188. Vomstein, K., et al., *Uterine microbiota plasticity during the menstrual cycle: Differences between healthy controls and patients with recurrent miscarriage or implantation failure.* J Reprod Immunol, 2022. **151**: p. 103634.
189. DiGiulio, D.B., et al., *Temporal and spatial variation of the human microbiota during pregnancy.* Proc Natl Acad Sci U S A, 2015. **112**(35): p. 11060-5.
190. MacIntyre, D.A., et al., *The vaginal microbiome during pregnancy and the postpartum period in a European population.* Sci Rep, 2015. **5**: p. 8988.
191. Serrano, M.G., et al., *Racioethnic diversity in the dynamics of the vaginal microbiome during pregnancy.* Nat Med, 2019. **25**(6): p. 1001-1011.
192. Li, D., et al., *Vaginal microbiome analysis of healthy women during different periods of gestation.* Biosci Rep, 2020. **40**(7).
193. Li, K.T., et al., *Changes in the Vaginal Microbiome During Pregnancy and the Postpartum Period in South African Women: a Longitudinal Study.* Reprod Sci, 2024. **31**(1): p. 275-287.
194. Freitas, A.C., et al., *The vaginal microbiome of pregnant women is less rich and diverse, with lower prevalence of Mollicutes, compared to non-pregnant women.* Sci Rep, 2017. **7**(1): p. 9212.
195. Odogwu, N.M., et al., *Lactobacillus crispatus thrives in pregnancy hormonal milieu in a Nigerian patient cohort.* Sci Rep, 2021. **11**(1): p. 18152.
196. Siiteri, P.K. and P.C. MacDonald, *Placental estrogen biosynthesis during human pregnancy.* J Clin Endocrinol Metab, 1966. **26**(7): p. 751-61.
197. Nunn, K.L., et al., *Changes in the Vaginal Microbiome during the Pregnancy to Postpartum Transition.* Reprod Sci, 2021. **28**(7): p. 1996-2005.
198. Leoni, C., et al., *Human Endometrial Microbiota at Term of Normal Pregnancies.* Genes (Basel), 2019. **10**(12): p. 1-11.
199. Leitich, H., et al., *Bacterial vaginosis as a risk factor for preterm delivery: a meta-analysis.* Am J Obstet Gynecol, 2003. **189**(1): p. 139-47.
200. Hyman, R.W., et al., *The dynamics of the vaginal microbiome during infertility therapy with in vitro fertilization-embryo transfer.* J Assist Reprod Genet, 2012. **29**(2): p. 105-15.
201. Haahr, T., et al., *Abnormal vaginal microbiota may be associated with poor reproductive outcomes: a prospective study in IVF patients.* Hum Reprod, 2016. **31**(4): p. 795-803.
202. Vladislavovna, B.V., et al., *Microbiome of the Uterus in Women With Unsuccessful in Vitro Fertilization Attempts.* International Journal of Women's Health and Reproduction Sciences, 2020. **8**(4): p. 423-427.
203. Kitaya, K., et al., *Characterization of Microbiota in Endometrial Fluid and Vaginal Secretions in Infertile Women with Repeated Implantation Failure.* Mediators Inflamm, 2019. **2019**: p. 4893437.
204. Garcia-Grau, I., et al., *Taxonomical and Functional Assessment of the Endometrial Microbiota in A Context of Recurrent Reproductive Failure: A Case Report.* Pathogens, 2019. **8**(4): p. 205.
205. Su, W., et al., *Vaginal and endometrial microbiome dysbiosis associated with adverse embryo transfer outcomes.* Reprod Biol Endocrinol, 2024. **22**(1): p. 111.
206. Kyono, K., et al., *A pilot study and case reports on endometrial microbiota and pregnancy outcome: An analysis using 16S rRNA gene sequencing among IVF patients, and trial therapeutic intervention for dysbiotic endometrium.* Reprod Med Biol, 2019. **18**(1): p. 72-82.

207. Riganelli, L., et al., *Structural Variations of Vaginal and Endometrial Microbiota: Hints on Female Infertility.* Front Cell Infect Microbiol, 2020. **10**: p. 350.
208. Wei, Q., et al., *Impact of vaginal microecological differences on pregnancy outcomes and endometrial microbiota in frozen embryo transfer cycles.* J Assist Reprod Genet, 2024. **41**(4): p. 929-938.
209. Bailén, M., et al., *Bioinformatic strategies to address limitations of 16rRNA short-read amplicons from different sequencing platforms.* Journal of Microbiological Methods, 2020. **169**: p. 105811.
210. Bednarska-Czerwińska, A., et al., *Marking the Profile of the Microflora of the Endometrium and Uterine Cervix in Women as a Potential Factor Determining the Effectiveness of In Vitro Fertilization.* Journal of Clinical Medicine, 2022. **11**(12): p. 3348.
211. Fujii, S. and T. Oguchi, *Age- and endometrial microbiota-related delay in development of endometrial receptivity.* Reprod Med Biol, 2023. **22**(1): p. e12523.
212. Chen, P., et al., *Interaction between endometrial microbiota and host gene regulation in recurrent implantation failure.* Journal of Assisted Reproduction and Genetics, 2022. **39**(9): p. 2169-2178.
213. Zhang, R., et al., *Altered Endometrial Microbiota Profile Is Associated With Poor Endometrial Receptivity of Repeated Implantation Failure.* Am J Reprod Immunol, 2024. **92**(5): p. e70005.
214. Cela, V., et al., *Endometrial Dysbiosis Is Related to Inflammatory Factors in Women with Repeated Implantation Failure: A Pilot Study.* J Clin Med, 2022. **11**(9).
215. Chen, P., et al., *Endometrial microbial alterations disrupt endometrial immune homeostasis by overactivation of Eicosapentaenoic acid biosynthesis leading to altered endometrial receptivity.* J Reprod Immunol, 2023. **155**: p. 103787.
216. Chen, P., et al., *Interaction Between Chronic Endometritis Caused Endometrial Microbiota Disorder and Endometrial Immune Environment Change in Recurrent Implantation Failure.* Front Immunol, 2021. **12**: p. 748447.
217. Satokata, I., G. Benson, and R. Maas, *Sexually dimorphic sterility phenotypes in Hoxa10-deficient mice.* Nature, 1995. **374**(6521): p. 460-3.
218. Daikoku T, et al., *Uterine Msx-1 and Wnt4 Signaling Becomes Aberrant in Mice with the Loss of Leukemia Inhibitory Factor or Hoxa-10: Evidence for a Novel Cytokine-Homeobox-Wnt Signaling in Implantation.* Molecular Endocrinology., 2004. **18**: p. 1238-1250.
219. Lim, H.J. and S.K. Dey, *HB-EGF: a unique mediator of embryo-uterine interactions during implantation.* Exp Cell Res, 2009. **315**(4): p. 619-26.
220. Wang, H. and S.K. Dey, *Roadmap to embryo implantation: clues from mouse models.* Nat Rev Genet, 2006. **7**(3): p. 185-99.
221. Stewart, C.L., et al., *Blastocyst implantation depends on maternal expression of leukaemia inhibitory factor.* Nature, 1992. **359**(6390): p. 76-9.
222. Paulson, E.E. and P. Comizzoli, *Endometrial receptivity and embryo implantation in carnivores—commonalities and differences with other mammalian species.* Biology of reproduction, 2021. **104**(4): p. 771-783.
223. Wolfarth, A.A., et al., *A Human Microbiota-Associated Murine Model for Assessing the Impact of the Vaginal Microbiota on Pregnancy Outcomes.* Front Cell Infect Microbiol, 2020. **10**: p. 570025.

224. Mejia, M.E., et al., *Vaginal microbial dynamics and pathogen colonization in a humanized microbiota mouse model.* NPJ Biofilms Microbiomes, 2023. **9**(1): p. 87.
225. Maqsood, M.I., et al., *Immortality of cell lines: challenges and advantages of establishment.* Cell Biol Int, 2013. **37**(10): p. 1038-45.
226. Nishida, M., *The Ishikawa Cells from Birth to the Present.* Human Cell, 2002. **15**(3): p. 104-117.
227. Nishida M, et al., *Establishment of a new human endometrial adenocarcinoma cell line, Ishikawa cells, containing estrogen and progesterone receptors.* Japan Society of Obstetrics and Gynecology, 1985. **37**(7): p. 1103-1111.
228. Way, D.L., et al., *Characterization of a new human endometrial carcinoma (RL95-2) established in tissue culture.* In Vitro, 1983. **19**(3): p. 147-158.
229. Hannan, N.J., et al., *Models for Study of Human Embryo Implantation: Choice of Cell Lines?* Biology of Reproduction, 2010. **82**(2): p. 235-245.
230. Sundareshan, P. and M.J.C. Hendrix, *Growth, morphologic, and invasive characteristics of early and late passages of a human endometrial carcinoma cell line (RL95-2).* In Vitro Cellular & Developmental Biology - Animal, 1992. **28**(7-8): p. 544-552.
231. Maldonado-Estrada, J., et al., *Evaluation of Cytokeratin 7 as an accurate intracellular marker with which to assess the purity of human placental villous trophoblast cells by flow cytometry.* Journal of immunological methods, 2004. **286**(1): p. 21-34.
232. Hamada, A.L., et al., *Transfection of Antisense Chorionic Gonadotropin β Gene into Choriocarcinoma Cells Suppresses the Cell Proliferation and Induces Apoptosis.* The journal of clinical endocrinology and metabolism, 2005. **90**(8): p. 4873-4879.
233. White, T.E., et al., *Human choriocarcinoma (JAr) cells grown as multicellular spheroids.* Placenta, 1988. **9**(6): p. 583-598.
234. Wang, H., et al., *A novel model of human implantation: 3D endometrium-like culture system to study attachment of human trophoblast (Jar) cell spheroids.* Molecular Human Reproduction, 2012. **18**(1): p. 33-43.
235. Buckley, R.J., et al., *Macrophage polarisation affects their regulation of trophoblast behaviour.* Placenta, 2016. **47**: p. 73-80.
236. Mikhailova, V., et al., *Pro- and Anti-Inflammatory Cytokines in the Context of NK Cell-Trophoblast Interactions.* Int J Mol Sci, 2022. **23**(4).
237. Mikhailova, V., et al., *NK-92 cells change their phenotype and function when cocultured with IL-15, IL-18 and trophoblast cells.* Immunobiology, 2021. **226**(5): p. 152125.
238. Aldo, P.B., et al., *Effect of culture conditions on the phenotype of THP-1 monocyte cell line.* Am J Reprod Immunol, 2013. **70**(1): p. 80-6.
239. Maki, G., et al., *Factors regulating the cytotoxic activity of the human natural killer cell line, NK-92.* Journal of hematotherapy & stem cell research, 2001. **10**(3): p. 369-383.
240. Dimova, T., et al., *The modeling of human implantation and early placentation: achievements and perspectives.* Hum Reprod Update, 2025. **31**(2): p. 133-163.
241. Heidari-Khoei, H., et al., *Derivation of hormone-responsive human endometrial organoids and stromal cells from cryopreserved biopsies.* Experimental Cell Research, 2022. **417**(1): p. 113205.
242. Ahn, J., et al., *Three-dimensional microengineered vascularised endometrium-on-a-chip.* Hum Reprod, 2021. **36**(10): p. 2720-2731.

243. Gnecco, J.S., et al., *Hemodynamic forces enhance decidualization via endothelial-derived prostaglandin E2 and prostacyclin in a microfluidic model of the human endometrium.* Hum Reprod, 2019. **34**(4): p. 702-714.
244. Murphy, A.R., H. Campo, and J.J. Kim, *Strategies for modelling endometrial diseases.* Nature Reviews Endocrinology, 2022. **18**(12): p. 727-743.
245. Lund, M.E., et al., *The choice of phorbol 12-myristate 13-acetate differentiation protocol influences the response of THP-1 macrophages to a pro-inflammatory stimulus.* J Immunol Methods, 2016. **430**: p. 64-70.
246. Kotzur, R., et al., *NK-92 cells retain vitality and functionality when grown in standard cell culture conditions.* PLOS ONE, 2022. **17**(3): p. e0264897.
247. Shibata, S., et al., *Modeling embryo-endometrial interface recapitulating human embryo implantation.* Science Advances, 2024. **10**(8): p. eadi4819.
248. Chen, C., et al., *3D-printed microfluidic devices: fabrication, advantages and limitations—a mini review.* Analytical Methods, 2016. **8**(31): p. 6005-6012.
249. Voloshin, N., et al., *Practical Use of Immortalized Cells in Medicine: Current Advances and Future Perspectives.* Int J Mol Sci, 2023. **24**(16).
250. Jiang, Y., et al., *Proof-of-Concept for Long-Term Human Endometrial Epithelial Organoids in Modeling Menstrual Cycle Responses.* Cells, 2024. **13**(21): p. 1811.
251. Luddi, A., et al., *Organoids of Human Endometrium: A Powerful In Vitro Model for the Endometrium-Embryo Cross-Talk at the Implantation Site.* Cells, 2020. **9**(5): p. 1121.
252. Ho, H., et al., *A high-throughput in vitro model of human embryo attachment.* Fertility and Sterility, 2012. **97**(4): p. 974-8.
253. Turco, M.Y., et al., *Long-term, hormone-responsive organoid cultures of human endometrium in a chemically defined medium.* Nature Cell Biology, 2017. **19**(5): p. 568-577.
254. Ahmad, V., et al., *Development of polarity-reversed endometrial epithelial organoids.* Reproduction, 2024. **167**(3): p. e230478.
255. Chalak, M., et al., *Cell Immortality: In Vitro Effective Techniques to Achieve and Investigate Its Applications and Challenges.* Life (Basel), 2024. **14**(3).
256. van Meer, B.J., et al., *Small molecule absorption by PDMS in the context of drug response bioassays.* Biochem Biophys Res Commun, 2017. **482**(2): p. 323-328.
257. Fitzgerald, H.C., D.J. Schust, and T.E. Spencer, *In vitro models of the human endometrium: evolution and application for women's health+.* Biology of Reproduction, 2020. **104**(2): p. 282-293.
258. Luongo, F.P., et al., *Modeling the window of implantation: insights from endometrial biopsy and menstrual blood-derived organoids and endometrial stromal cells.* Human Reproduction Open, 2025. **2025**(4).
259. Cindrova-Davies, T., et al., *Menstrual flow as a non-invasive source of endometrial organoids.* Communications Biology, 2021. **4**(1): p. 651.
260. Rodríguez, C.F., et al., *Breaking the clean room barrier: exploring low-cost alternatives for microfluidic devices.* Front Bioeng Biotechnol, 2023. **11**: p. 1176557.
261. Korch, C., et al., *DNA profiling analysis of endometrial and ovarian cell lines reveals misidentification, redundancy and contamination.* Gynecologic Oncology, 2012. **127**(1): p. 241-248.
262. Leonovich, O.A., *Mycoplasma: Properties, Detection, and Decontamination Methods of Cell Cultures and Viral Strains (Review).* Applied Biochemistry and Microbiology, 2024. **60**(5): p. 785-793.

263. Hibaoui, Y. and A. Feki, *Organoid Models of Human Endometrial Development and Disease.* Frontiers in Cell and Developmental Biology, 2020. **Volume 8 - 2020**.
264. Regehr, K.J., et al., *Biological implications of polydimethylsiloxane-based microfluidic cell culture.* Lab Chip, 2009. **9**(15): p. 2132-9.
265. Zhao, Z., et al., *Organoids.* Nature Reviews Methods Primers, 2022. **2**(1): p. 94.
266. Harper, J.M., *Primary Cell Culture as a Model System for Evolutionary Molecular Physiology.* Int J Mol Sci, 2024. **25**(14).
267. Alzamil L, Nikolakopoulou K, and Turco MY, *Organoid systems to study the human female reproductive tract and pregnancy.* Cell Death & Differentiation, 2021. **28**: p. 35-51.
268. Li, Q., et al., *Human uterine natural killer cells regulate differentiation of extravillous trophoblast early in pregnancy.* Cell Stem Cell, 2024. **31**(2): p. 181-195.e9.
269. Zych, M.L., et al., *Decidual natural killer cells promote extravillous trophoblast developmental pathways: evidence from trophoblast organoid co-cultures*. 2024, Cold Spring Harbor Laboratory.
270. Wu, Z.M., et al., *Pro-inflammatory cytokine-stimulated first trimester decidual cells enhance macrophage-induced apoptosis of extravillous trophoblasts.* Placenta, 2012. **33**(3): p. 188-94.
271. Zhang, X., et al., *Investigating bacteria-induced inflammatory responses using novel endometrial epithelial gland organoid models.* Frontiers in Reproductive Health, 2024. **6**.
272. Zhang, X., et al., *Comparative analysis of organoid, air-liquid interface, and direct infection models for studying pathogen-host interactions in endometrial tissue.* Sci Rep, 2025. **15**(1): p. 8531.
273. Xiao S, et al., *A microfluidic culture model of the human reproductive tract and 28-day menstrual cycle.* Nature Communications, 2017. **8**: p. 1-13.
274. Busch, C., et al., *Functional, patient-derived 3D tri-culture models of the uterine wall in a microfluidic array.* Human Reproduction, 2024. **39**(11): p. 2537-2550.
275. Cho, H., et al., *A PDMS-Based Interdigitated Platform for Trophoblast Invasion Study Under Oxygen Stress Conditions.* BioChip Journal, 2021. **15**(4): p. 362-370.
276. Richardson, L.S., et al., *Modeling ascending infection with a feto-maternal interface organ-on-chip.* Lab Chip, 2020. **20**(23): p. 4486-4501.
277. Richardson, L.S., et al., *Testing of drugs using human feto-maternal interface organ-on-chips provide insights into pharmacokinetics and efficacy.* Lab Chip, 2022. **22**(23): p. 4574-4592.
278. Richardson, L., et al., *A Microphysiological Device to Model the Choriodecidual Interface Immune Status during Pregnancy.* J Immunol, 2023. **210**(9): p. 1437-1446.
279. Sood, A., et al., *Translational Nanomedicines Across Human Reproductive Organs Modeling on Microfluidic Chips: State-of-the-Art and Future Prospects.* ACS Biomaterials Science & Engineering, 2023. **9**(1): p. 62-84.
280. Zahra, A., et al., *Validation of vaginal microbiome proxies for in vitro experiments that biomimic Lactobacillus-dominant vaginal cultures.* American journal of reproductive immunology (1989), 2023. **90**(6): p. e13797-n/a.
281. Mahajan, G., et al., *Vaginal microbiome-host interactions modeled in a human vagina-on-a-chip.* Microbiome, 2022. **10**(1): p. 201.

282. Yu, B., et al., *Vaginal Bacteria Elicit Acute Inflammatory Response in Fallopian Tube Organoids.* Reproductive Sciences, 2024. **31**(2): p. 505-513.
283. Gurner, K.H., et al., *A microenvironment of high lactate and low pH created by the blastocyst promotes endometrial receptivity and implantation.* Reprod Biomed Online, 2022. **44**(1): p. 14-26.
284. Fu, M., et al., *Alterations in Vaginal Microbiota and Associated Metabolome in Women with Recurrent Implantation Failure.* mBio, 2020. **11**(3): p. e03242-19.
285. Nishio, E., et al., *Metabolomic and microbiome analysis of cervicovaginal mucus in in vitro fertilization-embryo transfer: Toward predicting pregnancy success.* Reprod Med Biol, 2024. **23**(1): p. e12568.
286. Chenoll, E., et al., *Selection of New Probiotics for Endometrial Health.* Front Cell Infect Microbiol, 2019. **9**: p. 114.
287. Mirmonsef P, et al., *The Effects of Commensal Bacteria on Innate Immune Responses in the Female Genital Tract.* American Journal of Reproductive Immunology, 2011. **65**: p. 190-195.
288. Chaudry, A.N., et al., *Analysis of vaginal acetic acid in patients undergoing treatment for bacterial vaginosis.* J Clin Microbiol, 2004. **42**(11): p. 5170-5.
289. Al-Mushrif, S., A. Eley, and B.M. Jones, *Inhibition of chemotaxis by organic acids from anaerobes may prevent a purulent response in bacterial vaginosis.* Journal of medical microbiology, 2000. **49**(11): p. 1023-1030.
290. Vergaro, P., et al., *Transcriptomic analysis of the interaction of choriocarcinoma spheroids with receptive vs. non-receptive endometrial epithelium cell lines: an in vitro model for human implantation.* J Assist Reprod Genet, 2019. **36**(5): p. 857-873.
291. Castelbaum, A.J., et al., *Characterization of Integrin Expression in a Well Differentiated Endometrial Adenocarcinoma Cell Line (Ishikawa)*.* The Journal of Clinical Endocrinology & Metabolism, 1997. **82**(1): p. 136-142.
292. John, N.J., M. Linke, and H.W. Denker, *Quantitation of human choriocarcinoma spheroid attachment to uterine epithelial cell monolayers.* In Vitro Cell Dev Biol Anim, 1993. **29**(6): p. 461-8.
293. Sakkas, D., et al., *A soluble molecule secreted by human blastocysts modulates regulation of HOXA10 expression in an epithelial endometrial cell line.* Fertility and Sterility, 2003. **80**(5): p. 1169-1174.
294. Ran, J., et al., *ZEB1 modulates endometrial receptivity through epithelial-mesenchymal transition in endometrial epithelial cells in vitro.* Biochemical and Biophysical Research Communications, 2020. **525**(3): p. 699-705.
295. Bi, Y., et al., *HOXA10 improves endometrial receptivity by upregulating E-cadherin.* Biol Reprod, 2022. **106**(5): p. 992-999.
296. Lei, C.X., et al., *Interactions between galectin-3 and integrin 3 in regulating endometrial cell proliferation and adhesion.* Human reproduction (Oxford), 2009. **24**(11): p. 2879-2889.
297. Pattillo, R., et al., *The JAR cell line: continuous human multihormone production and controls. In vitro*, 1971. **6**(5): p. 398-399.
298. Hohn, H.-P., M. Linke, and H.-W. Denker, *Adhesion of trophoblast to uterine epithelium as related to the state of trophoblast differentiation: In vitro studies using cell lines.* Molecular Reproduction and Development, 2000. **57**(2): p. 135-145.
299. Tinel, H., H.-W. Denker, and M. Thie, *Calcium influx in human uterine epithelial RL95-2 cells triggers adhesiveness for trophoblast-like cells. Model*

studies on signalling events during embryo implantation. Molecular Human Reproduction, 2000. **6**(12): p. 1119-1130.
300. John, N.J., M. Linke, and H.-W. Denker, *Quantitation of human choriocarcinoma spheroid attachment to uterine epithelial cell monolayers.* In Vitro Cellular & Developmental Biology-Animal, 1993. **29**: p. 461-468.
301. Tsuchiya , S., et al., *Establishment and characterization of a human acute monocytic leukemia cell line (THP-1).* International Journal of Cancer, 1980. **26**(2): p. 171-176.
302. Gong, J.H., G. Maki, and H.G. Klingemann, *Characterization of a human cell-line (NK-92) with phenotypical and functional-characteristics of activated natural-killer cells.* Leukemia, 1994. **8**(4): p. 652-658.
303. Park, E.K., et al., *Optimized THP-1 differentiation is required for the detection of responses to weak stimuli.* Inflammation Research, 2007. **56**(1): p. 45-50.
304. Chanput, W., J.J. Mes, and H.J. Wichers, *THP-1 cell line: an in vitro cell model for immune modulation approach.* Int Immunopharmacol, 2014. **23**(1): p. 37-45.
305. Robin, T., A. Capes-Davis, and A. Bairoch, *CLASTR: The Cellosaurus STR similarity search tool - A precious help for cell line authentication.* International Journal of Cancer, 2020. **146**(5): p. 1299-1306.
306. Nikfarjam, L. and P. Farzanenh, *Prevention and detection of Mycoplasma contamination in cell culture.* Cell Journal (Yakhteh), 2012. **13**(4): p. 203-212.
307. Riss, T.L., et al., *Cell viability assays.* Assay Guidance Manual [Internet], 2016.
308. Kamiloglu, S., et al., *Guidelines for cell viability assays.* Food Frontiers, 2020. **1**(3): p. 332-349.
309. *BS EN ISO 10993-5:2009: Biological evaluation of medical devices: Tests for in vitro cytotoxicity*. 2009, British Standards Institute.
310. López-García, J., et al., *HaCaT Keratinocytes Response on Antimicrobial Atelocollagen Substrates: Extent of Cytotoxicity, Cell Viability and Proliferation.* J Funct Biomater, 2014. **5**(2): p. 43-57.
311. Schmittgen, T.D. and K.J. Livak, *Analyzing real-time PCR data by the comparative CT method.* Nature Protocols, 2008. **3**(6): p. 1101-1108.
312. Rayarao, S.R., *Two-way Analysis of Variance: A Comprehensive Review of Theory, Applications, and Statistical Methodology.* Authorea Preprints, 2025.
313. Schwecht, I., et al., *Lactic acid enhances vaginal epithelial barrier integrity and ameliorates inflammatory effects of dysbiotic short chain fatty acids and HIV-1.* Scientific reports, 2023. **13**(1): p. 20065.
314. Giangrazi, F., et al., *Contribution of endometrial microbiome to inflammation-mediated infertility in women undergoing ART.* Human Reproduction, 2026: p. deaf252.
315. Yuan, J.S., et al., *Statistical analysis of real-time PCR data.* BMC Bioinformatics, 2006. **7**: p. 85.
316. Maess, M.B., S. Sendelbach, and S. Lorkowski, *Selection of reliable reference genes during THP-1 monocyte differentiation into macrophages.* BMC Mol Biol, 2010. **11**: p. 90.
317. Vestergaard, A.L., et al., *Transcriptional expression of type-I interferon response genes and stability of housekeeping genes in the human endometrium and endometriosis.* Mol Hum Reprod, 2011. **17**(4): p. 243-54.
318. Navot, D., et al., *The window of embryo transfer and the efficiency of human conception in vitro.* Fertility and Sterility, 1991. **55**(1): p. 114-118.
319. Nikas G, et al., *Endometrial pinopodes indicate a shift in the window of receptivity in IVF cycles.* Human Reproduction, 1999. **14**(3): p. 787-792.

320. Cousins, F.L., et al., *Evidence from a mouse model that epithelial cell migration and mesenchymal-epithelial transition contribute to rapid restoration of uterine tissue integrity during menstruation.* PLoS One, 2014. **9**(1): p. e86378.
321. Oghbaei, F., et al., *Epithelial-mesenchymal transition process during embryo implantation.* Cell Tissue Res, 2022. **388**(1): p. 1-17.
322. Buck, V.U., et al., *Redistribution of adhering junctions in human endometrial epithelial cells during the implantation window of the menstrual cycle.* Histochem Cell Biol, 2012. **137**(6): p. 777-90.
323. Wang, X., et al., *Embryonic signals direct the formation of tight junctional permeability barrier in the decidualizing stroma during embryo implantation.* J Cell Sci, 2004. **117**(Pt 1): p. 53-62.
324. Rabaglino, M.B. and K.P. Conrad, *Evidence for shared molecular pathways of dysregulated decidualization in preeclampsia and endometrial disorders revealed by microarray data integration.* FASEB J, 2019. **33**(11): p. 11682-11695.
325. Li, Q., et al., *Transforming growth factor beta receptor type 1 is essential for female reproductive tract integrity and function.* PLoS Genet, 2011. **7**(10): p. e1002320.
326. Aikawa, S., et al., *Spatiotemporal functions of leukemia inhibitory factor in embryo attachment and implantation chamber formation.* Cell Death Discov, 2024. **10**(1): p. 481.
327. Stewart, C.L., et al., *Blastocyst implantation depends on maternal expression of leukaemia inhibitory factor.* Nature, 1992. **359**(6390): p. 76-79.
328. Hiraoka, T., et al., *Differential roles of uterine epithelial and stromal STAT3 coordinate uterine receptivity and embryo attachment.* Sci Rep, 2020. **10**(1): p. 15523.
329. Cheng, J.G., et al., *Dual control of LIF expression and LIF receptor function regulate Stat3 activation at the onset of uterine receptivity and embryo implantation.* Proc Natl Acad Sci U S A, 2001. **98**(15): p. 8680-5.
330. Fan, X., et al., *VEGF blockade inhibits angiogenesis and reepithelialization of endometrium.* FASEB J, 2008. **22**(10): p. 3571-80.
331. Gipson, I.K., et al., *Mucin Genes Expressed by Human Female Reproductive Tract Epithelia1.* Biology of Reproduction, 1997. **56**(4): p. 999-1011.
332. Meseguer, M., et al., *Human Endometrial Mucin MUC1 Is Up-Regulated by Progesterone and Down-Regulated In Vitro by the Human Blastocyst.* Biology of Reproduction, 2001. **64**(2): p. 590-601.
333. King, A.E., H.O.D. Critchley, and R.W. Kelly, *The NF-κB pathway in human endometrium and first trimester decidua.* Molecular Human Reproduction, 2001. **7**(2): p. 175-183.
334. Laird, S.M., et al., *Expression of nuclear factor κ B in human endometrium; role in the control of interleukin 6 and leukaemia inhibitory factor production.* Molecular Human Reproduction, 2000. **6**(1): p. 34-40.
335. Ersahin, A., et al., *Disturbed endometrial NF-κB expression in women with recurrent implantation failure.* European Review for Medical and Pharmacological Sciences, 2016. **20**(24): p. 5037-5040.
336. Ravel, J., et al., *Vaginal microbiome of reproductive-age women.* Proceedings of the National Academy of Sciences, 2011. **108**(1): p. 4680-4687.
337. Heng, S., et al., *The significance of post-translational removal of α-DG-N in early stage endometrial cancer development.* Oncotarget, 2017. **8**(47): p. 81942-81952.

338. Haggerty, C.L., et al., *Presence and concentrations of select bacterial vaginosis-associated bacteria are associated with increased risk of pelvic inflammatory disease.* Sex Transm Dis, 2020. **47**(5): p. 344-346.
339. Srinivasan, B., et al., *TEER Measurement Techniques for In Vitro Barrier Model Systems.* SLAS Technology, 2015. **20**(2): p. 107-126.
340. Liang, C.-C., A.Y. Park, and J.-L. Guan, *In vitro scratch assay: a convenient and inexpensive method for analysis of cell migration in vitro.* Nature Protocols, 2007. **2**(2): p. 329-333.
341. Gastiazoro, M.P., et al., *Glyphosate induces epithelial mesenchymal transition-related changes in human endometrial Ishikawa cells via estrogen receptor pathway.* Mol Cell Endocrinol, 2020. **510**: p. 110841.
342. Schneider, C.A., W.S. Rasband, and K.W. Eliceiri, *NIH Image to ImageJ: 25 years of image analysis.* Nature Methods, 2012. **9**(7): p. 671-675.
343. Suarez-Arnedo, A., et al., *An image J plugin for the high throughput image analysis of in vitro scratch wound healing assays.* PLoS One, 2020. **15**(7): p. e0232565.
344. Grada, A., et al., *Research Techniques Made Simple: Analysis of Collective Cell Migration Using the Wound Healing Assay.* Journal of Investigative Dermatology, 2017. **137**(2): p. e11-e16.
345. Pijuan, J., et al., *In vitro Cell Migration, Invasion, and Adhesion Assays: From Cell Imaging to Data Analysis.* Front Cell Dev Biol, 2019. **7**: p. 107.
346. Cappiello, F., B. Casciaro, and M.L. Mangoni, *A Novel In Vitro Wound Healing Assay to Evaluate Cell Migration.* J Vis Exp, 2018(133).
347. Radstake, W.E., et al., *Comparison of in vitro scratch wound assay experimental procedures.* Biochem Biophys Rep, 2023. **33**: p. 101423.
348. Buck, V.U., et al., *Interaction of human trophoblast cells with gland-like endometrial spheroids: a model system for trophoblast invasion.* Hum Reprod, 2015. **30**(4): p. 906-16.
349. Buckley, A.G., et al., *Visualisation of Multiple Tight Junctional Complexes in Human Airway Epithelial Cells.* Biological Procedures Online, 2018. **20**(1).
350. Anwer, S. and K. Szászi, *Immunofluorescent Staining of Claudin-2 in Cultured Kidney Tubular Cells.* BIO-PROTOCOL, 2020. **10**(14).
351. Linkert, M., et al., *Metadata matters: access to image data in the real world.* J Cell Biol, 2010. **189**(5): p. 777-82.
352. Shihan, M.H., et al., *A simple method for quantitating confocal fluorescent images.* Biochem Biophys Rep, 2021. **25**: p. 100916.
353. Liu, X.M., et al., *Down-regulation of S100A11, a calcium-binding protein, in human endometrium may cause reproductive failure.* J Clin Endocrinol Metab, 2012. **97**(10): p. 3672-83.
354. Zhang, H., et al., *O-GlcNAc modification mediates aquaporin 3 to coordinate endometrial cell glycolysis and affects embryo implantation.* J Adv Res, 2022. **37**: p. 119-131.
355. Engel, B.J., et al., *MUC1 stimulates EGFR expression and function in endometrial cancer.* Oncotarget, 2016. **7**(22): p. 32796-32809.
356. Zhong, G., Y. Wang, and X. Liu, *Expression of HOXA10 in endometrial hyperplasia and adenocarcinoma and regulation by sex hormones in vitro.* Int J Gynecol Cancer, 2011. **21**(5): p. 800-5.
357. Au, H.-K., et al., *TGF-βI Regulates Cell Migration through Pluripotent Transcription Factor OCT4 in Endometriosis.* PLOS ONE, 2015. **10**(12): p. e0145256.

358. Zhang, H., et al., *Progesterone Regulates Glucose Metabolism Through Glucose Transporter 1 to Promote Endometrial Receptivity.* Front Physiol, 2020. **11**: p. 543148.
359. Amabebe, E. and D.O.C. Anumba, *The Vaginal Microenvironment: The Physiologic Role of Lactobacilli.* Front Med (Lausanne), 2018. **5**: p. 181.
360. Shan, T., et al., *M2-TAM subsets altered by lactic acid promote T-cell apoptosis through the PD-L1/PD-1 pathway.* Oncol Rep, 2020. **44**(5): p. 1885-1894.
361. Apostolova, P. and E.L. Pearce, *Lactic acid and lactate: revisiting the physiological roles in the tumor microenvironment.* Trends Immunol, 2022. **43**(12): p. 969-977.
362. Redel, B.K., et al., *Glycolysis in preimplantation development is partially controlled by the Warburg Effect.* Mol Reprod Dev, 2012. **79**(4): p. 262-71.
363. Chen, C., et al., *Lactic Acid Inhibits the Cytotoxicity of NK-92 Cells via Activating the Lactate Receptor GPR81.* Annual Research & Review in Biology, 2023: p. 1-10.
364. Brand, A., et al., *LDHA-Associated Lactic Acid Production Blunts Tumor Immunosurveillance by T and NK Cells.* Cell Metabolism, 2016. **24**(5): p. 657-671.
365. Okabe, S., et al., *Acetic acid induces cell death: an in vitro study using normal rat gastric mucosal cell line and rat and human gastric cancer and mesothelioma cell lines.* J Gastroenterol Hepatol, 2014. **29 Suppl 4**: p. 65-9.
366. Iplik, E.S., T. Catmakas, and B. Cakmakoglu, *A new target for the treatment of endometrium cancer by succinic acid.* Cell Mol Biol (Noisy-le-grand), 2018. **64**(1): p. 60-63.
367. Ertugrul, B., E.S. Iplik, and B. Cakmakoglu, *In Vitro Inhibitory Effect of Succinic Acid on T-Cell Acute Lymphoblastic Leukemia Cell Lines.* Arch Med Res, 2021. **52**(3): p. 270-276.
368. Meresman, G.F., et al., *Apoptosis is increased and cell proliferation is decreased in out-of-phase endometria from infertile and recurrent abortion patients.* Reproductive Biology and Endocrinology, 2010. **8**(1): p. 126.
369. von Wolff, M., et al., *Glucose transporter proteins (GLUT) in human endometrium: expression, regulation, and function throughout the menstrual cycle and in early pregnancy.* J Clin Endocrinol Metab, 2003. **88**(8): p. 3885-92.
370. Maeyama, M., et al., *Glycogen Estimation by a Rapid Enzymic Method in Very Small Samples of Human Endometrium: Glycogen Content in the Endometrium of Infertile Patients During the Menstrual Cycle.* Fertility and Sterility, 1977. **28**(2): p. 159-162.
371. O'Brien, K.L. and D.K. Finlay, *Immunometabolism and natural killer cell responses.* Nat Rev Immunol, 2019. **19**(5): p. 282-290.
372. Yan, S., et al., *The mTORC1 Signaling Support Cellular Metabolism to Dictate Decidual NK Cells Function in Early Pregnancy.* Front Immunol, 2022. **13**: p. 771732.
373. Chung, S.T., et al., *Measurements of Gluconeogenesis and Glycogenolysis: A Methodological Review.* Diabetes, 2015. **64**(12): p. 3996-4010.
374. Freitas, A.C. and J.E. Hill, *Quantification, isolation and characterization of Bifidobacterium from the vaginal microbiomes of reproductive aged women.* Anaerobe, 2017. **47**: p. 145-156.
375. Zevin, A.S., et al., *Microbiome Composition and Function Drives Wound-Healing Impairment in the Female Genital Tract.* PLoS Pathog, 2016. **12**(9): p. e1005889.

376. Paria, B.C., et al., *Zonula Occludens-1 and E-cadherin Are Coordinately Expressed in the Mouse Uterus with the Initiation of Implantation and Decidualization.* Developmental Biology, 1999. **208**(2): p. 488-501.
377. Edwards, V.L., et al., *Neisseria gonorrhoeae breaches the apical junction of polarized epithelial cells for transmigration by activating EGFR.* Cell Microbiol, 2013. **15**(6): p. 1042-57.
378. Mukura, L.R., et al., *Chlamydia trachomatis regulates innate immune barrier integrity and mediates cytokine and antimicrobial responses in human uterine ECC-1 epithelial cells.* Am J Reprod Immunol, 2017. **78**(6).
379. Buck, V.U., et al., *Steroid hormones and human choriogonadotropin influence the distribution of alpha6-integrin and desmoplakin 1 in gland-like endometrial epithelial spheroids.* Histochemistry and Cell Biology, 2021. **155**(5): p. 581-591.
380. Classen-Linke, I., et al., *Changes in Epithelial Cell Polarity and Adhesion Guide Human Endometrial Receptivity: How In Vitro Systems Help to Untangle Mechanistic Details.* Biomolecules, 2025. **15**(8).
381. Whitby, S., L.A. Salamonsen, and J. Evans, *The Endometrial Polarity Paradox: Differential Regulation of Polarity Within Secretory-Phase Human Endometrium.* Endocrinology, 2017. **159**(1): p. 506-518.
382. Luddi A, et al., *Organoids of Human Endometrium: A Powerful In Vitro Model for the Endometrium-Embryo Cross-Talk at the Implantation Site.* Cells, 2020. **9**: p. 1-16.
383. Ni, N. and Q. Li, *TGFbeta superfamily signaling and uterine decidualization.* Reprod Biol Endocrinol, 2017. **15**(1): p. 84.
384. Gao, Y., S. Li, and Q. Li, *Uterine epithelial cell proliferation and endometrial hyperplasia: evidence from a mouse model.* Mol Hum Reprod, 2014. **20**(8): p. 776-86.
385. Peng, J., et al., *Uterine activin receptor-like kinase 5 is crucial for blastocyst implantation and placental development.* Proc Natl Acad Sci U S A, 2015. **112**(36): p. E5098-107.
386. Wang, Z., et al., *Mice with dysfunctional TGF-beta signaling develop altered intestinal microbiome and colorectal cancer resistant to 5FU.* Biochim Biophys Acta Mol Basis Dis, 2021. **1867**(10): p. 166179.
387. Xue, V.W., et al., *Transforming Growth Factor-beta: A Multifunctional Regulator of Cancer Immunity.* Cancers (Basel), 2020. **12**(11).
388. Hannan, N.J., et al., *Analysis of fertility-related soluble mediators in human uterine fluid identifies VEGF as a key regulator of embryo implantation.* Endocrinology, 2011. **152**(12): p. 4948-56.
389. Sui, Y.-L., L. Li, and X.-X. Sun, *Integrated bioinformatics analysis to identify key genes and pathways involved in the endometria of patients with recurrent implantation failure undergoing in vitro fertilization and embryo transfer.* Reproductive and Developmental Medicine, 2023. **7**(4): p. 230-237.
390. Peter Durairaj, R.R., et al., *Deregulation of the endometrial stromal cell secretome precedes embryo implantation failure.* Mol Hum Reprod, 2017. **23**(7): p. 478-487.
391. Otsugu, M., et al., *Low pH induces amiloride-sensitive expression of leukemia inhibitory factor in endometrial cells.* J Reprod Dev, 2025. **71**(3): p. 115-123.
392. Okada, H., et al., *Estrogen and selective estrogen receptor modulators regulate vascular endothelial growth factor and soluble vascular endothelial growth factor receptor 1 in human endometrial stromal cells.* Fertil Steril, 2010. **93**(8): p. 2680-6.

393. Kim, M., et al., *VEGF-A regulated by progesterone governs uterine angiogenesis and vascular remodelling during pregnancy.* EMBO Mol Med, 2013. **5**(9): p. 1415-30.
394. Ali, R., et al., *An interplay of Progesterone, Leukemia Inhibitor Factor and Interleukin-6 in the window of implantation; Impact on fertility.* Cytokine, 2023. **170**: p. 156332.
395. Amjadi, F., et al., *The Uterine Immunological Changes may be responsible for Repeated Implantation Failure.* Journal of Reproductive Immunology, 2020. **138**: p. 103080.
396. Yue, X., L. Wu, and W. Hu, *The regulation of leukemia inhibitory factor.* Cancer Cell Microenviron, 2015. **2**(3).
397. Hu, W., et al., *p53 regulates maternal reproduction through LIF.* Nature, 2007. **450**(7170): p. 721-4.
398. Wu, F., et al., *Improvement of vaginal probiotics Lactobacillus crispatus on intrauterine adhesion in mice model and in clinical practice.* BMC Microbiol, 2023. **23**(1): p. 78.
399. Lu, W., et al., *Dysbiosis of the endometrial microbiota and its association with inflammatory cytokines in endometrial cancer.* Int J Cancer, 2021. **148**(7): p. 1708-1716.
400. Zaiatz-Bittencourt, V., et al., *Butyrate limits human natural killer cell effector function.* Sci Rep, 2023. **13**(1): p. 2715.
401. Ramaswami, S. and M.S. Hayden, *Electrophoretic Mobility Shift Assay Analysis of NF-κB DNA Binding*, in *NF-kappa B: Methods and Protocols*, M.J. May, Editor. 2015, Springer New York: New York, NY. p. 3-13.
402. Li, C.C., et al., *Phosphorylation of NF-KB1-p50 is involved in NF-kappa B activation and stable DNA binding.* Journal of Biological Chemistry, 1994. **269**(48): p. 30089-30092.
403. Turco, M.Y., et al., *Trophoblast organoids as a model for maternal–fetal interactions during human placentation.* Nature, 2018. **564**(7735): p. 263-267.
404. Rajaei, S., et al., *Cytokine profile in the endometrium of normal fertile and women with repeated implantation failure.* Iranian Journal of Immunology, 2011. **8**(4): p. 201-208.
405. Basatvat, S., et al., *Potential innate immunity-related markers of endometrial receptivity and recurrent implantation failure (RIF).* Reprod Biol, 2021. **21**(4): p. 100569.
406. Boomsma, C.M., et al., *Cytokine profiling in endometrial secretions: a non-invasive window on endometrial receptivity.* Reprod Biomed Online, 2009. **18**(1): p. 85-94.
407. Arici, A., et al., *Interleukin-8 in the human endometrium.* Journal of Clinical Endocrinology and Metabolism, 1998. **83**(5).
408. Hirota, Y., et al., *Interleukin (IL)-1beta stimulates migration and survival of first-trimester villous cytotrophoblast cells through endometrial epithelial cell-derived IL-8.* Endocrinology, 2009. **150**(1): p. 350-6.
409. Srivastava, A., et al., *Profiles of cytokines secreted by isolated human endometrial cells under the influence of chorionic gonadotropin during the window of embryo implantation.* Reprod Biol Endocrinol, 2013. **11**: p. 116.
410. von Wolff, M., et al., *Tumour necrosis factor-α (TNF-α) in human endometrium and uterine secretion: an evaluation by immunohistochemistry, ELISA and semiquantitative RT–PCR.* Molecular Human Reproduction, 1999. **5**(2): p. 146-152.

411. Tu, Y.A., et al., *Intentional endometrial injury enhances angiogenesis through increased production and activation of MMP-9 by TNF-alpha and MMP-3 in a mouse model.* Mol Hum Reprod, 2021. **27**(10).
412. Lai, T.H., H.T. Chen, and W.B. Wu, *Trophoblast coculture induces intercellular adhesion molecule-1 expression in uterine endometrial epithelial cells through TNF-alpha production: Implication of role of FSH and ICAM-1 during embryo implantation.* J Reprod Immunol, 2022. **152**: p. 103650.
413. Arima, K., et al., *Effects of lipopolysaccharide and cytokines on production of RANTES by cultured human endometrial stromal cells.* Molecular Human Reproduction, 2000. **6**(3): p. 246-251.
414. Rossi, M., et al., *Identification of genes regulated by interleukin-1beta in human endometrial stromal cells.* Reproduction, 2005. **130**(5): p. 721-9.
415. Schaefer, T.M., et al., *IL-1β-Mediated Proinflammatory Responses Are Inhibited by Estradiol via Down-Regulation of IL-1 Receptor Type I in Uterine Epithelial Cells.* Journal of Immunology, 2005. **175**(10): p. 6509-6516.
416. Bulmer, J.N., et al., *Granulated lymphocytes in human endometrium: histochemical and immunohistochemical studies.* Human Reproduction, 1991. **6**(6): p. 791-798.
417. Saito, S., et al., *Cytokine production by CD16^{-}CD56^{bright} natural killer cells in the human early pregnancy decidua.* International Immunology, 1993. **5**(5): p. 559-563.
418. Wang, F., et al., *Biology and pathology of the uterine microenvironment and its natural killer cells.* Cellular & Molecular Immunology, 2021. **18**(9): p. 2101-2113.
419. Robson, A., et al., *Uterine natural killer cells initiate spiral artery remodeling in human pregnancy.* FASEB J, 2012. **26**(12): p. 4876-85.
420. Hu, Y., et al., *Decidual NK cells alter in vitro first trimester extravillous cytotrophoblast migration: a role for IFN-γ.* The Journal of Immunology, 2006. **177**(12): p. 8522-8530.
421. Duriez, M., et al., *Human decidual macrophages and NK cells differentially express Toll-like receptors and display distinct cytokine profiles upon TLR stimulation.* Front Microbiol, 2014. **5**: p. 316.
422. Jiang, X., et al., *Three macrophage subsets are identified in the uterus during early human pregnancy.* Cellular & Molecular Immunology, 2018. **15**(12): p. 1027-1037.
423. Li, M., et al., *Tim-3(+) decidual Mphis induced Th2 and Treg bias in decidual CD4(+)T cells and promoted pregnancy maintenance via CD132.* Cell Death Dis, 2022. **13**(5): p. 454.
424. Wang, H., et al., *Role of decidual CD14(+) macrophages in the homeostasis of maternal-fetal interface and the differentiation capacity of the cells during pregnancy and parturition.* Placenta, 2016. **38**: p. 76-83.
425. Lidström, C., et al., *Cytokine Secretion Patterns of NK Cells and Macrophages in Early Human Pregnancy Decidua and Blood: Implications for Suppressor Macrophages in Decidua.* American journal of reproductive immunology (1989), 2003. **50**(6): p. 444-452.
426. Asarat, M., et al., *Short-Chain Fatty Acids Regulate Secretion of IL-8 from Human Intestinal Epithelial Cell Lines in vitro.* Immunol Invest, 2015. **44**(7): p. 678-93.
427. Mishra, P., et al., *Application of student's t-test, analysis of variance, and covariance.* Ann Card Anaesth, 2019. **22**(4): p. 407-411.

428. Thomas, M.J., *Elucidating the chlamydial growth characteristics, infection factors, and host responses to persistent chlamydial infection in women*, in *School of Life Sciences*. 2019, University of Technology Sydney: Open Publications of UTS Scholars. p. 273.
429. Tian, C.Q., et al., *Inhibition of the BET family reduces its new target gene IDO1 expression and the production of L-kynurenine.* Cell Death Dis, 2019. **10**(8): p. 557.
430. Honig, A., et al., *Indoleamine 2,3-dioxygenase (IDO) expression in invasive extravillous trophoblast supports role of the enzyme for materno-fetal tolerance.* J Reprod Immunol, 2004. **61**(2): p. 79-86.
431. Zhai, L., et al., *IDO1 in cancer: a Gemini of immune checkpoints.* Cell Mol Immunol, 2018. **15**(5): p. 447-457.
432. Morris, H., et al., *Endometrial lymphoid tissue: an immunohistological study.* Journal of Clinical Pathology, 1985. **38**(6): p. 644.
433. King, A., et al., *Immunocytochemical characterization of the unusual large granular lymphocytes in human endometrium throughout the menstrual cycle.* Human Immunology, 1989. **24**(3): p. 195-205.
434. Miyagi, M., et al., *Endometrial and vaginal microbiomes influence assisted reproductive technology outcomes.* JBRA Assist Reprod, 2022.
435. Caselli, E., et al., *Atopobium vaginae And Porphyromonas somerae Induce Proinflammatory Cytokines Expression In Endometrial Cells: A Possible Implication For Endometrial Cancer?* Cancer Management and Research, 2019. **11**: p. 8571-8575.
436. Tsui, K.-H., et al., *Interleukin-8 can stimulate progresterone secretion from a human trophoblast cell line, BeWo.* In Vitro Cellular & Developmental Biology - Animal, 2004. **40**(10): p. 331-336.
437. Rizzo, A., A. Losacco, and C.R. Carratelli, *Lactobacillus crispatus modulates epithelial cell defense against Candida albicans through Toll-like receptors 2 and 4, interleukin 8 and human beta-defensins 2 and 3.* Immunol Lett, 2013. **156**(1-2): p. 102-9.
438. Alhousseini, A., et al., *Differential Secretion of Inflammatory Cytokines by Human Trophoblasts in the Presence of Escherichia coli, Lactobacillus crispatus, and Lactobacillus jensenii.* Gynecol Obstet Invest, 2020. **85**(3): p. 277-283.
439. Young, S.L., et al., *Expression of Toll-like Receptors in Human Endometrial Epithelial Cells and Cell Lines.* American Journal of Reproductive Immunology, 2004. **52**(1): p. 67-73.
440. Bischoff, D.S., et al., *Acidic pH stimulates the production of the angiogenic CXC chemokine, CXCL8 (interleukin-8), in human adult mesenchymal stem cells via the extracellular signal-regulated kinase, p38 mitogen-activated protein kinase, and NF-kappaB pathways.* J Cell Biochem, 2008. **104**(4): p. 1378-92.
441. Xu, L. and I.J. Fidler, *Acidic pH-induced elevation in interleukin 8 expression by human ovarian carcinoma cells.* Cancer research, 2000. **60**(16): p. 4610-4616.
442. Japp, N.C., et al., *Tumor Biomarker In-Solution Quantification, Standard Production, and Multiplex Detection.* Journal of Immunology Research, 2021. **2021**: p. 1-12.
443. Van, K., J.L. Burns, and J.M. Monk, *Effect of Short-Chain Fatty Acids on Inflammatory and Metabolic Function in an Obese Skeletal Muscle Cell Culture Model.* Nutrients, 2024. **16**(4).

444. Ramhorst, R., et al., *Induction of maternal tolerance to fetal alloantigens by RANTES production.* Am J Reprod Immunol, 2006. **56**(5-6): p. 302-11.
445. Kamrani, A., et al., *The role of probiotics in restoring the Th1 to Th2 ratio in women experiencing recurrent implantation failure; a double-blind randomized clinical trial.* Hum Immunol, 2025. **86**(1): p. 111220.
446. You, Y., et al., *TNF-alpha Regulated Endometrial Stroma Secretome Promotes Trophoblast Invasion.* Front Immunol, 2021. **12**: p. 737401.
447. Simon, C., et al., *Localization of interleukin-1 type I receptor and interleukin-1β in human endometrium throughout the menstrual cycle.* The journal of clinical endocrinology and metabolism, 1993. **77**(2): p. 549-555.
448. Vacca, P., et al., *Analysis of natural killer cells isolated from human decidua: Evidence that 2B4 (CD244) functions as an inhibitory receptor and blocks NK-cell function.* Blood, 2006. **108**(13): p. 4078-85.
449. Von Woon, E., et al., *Number and function of uterine natural killer cells in recurrent miscarriage and implantation failure: a systematic review and meta-analysis.* Hum Reprod Update, 2022. **28**(4): p. 548-582.
450. Fukui, A., et al., *Intracellular cytokine expression of peripheral blood natural killer cell subsets in women with recurrent spontaneous abortions and implantation failures.* Fertil Steril, 2008. **89**(1): p. 157-65.
451. Blazheva, S., et al., *Unlocking the Uterine Code: Microbiota, Immune Cells, and Therapy for Recurrent Reproductive Failure.* Microorganisms, 2024. **12**(3).
452. Takeda, K., et al., *Interleukin-12 is involved in the enhancement of human natural killer cell activity by Lactobacillus casei Shirota.* Clin Exp Immunol, 2006. **146**(1): p. 109-15.
453. Tonn, T., et al., *Treatment of patients with advanced cancer with the natural killer cell line NK-92.* Cytotherapy, 2013. **15**(12): p. 1563-1570.
454. Nowakowska, P., et al., *Clinical grade manufacturing of genetically modified, CAR-expressing NK-92 cells for the treatment of ErbB2-positive malignancies.* Cancer Immunology, Immunotherapy, 2018. **67**(1): p. 25-38.
455. Grebenkina, P., et al., *Modulation of NK Cell Properties by ESKAPE Group Bacteria.* International Journal of Molecular Sciences, 2025. **26**(17): p. 8449.
456. Elshal, M.F. and J.P. McCoy, *Multiplex bead array assays: performance evaluation and comparison of sensitivity to ELISA.* Methods, 2006. **38**(4): p. 317-23.
457. Perez, M., et al., *Microbiota-Derived Short-Chain Fatty Acids Boost Antitumoral Natural Killer Cell Activity.* J Clin Med, 2024. **13**(13).
458. Cummings, J.H., et al., *Short chain fatty acids in human large intestine, portal, hepatic and venous blood.* Gut, 1987. **28**(10): p. 1221-7.
459. Lapides, L., et al., *Clustering of Uterine Natural Killer Cells Around Uterine Glands in Women with Recurrent Implantation Failure and Recurrent Pregnancy Loss: An Immunohistochemical Study.* Int J Mol Sci, 2025. **26**(20).
460. Arici A, et al., *Regulation of interleukin-8 gene in human endometrial cells in culture.* Molecular and Cellular Endocrinology, 1993. **94**: p. 195-204.
461. Peter, K., et al., *Lactic acid delays the inflammatory response of human monocytes.* Biochem Biophys Res Commun, 2015. **457**(3): p. 412-8.
462. Bar-Joseph, Z., A. Gitter, and I. Simon, *Studying and modelling dynamic biological processes using time-series gene expression data.* Nat Rev Genet, 2012. **13**(8): p. 552-64.
463. Yao, J., et al., *NK-92 cells activated by IL-2 inhibit the progression of endometriosis in vitro.* J Obstet Gynaecol, 2024. **44**(1): p. 2372682.

464. Kurmanova, A., et al., *Altered Expressions of IL-15, IFNG, and HPRT1 Genes in the Thin Endometria of Patients with Reproductive Disorders: A Prospective Comparative Study.* J Clin Med, 2024. **13**(20).
465. Fehniger, T.A., et al., *Differential cytokine and chemokine gene expression by human NK cells following activation with IL-18 or IL-15 in combination with IL-12: implications for the innate immune response.* J Immunol, 1999. **162**(8): p. 4511-20.
466. Mei, J., et al., *Inhibition of IDO1 suppresses cyclooxygenase-2 and matrix metalloproteinase-9 expression and decreases proliferation, adhesion and invasion of endometrial stromal cells.* Mol Hum Reprod, 2012. **18**(10): p. 467-76.
467. Zong, S., et al., *Dysregulated expression of IDO may cause unexplained recurrent spontaneous abortion through suppression of trophoblast cell proliferation and migration.* Sci Rep, 2016. **6**: p. 19916.
468. Wei, H., et al., *Abnormal Expression of Indoleamine 2, 3-Dioxygenase in Human Recurrent Miscarriage.* Reprod Sci, 2020. **27**(8): p. 1656-1664.
469. Obayashi, Y., et al., *Role of Indoleamine 2,3-Dioxygenase and Tryptophan 2,3-Dioxygenase in Patients with Recurrent Miscarriage.* Am J Reprod Immunol, 2016. **75**(1): p. 69-77.
470. Jurgens, B., et al., *Interferon-gamma-triggered indoleamine 2,3-dioxygenase competence in human monocyte-derived dendritic cells induces regulatory activity in allogeneic T cells.* Blood, 2009. **114**(15): p. 3235-43.
471. Martin-Gallausiaux, C., et al., *Butyrate Produced by Commensal Bacteria Down-Regulates Indolamine 2,3-Dioxygenase 1 (IDO-1) Expression via a Dual Mechanism in Human Intestinal Epithelial Cells.* Front Immunol, 2018. **9**: p. 2838.
472. Rovira Gonzalez, Y.I., et al., *In vitro cytokine licensing induces persistent permissive chromatin at the Indoleamine 2,3-dioxygenase promoter.* Cytotherapy, 2016. **18**(9): p. 1114-28.
473. Huang, H.L., et al., *Decidual IDO(+) macrophage promotes the proliferation and restricts the apoptosis of trophoblasts.* J Reprod Immunol, 2021. **148**: p. 103364.
474. Tan, W., et al., *Relationship between macrophages in mouse uteri and angiogenesis in endometrium during the peri-implantation period.* Theriogenology, 2014. **82**(7): p. 1021-7.
475. Liu, Y., X.-M. Tan, and T.-T. He, *Macrophage polarization disorder in the endometrial immune microenvironment may contribute to recurrent implantation failure.* Reproductive and Developmental Medicine, 2024. **8**(3): p. 162-168.
476. Diao, L., et al., *New endometrial immune cell-based score (EI-score) for the prediction of implantation success for patients undergoing IVF/ICSI.* Placenta, 2020. **99**: p. 180-188.
477. Tsao, F.Y., et al., *M1 macrophages decrease in the deciduae from normal pregnancies but not from spontaneous abortions or unexplained recurrent spontaneous abortions.* J Formos Med Assoc, 2018. **117**(3): p. 204-211.
478. Samuvel, D.J., et al., *Lactate boosts TLR4 signaling and NF-kappaB pathway-mediated gene transcription in macrophages via monocarboxylate transporters and MD-2 up-regulation.* J Immunol, 2009. **182**(4): p. 2476-84.
479. Yanagihara, S., et al., *Lactobacillus acidophilus L-92 Cells Activate Expression of Immunomodulatory Genes in THP-1 Cells.* Biosci Microbiota Food Health, 2014. **33**(4): p. 157-64.

480. Chen, X., et al., *Hypoxia-induced polarization of M2 macrophages and C-C motif chemokine ligand 5 secretion promotes the migration and invasion of trophoblasts.* Biol Reprod, 2022. **107**(3): p. 834-845.
481. Ono, Y., et al., *CD206+ M2-Like Macrophages Are Essential for Successful Implantation.* Front Immunol, 2020. **11**: p. 557184.
482. Eyster, K.M., et al., *Reciprocal communication between endometrial stromal cells and macrophages.* Reprod Sci, 2010. **17**(9): p. 809-22.
483. Zhuang, B.M., et al., *Single-cell characterization of self-renewing primary trophoblast organoids as modeling of EVT differentiation and interactions with decidual natural killer cells.* BMC Genomics, 2023. **24**(1): p. 618.
484. Gardner, D.K., et al., *Glucose consumption of single post-compaction human embryos is predictive of embryo sex and live birth outcome.* Hum Reprod, 2011. **26**(8): p. 1981-6.
485. Gott, A.L., et al., *Non-invasive measurement of pyruvate and glucose uptake and lactate production by sigle human preimplantation embryos.* Human Reproduction, 1990. **5**(1): p. 104-108.
486. Zhang, H., et al., *Low-level pyruvate inhibits early embryonic development and maternal mRNA clearance in mice.* Theriogenology, 2021. **166**: p. 104-111.
487. Wang, M., et al., *Glucose promoting the early embryonic development by increasing the lipid synthesis at 2-cell stage.* Front Cell Dev Biol, 2023. **11**: p. 1208501.
488. Cao, D., et al., *Selective utilization of glucose metabolism guides mammalian gastrulation.* Nature, 2024. **634**(8035): p. 919-928.
489. Chi, F., et al., *Glycolysis-Independent Glucose Metabolism Distinguishes TE from ICM Fate during Mammalian Embryogenesis.* Dev Cell, 2020. **53**(1): p. 9-26 e4.
490. Ferrick, L., Y.S.L. Lee, and D.K. Gardner, *Metabolic activity of human blastocysts correlates with their morphokinetics, morphological grade, KIDScore and artificial intelligence ranking.* Hum Reprod, 2020. **35**(9): p. 2004-2016.
491. Gardner, D.K., *Lactate production by the mammalian blastocyst: Manipulating the microenvironment for uterine implantation and invasion?* BioEssays, 2015. **37**(4): p. 364-371.
492. Gardner, D.K. and H.J. Leese, *Concentrations of nutrients in mouse oviduct fluid and their effects on embryo development and metabolism in vitro.* Journal of reproduction & fertility, 1990. **88**(1): p. 361-368.
493. Norwitz, E.R., D.J. Schust, and S.J. Fisher, *Implantation and the Survival of Early Pregnancy.* New England Journal of Medicine, 2001. **345**(19): p. 1400-1408.
494. Anacker, J., et al., *Human decidua and invasive trophoblasts are rich sources of nearly all human matrix metalloproteinases.* Mol Hum Reprod, 2011. **17**(10): p. 637-52.
495. Udayashankar, R., et al., *Characterization of invasive trophoblasts generated from human embryonic stem cells.* Hum Reprod, 2011. **26**(2): p. 398-406.
496. Plaks, V., et al., *Matrix metalloproteinase-9 deficiency phenocopies features of preeclampsia and intrauterine growth restriction.* Proc Natl Acad Sci U S A, 2013. **110**(27): p. 11109-14.
497. Zhang, H., et al., *The chemokine CXCL6 restricts human trophoblast cell migration and invasion by suppressing MMP-2 activity in the first trimester.* Hum Reprod, 2013. **28**(9): p. 2350-62.

498. Cabral-Pacheco, G.A., et al., *The Roles of Matrix Metalloproteinases and Their Inhibitors in Human Diseases.* Int J Mol Sci, 2020. **21**(24).
499. Wang, H., et al., *Matrix metalloproteinase and tissue inhibitor of matrix metalloproteinase expression in human preimplantation embryos.* Fertil Steril, 2003. **80 Suppl 2**: p. 736-42.
500. Stsepetova, J., et al., *The complex microbiome from native semen to embryo culture environment in human in vitro fertilization procedure.* Reprod Biol Endocrinol, 2020. **18**(1): p. 3.
501. Alqawasmeh, O.A.M., et al., *Vertical transmission of microbiomes into embryo culture media and its association with assisted reproductive outcomes.* Reprod Biomed Online, 2024. **49**(2): p. 103977.
502. Yoshida, T., et al., *Lactobacillus crispatus promotes invasion of the HTR-8/SVneo trophoblast cell line.* Placenta, 2021. **111**: p. 76-81.
503. Chen, L., et al., *Mechanisms of YAP1-mediated trophoblast ferroptosis in recurrent pregnancy loss.* J Assist Reprod Genet, 2024.
504. Shyu, M.K., et al., *Mucin 15 is expressed in human placenta and suppresses invasion of trophoblast-like cells in vitro.* Hum Reprod, 2007. **22**(10): p. 2723-32.
505. Wang, H., et al., *A novel model of human implantation: 3D endometrium-like culture system to study attachment of human trophoblast (Jar) cell spheroids.* Mol Hum Reprod, 2012. **18**(1): p. 33-43.
506. Lan, J. and C. Chen, *The role of lactic acid bacteria in maintaining vaginal internal environment homeostasis in patients with infertility.* Microb Pathog, 2023. **176**: p. 106004.
507. Gardner, D.K., et al., *Environment of the preimplantation human embryo in vivo: metabolite analysis of oviduct and uterine fluids and metabolism of cumulus cells.* Fertility and Sterility, 1996. **65**(2): p. 349-353.
508. Yu, X., et al., *Acetyl-CoA metabolism maintains histone acetylation for syncytialization of human placental trophoblast stem cells.* Cell Stem Cell, 2024. **31**(9): p. 1280-1297 e7.
509. Ain, R. and P.B. Seshagiri, *Succinate and malate improve development of hamster eight-cell embryos in vitro: Confirmation of viability by embryo transfer.* Molecular Reproduction and Development, 1998. **47**(4): p. 440-447.
510. Lane, M. and D.K. Gardner, *Lactate regulates pyruvate uptake and metabolism in the preimplantation mouse embryo.* Biology of Reproduction, 2000. **62**(1): p. 16-22.
511. Waugh, E.E. and R.G. Wales, *Oxidative utilization of glucose, acetate and lactate by early preimplantation sheep, mouse and cattle embryos.* Reproduction, fertility, and development, 1993. **5**(1): p. 123–133.
512. Zhao, J., et al., *Metabolic remodelling during early mouse embryo development.* Nature metabolism, 2021. **3**(10): p. 1372-1384.
513. Karachrysafi, S., et al., *Immunohistochemical study of MMP-2, MMP-9, EGFR and IL-8 in decidual and trophoblastic specimens of recurrent pregnancy loss cases.* J Matern Fetal Neonatal Med, 2023. **36**(1): p. 2218523.
514. Turpeenniemi-Hujanen, T., et al., *Extracellular matrix interactions in early human embryos: implications for normal implantation events.* Fertility and Sterility, 1995. **64**(1): p. 132-138.
515. Gu, J., et al., *The correlation analysis of human embryonic MMP-9 secretion and embryo quality.* Eur Rev Med Pharmacol Sci, 2015. **19**(13): p. 2354-8.

516. Baumann, F., et al., *Lactate promotes glioma migration by TGF-β2–dependent regulation of matrix metalloproteinase-2.* Neuro-oncology (Charlottesville, Va.), 2009. **11**(4): p. 368-380.
517. Chen, S., et al., *Effect of Vaginal Microecological Alterations on Female Pelvic Organ Prolapse.* Int Urogynecol J, 2024. **35**(4): p. 881-891.
518. Sheng, S.L., et al., *Knockdown of lactate dehydrogenase A suppresses tumor growth and metastasis of human hepatocellular carcinoma.* FEBS J, 2012. **279**(20): p. 3898-910.
519. Hua, Y., et al., *Expression of lactate dehydrogenase C correlates with poor prognosis in renal cell carcinoma.* Tumour Biol, 2017. **39**(3): p. 1010428317695968.
520. Emenaker, N.J. and M.D. Basson, *Short Chain Fatty Acids Inhibit Human (SW1116) Colon Cancer Cell Invasion by Reducing Urokinase Plasminogen Activator Activity and Stimulating TIMP-1 and TIMP-2 Activities, Rather Than via MMP Modulation.* Journal of Surgical Research, 1998. **76**(1): p. 41-46.
521. Onogi, A., et al., *Hypoxia inhibits invasion of extravillous trophoblast cells through reduction of matrix metalloproteinase (MMP)-2 activation in the early first trimester of human pregnancy.* Placenta, 2011. **32**(9): p. 665-670.
522. Schröpfer, A., et al., *Expression pattern of matrix metalloproteinases in human gynecological cancer cell lines.* BMC Cancer, 2010. **10**(1): p. 553.
523. Yu, N., et al., *HCG-Activated Human Peripheral Blood Mononuclear Cells (PBMC) Promote Trophoblast Cell Invasion.* PLoS One, 2015. **10**(6): p. e0125589.
524. Chénais, B., *Matrix metalloproteinase-2 and -9 secretion by the human JAR choriocarcinoma cell line is stimulated by TNF-α.* Advances in Bioscience and Biotechnology, 2012. **03**(01): p. 51-56.
525. Kobara, H., et al., *Lipocalin2 enhances the matrix metalloproteinase-9 activity and invasion of extravillous trophoblasts under hypoxia.* Placenta, 2013. **34**(11): p. 1036-43.
526. Weimar, C.H., et al., *In-vitro model systems for the study of human embryo-endometrium interactions.* Reprod Biomed Online, 2013. **27**(5): p. 461-76.
527. Hu, W., et al., *Nucleolar stress regulation of endometrial receptivity in mouse models and human cell lines.* Cell Death Dis, 2019. **10**(11): p. 831.
528. Mao, J., et al., *GPR65 inhibits human trophoblast cell adhesion through upregulation of MYLK and downregulation of fibronectin via cAMP-ERK signaling in a low pH environment.* Cell Commun Signal, 2023. **21**(1): p. 238.
529. Vento-Tormo, R., et al., *Single-cell reconstruction of the early maternal-fetal interface in humans.* Nature, 2018. **563**(7731): p. 347-353.
530. Evans, J., et al., *Prokineticin 1 signaling and gene regulation in early human pregnancy.* Endocrinology, 2008. **149**(6): p. 2877-87.
531. Klingemann, H., *The NK-92 cell line—30 years later: its impact on natural killer cell research and treatment of cancer.* Cytotherapy, 2023. **25**(5): p. 451-457.
532. Collins, J., et al., *Humanized microbiota mice as a model of recurrent Clostridium difficile disease.* Microbiome, 2015. **3**(1): p. 35.
533. Ka, Y., et al., *Establishment of a human microbiome- and immune system-reconstituted dual-humanized mouse model.* Experimental Animals, 2023. **72**(3): p. 402-412.
534. Wege, A.K., et al., *Functional and phenotypic characterization of the humanized BLT mouse model.* Curr Top Microbiol Immunol, 2008. **324**: p. 149-65.

535. Lan, P., et al., *Reconstitution of a functional human immune system in immunodeficient mice through combined human fetal thymus/liver and CD34+ cell transplantation.* Blood, 2006. **108**(2): p. 487-92.
536. Daharsh, L., et al., *Characterization of double humanized BLT-mice with stable engraftment of a human gut bacterial microbiome.* Frontiers in Microbiomes, 2024. **Volume 3 - 2024**.
537. Williams, N.S., et al., *Natural killer cell differentiation: insights from knockout and transgenic mouse models and in vitro systems.* Immunological reviews, 1998. **165**(1): p. 47-61.
538. Croy, B.A., et al., *Histological studies of gene-ablated mice support important functional roles for natural killer cells in the uterus during pregnancy.* Journal of Reproductive Immunology, 1997. **35**(2): p. 111-133.
539. Guimond, M.-J., et al., *Absence of Natural Killer Cells during Murine Pregnancy is Associated with Reproductive Compromise in TgE26 Mice.* Biology of Reproduction, 1997. **56**(1): p. 169-179.
540. Lozano, F.M., et al., *Characterization of the Endometrial Microbiome in Patients with Recurrent Implantation Failure.* Microorganisms, 2023. **11**(3).
541. Kusama, K., et al., *Endometrial epithelial-mesenchymal transition (EMT) by menstruation-related inflammatory factors during hypoxia.* Mol Hum Reprod, 2021. **27**(6).
542. So, K.A., et al., *Interleukin-6 expression by interactions between gynecologic cancer cells and human mesenchymal stem cells promotes epithelial-mesenchymal transition.* Int J Oncol, 2015. **47**(4): p. 1451-9.
543. Fernando, R.I., et al., *IL-8 signaling plays a critical role in the epithelial-mesenchymal transition of human carcinoma cells.* Cancer Res, 2011. **71**(15): p. 5296-306.
544. Dong, W., et al., *Exposure to TNF-alpha combined with TGF-beta induces carcinogenesis in vitro via NF-kappaB/Twist axis.* Oncol Rep, 2017. **37**(3): p. 1873-1882.
545. Li, J., et al., *Inflammation-related downregulation of zonula Occludens-1 in fetal membrane contributes to development of prelabor rupture of membranes.* Placenta, 2020. **99**: p. 173-179.
546. Brysse, A., et al., *Regulation of CXCL8/IL-8 expression by zonula occludens-1 in human breast cancer cells.* Mol Cancer Res, 2012. **10**(1): p. 121-32.
547. Musso, T., et al., *Leukemia Inhibitory Factor Induces Interleukin-8 and Monocyte Chemotactic and Activating Factor in Human Monocytes: Differential Regulation by Interferon-γ.* Blood, 1995. **86**(5): p. 1961-1967.
548. Ottosen, L.D., et al., *Observations on intrauterine oxygen tension measured by fibre-optic microsensors.* Reprod Biomed Online, 2006. **13**(3): p. 380-5.
549. Kigawa, J., *[Studies on the levels of pO2 and pCO2 in the uterine cavity and uterine tissue (author's transl)].* Nihon Sanka Fujinka Gakkai Zasshi, 1981. **33**(10): p. 1646-54.
550. Yedwab, G.A., et al., *The temperature, pH, and partial pressure of oxygen in the cervix and uterus of women and uterus of rats during the cycle.* Fertil Steril, 1976. **27**(3): p. 304-9.
551. Ortiz-Prado, E., et al., *Partial pressure of oxygen in the human body: a general review.* Am J Blood Res, 2019. **9**(1): p. 1-14.
552. Ng KYB, et al., *In vivo oxygen, temperature and pH dynamics in the female reproductive tract and their importance in human conception: a systematic review.* Human Reproduction Update, 2018. **24**: p. 15-34.

553. Matsumoto, L., et al., *HIF2alpha in the uterine stroma permits embryo invasion and luminal epithelium detachment.* J Clin Invest, 2018. **128**(7): p. 3186-3197.
554. Ramirez-Bergeron, D.L., et al., *HIF-dependent hematopoietic factors regulate the development of the embryonic vasculature.* Dev Cell, 2006. **11**(1): p. 81-92.
555. Yao, F., et al., *Single-embryo transcriptomic atlas of oxygen response reveals the critical role of HIF-1alpha in prompting embryonic zygotic genome activation.* Redox Biol, 2024. **72**: p. 103147.
556. Xie, Y., et al., *Downregulation of HIF-2alpha Enhances Apoptosis and Limits Invasion in Human Placental JEG-3 Trophoblast Cells.* Reprod Sci, 2021. **28**(9): p. 2710-2717.
557. Shigemitsu, A., K. Naruse, and H. Kobayashi, *Hypoxia Promotes Extravillous Trophoblast Cell Invasion through the Hypoxia-Inducible Factor Urokinase-Type Plasminogen Activator Receptor Pathway.* Gynecol Obstet Invest, 2022. **87**(3-4): p. 232-241.
558. Liang, L., et al., *HIF-1alpha is positively associated with endometrial receptivity by regulating PKM2.* J Obstet Gynaecol Res, 2023. **49**(11): p. 2734-2745.
559. Hashimoto, Y., et al., *Inflammatory Cytokine-Induced HIF-1 Activation Promotes Epithelial-Mesenchymal Transition in Endometrial Epithelial Cells.* Biomedicines, 2023. **11**(1).
560. Herbemont, C., et al., *Impact of oxygen tension according to embryo stage of development: a prospective randomized study.* Sci Rep, 2021. **11**(1): p. 22313.
561. Tamm-Rosenstein, K., et al., *Changes in the transcriptome of the human endometrial Ishikawa cancer cell line induced by estrogen, progesterone, tamoxifen, and mifepristone (RU486) as detected by RNA-sequencing.* PLoS One, 2013. **8**(7): p. e68907.
562. Pinelli, D.M., et al., *Hormonal Modulation of Ishikawa Cells During Three-Dimensional Growth In Vitro.* Journal of the Society for Gynecologic Investigation, 1998. **5**(4): p. 217-223.
563. Tamm K, et al., *Genes targeted by the estrogen and progesterone receptors in the human endometrial cell lines HEC1A and RL95-2.* Reproductive Biology and Endocrinology, 2009. **7**.
564. Lykke, M.R., et al., *Vaginal, Cervical and Uterine pH in Women with Normal and Abnormal Vaginal Microbiota.* Pathogens, 2021. **10**(2).
565. Tarahomi, M., et al., *In vivo human uterine temperature, pH, and uterine fluid composition analysis.* bioRxiv, 2024: p. 2024.11.18.623470.
566. Kapalczynska, M., et al., *2D and 3D cell cultures - a comparison of different types of cancer cell cultures.* Arch Med Sci, 2018. **14**(4): p. 910-919.
567. Fitzgerald, H.C., et al., *Self-renewing endometrial epithelial organoids of the human uterus.* Proc Natl Acad Sci U S A, 2019. **116**(46): p. 23132-23142.
568. Cindrova-Davies, T., et al., *Menstrual flow as a non-invasive source of endometrial organoids.* Commun Biol, 2021. **4**(1): p. 651.
569. Zhou, W., et al., *Infertile human endometrial organoid apical protein secretions are dysregulated and impair trophoblast progenitor cell adhesion.* Front Endocrinol (Lausanne), 2022. **13**: p. 1067648.
570. Wu, Q., et al., *Organ-on-a-chip: recent breakthroughs and future prospects.* Biomed Eng Online, 2020. **19**(1): p. 9.
571. Clarke, G.A., et al., *Advancement of Sensor Integrated Organ-on-Chip Devices.* Sensors (Basel), 2021. **21**(4).

572. Chang, K.-W., et al., *Womb-on-a-chip biomimetic system for improved embryo culture and development.* Sensors and Actuators B: Chemical, 2016. **226**: p. 218-226.
573. Kim, R., et al., *A Platform for Co-Culture of Primary Human Colonic Epithelium With Anaerobic Probiotic Bacteria.* Front Bioeng Biotechnol, 2022. **10**: p. 890396.
574. Rosca, A.S., et al., *Gardnerella and vaginal health: the truth is out there.* FEMS Microbiol Rev, 2020. **44**(1): p. 73-105.
575. Ruiz-Alonso M, et al., *The endometrial receptivity array for diagnosis and personalized embryo transfer as a treatment for patients with repeated implantation failure.* Fertility and Sterility, 2013. **100**: p. 818-824.
576. Tan, J., et al., *The role of the endometrial receptivity array (ERA) in patients who have failed euploid embryo transfers.* J Assist Reprod Genet, 2018. **35**(4): p. 683-692.
577. Iwami, N., et al., *Therapeutic intervention based on gene sequencing analysis of microbial 16S ribosomal RNA of the intrauterine microbiome improves pregnancy outcomes in IVF patients: a prospective cohort study.* Journal of Assisted Reproduction and Genetics, 2023. **40**(1): p. 125-135.
578. Iwami, N., et al., *Shortening time to pregnancy in infertile women by personalizing treatment of microbial imbalance through Emma & Alice: A multicenter prospective study.* Reproductive medicine and biology, 2025. **24**(1): p. e12634-n/a.
579. Shamugia, N., P. Varlakova, and N. Podzolkova, *Correction of Uterine Microflora Composition Disorders and Embryo Transfer Timing in Patients with Recurrent Implantation Failure: Clinical Effects and Prognostic Factors.* Medical Times, 2025. **3**(1).
580. Lédée, N., et al., *The uterine immune profile: A method for individualizing the management of women who have failed to implant an embryo after IVF/ICSI.* Journal of Reproductive Immunology, 2020. **142**: p. 103207.
581. Lédée, N., et al., *The Uterine Immune Profile May Help Women With Repeated Unexplained Embryo Implantation Failure After In Vitro Fertilization.* American journal of reproductive immunology (1989), 2016. **75**(3): p. 388-401.
582. Lédée, N., et al., *Uterine immune profiling for increasing live birth rate: A one-to-one matched cohort study.* Journal of Reproductive Immunology, 2017. **119**: p. 23-30.
583. Lédée, N., et al., *Endometrial immune profiling and precision therapy increase live birth rate after embryo transfer: a randomised controlled trial.* Frontiers in Immunology, 2025. **Volume 16 - 2025**.